# Pneumococcus morphogenesis and resistance to beta-lactams

Jules Philippe

UNIVERSITÉ DE GRENOBLE

## Thesis

to obtain the grade of

## PhD for the UNIVERSITY OF GRENOBLE

Specialty: **Virology – Microbiology – Immunology**

Presented by


## Jules PHILIPPE


Thesis directed by **André ZAPUN**

prepared within the **Pneumococcus Group – Institute for Structural Biology – UMR 5075**
at the **Doctoral School of Chemistry and Life Sciences**

# Pneumococcus Morphogenesis and resistance to beta-lactams

Thesis defended in public on September 29th, 2014
to the following jury:

**Dr. Rut Carballido-López**
Research director at INRA, Reporter
**Pr. Leiv Sigve Håvarstein**
Professor at the Norwegian University of Life Sciences, Reporter
**Pr. Christelle Breton**
Professor at the University Joseph Fourier, Examiner
**Dr. Christophe Grangeasse**
Research director at CNRS, Examiner
**Pr. Malcolm G. P. Page**
Head of Biology at Basilea Pharmaceutica International Ltd, Examiner
**Dr. André Zapun**
Researcher at CNRS, Thesis director





*Université Joseph Fourier / Université Pierre Mendès France /*
*Université Stendhal / Université de Savoie / Grenoble INP*

UNIVERSITÉ DE GRENOBLE

# THÈSE

Pour obtenir le grade de

## DOCTEUR DE L'UNIVERSITÉ DE GRENOBLE

Spécialité : **Virologie – Microbiologie – Immunologie**

Arrêté ministériel : 7 août 2006


Présentée par

## Jules PHILIPPE

Thèse dirigée par **André ZAPUN**

préparée au sein du **Groupe Pneumocoque – Institut de Biologie Structurale – UMR 5075**
dans **l'École Doctorale Chimie et Sciences du Vivant**


# Morphogénèse du pneumocoque et résistance aux bêta-lactamines

Thèse soutenue publiquement le 29 septembre 2014,
devant le jury composé de :

**Dr. Rut Carballido-López**
Directrice de recherches à l'INRA, Rapporteur
**Pr. Leiv Sigve Håvarstein**
Professeur à l'Université de Norvège, Rapporteur
**Pr. Christelle Breton**
Professeur à l'Université Joseph Fourier, Examinatrice
**Dr. Christophe Grangeasse**
Directeur de recherches au CNRS, Examinateur
**Pr. Malcolm G. P. Page**
Directeur Biologie chez Basilea Pharmaceutica International Ltd, Examinateur
**Dr. André Zapun**
Chargé de recherches au CNRS, Directeur de thèse





*Université Joseph Fourier / Université Pierre Mendès France /*
*Université Stendhal / Université de Savoie / Grenoble INP*

M. PASTEUR : J'ai été obligeamment averti, le 10 décembre, par M. Lannelongue, de la présence dans son service de l'enfant atteint d'hydrophobie dont M. Maurice Raynaud vient de vous entretenir. Avec la salive, quatre heures après la mort, j'ai inoculé deux lapins qui sont morts en trente-six heures. Dans leur sang se trouvait un organisme microscopique nouveau qui a pu être cultivé dans le bouillon de veau. Cet organisme, que je figure sur le tableau, se présente sous la forme d'un bâtonnet, légèrement rétréci en son milieu, analogue à un 8; il a $\frac{1}{1000}$ de millimètre de diamètre et est entouré d'une substance gélatiniforme ayant l'aspect d'une auréole pâle. Dans le liquide de culture, l'auréole disparaît et les bâtonnets se disposent en chapelets de formes variées, qui en contiennent 100, 150 et plus; lorsque la culture est abandonnée à elle-même, les bâtonnets disparaissent pour faire place à des globules sphériques d'un plus petit diamètre. Les cultures successives de cet organisme ont manifesté leur virulence sur des lapins et des chiens, et l'existence constante dans le sang du même organisme. J'ignore absolument les relations de cette nouvelle maladie avec la rage. Ce que j'affirme, contrairement à ce que vient de dire M. Colin, c'est que cette maladie n'est pas la septicémie, et qu'il en est ainsi de la maladie étudiée par MM. Raynaud et Lannelongue. Bien entendu, je ne parle que de la série de leurs essais relatifs à l'inoculation de la salive de l'enfant, puisque c'est là seulement que nous avons procédé de même.

*First description of the pneumococcus by Louis Pasteur.*
*Extract of the French 'Bulletin de l'Académie de médecine', 1881.*

# Acknowledgements

First, I would like to thank Dr. Rut Rut Carballido-López and Pr. Leiv Sigve Håvarstein to have accepted to review this manuscript, as reporters of the jury. I am also grateful to Pr. Christelle Breton, Dr. Christophe Grangeasse and Pr. Malcolm G. P. Page to participate in the evaluation as examinators.

I would like to acknowledge Thierry VERNET to have welcomed me in the Pneumococcus Group from 2009 to 2014. Thierry always made sure to provide me with a pleasant and fruitful environment. He has always been of very good advice and appreciable company in scientific discussion, but also speaking about travelling and mountain outdoor activities. Thank you Thierry, I guess I have been lucky to spend these years in your lab.

Many thanks go to André Zapun, a great PhD director that knew how to deal with a wild PhD student. André, when I met you the first time, you had a cast to recover from the thumb you broke in climbing. During the "interview" and later on, you told me about your backpacking experiences around the world, your mountaineering expeditions, the incredible variety of birds and if I remember well, about a bug I think you called "pneumococcus". How could I miss it, I could not refuse! Thank you for the supervision you finely adapted to my personality. Thank you for being so logical that any unexpected result can make sense. Thank you for keeping the energy to transmit your great knowledge of Biochemistry to a student that always privileged Microbiology classes at the expense of Biochemistry at the University. You taught me how to plan experiments, how to avoid useless ones, how to interpret results and (I don't know if it is appropriate here, but) how to write. Thank you again.

I would like to thank the other researchers of the lab for their help and precious advices to make not-working experiments work, and explaining me various incredible molecular mechanisms of the pneumococcus. Claire, thank you for the rhubarb, Cécile thank you for the white wine at each occasion we could celebrate something, Marjolaine, thank you for your smile and showing me how to subjugate membrane proteins with detergents, Anne-Marie D.G., thank you for your advices. Also Anne-Marie V, thank you for your pleasant company.

I would like to thank Laure Roux, the best lab technician ever, always happy, taking care of the people, easy going, accommodating, I think my English vocabulary becomes limiting. Thank you for making things easy in the lab, and for your great company outside the lab. Greetings to your family!

My acknowledgements also go to the Eefjan Breukink that hosted me for three weeks in his laboratory of the University of Utrecht. Thank you for the supervision in lipid II synthesis. I also thank Martijn Koorengevel that also helped me in the experiments in Utrecht. I also thank Régine

Hakenbeck and Dalia Denapaite for the generous gift of the GFP:PBP2x encoding strain of pneumococcus.

I would like to acknowledge Nordine Helassa, who built many constructs I used and Fany Couppey that initiated the work on piperacillin prior to my arrival at the laboratory. This work would not have been the same without the tools and knowledge you generated.

Thanks to Yann Huon de Kermadec tried to convert me to the world of nanodiscs. Thank you for the introduction to the "nanos", but also for the enjoyable time we have outside the lab.

Gravier, thanks for introducing me to the world of the good beer. OK, I'll never be a fine Belgium beer taster as you, but it has always been a pleasure to share a drink with you. Also at the lab, my office-mate, always here to give me precious advices and transmitting your wide knowledge on PBPs, thank you.

Max, Rémi and Julie, the other PhD students of the lab. Many thanks for the nice environment you brought at work, for the meals and beers we had together to forget about our heavy student duty…

Louise, Widade, Yann H2K, Papa Jimmy, Yann Fichou, Gianluca, Mathieu (with 1 or 2 "t", I never remember), Hicham, Michel (not PhD, but it's the same) and Didier, thank you for being PhD students at the same time as me, it's always good to know we are not alone. I'll miss the Wednesday H2 meals!

Of course, many thanks to anybody that worked at the lab and brought a nice atmosphere as Ana, Guillaume, Benjamin, Flo, Justine, Lucie, Violaine, Iza it was great to "work" with you!

Thank you Lorraine, for the support, for the best meals when I had only chineese noodles to survive, for the soft words that made me keeping a good mood even when printing spoiled the whole formatting!

Thank you Jérôme and Steph, the roomates without whom I'd be 5kg lighter… Thanks to all the potes grenoblois, these studies where rich in people and mountains!

Thank you papa and maman for all the support and for allowing me to complete these studies and to have let me travelling for several years as far and as much as I could!

This work used the platforms of the Grenoble Instruct center (ISBG ; UMS3518 CNRS-CEA-UJF-EMBL) with support from FRISBI (ANR-10-INSB-05-02) and GRAL (ANR-10-LABX-49-01) within the Grenoble Partnership for Structural Biology (PSB).

I would like to thank Daphna Fenel and Dr Guy Schoehn from the Electron Microscopy platform, I thank Aline Leroy and Christine Ebel from the PAOL platform and Lionel Imbert from the cell free platform. I thank Anne Marie Villard and Dr. Marjolaine Noirclerc-Savoye, for the detergent

screening for membrane protein solubilization and purification; and Céline Charavay and Stéphane Segard (GIPSE, CEA, Grenoble) for the RoBioLIMS database development.

Finally, I would like to thank the Région Rhône Alpes and the ARC1 Santé for financing my PhD. I also thank the CEA, the UJF and the CNRS that are the three institutes of the UMR 5075.

# Contents

# Abbreviations

| | |
|---|---|
| 3D-SIM: | three-dimensional structured illumination microscopy |
| aLII: | amidated lipid II |
| AT: | amidotransferase |
| ATP: | adenosin triphosphate |
| AU: | arbitrary units |
| CDC: | center for disease control |
| CMC: | critical micelle concentration |
| CSP: | competence-simulating peptide |
| CV: | column volume |
| DDM: | *n*-dodecyl-β-D-maltopyranoside |
| DEAE: | Diethylaminoethyl |
| DIC: | differential interference contrast microscopy |
| DMSO: | dimethyl sulfoxide |
| DNA: | deoxyribonucleic acid |
| EM: | electron microscopy |
| FosC12: | fos-choline-12 |
| g: | gram |
| Glc*N*Ac: | *N*-acetylglucosamine |
| GT: | glycosyltransferase |
| h: | hour |
| HPLC: | high-performance liquid chromatography |
| HRP: | horseradish peroxidase |
| IPD: | invasive pneumococcal diseases |
| IPTG: | isopropyl β-D-1-thiogalactopyranoside |
| k: | kilo |
| Da: | dalton |
| L: | liter |
| LII: | lipid II |
| LII-DNS: | dansylated lipid II |
| LTA: | lipoteichoic acids |
| m: | meter |
| m…: | milli… |
| µ: | micro |
| M: | molar (mole / liter) |
| MALLS: | multi-angle laser light scattering |
| MCS: | multiple cloning site |
| MIC: | minimum inhibitory concentration |
| min: | minute |
| Mur*N*Ac: | *N*-acetylmuramic acid |
| n: | nano |
| OD: | optical density (in nanometer) |
| PBP: | penicillin-binding protein |
| PBS: | phosphate buffer saline |

| | |
|---|---|
| PCR: | polymerase chain reaction |
| PCV: | pneumococcal conjugate vaccine |
| PEG: | polyethylene glycol |
| PLP: | protéine liant la pénicilline |
| psi: | pound per square inch |
| QELS: | quasi-elastic light scattering |
| *qs*: | quantity sufficient |
| RI: | refractive index |
| RNA: | ribonucleic acid |
| ROS: | reactive oxygen species |
| rpm: | rotation per minute |
| SEC: | size exclusion chromatography |
| SDS-PAGE: | sodium dodecyl sulfate – polyacrylamide gel electrophoresis |
| SEDS: | shape, elongation, division and sporulation proteins |
| TLC: | thin layer chromatography |
| TM: | transmembrane |
| TP: | transpeptidase |
| tRNA: | transfer RNA |
| UDP: | uridine diphosphate |
| UV: | ultra-violet |
| V: | volt |
| WHO: | world health organization |
| WTA: | wall teichoic acids |

# I- Introduction

*Louis Pasteur (left) and George Miller Sternberg (right) simultaneously discovered Streptococcus pneumoniae in the blood of rabbits inoculated with human saliva in 1881.*

## Le pneumocoque – résumé

*Streptococcus pneumoniae*, communément appelé le pneumocoque, est une bactérie à Gram positif souvent rencontrée dans la flore commensale du nasopharynx de l'humain. Dans certaines conditions, elle peut engendrer des maladies, tout particulièrement chez les personnes au système immunitaire faible (nourrissons, personnes âgées ou immunodéprimées). Les infections à pneumocoques peuvent être diverses selon le site de propagation de la bactérie dans le corps humain. Les plus communes sont les otites chez les enfants, mais on rencontre aussi des sinusites, pneumonies ou septicémies qui entraînent dans les cas les plus graves des méningites. Dans le monde, plus d'un million et demi de personnes meurent chaque année d'infections à pneumocoques. Les enfants des pays en voie de développement sont les plus touchés.

Le pneumocoque adopte une forme caractéristique en diplocoque et peut former des chainettes lorsqu'elle est cultivée en milieu liquide en laboratoire. A sa surface, il possède une membrane cytoplasmique entourée d'une paroi et éventuellement d'une capsule. La paroi (qui fait l'objet du chapitre suivant) est une structure essentielle qui protège la bactérie contre la pression osmotique. Elle donne sa forme à la bactérie et permet l'ancrage de diverses molécules de surface, telles que les polysaccharides qui constituent la capsule du pneumocoque. En tant que structure de surface (la plus à l'extérieure de cette bactérie), la capsule est un facteur de virulence majeur qui gêne la reconnaissance par le système immunitaire de l'hôte.

Le pneumocoque est capable de s'adapter à diverses conditions, ce qui lui permet d'évoluer au travers d'environnements très différents au cours de l'infection. En temps qu'anaérobe aéro-tolérant, il peut passer du nasopharynx au sang où les concentrations d'oxygène sont très différentes. Aussi, la génération d'une forte concentration de peroxyde d'hydrogène lui permet d'évoluer lors d'infections, en particulier dans les pneumonies ou septicémies. Le pneumocoque est aussi naturellement résistant au lysozyme, une des défenses majeures de l'hôte contre les bactéries.

L'importante capacité d'adaptation du pneumocoque est renforcée par sa facilité à intégrer les caractères génétiques des bactéries de son environnement. Deux caractéristiques du pneumocoque y jouent un rôle clé. Premièrement, il est naturellement compétant, ce qui lui permet d'intégrer dans son génome des fragments d'ADN contenant des informations génétiques pouvant être sélectionnées si elles lui sont avantageuses. De plus, le pneumocoque autolyse, c'est-à-dire que lorsque la densité de pneumocoques est trop importante, une enzyme entraîne la lyse des bactéries, relâchant du matériel génétique dans le milieu extérieur, disponible pour les pneumocoques restants. Le phénomène de compétence est impliqué dans la résistance aux antibiotiques et l'évasion des vaccins.

A ce jour, plus de 90 sérotypes de pneumocoques ont été identifiés qui diffèrent par la composition de la capsule. Les vaccins disponibles étant basé sur l'immunisation par injection de polysaccharides de surface, seuls certains sérotypes sont pris en compte. Le Pneumovax®23 (Merck) protège les adultes contre 23 sérotypes de pneumocoque mais est faiblement immunogénique chez l'enfant. Deux vaccins utilisés chez l'enfant, le Prevenar®7 et le Prevenar®13 (Pfizer) sont plus efficaces dans ce contexte, grâce à la conjugaison de 7 ou 13 polysaccharides de surface à une protéine porteuse. Ces vaccins, développés aux Etats-Unis, ciblent les sérotypes qui étaient les plus présents et résistants dans les isolats cliniques de ce pays au moment de leur confection. Leur utilisation a permis de faire baisser la proportion des sérotypes concernés dans les infections à pneumocoques recensées dans les pays occidentaux. Cependant, ils sont moins adaptés aux sérotypes présents en Asie et en Amérique du Sud, particulièrement.

Le développement précoce des bêta-lactamines a procuré un traitement de choix pour les infections à pneumocoques grâce à sa forte sensibilité pour ces antibiotiques. Aussi, leur utilisation de manière intensive a-t-elle engendré l'émergence de souches résistantes dès la fin des années 70. En France, la fréquence des souches cliniques de pneumocoques résistantes à la pénicilline a cessé d'augmenter en 2002 grâce à la mise en place d'un plan national pour l'efficacité des antibiotiques et l'augmentation de la vaccination des nourrissons.

# The pneumococcus

The pneumococcus is only 1 µm long. Behind its tiny appearance, this bacterium hides many properties and characteristics that make it of great scientific and medical interest. First, it causes major health problems around the world, from the poorest to the richest country and treatments must be continuously developed to limit infections. Then, many mechanisms are used by this opportunistic pathogen to cope with its environment and the strategies used by humans to fight it. This part intends to give a general overview of *Streptococcus pneumoniae* that shall help the reader to understand why the pneumococcus is of interest.

## Discovery

*Streptococcus pneumoniae* – the pneumococcus – was first described in 1881 from two independent accidental observations. George Miller Sternberg, one of the first scientists studying bacteria in the United States was intending to identify the cause of malaria. He injected rabbits with different samples collected in swamps of the suburbs of New Orleans. As a "sterile" control, he used his own saliva. The "control" rabbit died in forty eight hours and Sternberg observed in its blood some micro-organisms he called *micrococci* (Sternberg, 1881). Almost eight thousand kilometers away, the same year, Louis Pasteur could isolate the same organism from the blood of two rabbits that died in thirty six hours after inoculation with the saliva of a dead patient with rabies (Pasteur, 1881). Because of its capacity to cause pulmonary diseases, this bacterium was soon renamed pneumococcus, and *Diplococcus pneumoniae* for its shape. It was eventually called *S. pneumoniae* in 1974 for its propensity to form chains of cocci in liquid cultures (Watson*, et al.*, 1993).

## General description and characteristics

### *Bacteriology*

*S. pneumoniae* is a 1 µm Gram-positive bacterium that has an ovoid shape (slightly elongated coccus with an "American football" shape). In liquid cultures, it is often observed as diplococci (a pair of cocci), but it can also be seen as isolated cells or in chains (Figure 1). A pneumococcus cell is not motile and does not form spores. Its density must be close to that of water as liquid cultures in exponential phase without stirring appear turbid from surface to bottom. In these conditions, the generation time is typically forty minutes. *S. pneumoniae* is an aero-tolerant anaerobic bacterium that prefers an environment enriched in carbon dioxide (typically, an atmosphere containing 5% of carbon dioxide is used for cultivation), where it ferments glucose to lactic acid for growth. The

pneumococcus does not produce catalase, which is often added to the cultivation media (by adding blood, for example) in order to protect it against the hydrogen peroxide it produces as a byproduct of its metabolism. One convenient property of *S. pneumoniae* is that it is α-hemolytic: the hydrogen peroxide it produces oxidizes hemoglobin (red, with a $Fe^{2+}$ ferrous ion in the heme) to methemoglobin (green, with a $Fe^{3+}$ ferric ion in the heme). Thus, colonies of pneumococci grown on blood agar medium are characterized by the dark green halo surrounding them, which enables an easy identification. The pneumococcus can be differentiated from other α-hemolytic streptococci by its unique sensitivity to optochin (a quinine derivative).

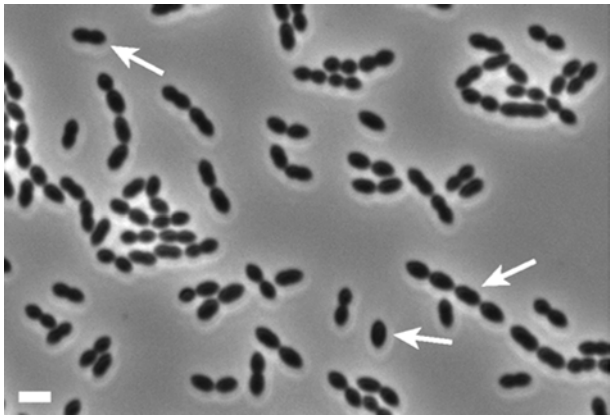

**Figure 1: Phase contrast image of pneumococcus R6 cells. Arrows indicate a single cell, a diplococcus and a chain of pneumococci. Scale bar: 2µm.**

*S. pneumoniae* belongs to the phylum Firmicutes, the class Bacilli, the order Lactobacillales, the family Streptococcaceae and the genus *Streptococcus*. This genus includes six major clusters, as defined by 16S rRNA sequencing: pyogenic, anginosus, mitis (including *S. pneumoniae*), salivarius, bovis and mutans (Kawamura*, et al.*, 1995).

### *Pneumococcus cell surface*

The surface of the pneumococcus is comprised of two major layers surrounding the plasma membrane: the cell wall and the capsule (Figure 2).

The cell wall contains peptidoglycan, a single macromolecule made of glycan chains reticulated by peptide bridges. This molecule is described in details in the next chapter. Cell wall also comprises the teichoic acids (40 - 50 % of the cell wall dry weight (Bui*, et al.*, 2012)). Teichoic acids are polysaccharides that contain glycerol-phosphate or ribitol-phosphate subunits, found in Gram-positive bacteria. They can be anchored to the plasma membrane (lipoteichoic acids, or LTA) or to the peptidoglycan (wall teichoic acids, or WTA). In *S. pneumoniae*, the teichoic acids are unusual

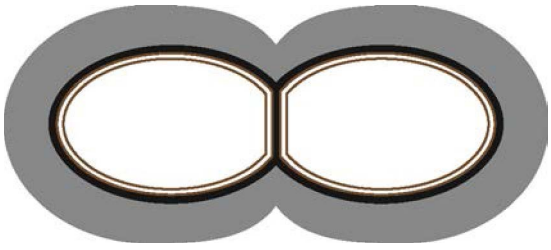

**Figure 2: Schematic representation of *S. pneumoniae* cell surface. Grey: capsule, black: cell wall, brown: plasma membrane**

for several reasons. Contrary to most bacteria, the repeating unit of WTA is identical to that of LTA (Fischer, 1997). It is composed of the rare amino sugar 2-acetamido-4-amino-2,4,6-trideoxy-galactose, glucose, ribitol-phosphate, *N*-acetylgalactosamine, and phosphocholine, repeated 6 to 7 times in one WTA molecule (Figure 3, (Bui*, et al.*, 2012)). The phosphocholines are particular to the pneumococcus. They enable the binding of several surface proteins to the cell wall through non-covalent linkage (the choline-binding proteins, or CBPs). Also, choline is essential for the growth of pneumococcus, which is the only bacterium known with this requirement. The phosphocholines play a role in multiple mechanisms involved in the formation of chains, competence, autolysis (Tomasz, 1968) and penicillin-induced lysis (Tomasz*, et al.*, 1970). This is explained by the fact that some of the CBPs are peptidoglycan hydrolases required for all these mechanisms.

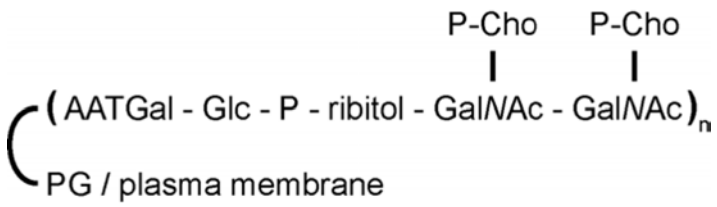


**Figure 4: Composition of pneumococcal teichoic acids, modified from (Bui*, et al.*, 2012). WTA are anchored to peptidoglycan and LTA to the plasma membrane. AATGal: 2-acetamido-4-amino-2,4,6-trideoxy-galactose, Glc: glucose, P: phosphate, Gal*N*Ac: *N*-acetylgalactosamine, P-Cho: phosphocholine, PG: peptidoglycan.**

The polysaccharide capsule overlays the peptidoglycan layer and its composition determines the serotype of a given strain. Generally, the capsule is covalently attached to the cell wall of pneumococcus, with some exceptions (serotype 3, for example (Sorensen*, et al.*, 1990)), and is typically 200 to 400 nm thick. The capsule increases the virulence of this pathogen (Kelly*, et al.*, 1994). Of note though, two cases of conjunctivitis have been reported to be caused by non-encapsulated isolates (Martin*, et al.*, 2003), (Crum*, et al.*, 2004), indicating that this structure is not essential for the development of pneumococcal conjunctivitis, at least. The capsule was shown to help pneumococci evade the host immune system (Avery & Dubos, 1931). Globally, the capsule reduces the interaction with phagocytes by charge at physiological pH, it impairs phagocyte recognition of immunoglobulins and complement molecules bound to surface molecules (teichoic acids or surface proteins) because the latter are shorter than the capsule thickness, it reduces the complement deposition at the pneumococcus

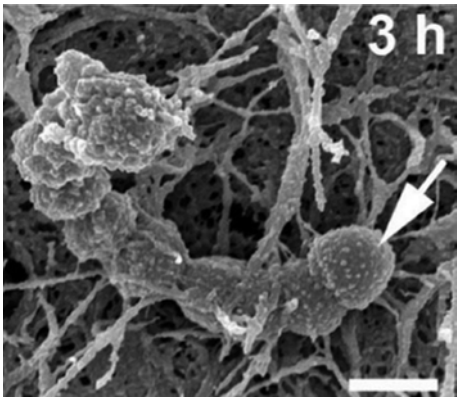


**Figure 3: Scanning electron microscopy picture of A66 encapsulated pneumococci after 3 h of incubation with HEp-2 larynx cells. The arrow indicates a pneumococcus in close interaction with the cell, with a thinner capsule than the other pneumococci of the chain. Adapted from (Hammerschmidt*, et al.*, 2005).**

surface and the trapping by neutrophil extracellular traps (reviewed in (Kadioglu*, et al.*, 2008)).

During colonization of the host, the capsule layer becomes thinner upon adhesion to epithelial tissues to favor the interaction (Figure 4, (Hammerschmidt*, et al.*, 2005)). Also, *S. pneumoniae* can switch the composition of their capsule (hence serotype) by transformation to evade immunity, for example.

### *Serotypes*

In 1910, a typing method was developed by Franz Neufeld and Ludwig Händel providing evidence, for the first time, that pneumococci can belong to different serotypes. This method consisted in injecting clinical pneumococcal strains to mice previously immunized with different types of pneumococci, and observing death or survival of the animal (Neufeld & Haendel, 1910). A series of additional serotypes were later identified in the United States by Dochez and Gillespie and in South Africa by Lister, present in the latter case only in South Africa (Watson*, et al.*, 1993). Nowadays, serotyping is performed by coagglutination with antibodies, and recently by multiplex PCR or the use of DNA microarrays.

The serotype of an organism is determined by its antigenic constitution, which differs from other organisms of the same species. To date, at least 93 distinct pneumococcus serogroups with distinct capsular poly-saccharides structures have been described (Henriques-Normark & Tuomanen, 2013). The different serotypes are associated with distinct characteristics in terms of virulence or antibiotic resistance (Song*, et al.*, 2012).

Note that the R6 laboratory strain, used in the present study, is not encapsulated and therefore avirulent.

### *Natural environment*

The pneumococcus naturally inhabits as a commensal organism the nasopharynx of humans. In healthy persons, the nasopharyngeal microbiota comprises several bacterial species that cohabit or compete with each other. This microbiota was recently investigated in healthy children and compared with that of children with pneumonia from three Swiss hospitals (Sakwinska*, et al.*, 2014). It showed that three genera are dominant in the nasopharynx of both healthy children and pneumonia patients: *Moraxella*, *Streptococcus* and *Haemophilus* (Figure 5). As one could expect, the abundance of the *Streptococcus* and the *Haemophilus* genera is increased in patients with pneumonia. Of note is that the nasopharyngeal microbiota strongly differs from one person to another.

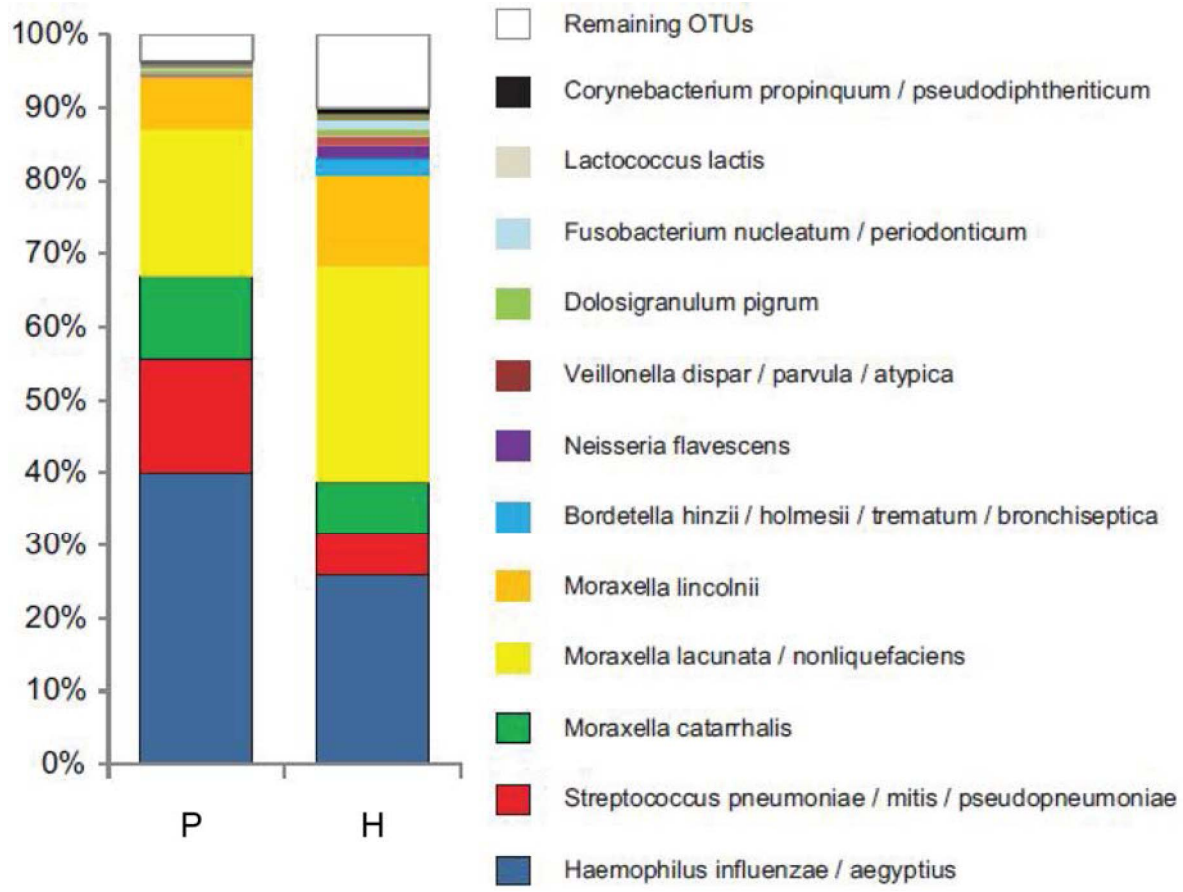


**Figure 5: Relative abundance of the 12 most common micro-organisms of the nasopharyngeal microbiota of 50 healthy (H) and 50 pneumonia (P) children (2 months to 16 years old) from 3 Swiss hospitals. OTUs stands for operational taxonomic unit. Adpated from (Sakwinska*, et al.*, 2014).**

In the nasopharynx, the pneumococcus can be exposed to high oxygen concentrations (likely up to 20 % at the surface of the mucus layer) whereas it deals with low oxygen concentrations in deeper layers (5 %) (Yesilkaya*, et al.*, 2013). In some instances, the pneumococcus can lead to infection by colonizing the lower respiratory tract, or even the blood and the cerebrospinal fluid. In those latter cases, the pneumococcus copes with nearly anaerobic conditions.

*S. pneumoniae* encounters several reactive oxygen species (ROS) in the different environments it occupies. Hydrogen peroxide ($H_2O_2$) is one of them that is produced as a byproduct of its own metabolism at a concentration that can reach 2 mM. This compound contributes to the virulence of the pneumococcus and is required for the colonization of the nasopharynx and the development of pneumonia and sepsis (Spellerberg*, et al.*, 1996). A drawback of hydrogen peroxide is that it is detrimental for *S. pneumoniae* cells, as the other ROS. Indeed, it damages proteins by oxidation, and this is used by the immune system to fight infections. In inflammation, neutrophils and macrophages release several ROS including $H_2O_2$, superoxide anion ($O_2^{\bullet -}$) and hydroxyl radicals ($OH^{\bullet}$) that also damage other molecules such as DNA. The lactic acid bacteria of the nasopharynx can also be a source of ROS.

The pneumococcus lacks catalase, which is utilized by most bacteria to eliminate $H_2O_2$. It also lacks the main Gram-negative proteins known to confer resistance to oxidative stress. A set of proteins has been described to date that allows the pneumococcus to live in the presence of ROS (reviewed in (Yesilkaya*, et al.*, 2013)), but the mechanisms are not completely understood yet.

One of the primary defense of the host is the use of lysozyme to disrupt the peptidoglycan of the pathogens (Nonomura*, et al.*, 1991), (Bercovici*, et al.*, 1975). The pneumococcus is naturally resistant to this enzyme thanks to its largely de-acetylated peptidoglycan.

### *Competence*

An interesting property of the pneumococcus is its intrinsic competence. The competence is the capacity of a cell to integrate DNA from the environment. This mechanism enables the cell to beneficiate of advantageous characteristics possibly encoded by the fragment of DNA incorporated. Competence occurs naturally, and it can be artificially induced under specific conditions . The analysis of competence genes revealed that it is conserved among the genus *Streptococcus* (Berg*, et al.*, 2012).

In 1928, a British bacteriologist, Frederick Griffith, described competence for the first time by using *S. pneumoniae* cells. First, he injected mice with an avirulent strain of pneumococcus with no effect on the survival of the rodents. However, the co-injection of this avirulent strain and a heat-killed virulent strain of pneumococcus caused the injected mice to die (Griffith, 1928). In fact, the avirulent strain of pneumococcus underwent transformation, which had never been described before. In 1931 in New York, Dawson and Sia could perform pneumococcus transformation *in vitro*, *i.e.* with no passage in an animal: the dead "donor" pneumococci where added in the culture medium for transformation (Dawson & Sia, 1931). Twelve years later, Avery *et al* identified the factor containing the transferred information: the deoxyribonucleic acid (DNA) (Avery*, et al.*, 1944). At this time, DNA was shown to provide transformants with their new property, but the molecular mechanisms responsible for competence activation remained unclear.

Half a century later, the pheromone-like signal that induces competence was identified in the pneumococcus (Havarstein*, et al.*, 1995). It was called CSP for competence-simulating peptide. CSP is a 17 amino-acids peptide, ribosomally synthesized as a precursor peptide that is then exported and cleaved by the ComA ABC transporter (Havarstein*, et al.*, 1995). Subsequently, the pneumococcus *comCDE* operon was described, encoding for the three core-proteins of the competence: *comC* encodes for CSP, *comD* and *comE* encode for a two-component signal transduction system, including the CSP-specific receptor (ComD) and its cognate response regulator (ComE, (Pestova*, et al.*, 1996)).

CSP and ComD are species-specific (Johnsborg & Havarstein, 2009), which enables species-dependent competence signaling. This can be useful in an environment where multiple species cohabit or compete with each other.

The expression of more than 180 genes is influenced by the competence state of the pneumococcus, from which only 10 to 20% were shown to be required for natural transformation. Further details on those genes are in (Johnsborg & Havarstein, 2009) and (Berg, *et al.*, 2012).

The natural competence ability provides an important advantage to *S. pneumoniae* in terms of resistance. Indeed, β-lactam resistance genes are exchanged from strain to strain, and even between different species co-habiting the same niche that have developped resistance due to in-adequate antibiotic exposure (Dowson, *et al.*, 1989), (Laible, *et al.*, 1991). Other types of antibiotic resistance has also been associated with recombinantion events, such as the macrolides, the fluoroquinolones and the rifampicin (Croucher, *et al.*, 2011). Also, the combination of genetic transformation and recombination events has allowed serotype switching, enabling pneumococci to evade vaccine immunization (Croucher, *et al.*, 2011).

### *Autolysis*

Another property of *S. pneumoniae* is the autolysis. The growth of this organism is characterized by a short stationary phase followed by a strong decrease of the optical density (OD) in laboratory conditions. The major autolysin responsible for autolysis in the pneumococcus is LytA. Its depletion restores the stationary phase (Figure 6). This property is related to competence in that cells in the competent state are more prone to autolysis (Seto & Tomasz, 1975). Also, it was shown in 2004 that the release of DNA in the medium upon competence induction was mainly due to the action of two proteins in the pneumococcus: the major autolysin LytA and LytC, two peptidoglycan hydrolases (Moscoso & Claverys, 2004).

LytA has an *N*-acetylmuramoyl L-alanine amidase activity (Howard & Gooder, 1974), (Mellroth, *et al.*, 2012). In other words, it separates the glycan chains of peptidoglycan from their peptide crosslinks. This protein includes two domains: a *N*-

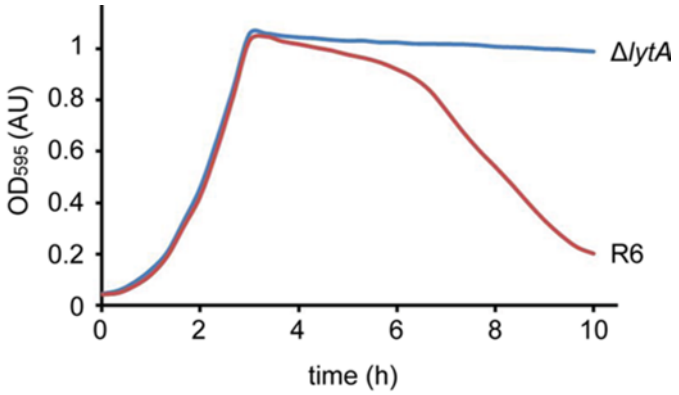


**Figure 6: Growth curves of *S. pneumoniae* R6 and its Δ*lytA* derivative in laboratory conditions.**

acetylmuramoyl L-alanine amidase domain and a choline-binding domain. The latter allows to localize it to the cell wall via its interaction with the phosphocholine residues of the teichoic acids, confirming an early observation (Briese & Hakenbeck, 1985). LytA is a cytoplasmic protein. It is thought to be released in the extracellular medium through bacterial lysis, resulting in a cascade lysis event, which in turn kills the whole population of pneumococci in laboratory conditions (Mellroth*, et al.*, 2012).

The exact role of LytA *in vivo* is not fully understood, although several suggestions have been made. First, LytA deficient mutants have no morphological deffects (Tomasz*, et al.*, 1988), (Berg*, et al.*, 2013), but only a higher propensity for the formation of chains in liquid culture. Thus, its role in cell wall maturation or in the division process is probably limited. Rather, LytA is involved in the virulence of the pneumococcus, as demonstrated in a rat model of meningitis (Hirst*, et al.*, 2008). Also, it was shown to reduce the secretion of some cytokines that activate phagocytosis, in addition of preventing phagocytosis by unclear mechanisms (Martner*, et al.*, 2009). The authors suggest that the fragments of autolyzed bacteria could constitute a diversion, in turn diminishing phagocytosis of living bacteria.

Under penicillin treatment, pneumococcus lysis is mainly due to the action of LytA. Indeed, in a LytA-negative mutant, penicillin addition at the minimum inhibitory concentration (MIC) inhibits growth, but does not result in lysis contrary to the same treatment in a LytA-positive background (Tomasz & Waks, 1975). Addition of exogeneous LytA restores lysis in β-lactam treated cells but it does not induce lysis of pneumococci treated with antibiotics that do not target peptidoglycan synthesis (chloramphenicol) (Tomasz & Waks, 1975). In exponential growth phase, it seems that pneumococci are protected from LytA activity, which is not the case in stationary phase or under peptidoglycan-directed antibiotic treatment (Mellroth*, et al.*, 2012). The mechanisms of activation of LytA are not fully understood to date, but Mellroth *et al* proposed it to be through the recognition of its peptidoglycan substrate (Figure 7).

### *Pathogenicity*

Before the beginning of the twentieth century, the pneumococcus was already shown to cause meningitis, otitis media, arthritis and endocarditis (Netter, 1887), (Zaufal, 1887). Nowadays, it has been described in many infections that also include pneumonia, sinusitis and septicemia.

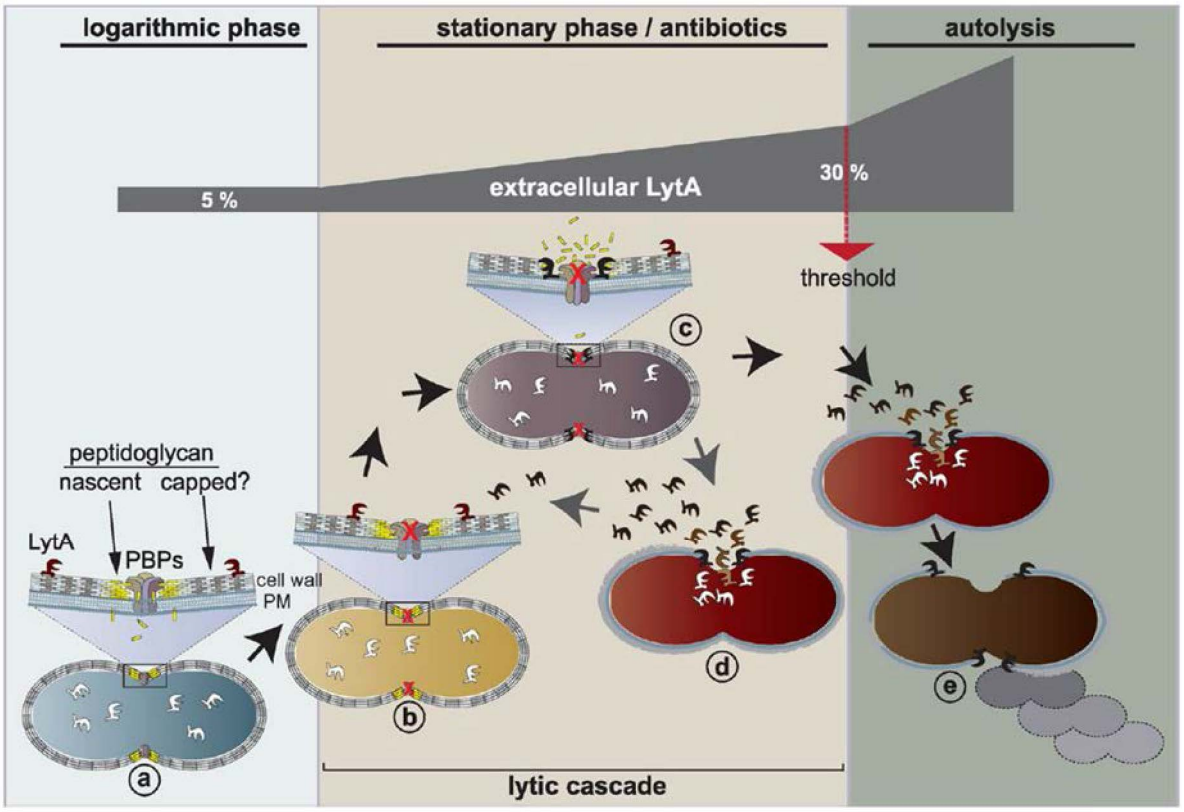


**Figure 7: Model of the mode of action of LytA during pneumococcus growth, from (Mellroth, *et al.*, 2012). Cytoplasmic LytA is released through lysis and can access peptidoglycan when its synthesis is stopped (in stationary phase or in the presence of peptidoglycan-targeting antibiotics). More than 30 % of LytA in the medium results in extensive lysis of the bacteria contained in the culture.**

The pneumococcus is a commensal of the human nasopharyngeal flora. However, it can initiate a variety of non-invasive diseases (sinusitis and otitis media), or more severe invasive diseases (pneumonia, septicemia and meningitis). According to a 2005 estimate of the world health organization (WHO), 1.6 million people die of pneumococcal diseases in the world each year. The most at risk populations are people with a weak immune system. The elderly and the youth are especially vulnerable. 700,000 to 1 million children under five years old die of pneumococcal infections every year worldwide: (WHO – http://www.who.int/ith/diseases/pneumococcal/en/). Immuno-compromised patients are also at risk (with AIDS, for example).

*S. pneumoniae* cells present in the upper respiratory tract are transmitted to another person in droplets of respiratory secretions (*eg*: saliva or mucus). They will first establish in the nasopharynx from which they are usually cleared. In some cases, they will move to the ear and cause otitis, which is common in children under 5 years old. Invasive diseases result from the propagation of pneumococci to the lungs, the blood stream and the cerebrospinal fluid, the latter case being the most life-threatening (Figure 8).

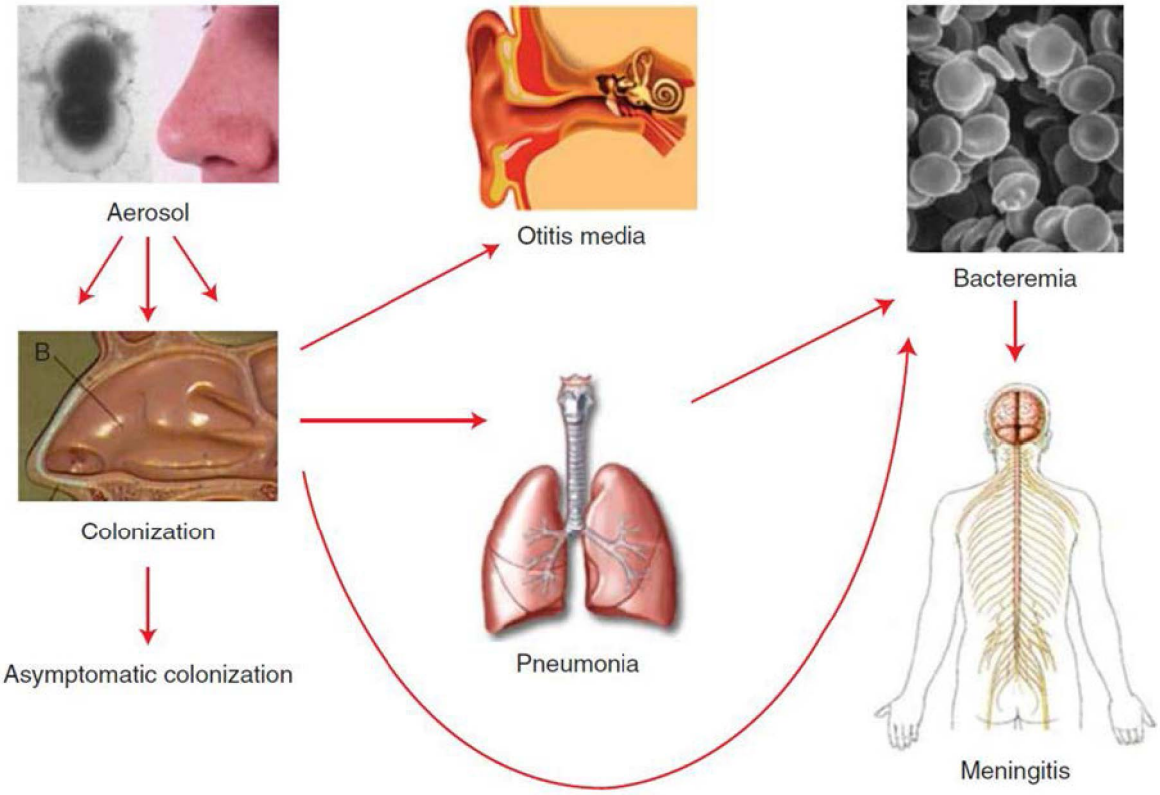


Figure 8: **Pneumococcus pathogenesis (Henriques-Normark & Tuomanen, 2013).**

## Prophylaxis and treatment

### *Vaccines*

The capsular polysaccharides protect the pneumococcus from phagocytosis. Nevertheless, opsonization of *S. pneumoniae* cells by antibodies directed against the capsule results in recognition by the host phagocytes and elimination of the pathogen. Several vaccines against pneumococcal infections have been developed based on this principle.

The longest lasting pneumococcus vaccine is on the market since 1983. The Pneumovax®23 (Merck) consists of a mixture of purified polysaccharides of 23 different serotypes. The use of this vaccine is limited to the adults (mainly the elderly and immunocompromised patients) because of its low immunogenicity in children under 2 years old. Also, it does not prevent pneumococcus carriage without symptoms.

In the year 2000, a vaccine comprised of pneumococcal polysaccharides from 7 serotypes conjugated to a protein carrier was licensed in the United States (PCV7, Prevenar®, Pfizer), and adopted one year later by several European countries. The protein carrier, CRM197™, allows better immunization of the children under 2 years old. Furthermore, the 7 serotypes covered by this

vaccine were dominant in the United States at the time it was developed. As a consequence, the rate of pediatric invasive pneumococcal diseases (IPD) and nasopharyngeal carriage was reduced for the vaccine-targeted serotypes (Pilishvili*, et al.*, 2010). Furthermore, the proportion of IPD in the non-vaccinated population (children too young for vaccination and people above 50 years old) diminished, indicating that the global immunization programs consistently impaired the spread of targeted serotypes.

Unfortunately, the reduced prevalence of PCV7 serogroups left a free ecological niche for others, and they became more and more common. Also, some emerging serotypes, such as 19A, have been associated with increased virulence and antibiotic resistance (McGee, 2007). Another drawback of the PCV7 is that it is not as efficient in preventing pneumonia or acute otitis media as bacteremia.

Therefore, additional conjugated vaccines were developed, covering more serotypes: 10- and 13-valent vaccines for example. The later, PCV13, Prevenar® (Pfizer) has replaced the PCV7 in the French vaccination program in 2010. It led to a decreased prevalence of the serogroups 19A, 7F and 1 (Varon*, et al.*, 2013).

PCVs are expensive due to complex development and production that limit their use in developing countries where the burden of pneumococcal infections is the most substantial. Also, as polysaccharide vaccines, PCVs target limited sets of serotypes and replacement has been observed. Moreover, serotype distribution is area dependent, and the efficacy of the existing vaccines depends on the country. For example, the PCV7 covered 70 to 88 % of the serogroups found in children from the United States, Canada, Africa and Europe at the time of its development, while it covered less than 65 % of the serotypes causing IPD in Asia and South America (Hausdorff*, et al.*, 2000).

An affordable vaccine with a target independent of the capsular layer would be ideal, but several approaches are considered (Moffitt & Malley, 2011). Briefly, the adaptation of conjugate vaccines to serotypes prevalent in low-income countries is envisaged in China. Also, the development of polysaccharides associated to a conserved pneumococcus protein carrier could have a better efficacy. Another promising approach would be to develop a vaccine that targets proteins conserved among the different pneumococcal serogroups. Several of those proteins have been studied and tested in clinical trials, some of them giving encouraging results. A combination of those proteins may provide robust and serotype-independent protection to pneumococcal infections. Finally, a very low-cost and promising strategy is the use of whole pneumococcal killed cells as a vaccine, with the advantage of presenting many antigens at once. Recently, this strategy was shown

to protect mice from pneumococcal infections to a similar extent as currently used polysaccharide vaccines, in a serotype-independent manner (Xu*, et al.*, 2014).

### *Antibiotics*

The first antimicrobial used to treat pneumococcus infections appeared in the early forties with the development of sulfonamide drugs (Whitby, 1938). However, a pneumococcus resistant to sulfonamide was rapidly found in a patient (Tillett*, et al.*, 1943). This isolate, however, was sensitive to another antimicrobial compound first described in 1929: the penicillin (Fleming, 1929). Penicillin was then intensively and successfully used to fight various bacterial infections (Keefer, 1943), (Tillett*, et al.*, 1944). However, the extensive use of antibiotics was followed by the emergence of resistant pneumococcus strains, first reported in 1967 (Hansman, 1967). Multi-resistant strains were reported half a century after the introduction of antibiotics in healthcare (Appelbaum*, et al.*, 1977). Recently, extensively drug-resistant pneumococci have emerged (Kang*, et al.*, 2012). These strains resist to at least one antibiotic in all classes, except vancomycin and linezolid.

Nowadays, pneumococcal infections are treated with antibiotics. In the case of invasive diseases, the treatment should be initiated quickly to limit the progression of the infection. In France, if a bacterial infection is suspected in the case of otitis media, meningitis or pneumonia, the first antibiotic treatment is usually assuming pneumococcal infections as for those diseases, it is the most probable etiologic agent. Guidelines are provided by the heath products and medicine safety national agency (ANSM, in French) for the choice of treatment of the different diseases. The following paragraphs sum up the major treatments utilized in France against infections that can be cause by *S. pneumoniae* (from (Brisou*, et al.*, 2004)).

Community-acquired pneumopathies are mostly treated with amoxicillin, a bacteriolytic β-lactam with good absorption properties (oral administration). If there is no sign of improvement after 2 – 3 days, recommendation should be asked to a specialist or at the hospital. A better-adapted treatment can be another β-lactam or antibiotics of a different class in the case of β-lactam-resistant pneumococcus strain, or β-lactam allergy.

In the case of meningitis, the patient should be immediately hospitalized and a lumbar puncture (cerebrospinal fluid sampling) will be performed to determine the etiology of the disease. Depending on the age, the gravity of the infection and the probability that the meningitis is caused by the pneumococcus, different antibiotic treatments are recommended, including cefotaxime, ceftriaxone, amoxicillin (β-lactams) and / or vancomycin (a glycopeptide). The treatment is then adapted by considering the results of the lumbar puncture. No codified recommendations exist and

the best-suited treatment is usually determined by consultation of the medical doctor, the pharmacist and the microbiologist.

Acute otitis media are also treated on a different manner depending on the age. Before 2 years old, antibiotic therapies are systematic while it is recommended only in the case of strong symptoms after 2 years old. The antibiotics utilized in acute otitis media treatment are β-lactam including amoxicillin, cefuroxime and cefpodoxime, or macrolide (erythromycin) in the case of β-lactam allergies. β-Lactamase inhibitors are associated to these β-lactam antibiotics because *Haemophilus influenzae* is common in young children. This organism produces β-lactamases that inactivate the β-lactams. Again, the treatment should be evaluated 2 – 3 days after initiation. If it is not efficient, the etiology of the infection should be determined and the treatment adapted.

## Epidemiology

The world-wide spread of pneumococcus strains is facilitated by two properties of the organism. First, most people naturally carry this pathogen at least once in their lifetime (Center for Disease Control, CDC – http://www.cdc.gov/pneumococcal/about/risk-transmission.html). Second, transmission by direct contact with respiratory secretions of carrier persons allows it to quickly propagate through the population. Despite its global repartition, the mortality rate does not correlate with the incidence rate in several countries, due to distinct policies in terms of prevention or accessibility to the treatment (Figure 9).

In developing countries, the young children constitute the most at-risk population because of low access to adapted treatments and bad living conditions. By contrast in developed countries, the elderly and immunocompromised persons are most at-risk. However, pneumococcus diseases also occur in persons recovering from influenza, cigarette smokers or alcohol abusers, for example (Grau*, et al.*, 2014).

In France, the Pneumococcus Reference National Center (CNRP, in French) is in charge of the surveillance of pneumococcus infections and pneumococcus antibiotics resistance. It relies on 23 Regional Pneumococcus Observatories (ORP, in French) that collect data in about 500 healthcare centers. A yearly activity report summarizes the epidemiology of the pneumococcus of the previous year (Varon*, et al.*, 2013).

In 2012, 993 strains were collected by the CNRP and serotyped. The prevalence of each serotype was determined and compared to that defined in previous years since 2001. The prevalence differs in distinct age groups and sampling types. We will focus herein on the global results of IPDs in the population (meningitis and bacteremia). In 2012, the serotype 12F was predominant, followed by the serotypes 19A, 3, 7F and 1 (Varon*, et al.*, 2013). In 2001, the most prevalent serogroups were the 14, 19A, 23F, 6B, 19F and 3 (1968 isolates). From those, the PCV7

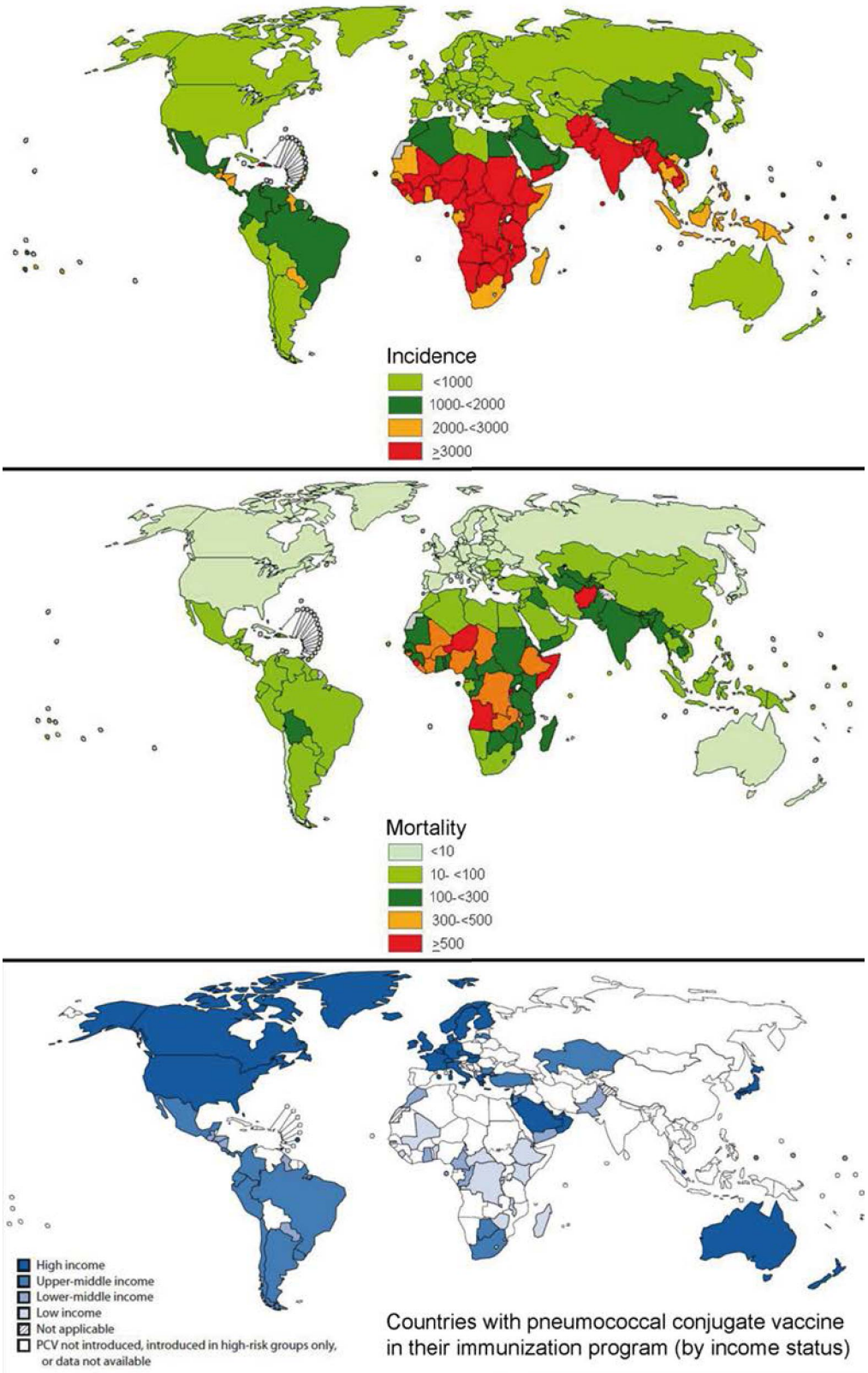


**Figure 9: Top 2 panels. Pneumococcus incidence and mortality rates in children (< 5 years old) in 2000. Legend is in number of case per 100,000 children. Adapted from the WHO slides available on the web: http://www.who.int/immunization/monitoring_surveillance/burden/estimates/Pneumo_hib_2000/en/index2.html). Lower panel: Countries that include pneumococcal conjugate vaccines in their national immunization programs, by incoming status. Adapted from (CDC, 2013).**

vaccine (which was introduced in 2003 in the French immunization program) covers the serotypes 14, 23F, 6B and 19F, which were not the most prevalent strains anymore in 2012. The replacement of PCV7 by PCV13 in June 2010 in the French vaccination program did not result yet in the removal serogroups 19A, 3, 7F and 1 from the most prevalent serotypes in 2012. However, this is probably a matter of time, as they all showed a drastic prevalence decrease since the records of 2009, except for serotype 3 (Varon*, et al.*, 2013).

The proportion of antibiotic resistance in pneumococcal invasive diseases dramatically increased in the eighties and nineties in France. However, the efforts of the health ministry in the prevention of abusive use of antibiotics and the introduction of the PCV7 and the PCV13 in the French immunization program have inverted the tendency. At its maximum, in 2002, the proportion of pneumococci with diminished susceptibility to penicillin reached the frightening value of 53 % of the investigated invasive disease pneumococcal clinical isolates. In 2012, it had diminished to 22 % and continuous efforts will hopefully bring resistance proportion back to reasonable level (Figure 10).

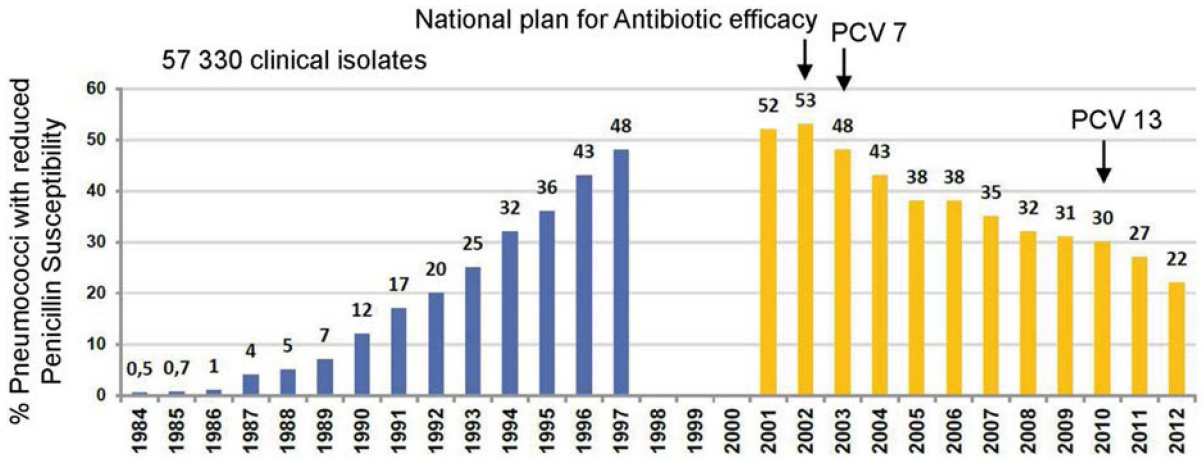


**Figure 10: Evolution of penicillin resistance in pneumococcal clinical isolates in France. Adapted from (Varon*, et al.*, 2013).**

## Concluding remarks

*S. pneumoniae* is of significant scientific and medical importance. It is an ideal Gram-positive model organism for several reasons. First, the pneumococcus has allowed to identify DNA as the molecule encoding the characteristics of living organisms. Many physiological processes have been discovered on the pneumococcus, comprising competence, autolysis and quorum sensing. Furthermore, the first Gram-positive genome sequence to be determined was that of the pneumococcus. Concerning medical interests, it allowed the development of polysaccharide vaccines, and revealed many aspects of the mechanisms of resistance against antibiotics. Also,

general characteristics of the Gram-positive bacterial pathogenesis have been understood thanks to studies on the pneumococcus.

For these reasons, one can reasonably claim that further investigations on this organism will answer many of the lasting questions on the microbial physiology and the pathogenesis of Gram-positive bacteria. Also, pneumococcal research efforts will participate in the fight against bacterial infections that are in constant evolution, as evidenced in *S. pneumoniae*.

## Le peptidoglycane du pneumocoque – résumé

Le peptidoglycane est le constituant majeur de la paroi et est une structure essentielle et très conservée dans le règne des bactéries. Cette molécule géante forme un sacculus qui entoure complètement la cellule. Cette structure permet à la bactérie de conserver son intégralité face à la pression osmotique et sert d'ancrage à plusieurs molécules de surface. Enfin, le peptidoglycane procure sa forme à la bactérie, ce qui a son importance car la forme d'une bactérie lui confère des avantages spécifiques à certains environnements. L'essentialité et la position du peptidoglycane à la surface de la cellule bactérienne en font la cible d'antibiotiques.

Le peptidoglycane est composé de chaines oligosaccharidiques réticulées par des ponts peptidiques. Ces chaînes glycanes sont formées d'une succession d'unités disaccharidiques constituées d'un résidu *N*-acetylglucosamine (NAG) liés à un acide *N*-acetylmuramique (NAM) par une liaison osidique β1→4. Dans le peptidoglycane naissant, les résidus NAM sont décorés du pentapeptide L-Ala-γ-D-iso-Gln-L-Lys-D-Ala-D-Ala. Ces pentapeptides sont utilisés pour la formation de liaisons entre les chaînes glycanes, constituant à terme le sacculus. Chez le pneumocoque, il est admis que les chaînes glycanes sont parallèles à la membrane plasmique, insérées de manière perpendiculaire à l'axe le plus long de la cellule.

La composition du peptidoglycane diffère entre espèces de bactéries, ce qui leur donne des propriétés différentes. Chez le pneumocoque, une caractéristique intéressante est la présence de peptides branchés dans le peptidoglycane. Il s'agit de dipeptides (L-Ser-L-Ala ou L-Ala-L-Ala) liés à la lysine en position 3 du pentapeptide, qui peuvent aussi être impliqués dans les ponts peptidiques entre chaînes glycanes. Ces peptides branchés sont plus abondants chez les souches cliniques résistantes aux antibiotiques, bien qu'on ne comprenne pas encore clairement pourquoi. D'autres modifications rencontrées chez le pneumocoque sont la dé-acétylation des NAG ou la O-acétylation des NAM, qui procurent la résistance au lysozyme.

La synthèse du peptidoglycane est une suite de réactions enzymatiques commençant dans le cytoplasme et finissant à l'extérieur de la cellule après transfert du précurseur à travers la membrane plasmique. Le lipide II est le précurseur du peptidoglycane synthétisé dans le cytoplasme de la cellule. Il s'agit de la sous-unité dissaccharide-pentapeptide NAG-NAM-L-Ala-D-(γ)Gln-L-Lys-D-Ala-D-Ala ancrée à la membrane plasmique par un undécaprényl-pyrophosphate lié au sucre NAM. La synthèse du lipide II est catalysée à partir d'un résidu NAG par l'intermédiaire de 8 enzymes Mur (MurA, B, D, D, E, F, G et T), MraY et GatD. Ensuite, le lipide II est transféré à travers la membrane par une « flippase » et la sous-unité dissaccharide-pentapeptide est utilisée pour l'assemblage du sacculus. Les protéines liant la pénicilline (PLPs, PBPs en anglais) sont responsables de l'activité glycosyl-transférase permettant l'élongation des chaînes glycanes et de l'activité transpeptidase

permettant leur réticulation. Ces activités sont complétées d'une activité « hydrolase », qui permet l'« ouverture » du sacculus requise pour l'insertion de nouveau matériel. Les modifications observées dans la composition du peptidoglycane sont effectuées à l'intérieur (ajout de dipeptides au pentapeptides par MurM et MurN) ou à l'extérieur de la cellule (dé-acétylation des résidus NAG par PgdA, O-acétylation des résidus NAM par Adr, raccourcissement du pentapeptide par PBP3 et LdcB).

Les différentes protéines impliquées dans la synthèse et les modifications du peptidoglycane chez le pneumocoque sont détaillées dans cette partie.

## Pneumococcus peptidoglycan

The peptidoglycan is the major component of the cell wall, and is extensively conserved in the bacterial kingdom (Liechti*, et al.*, 2014). It consists of a giant single molecule, the sacculus, which encases the plasma membrane of the bacterium. In Gram-negative bacteria the peptidoglycan is found in the periplasm between the plasma membrane and the outer membrane. The peptidoglycan is required by bacterial cells to maintain their integrity under the turgor pressure. This stress is imposed by the osmotic flow of water from the external environment to the cytoplasm induced by the difference of concentration of solutes in these compartments. The peptidoglycan also serves as a scaffold for several surface molecules, including proteins (*eg.* the pneumococcus pilus), wall teichoic acids and the capsular polysaccharides. The peptidoglycan is also involved in the interaction with the host in that peptidoglycan fragments are recognized by the immune system (Boneca, 2005). Finally, the peptidoglycan architecture determines the bacterial shape, and isolated sacculi retain the cell shape, even after elimination of all the other components of the cell. This feature is important because the shape confers specific advantages to the cell that can be essential in some environments (Young, 2006).

Given its essentiality and its localization at the surface of bacterial cells, peptidoglycan is the target of some antibiotics, reviewed in the last part of the introduction. In the present part, I intend to describe the peptidoglycan of the pneumococcus, in terms of chemical composition, architecture, and how it is synthesized and modified.

### Pneumococcus peptidoglycan composition

The peptidoglycan is a mesh of glycan strands cross-linked by short peptides (Vollmer*, et al.*, 2008). The glycan strands are comprised of a succession of alternating *N*-acetylmuramic acid (Mur*N*Ac) and *N*-acetylglucosamine (Glc*N*Ac) residues linked by β1 → 4 bonds. The Mur*N*ac residues are decorated with a peptide in substitution of the D-lactoyl group. In newly-synthesized pneumococcus peptidoglycan, this pentapeptide has the following composition: L-Ala-γ-D-iso-Gln-L-Lys-D-Ala-D-Ala (Bui*, et al.*, 2012). During peptidoglycan synthesis, the pentapeptides are used by DD-transpeptidases to covalently link adjacent glycan chains, resulting mostly in dimeric, but also in trimeric or tetrameric structures that attach 2, 3 or 4 glycan strands together, respectively. As a consequence, the peptidoglycan constitutes a giant mesh-like molecule that surrounds the entire cell. The presence of D-amino-acids in the composition of the peptidoglycan is probably not a random fact, as they confer this essential structure with resistance against most known proteases.

In *S. pneumoniae*, the peptidoglycan contains numerous variations (Figure 11). First, the monomers (term used to designate the peptides that are not part of cross-links) are mostly tripeptides, cumulated tetra- and pentapeptides representing only 20% of the total monomers (Bui*, et al.*, 2012), (Table I).

The glutamate in second position of the peptide is mostly amidated in the pneumococcus and in other Gram-positives species (*eg. Staphylococcus aureus*). This was recently shown to be required for the transpeptidation activity (Zapun*, et al.*, 2013). Furthermore, it is linked to the resistance against both β-lactam antibiotics and lysozyme digestion of the peptidoglycan (Figueiredo*, et al.*, 2014).

The peptide bridges (Figure 11) can be found with the following combinations: tetra-tri-, tetra-tetra- or tetra-pentapeptides, as the linkage is between the L-Lys and the first D-Ala residues of the peptides requiring at list a tetrapeptide and a tripeptide.

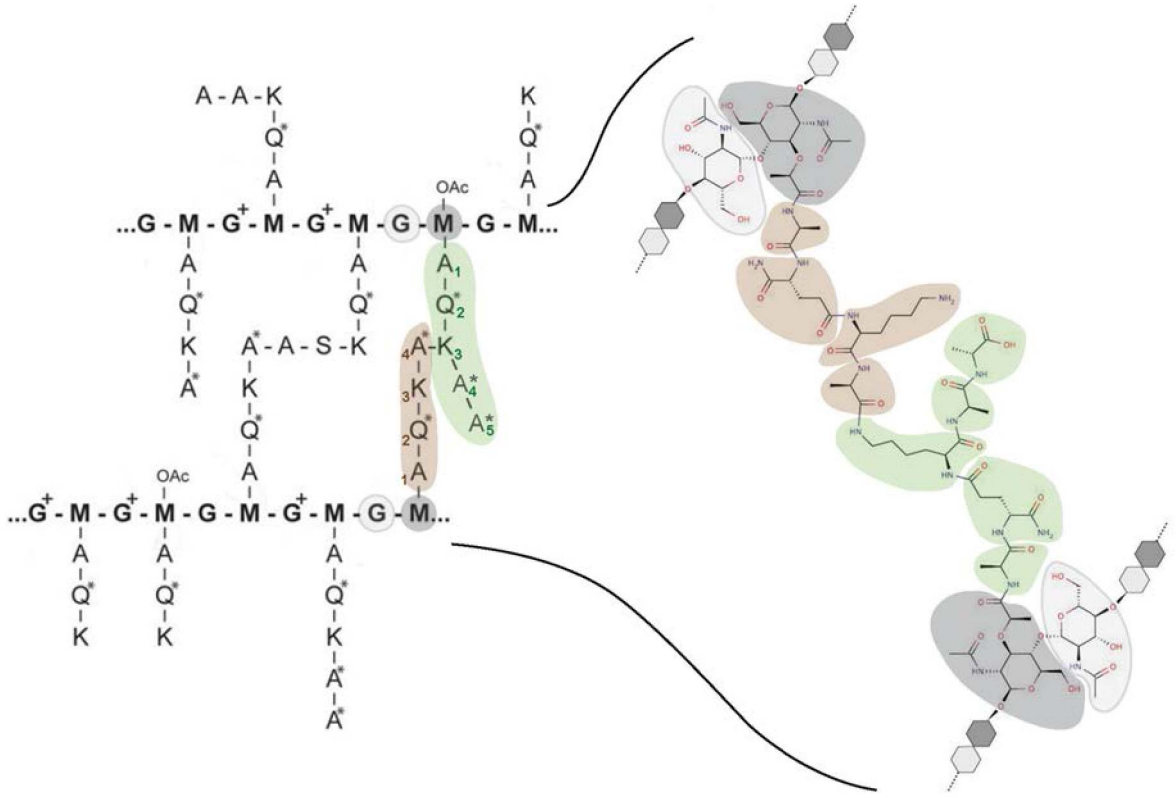


**Figure 11: Representation of the chemical variations found in the peptidoglycan of pneumococcus, and detail of a tetra-pentapeptide cross-link. M and G stand for Mur*N*ac (dark grey) and Glc*N*ac (light grey), respectively. A, Q and K represent alanine, isoglutamine and lysine residues, respectively (the amino-acids in D- configuration are designed by an asterisk *). G+ stand for Glc*N*, OAc-M are O-acetylated Mur*N*ac residues. Adapted from (Bui*, et al.*, 2012) and (Zapun*, et al.*, 2013).**

Another common variation found in pneumococcal peptidoglycan is the presence of "branched peptides", which are peptides containing two amino-acids (L-Ser-L-Ala or L-Ala-L-Ala) bound to the ε-amino group of the L-Lys in position 3. Interestingly, these branched peptides are more abundant in penicillin-resistant clinical isolates. In the study of 20 pneumococcal clinical isolates, Garcia-Bustos and Tomasz found < 30% of branched peptides in penicillin-susceptible pneumococci, while penicillin-resistant isolates had > 70 % of branched peptides (Garcia-Bustos & Tomasz, 1990). Of note is that the R6 laboratory strain has a slightly higher proportion of branched peptides than the clinical isolates studied by Garcia-Bustos and Tomasz. Globally, 45% of the peptides are branched in the R6 strain, and the cross-links between glycan chains are comprised of > 90% of branched peptides (Bui*, et al.*, 2012). This suggests that globally, branched peptides are

**Table I: The muropeptides of *S. pneumoniae* (R6 strain). n.d.: not detected, [a]: percentage in the mono-, di- or trimmers. (Bui*, et al.*, 2012)**

| Monomers/ oligomers (% of total) | Muropeptide or modification | Relative percentage[a] (%) |
|---|---|---|
| Monomers (35.9) | Tri | 79.9 |
| | Tetra | 11.8 |
| | Penta | 8.4 |
| | Unmodified | 43.7 |
| | Deacetylated | 18.5 |
| | Glutamate | 12.6 |
| | Deacetylated/glutamate | 5.0 |
| | O-Acetylated | n.d. |
| | -GlcNAc | 0.3 |
| | -GlcNAc-MurNAc | n.d. |
| | Ala-Ala | 8.1 |
| | Ser-Ala | 29.7 |
| Dimers (25.9) | TetraTri | 100.0 |
| | Unmodified | 19.0 |
| | Deacetylated | 45.1 |
| | Glutamate | 1.8 |
| | Deacetylated/glutamate | 1.8 |
| | O-Acetylated | n.d. |
| | Missing GlcNAc | n.d. |
| | Missing (GlcNAc-MurNAc) | n.d. |
| | Ala-Ala | 18.5 |
| | Ser-Ala | 74.8 |
| Trimers (9.6) | TetraTetraTri | 97.9 |
| | TetraTetraTetra | 2.1 |
| | Unmodified | 2.1 |
| | Deacetylated | 14.2 |
| | Glutamate | n.d. |
| | Deacetylated/glutamate | n.d. |
| | O-Acetylated | 8.1 |
| | Missing GlcNAc | 11.9 |
| | Missing (GlcNAc-MurNAc) | 8.1 |
| | Ala-Ala | 31.7 |
| | Ser-Ala | 45.6 |

preferred than linear peptides for transpeptidation.

The glycan chains also undergo secondary modifications. In the pneumococcus, 80% of the Glc*N*ac and 10% of the Mur*N*Ac residues are de-acetylated (Vollmer & Tomasz, 2000). Also, some Mur*N*Ac residues are O-acetylated.

The peptidoglycan composition of the R6 strain was investigated in-depth (Bui*, et al.*, 2012). First, specific digestion of purified peptidoglycan by cellosyl generated the muropeptides, the subunits of the peptidoglycan (Glc*N*Ac-Mur*N*ac-peptide). Thereafter, the muropeptides of different composition were separated by high-performance liquid chromatography (HPLC) and analyzed on-line by electrospray mass spectrometry, revealing a big heterogeneity in the composition of the peptidoglycan of *S. pneumoniae* (Table I). The variations observed in muropeptides were different in monomers, dimers and trimmers. Indeed, glutamate was virtually exclusively found in monomers, suggesting the fact that a glutamine is required for transpeptidation (Zapun*, et al.*, 2013). Also, Glc*N*Ac residues were often deacetylated in dimers (45 %) whereas deacetylation was found in less than 20 % of monomers and trimers. Finally, the branched peptides were most abundant in dimers and trimers, suggesting that they are preferred for transpeptidation.

## Architecture

In the early 2000s, cell wall architecture was investigated using computational methods. In Gram-positive bacteria with a thick cell wall, a scaffold model was proposed in which glycan strands are directed perpendicularly from the plasma membrane. The scaffold model fitted the experimentally available data of that time, including the length of glycan chains and the proportion of peptide cross-links (Dmitriev*, et al.*, 2003). This contrasted with the "classical" model of peptidoglycan architecture in which glycan strands are parallel to the plasma membrane (Holtje, 1998). With the advance of methodology, peptidoglycan architecture has been recently investigated experimentally in ovoid bacteria (*Lactococcus lactis*, *Enterococcus faecalis* and *S. pneumoniae*) by atomic force microscopy. It now appears that glycan strands are organized along the short axis of the cell, parallel to the plasma membrane (Andre*, et al.*, 2010), (Wheeler*, et al.*, 2011) (Figure 12).

The orientation is the same at the periphery and at the septum, suggesting that peptidoglycan insertion is organized similarly in both zones. Interestingly, the glycan chains of the three ovoid species have similar length to those of *Bacillus subtilis*, longer than in *S. aureus*. Indeed half of the glycan strands are longer than 50 disaccharides whereas most are 5- to 10-unit long in *S. aureus* (Wheeler*, et al.*, 2011). Also, similarly to *B. subtilis*, a lateral peptidoglycan band pattern was

observed in ovoid bacteria, which again contrasts with the "knobbles" observed in *S. aureus*, suggesting a different architecture between the true cocci and the slightly elongated "ovococci".

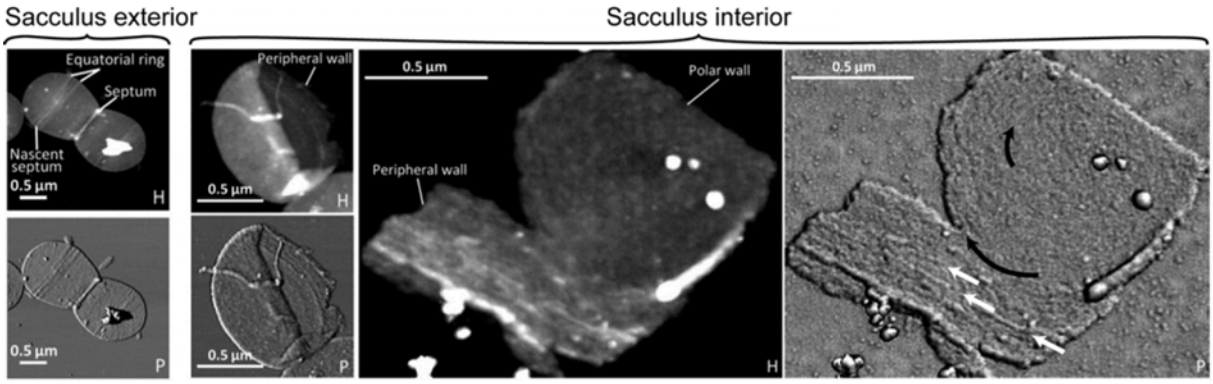


**Figure 12: Atomic Force Microscopy height (H) and phase (P) images of pneumococcus sacculi. Glycan strands are organized in the direction of the short axis of the cell, both in peripheral and polar wall (right panel: white and black arrows, respectively). Adapted from (Wheeler, *et al.*, 2011).**

## Peptidoglycan Biosynthesis

For cellular growth, new peptidoglycan has to be synthesized and incorporated in the sacculus. First, peptidoglycan synthesis involves cytoplasmic steps to assemble its precursor, the lipid II. The lipid II consists of a disaccharide pentapeptide (Glc*N*ac-Mur*N*Ac-L-Ala-D-(γ)Gln-L-Lys-D-Ala-D-Ala) anchored to the plasma membrane through an undecaprenyl-pyrophosphate bound to the Mur*N*Ac residue. In the pneumococcus, eight Mur proteins (MurA, B, C, D, E, F, G, T), MraY and GatD are involved in the synthesis and modification of the lipid II on the inner side of the plasma membrane. Then, lipid II is flipped across the membrane. This is thought to be performed by two proteins in the pneumococcus, RodA and FtsW (Mohammadi, *et al.*, 2011), although another candidate (MurJ) has been proposed as the bacterial flippase (Sham, *et al.*, 2014). Thereafter, the assembly of the peptidoglycan outside the cell requires two activities. The glycosyltransferase activity (GT) polymerizes the precursors to form glycan strands decorated with pentapeptides. The transpeptidase activity (TP) is responsible for the formation of peptide bridges that attach the glycan strands together. In *S. pneumoniae*, five PBPs are in charge of the TP and GT activities: the class A **PBP1a**, **PBP1b** and **PBP2a** have both activities whereas the class B **PBP2b** and **PBP2x** only perform transpeptidation. Those cytoplasmic, membrane-associated and external steps permit the incorporation of nascent peptidoglycan strands in the sacculus (Figure 13**Erreur ! Source du renvoi introuvable.**).

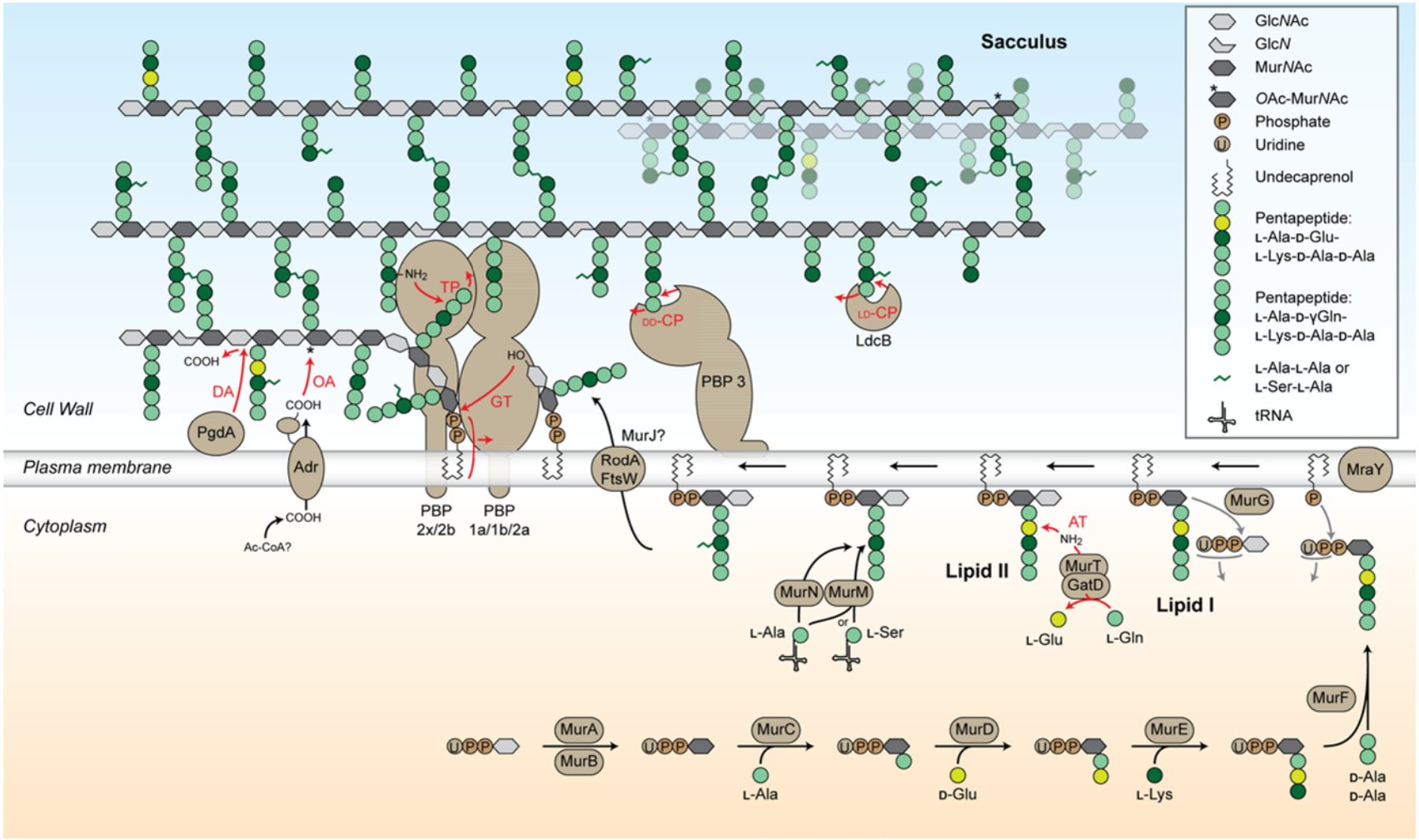


**Figure 13: Peptidoglycan synthesis and maturation in *S. pneumoniae*. The lipid II precursor is synthesized in the cytoplasm, flipped across the plasma membrane, and incorporated in the sacculus outside the cell. The glycan chains and stem peptides are modified at different stages. In red: AT: amidotransferase activity, GT: glycosyltransferase activity, TP: transpeptidase activity, CP: carboxypeptidase activity, DA: deacetylation, OA: O-acetylation. Note that the proteins are not represented to scale. The modifications in the sacculus are in the proportions found in pneumococcus peptidoglycan (Table I Erreur ! Source du renvoi introuvable.).**

An additional peptidoglycan degradation activity often referred to as “hydrolysis” is also required for growth (Vollmer, 2012). Indeed, “opening” the peptidoglycan mesh is a first step to incorporate new material and hydrolysis also acts in peptidoglycan maturation. The details of this activity are not fully known, even if a set of proteins, the “hydrolases”, have been described in the pneumococcus and other organisms. As hydrolysis is not crucial for understanding this thesis, it will not be reviewed herein.

### *Cytoplasmic steps: synthesis of the lipid II*

The cytoplasmic steps of peptidoglycan synthesis result in lipid II. First, uridine diphosphate Mur*N*Ac (UDP-Mur*N*Ac) is generated from UDP-Glc*N*Ac by the action of MurA and MurB (Skarzynski*, et al.*, 1996), (Benson*, et al.*, 1993). Thereafter, several amino-acids are added sequentially to the UDP-Mur*N*Ac residue by ATP-dependent ligases. MurC adds an L-Ala to UDP-Mur*N*Ac (position 1), followed by the ligation of a D-Glu (position 2), a L-Lys (position 3) and two D-Ala (position 4 and 5) by MurD, MurE and MurF, respectively (Bertrand*, et al.*, 1997), (Patin*, et al.*, 2010).

The next steps enable the association of the Mur*N*Ac-pentapeptide to the plasma membrane. It consists of the transfer of this residue to an undecaprenyl phosphate by the activity of the membrane-spanning transferase MraY, resulting in the lipid I (undecaprenyl-pyrophosphoryl-Mur*N*Ac-pentapeptide) (Chung*, et al.*, 2013). This step is followed by the addition of a Glc*N*Ac moiety to the lipid I from UDP-Glc*N*Ac, yielding lipid II (undecaprenyl-pyrophosphoryl-MurNAc-(pentapeptide)-GlcNAc), a reaction catalyzed by MurG (Hu*, et al.*, 2003).

The last cytoplasmic membrane-associated step of peptidoglycan biosynthesis in the pneumococcus consists of the amidation of the D-Glu in position 2 of the pentapeptide. As in *S. aureus* (Munch*, et al.*, 2012), (Figueiredo*, et al.*, 2012), a stable complex of the glutaminase GatD and the ligase MurT constitutes the amidotransferase that amidates most of the D-Glu to D-iso-Gln in the pneumococcus (Zapun*, et al.*, 2013). Amidated peptidoglycan is found in several Gram-positive bacterial pathogen including *Mycobacterium tuberculosis*, *S. pneumonia* and *Clostridium perfringens*. As it results in a less charged peptidoglycan (loss of a COO-), this modification was proposed to provide resistance to defensins and to play a general role in evasion of the immune system (Munch*, et al.*, 2012). Also, lack of amidation in *S. aureus* impaired growth and β-lactam and lysozyme resistance (Figueiredo*, et al.*, 2012). In the pneumococcus, the D-isoGln is required for the TP activity and is therefore essential for growth (Zapun*, et al.*, 2013). For these reasons, the Murt-GatD complex could be a promising therapeutic target.

A variation in the peptide cross-links of the pneumococcus peptidoglycan is referred-to as "branched" peptides. Branched peptides are peptidoglycan stem peptides harboring a di-peptide (L-Ser-L-Ala or L-Ala-L-Ala) bound on the ε-amino group of the L-Lys in position 3. The first amino-acid (a L-Ser or a L-Ala) is added by the action of MurM on the lipid II precursor on the cytoplasmic side of the membrane, the second (invariably a L-Ala) is then added by MurN (Filipe*, et al.*, 2000). MurM and MurN are seryl- or analyl-tRNA ligases as they use Ser-tRNA and / or Ala-tRNA as source of amino acids for the reaction (Lloyd*, et al.*, 2008). Inactivating the *murMN* operon totally eliminates the branched peptides from the peptidoglycan composition, which confirms their activity *in vivo* (Filipe & Tomasz, 2000). Although not all stem peptides are branched, at least half of them are, and almost no peptide bridges involve linear peptides in a strain with *murMN* (Table I).

### *Flipping the lipid II across the plasma membrane: the flippases*

Once the lipid II has been synthesized, it is to be flipped across the plasma membrane to allow the assembly of peptidoglycan outside the cell. This requires the activity of "flippases", some integral membrane proteins that belong to the SEDS family (for shape, elongation, division, and sporulation) (Ikeda*, et al.*, 1989), (Mohammadi*, et al.*, 2011), (Sieger*, et al.*, 2013). In the pneumococcus, two SEDS have been described, RodA and FtsW, the activity of the second being confirmed by a biochemical *in vitro* test (Mohammadi*, et al.*, 2011). FtsW is essential in the pneumococcus (Gerard*, et al.*, 2002) and RodA was suggested to be so (unpublished results mentioned in (Land & Winkler, 2011)).

The flippase activity of FtsW from *Escherichia coli* was recently investigated in details (Mohammadi*, et al.*, 2014). It was shown to require two charged amino-acids of the trans-membrane helix 4 (FtsW has 10 trans-membrane domains (Gerard*, et al.*, 2002)) that allow the lipid II to be translocated through a size-restricted pore formed by the protein in the plasma membrane. Note that the identity of the flippase remains controversial as another protein has been proposed to fulfill that role (MurJ) (Sham*, et al.*, 2014).

### *Extra-cellular steps: elongation and cross-linking of the glycan chains*

Once displayed on the outside of the plasma membrane, the lipid II is used as the substrate of the high molecular mass Penicillin-Binding Proteins (the PBPs). These membrane proteins have a short N-terminal cytoplasmic tail, a transmembrane segment and one (class B) or two (class A) enzymatic domains exposed on the outer surface of the plasma membrane (Goffin & Ghuysen, 1998). The class A PBPs catalyze both the elongation of the uncross-linked peptidoglycan chains by

their GT activity and the cross-linking of glycan strands by TP activity. In contrast, the class B PBPs only have the TP activity (Sauvage, *et al.*, 2008).

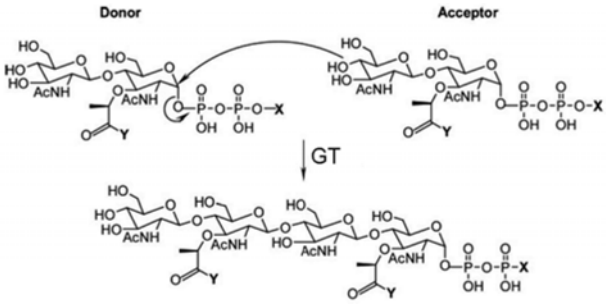


**Figure 14: GT reaction. The lipid II acceptor attacks the glycan strand donor, which releases its membrane anchor in the reaction. X: undecaprenol, Y: pentapeptide. Adapted from (Fraipont, *et al.*, 2006).**

In peptidoglycan synthesis, the GT reaction consists of the addition of a disaccharide pentapeptide to the reducing end of a glycan strand (Fraipont, *et al.*, 2006), (Perlstein, *et al.*, 2007). More especially, a glycan strand linked to the membrane by an undecaprenyl pyrophosphate is the donor. In the reaction, it is transferred to the hydroxyl in position 4 of the Glc*N*Ac moiety of a lipid II acceptor (Figure 14).

The GT domain of class A PBPs is associated to the membrane, independently of the membrane-spanning segment of the protein (di Guilmi, *et al.*, 1999). This may provide proximity between the GT active site and the lipid II precursors to facilitate the extension of glycan strands by the use of the lipid-anchored precursor. Moenomycin is the main transglycosylase inhibiting antibiotic, but it is not used for treatment because of its limiting pharmacokinetic properties (Ostash & Walker, 2005). The GT activity of the 3 *S. pneumoniae* class A PBPs has been extensively studied in the laboratory (Di Guilmi, *et al.*, 2003), (Di Guilmi, *et al.*, 2003), (Helassa, *et al.*, 2012), (Zapun, *et al.*, 2013). The GT reaction can be investigated *in vitro* by adding lipid II to the enzyme in the appropriate buffer, and running the sample on SDS-PAGE (Wang, *et al.*, 2008). This technique enables a quick monitoring of the GT activity providing a visual control of the size of the polymerized glycan chains.

The TP reaction is catalyzed by the penicillin-binding domain of the PBPs. The active site of this domain consists of 3 specific motifs characteristic of the active-site serine penicillin-recognizing enzymes family (ASPRE): SxxK, (S/Y)xN and (K/H)(S/T)G. The TP reaction involves three steps (Sauvage, *et al.*, 2008). First, a noncovalent Henri-Michaelis complex is formed between the enzyme and the pentapeptide. Second, the serine of the SXXK motif attacks the carbonyl of the D-Ala in position 4. This results in the release of the D-Ala in position 5 and the formation of a covalent link between the donor peptide and the PBP, forming an acyl-enzyme complex (acylation step). Eventually, the primary amine of the L-Lys in position 3 of the acceptor strand attacks the carbonyl in the bond linking the D-Ala of the donor strand and the active site of the PBP (deacylation step). Thus, a peptide link is formed between the D-Ala in position 4 of the donor peptide and the L-Lys in position 3 of the acceptor peptide (Figure 15a).

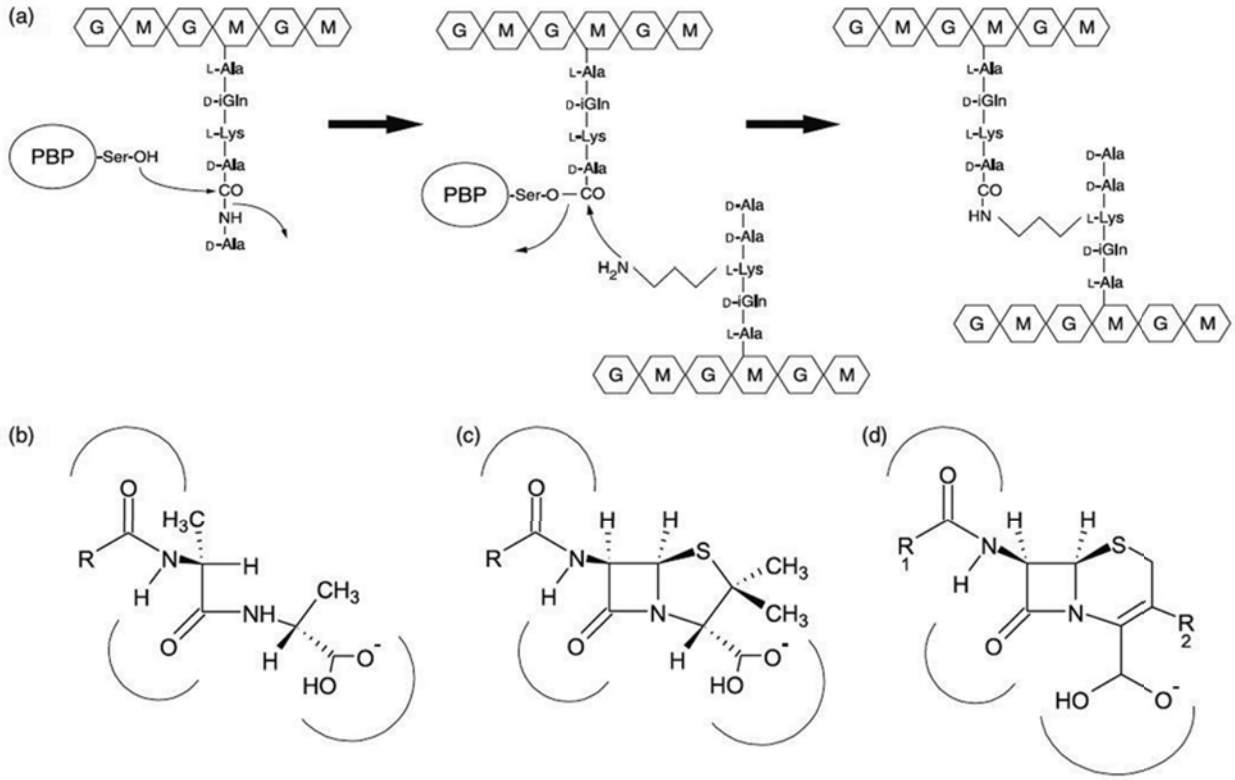


**Figure 15: The TP reaction, its D-Ala-D-Ala substrate and structurally similar inhibitors (Zapun, *et al.*, 2008). (a) In the first step, an ester bond is formed between the active serine of the PBP and the D-Ala in position 4 of the donor peptide stem. This link is then disrupted in the formation of a peptide link between the carbonyl group of the latter residue and the primary amine group of the L-Lys in position 3 of the acceptor stem peptide. G: Glc*N*Ac, M: Mur*N*Ac. (b) *N*-Acyl-D-Ala-D-Ala peptide. (c) Penicillin core structure. (d) Cephalosporin core structure.**

β-Lactam antibiotics such as penicillins and cephalosporins mimic the two D-Ala residues present at the extremity of the pentapeptide (Figure 15b-d). By forming a stable covalent adduct with the active site serine, β-lactams prevent the TP activity and impair cell growth or induce lysis depending on the nature of the β-lactam and its concentration. The transpeptidation and β-lactam inhibition reactions can be sketched as follows:

$$E + I \underset{k_{-1}}{\overset{k_1}{\rightleftharpoons}} EI \xrightarrow{k_2} EI^* \xrightarrow{k_3} E + P$$

E is the enzyme (PBP), I is the substrate (donor stem peptide or β-lactam), EI is the noncovalent Henri-Michaelis complex, EI* is the covalent acyl-enzyme complex, and P is the product (cross-linked stem peptides or inactivated β-lactam). Several kinetic parameters are associated to this reaction. The noncovalent complex EI has the dissociation constant $K_d = k_{-1}/k_1$. The acylation rate corresponds to $k_2$. Finally, $k_3$ represents the rate at which deacylation occurs, which, in the case of β-lactams, corresponds to the hydrolysis of EI* to regenerate the PBP and inactivate the β-lactam. With β-lactams, this rate is negligible on the pneumococcus doubling time-scale, which means that once a PBP is covalently bound to a β-lactam, its activity is irreversibly inhibited. In the TP reaction,

$k_3$ corresponds to the attack by the lysine of the acceptor stem peptide and is significant,which enables enzyme turnover. The details of the TP reaction remain to be determined biochemically.

Studying the TP activity *in vitro* is of importance to explore the biochemical details of the reaction. This is also a key step to understand how PBP variants with low-susceptibility to β-lactams do not react with those antibiotics while they keep reacting with their structurally similar natural substrate. It is only recently that synthesis *in vitro* of the precursor lipid II has been achieved in sufficient quantities for such studies (Schwartz*, et al.*, 2001), (Breukink*, et al.*, 2003). Following this development, several studies reported the *in vitro* reconstitution of TP reactions using purified PBPs from Gram-negative bacteria.

*In vitro* TP activity of purified class A PBPs from *E. coli* has been reported in several studies (*e.g.* (Bertsche*, et al.*, 2005), (Born*, et al.*, 2006), (Typas*, et al.*, 2010)). The TP activity of class B PBPs was reported only once in *E. coli*, but it was shown to co-operate with both GT and TP activities of class A PBPs (Banzhaf*, et al.*, 2012).

Gram-positive peptidoglycan had never been synthesized *in vitro* before the beginning of my thesis. This has been made possible with the discovery of the amidotransferase MurT-GatD complex (Munch*, et al.*, 2012), (Figueiredo*, et al.*, 2012). Indeed, in Gram-positive bacteria such as the pneumococcus, the TP activity requires preliminary amidation of the 2$^{nd}$ residue found on the stem peptide used as a substrate for the reaction. As André Zapun developed an amidation assay of purified lipid II, I could participate in the first experiments that enabled to reconstitute the TP activity of pneumococcus class A and class B PBPs *in vitro* (Zapun*, et al.*, 2013). This will be described later in this manuscript.

## Peptidoglycan Maturation

The peptidoglycan is a highly dynamic structure conferring bacteria with their great capability of resisting chemical, physical and biological challenges. After incorporation in the sacculus, the nascent peptidoglycan undergoes maturation, resulting in the various muropeptides described above (Figure 11, Figure 13).

In pneumococcus, the last D-Ala of the pentapeptide can be trimmed by the DD-carboxypeptidase PBP3 (DacA) (Severin*, et al.*, 1992), (Morlot*, et al.*, 2004). This activity is the same as the DD-transpeptidase activity of the PBPs until the deacylation step, where hydrolysis occurs instead of transpeptidation and results in the formation of a monomeric tetrapeptide instead of the dimeric penta-tetrapeptide formed by transpeptidases. The carboxypeptidase activity of PBP3 is

thought to participate to the spatial regulation of the cross-linking of the peptidoglycan. The reduction in the amount of pentapeptides where PBP3 is active should limit the reticulation of the peptidoglycan (by lack of pentapeptide substrate). Also, PBP3 localizes evenly throughout the cell surface, except at the site of new peptidoglycan insertion (Morlot*, et al.*, 2004). Moreover, PBP3-deficient pneumococci have aberrant shapes and multiple mislocalized septa (Schuster*, et al.*, 1990). This suggests that the positioning of the peptidoglycan synthesis machineries relies somehow on the availability of pentapeptides, which enable their cross-linking activity.

In the pneumococcus, the penultimate D-Ala of the pentapeptide can be trimmed by the LD-carboxypeptidase LdcB (also called DacB) on tetrapeptides preliminarily trimmed by PBP 3 (Barendt*, et al.*, 2011), (Hoyland*, et al.*, 2014). As with PBP3, cells lacking this zinc-dependent peptidase had morphological defects. Their peptidoglycan did not contain any monomeric trimers, and purified LdcB successfully trimmed tetrapeptides to tripeptides, an activity specific to LD linkages, confirming the role of LdcB in removing the 4$^{th}$ D-Ala of the pentapeptide (Hoyland*, et al.*, 2014). The physiological role of this enzyme remains hypothetical in the pneumococcus. Hoyland *et al.* suggested that it could provide D-Ala for further peptidoglycan synthesis, or allow to distinguish between "new" and "old" peptidoglycan. This latter statement could be of importance in that it would provide pneumococci with a way to correctly localize their morphogenesis machineries.

In an elegant study of the composition of nascent and "old" peptidoglycan in the pneumococcus, Laitinen and Tomasz reported changes in the reticulation of peptidoglycan strands (Laitinen & Tomasz, 1990). In order to isolate nascent or old peptidoglycan, they took advantage of the fact that LytA only digests peptidoglycan when choline is present on the neighboring teichoic acids (Mosser & Tomasz, 1970). A medium lacking choline but containing ethanolamine allows growth of pneumococci, which results in the substitution of the choline moieties by ethanolamine on the

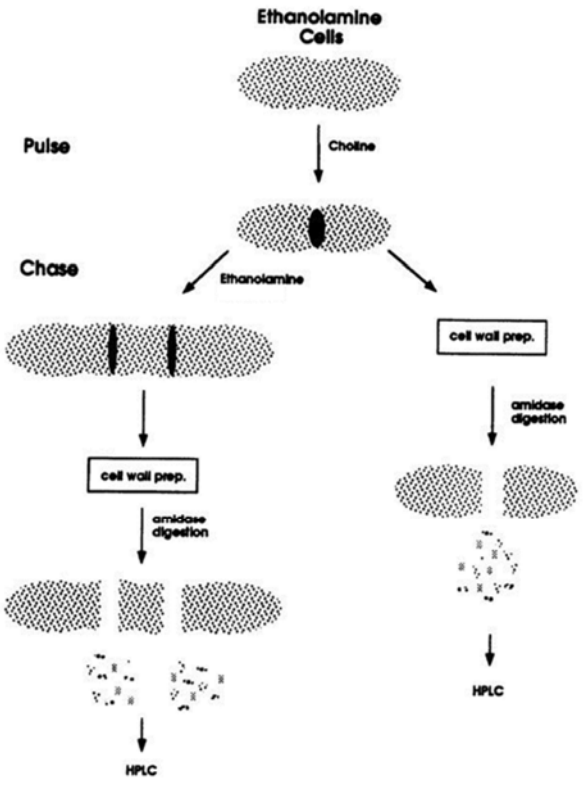


**Figure 16: Method used by Laitinen and Tomasz to analyze nascent and "old" peptidoglycan in *S. pneumoniae* (Laitinen & Tomasz, 1990).**

teichoic acids. After a pulse of choline in ethanolamine-containing cultures of pneumococci, the digestion of peptidoglycan by LytA enabled to solubilize selectively nascent peptidoglycan. On the other hand, when the choline pulse was followed by a chase in ethanolamine, "old" peptidoglycan was digested by LytA. The soluble peptidoglycan fragments where then analyzed by HPLC, which allowed the authors to compare the composition of nascent and "old" peptidoglycan (Figure 16). They observed that "old" peptidoglycan contains more cross-linked peptides than "new" peptidoglycan (31 % and 14 % of the peptides, respectively). This suggests that the PBPs not only synthesize peptidoglycan, but also participate in the maturation of the sacculus. This was already suggested in the seventies by Higgins and Shockmann, who observed that the cell wall in *Enterococcus hirae* was thicker in surface regions far from the zone of insertion of "new" cell wall (Higgins & Shockman, 1976).

Several clinical pneumococcus isolates with penicillin resistance have been reported to have highly branched peptidoglycan (Garcia-Bustos & Tomasz, 1990). Also, the inactivation of the *murMN* operon resulting in the removal of branched peptides is accompanied by a total loss of penicillin resistance (Filipe & Tomasz, 2000), (Filipe*, et al.*, 2002). Surprisingly however, the transformation of a highly active MurM is not sufficient to confer resistance to a susceptible pneumococcus strain, even though its peptidoglycan has increased branched stem peptides (Filipe*, et al.*, 2002). This demonstrates that although they are necessary in the isolates described in this study, branched peptides are not sufficient to provide resistance.

Recently, it was proposed that a higher rate of branched peptides could be a compensating mechanism for a low activity of PBP2b, an essential transpeptidase of the pneumococcus (Berg*, et al.*, 2013). Indeed, pneumococci expressing very low amounts of PBP2b still grow but they have abnormally high amounts of branched peptides in their peptidoglycan. The authors suggested that the highly branched composition of the peptidoglycan of β-lactam resistant *S. pneumoniae* isolates may be due to a low activity of the low-affinity PBP2b variant in these stains. This is supported by the fact that the low-susceptibility PBPs found in β-lactam-resistant strains were proposed to have an impaired activity (Zhao*, et al.*, 1997). However, the assay used in this early study was probably not appropriate to evaluate the TP activity. The exact reason why β-lactam resistant isolates have more branched peptides than susceptible isolates and the potential role of this phenotype remain unclear to date.

Another secondary modification observed in the peptidoglycan of pneumococcus is the deacetylation of the Glc*N*Ac residues. The *pgdA* gene encoding the peptidoglycan *N*-acetylglucosamine deacetylase A was shown to be responsible for Glc*N*ac de-acetylation (Vollmer &

Tomasz, 2000). It is exported by the pneumococcus and remains anchored to the plasma membrane through its uncleaved N-terminal signal sequence, which is probably required to maintain it in the vicinity of its substrate. PgdA does not seem to be important in laboratory condition as its depletion does not induce morphological or growth defects (Vollmer & Tomasz, 2000). However, it is a virulence factor in that it protects the pneumococcus from lysozyme peptidoglycan digestion, which is known since 1922 to have a bacteriolytic activity (Fleming, 1922) and constitutes a first defense against bacterial infections (Wang, 2014). Moreover, since the resolution of its 3-dimensional structure (Blake*, et al.*, 1965), the lysozyme is known to require the acetyl moiety of Glc*N*Ac residues for binding peptidoglycan.

The Mur*N*Ac residues can be *O*-acetylated in pneumococcus peptidoglycan. This modification consists in the addition of an acetyl group to the C6-OH position of some Mur*N*Ac residues. In the pneumococcus, *O*-acetylation is performed by a membrane protein encoded by the open reading frame *spr1868*, provisionally referred to as Adr (for attenuated drug resistance). Depletion of this protein eliminated *O*-acetyl groups in the peptidoglycan and induced hypersensitivity to lysozyme and reduced penicillin resistance (Crisostomo*, et al.*, 2006). This protein is homologous to the better characterized *O*-acetyl transferase A (OatA) of *S. aureus*, an integral membrane protein which was proposed to use activated acetate (acteyl-CoA) in the cytoplasm as an acetate donor and transfer it through the membrane (Bera*, et al.*, 2005).

## Concluding remarks

The various peptidoglycan modifications mentioned above are of clinical importance. Indeed, most of them seem to play a role either in impairing recognition by the immune system, its evasion or in antibiotic resistance. Targeting the enzymes responsible for those modifications could weaken bacterial pathogens, including the pneumococcus by making them easier to recognize by the immune system, and / or more sensitive to host immune defenses (lysozyme) or antibiotics (β-lactams). Interestingly, those modifications are mainly found in pathogenic bacteria (Moynihan*, et al.*, 2014). This means that if treatments are designed that inhibit them, they will impair the development of pathogens while not affecting the commensal flora.

## Morphogenèse du pneumocoque – résumé

Bien qu'il existe une multitude de formes de bactéries dans la nature, trois d'entre elles ont été particulièrement étudiées. Les bacilles en forme de bâtonnets, les coques sphériques, et les ovocoques comme le pneumocoque. Le terme d'ovocoque désigne les coques qui ont des cycles de divisions successives selon des plans parallèles, résultant pour le pneumocoque en une bactérie légèrement allongée en forme d'œuf. Dans cette partie, les protéines ayant une implication prouvée ou hypothétique dans la morphogenèse du pneumocoque sont revues.

Chez le pneumocoque, la synthèse du peptidoglycane est assurée par deux machineries. La première est responsable de l'élongation de la bactérie, permettant l'insertion de peptidoglycane à la périphérie tandis que la seconde machinerie permet la formation d'un septum au milieu de la cellule, suivie de son clivage et de la séparation des cellules filles qui génèrent les nouveaux pôles. L'inhibition de l'élongation par traitement aux antibiotiques ou inhibition de l'activité des protéines de l'élongation engendre des défauts morphologiques se traduisant par l'apparition de cellules raccourcies sous forme de « lentilles ». Quand la division est empêchée, des cellules allongées apparaissent. Ces observations indiquent la présence de deux machineries.

Six protéines au moins semblent être impliquées dans l'élongation du pneumocoque. PBP2b présente l'activité transpeptidase requise pour l'insertion de peptidoglycane dans le sacculus. PBP1a est supposée apporter l'activité glycosyl-transférase permettant l'élongation des chaînes de peptidoglycane. Cependant, cela n'a pas été démontré de manière expérimentale et cette implication reste spéculative, d'autant plus que le pneumocoque possède 3 PLPs possédant l'activité glycosyl-transférase. RodA est supposée jouer le rôle de flippase requise pour l'apport de lipide II. MreC et MreD ont un rôle inconnu dans l'élongation, mais leur déplétion engendre les défauts morphologiques caractéristiques des protéines de l'élongation. Pour finir, RodZ a été caractérisée chez les bacilles, où elle lie l'homologue bactérien des filaments d'actine à la membrane, ce qui constitue une plateforme utilisée par les protéines de l'élongation pour organiser leur action. Cette protéine du cytosquelette bactérien n'existe pas chez le pneumocoque, bien que RodZ ait été identifié dans le génome. Le rôle de RodZ est donc spéculatif, mais sa conservation chez les ovocoques suggère qu'elle a son importance. D'autres protéines, comme des hydrolases sont probablement aussi impliquées dans l'élongation, mais aujourd'hui, aucune évidence n'a été apportée quant à la spécificité de certaines hydrolases dans l'élongation.

Un nombre plus important de protéines a été assigné à la division du pneumocoque. Je les ai divisées en trois classes par rapport à leurs rôles respectifs. La division est orchestrée autour d'un équivalent procaryote du cytosquelette de tubuline, un polymère de FtsZ qui forme un anneau au milieu de la cellule au tout début de la phase de division du cycle cellulaire. Cet anneau de division

est associé à la membrane par SepF et FtsA également trouvés sous forme de filaments, alors que ZapA et ZapB semblent impliquées dans la régulation de la polymérisation de FtsZ. Six protéines jouent un rôle dans l'insertion de peptidoglycane au niveau du site de division, permettant la formation du septum. PBP2x apporte l'activité transpeptidase tandis que PBP1a semble impliquée dans la division (en plus de son rôle dans l'élongation). FtsW pourrait apporter l'activité flippase requise pour l'export du précurseur du peptidoglycane. DivIB, DivIC et FtsL forment un complexe requis pour la division bien qu'aucun rôle précis n'ait pu être démontré pour ces protéines pour l'instant. Enfin, 4 protéines sont connues pour permettre la séparation des cellules filles une fois le septum fermé. FtsE et FtsX forment un ABC transporteur au site de division et forment un piédestal pour PcsB. Cette dernière digère le peptidoglycane au septum grâce à son activation par le complexe FtsE-FtsX. Enfin, LytB permet la séparation de cellules filles n'étant plus attachées que par un fin lien de peptidoglycane.

La forme des pneumocoques est très conservée au sein d'une population. Pour permettre une telle précision, élongation et division se doivent d'être finement coordonnées dans l'espace et le temps. Les mécanismes de régulation de la morphogenèse du pneumocoque restent très peu connus à l'heure qu'il est. Cependant, il existe des liens entre les deux machineries qui permettent peut-être un niveau de régulation. En effet, division et élongation sont toutes deux FtsZ-dépendantes, similaire à la phase pré-septale de la morphogenèse des bacilles. PBP1a semble impliquée dans les deux processus, jouant peut-être un rôle dans la quantité de chaînes glycanes polymérisées avec succès aux deux sites d'assemblage du peptidoglycane. En outre, plusieurs protéines ont des rôles dont la spécificité pour l'élongation ou la division est ambigüe. EzrA, GpsB et DivIVA en font partie. Souvent, bien que la déplétion ou l'inhibition d'une protéine de l'élongation ou de la division entraîne une morphologie témoignant de la spécificité de son activité, des effets morphologiques secondaires sont aussi observés. Ceci renforce l'idée que les différentes machineries de la morphogenèse du pneumocoque sont fonctionnellement liées.

La complexité des mécanismes de morphogenèse, l'essentialité des protéines impliquées, et la nature membranaire de la plupart de ces protéines rendent la tâche difficile. Cependant, l'importance des infections bactériennes dans le monde et le potentiel impact de ces études dans le développement de traitements ou de vaccins motivent la recherche dans ce domaine.

## Morphogenesis of the pneumococcus

The simple observation of various bacterial samples under the microscope reveals a variety of organisms with different shapes (Figure 17). These shapes depend partly on the environment and confer specific advantages to the organisms (Young, 2006). For example, a coccoid organism can protect itself against shear forces by accessing to a small pore a rod could not access. Also, a coccus is a smaller target than a rod, and Young proposed that a chemical or physical attack has lower probability to reach a coccus than a bigger bacterium (Young, 2006). Among the variety of bacterial shapes that exist in the nature, three of them have been studied to a larger extent: cylinders, also called bacilli or rod-shaped cells (*e.g. B. subtilis*, *E. coli*); spheres, or cocci (*e.g. S. aureus*); ellipses,

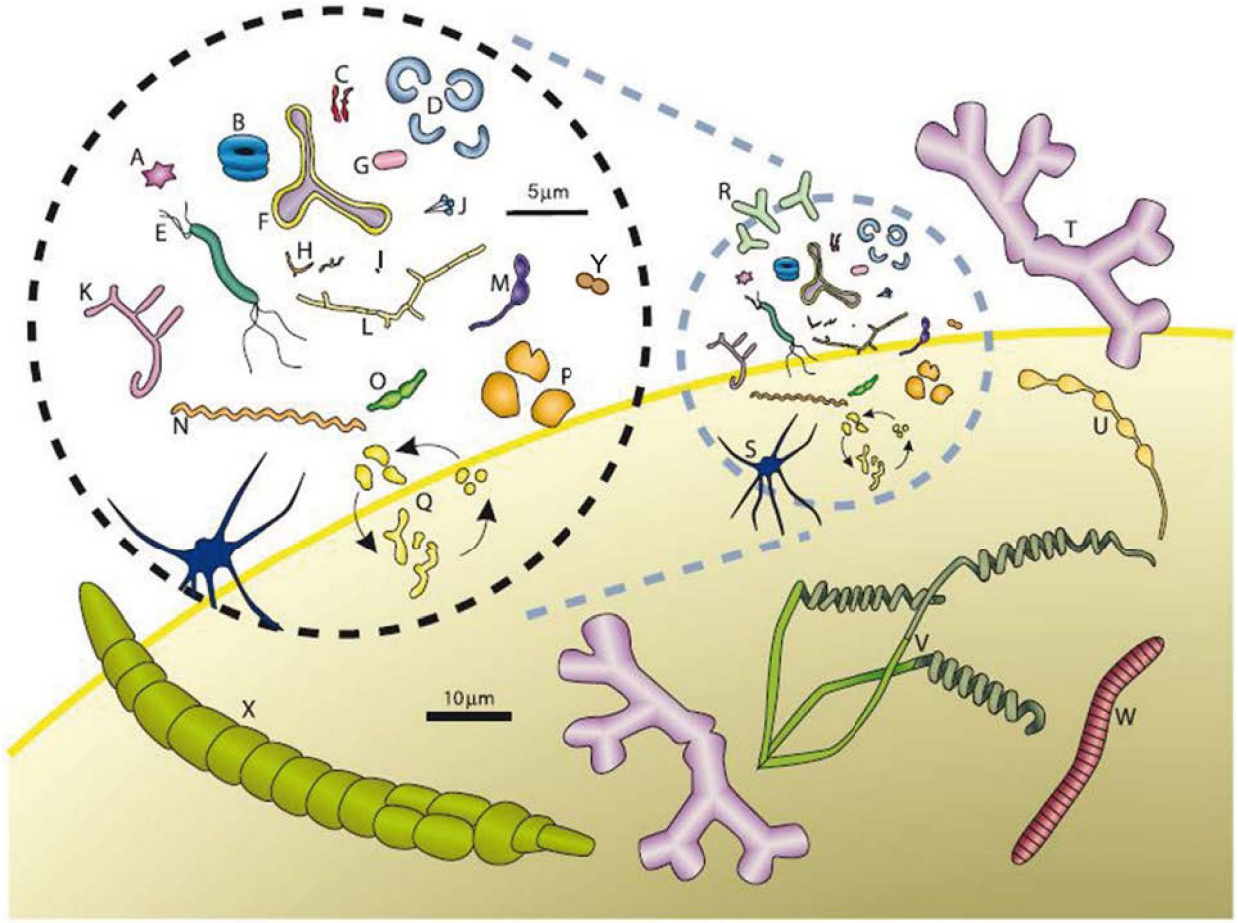


**Figure 17: Bacterial shapes, adapted from (Young, 2006). Bacteria are represented according to the scale bars. (A) *Stella* strain IFAM1312; (B) *Microcyclus* (now called *Ancylobacter) flavus*; (C) *Bifidobacterium bifidum*; (D) *Clostridium cocleatum*; (E) *Aquaspirillum autotrophicum*; (F) *Pyroditium abyssi*; (G) *Escherichia coli*; (H) *Bifidobacterium* sp.; (I) transverse section of ratoon stunt-associated bacterium; (J) *Planctomyces* sp.; (K) *Nocardia opaca*; (L) Chain of ratoon stunt-associated bacteria; (M) *Caulobacter* sp.; (N) *Spirochaeta halophila*; (O) *Prosthecobacter fusiformis*; (P) *Methanogenium cariaci*; (Q) *Arthrobacter globiformis* growth cycle; (R) gram-negative Alphaproteobacteria from marine sponges; (S) *Ancalomicrobium* sp.; (T) *Nevskia ramosa*; (U) *Rhodomicrobium vanniellii*; (V) *Streptomyces* sp.; (W) *Caryophanon latum*; (X) *Calothrix* sp.; (Y) *Streptococcus pneumoniae*. The yellow background is a portion of the giant bacterium *Thiomargarita namibiensis*.**

referred to as ovococci, “American football”-shaped cells or lancet-shaped bacteria (*e.g. S. pneumoniae*, *L. lactis*, *E. faecalis*). During growth, cocci have successive rounds of division, which are separated by long elongation periods in bacilli. In ovococci, both elongation and division phases exist, with a predominant division phase, in contrast to bacilli.

In this part, I intend to provide the reader with a global background concerning the morphogenesis of ovococci, more especially that of *S. pneumoniae*. Compared to rods, little is known about the morphogenesis of ovococci. In cases where a link to the morphogenesis of the pneumococcus is likely, but without direct evidence, I will also review what is known from other organisms to give a more thorough overview.

## Elongasome and divisome, the current model.

The growth of ellipsoid bacteria or ovococci was extensively described in the seventies, when Higgins and Shockman published a series of electron microscopy studies of thin slices of *E. hirae* ATCC 9790 (Higgins & Shockman, 1970). Reconstitution of a cell cycle from these pictures showed that the cell wall is first inserted at the middle part of the cell called the equator. As new material is inserted, a septum (or spetal disc, or cross-wall) grows towards the center of the cells and is simultaneously split at the periphery. Splitting of the septum results in the formation of the poles of the daughter cells. Eventually, the two daughter cells, which have already started incorporation of peptidoglycan at their respective equator, are separated (Higgins & Shockman, 1970). A subtle observation was interestingly made: the septal cross-wall is thinner than the cell wall located on each side of the septum, despite the fact that the septum is not strained by the osmotic pressure. Simple splitting of the

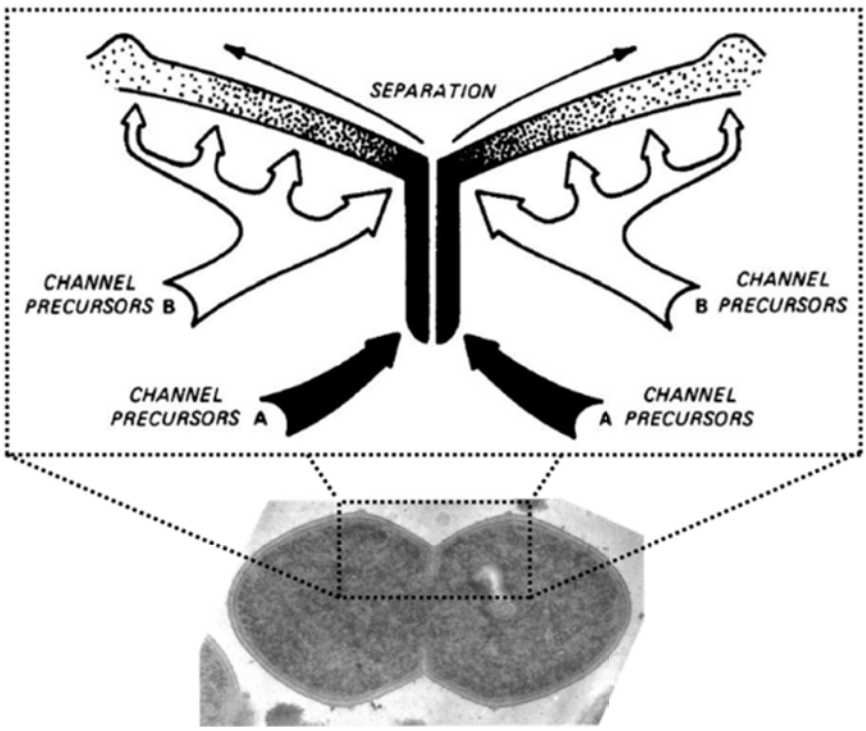


**Figure 18: Model integrating two independent machineries of insertion of precursors in the cell wall of *E. hirae*. Adapted from (Higgins & Shockman, 1976).**

septum cannot not explain this observation, and a model was proposed that includes two machineries of cell wall assembly, a septal and a peripheral one (Figure 18, (Higgins & Shockman, 1976)).

Several functional observations have supported this model. Indeed, when division was inhibited with antibiotics or by mutations of division proteins in several ovococcal species, these organisms elongated, which confirmed that elongation and division are performed independently (Lorian & Atkinson, 1976),(Lleo*, et al.*, 1990). Further, it was shown that depending on the composition of the culture medium, *Streptococcus mutans* NCTC 10449S and *L. lactis* IL1403 can adopt either an ellipsoid or a rod shape (Tao*, et al.*, 1987), (Tao*, et al.*, 1988), (Perez-Nunez*, et al.*, 2011). The former adapts its morphology to the salt composition of the medium whereas the latter momentarily undergoes coccus-to-rod transition during the late exponential phase of growth in a chemically defined medium, but not in a rich medium. Interestingly, *L. lactis* biofilms grown in this minimum medium had elongated bacteria at their surface, but not in deeper layers of the biofilm (Perez-Nunez*, et al.*, 2011). These observations confirm that peripheral elongation and septation can be dissociated in ovococcal species.

## Elongation proteins

To date, six proteins have been assigned to the elongation of the pneumococcus: PBP2b, RodA, PBP1a, MreC, MreD and RodZ (Claessen*, et al.*, 2008), (Sham*, et al.*, 2012), (Typas*, et al.*, 2012), (Zapun*, et al.*, 2008), (Philippe*, et al.*, 2014) (Figure 19). However, the full set of six proteins is not present in all ovococci species (Table II).

PBP2b is one of the two mono-functional class B PBPs of most ovococci species (Table II). In the rod-shaped species *B. subtilis*, the orthologue of PBP2b (PBP2) is involved in elongation (Sauvage*, et al.*, 2008). In *Streptococcus thermophilus*, PBP2b depletion results in shorter and more spherical cells, which grow twice slower than the ovoid parent strain (Thibessard*, et al.*, 2002). Interestingly, this strain has increased resistance to oxidative stress, although the reason of this phenotype remains mysterious. In *L. lactis*, PBP2b depletion causes a similar

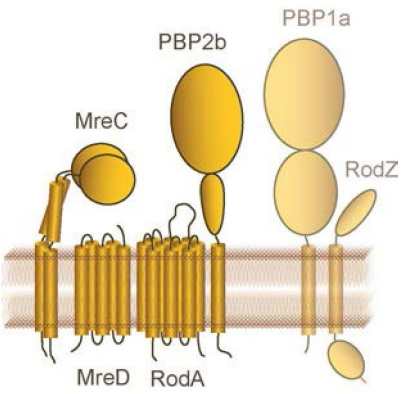


**Figure 19: Topology of the proteins assigned to the elongation of the pneumococcus. Deep yellow: proteins experimentally shown to participate in the elongation of ovococci. Light yellow: hypothetical implication. Adapted from (Philippe*, et al.*, 2014).**

**Table II: Proteins thought to participate in the elongation of ovococci. Adapted from (Philippe, *et al.*, 2014)**

| *Species*, strain | PBP2b | PBP1a | RodA | MreC | MreD | RodZ |
|---|---|---|---|---|---|---|
| *S. pneumoniae* R6 | spr1517 | spr0329 | spr0712 | spr2023 | spr2022 | spr2028 |
| *S. thermophilus* CNRZ1066 | str0613 | str0230 | str1229 | str0020 | str0021 | str2011 |
| *S. mutans* UA159 | SMU_597 | SMU_467 | SMU_1279c | SMU_20 | SMU_21 | SMU_2152c |
| *S. agalactiae* 2603V/R | SAG0765 | SAG0298 | SAG0621 | **A** | **A** | **A** |
| *S. dysgalactiae* D166B | SDE12394_07630 | SDE12394_08565 | SDE12394_03755 | **A** | **A** | SDE12394_10950 |
| *S. pyogenes* MGAS10394 | **A** | M6_Spy1401 | **A** | **A** | **A** | M6_Spy1865 |
| *L. lactis* IL1403 | L137682 | L129183 | L115706 | L98749 | L98132 | L30285 |
| *E. faecalis* V583 | EF_2857 | EF_1148 | EF_2502 | EF_3062 | EF_3061 | EF_3149 |
| *E. faecium* Aus0004 | EFAU004_01299 | EFAU004_00997 | EFAU004_00554 | EFAU004_02614 | EFAU004_02614 | EFAU004_02645 |
| *E. hirae* ATCC 9790 | EHR_14050 | EHR_12290 | EHR_01910 | EHR_05725 | EHR_05730 | EHR_05540 |

**Left: species and strain. For each protein, the name of the locus is given. A: absent.**

morphological defect (Perez-Nunez, *et al.*, 2011). Finally, in *S. pneumoniae*, PBP2b is essential. Also, it is known to be a major determinant of β-lactam resistance in the pneumococcus (Hakenbeck, *et al.*, 2012). Progressive depletion of the protein by an ingenious system of serial dilutions of a conditional knocked-out mutant in medium lacking an inducer results in chains of lentil-shaped cells with a shortened longitudinal axis (Berg, *et al.*, 2013) (Figure 20). In this paper, PBP2b depletion was also performed in cells devoid of LytA, the major pneumococcus autolysin, simplifying the analysis as cells were less prone to lysis due to depletion of an essential protein. The same morphological defects are observed in this background (Figure 20). Of note is the composition of the peptidoglycan of cells lacking PBP2b. A higher proportion of branched peptidoglycan peptides was found in absence of this elongation protein (Berg, *et al.*, 2013). All together, these observations confirm the role of PBP2b in the peripheral cell wall growth of ovococcal species. The role of PBP2b in the peptidoglycan composition is not clearly understood yet.

Little experimental evidence directly assigns a role of RodA in elongating ovococci. To date, it was depleted in only one ovococcus: *S. thermophilus*. This caused the same morphological defects

as PBP2b depletion: round cells (Thibessard*, et al.*, 2002). Preliminary results suggest essentiality of RodA in *S. pneumoniae* (Land & Winkler, 2011), which could be the reason why the observation of morphological defects on knocked-out strains has not been reported yet. However, it is known that SEDS genes (encoding for a family of proteins called "shape, elongation, division and sporulation" that includes RodA) are often found in the same operon as their cognate monofunctional PBPs in the genomes (Zapun*, et al.*, 2008), which suggests a role of RodA in the same process as PBP2b. These assumptions are reinforced by the fact that at non-permissive temperature, a thermo sensitive mutant of *rodA* grows as balls in *E. coli* (Matsuzawa*, et al.*, 1973). Furthermore, RodA is essential and involved in the elongation of *B. subtilis*. Indeed, in a strain where the gene encoding for RodA is under an inducible promoter, the absence of inducer prevents cell growth, and limited amounts of this inducer result in spherical cells that eventually lyse (Henriques*, et al.*, 1998).

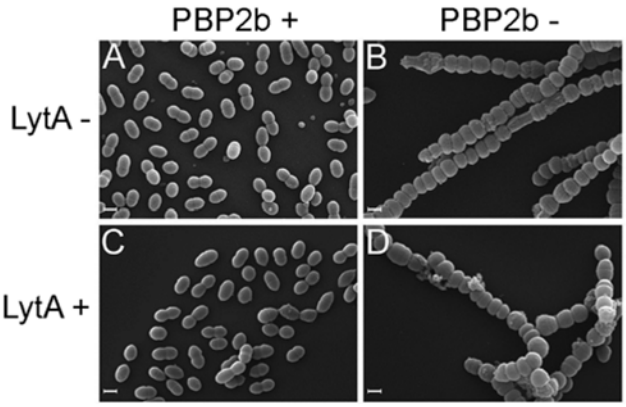


**Figure 20: Morphological defects of *S. pneumoniae* cells devoid of PBP2b in a LytA + or LytA – background. Scale bars: 1 µm. Adapted from (Berg*, et al.*, 2013).**

As mentioned before, PBP1a is one of the three bi-functional class A PBPs of *S. pneumoniae*. Although the implication of this protein in the elongation process of ovococci has not been firmly established yet, several clues support this hypothesis. First, 3D structured illumination microscopy (SIM) localization of PBP1a revealed that in late division stages, it lags behind PBP2x, the division class B PBP, suggesting a role at the periphery (Land*, et al.*, 2013). In an unencapsulated variant of *S. pneumoniae* D39, the depletion of PBP1a results in bacteria with a smaller diameter (Land & Winkler, 2011). This is possibly a clue supporting a role of PBP1a in pneumococci elongation because it has been proposed that the elongation machinery affects the diameter of bacterial cells (Young, 2010). In the same PBP1a-depleted strain, Land *et al.* showed that two other elongation proteins, MreC and MreD are not essential, while they are when PBP1a is expressed and is normally active (Land & Winkler, 2011). In the laboratory strain *S. pneumoniae* R6, the operon encoding MreC and MreD can be deleted, but it becomes essential if the R6 gene *pbp1a* is artificially replaced by the D39 allele (Land & Winkler, 2011). This genetic relationship of PBP1a with the elongation proteins also suggests a role in elongation. Moreover, the *B. subtilis* orthologue of PBP1a (PBP1) was proposed to act not only in division, but also in elongation (Claessen*, et al.*, 2008).

Three types of Mre proteins (for Murein region e) have been described to date: the cytoskeletal MreB (and the likes Mbl and MreBH of *B. subtilis*), MreC and MreD, the two latter being

membrane proteins (Figure 19). Their roles remain unclear to date. In the rod-shaped species *E. coli*, mutation of the *mre* genes caused bacterial rounding, demonstrating a role in elongation (Wachi*, et al.*, 1987). Ovococci lack the actin-like MreB protein, but most of them possess MreC and MreD (Table II). Exceptions are *Streptococcus pyogenes*, *Streptococcus agalactiae* and *Streptococcus dysgalactiae*. These three species are ovococci in that they divide in successive parallel plans and can be found as diplococci, but not in tetrads or in cubes comprising eight cells, as true cocci (Zapun*, et al.*, 2008). However, they appear less elongated than other ovococci like *S. pneumoniae* and *L. lactis*, which is consistent with the fact that they lack MreC and MreD. These two proteins were shown to be essential in strains of *S. pneumoniae* having the D39 allele of the *pbp1a* gene (Land & Winkler, 2011). In this strain, depletion led to cell rounding and eventually lysis. This was the first experimental demonstration that MreC and MreD participate in elongation.

RodZ has been assigned to the elongation of *E. coli* (Shiomi*, et al.*, 2008). Indeed, depleted cells were shorter whereas cells that overexpressed this protein were longer. In this bacterium, RodZ links MreB to the membrane (van den Ent*, et al.*, 2010), and it was proposed to help the polymerization and to stabilize the MreB cytoskeleton (Bendezu*, et al.*, 2009). Despite its wide conservation among the bacterial kingdom, RodZ is generally absent in species lacking MreB, but is surprisingly found in ovococci, except in *S. agalactiae* (Alyahya*, et al.*, 2009). One could expect RodZ function to be linked to that of the MreC/MreD complex in ovococci that are devoid of MreB. Interestingly however, RodZ encoding sequence was found in the genome of *S. pyogenes* and *S. dysgalactiae* that lack MreC and MreD (Table II, (Philippe*, et al.*, 2014)). Although RodZ is likely to be involved in elongation, its specific function remains to be deciphered in ovococci.

The six proteins described above are known or thought to participate in the peripheral growth of ovococci. Other proteins are probably involved in this mechanism, such as additional class A PBPs and hydrolases (Zapun*, et al.*, 2008). An insertional mutant of PBP1a had no elongation defect (Hoskins*, et al.*, 1999), which indicates that the GT activity was replaced, presumably by either PBP1b or PBP2a. Also, peripheral peptidoglycan synthesis is likely to require “opening” of the sacculus to allow for insertion of new peptidoglycan, which would necessitate an enzymatic activity. Also, ovococcal species have two other bi-functional PBPs, PBP1b and PBP2a, for which no precise role has been determined yet, (Zapun*, et al.*, 2008). A striking observation was made in *S. pyogenes*, where the presence of precisely 0.2 µg/mL of methicillin caused coccus to rod transition (Raz*, et al.*, 2012), even though this bacterium is devoid of the elongation proteins MreC, MreD, RodA and PBP2b (Table II). As this antibiotic is known to inhibit specifically PBP2x activity in *S. pneumoniae* (Land*, et al.*, 2013) and *L. lactis* (Perez-Nunez*, et al.*, 2011), a possible explanation is that residual activity of the class A PBPs could be responsible for the observed elongation.

## Division proteins

The division process has been extensively studied in rod model organisms such as *E. coli*, involving more than twenty different proteins. A number of proteins have also been assigned to the division of *S. pneumoniae* (Figure 21 and Table III). Little is known about the exact role of these proteins in the pneumococcus. The proteins described below are separated in three groups, according to their likely function (Figure 21). FtsZ, FtsA, SepF, ZapA and ZapB have a role related to the division ring. FtsW, PBP2x, DivIB, DivIC, FtsL and PBP1a are thought to work together in the assembly of peptidoglycan at the septum. Finally, LytB, PcsB, FtsX and FtsE are involved in the separation of daughter cells after the septum has been completed. The role of some of these proteins has never been experimentally evidenced in the pneumococcus. In this case, the reason why they are thought to participate in the division process is discussed.

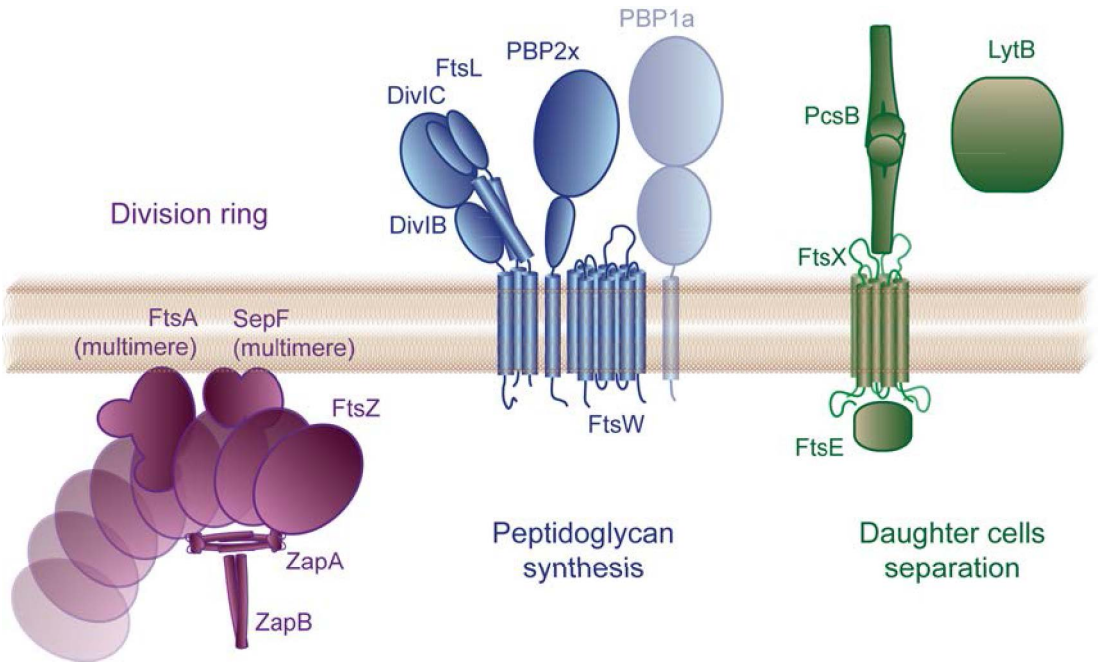


**Figure 21: Topology of the proteins assigned to the division of the pneumococcus. Deep colors: proteins experimentally shown to participate in the division of ovococci. Light colors: hypothetical implication. The role and interaction network of each of these proteins is described in the text.**

**Table III: Proteins thought to participate in the division of the pneumococcus.**

| Protein | Locus (R6) | Function |
|---|---|---|
| **Division ring organization** | | |
| FtsZ | spr1510 | Tubulin scaffold |
| FtsA | spr1511 | Actin scaffold, tethering of FtsZ to the membrane |
| SepF (YlmF) | spr1508 | Membrane bending at the septum, tethering of FtsZ to the membrane |
| ZapA | spr0366 | FtsZ-ring regulator |
| ZapB | spr0367 | FtsZ-ring regulator |
| **Peptidoglycan synthesis** | | |
| PBP2x (FtsI) | spr0304 | TP activity required for division |
| PBP1a | spr0329 | GT and TP activities |
| FtsW | spr0973 | Flippase involved in division |
| DivIB (FtsQ) | spr0605 | Hypothetical structural role |
| DivIC (FtsB) | spr0008 | Hypothetical structural role |
| FtsL | spr0303 | Hypothetical structural role |
| **Separation of the daughter cells** | | |
| LytB | spr0867 | Peptidoglycan hydrolase |
| PcsB | spr2021 | Peptidoglycan hydrolase |
| FtsX | spr0667 | ABC transporter with FtsE, PcsB localization and activation |
| FtsE | spr0666 | ABC transporter with FtsX, PcsB localization and activation |

**The loci names are from the genome of *S. pneumoniae* R6. GT: glcosyltransferase, TP: transpeptidase.**

### *Proteins involved in the organization of the division ring*

The central division protein is FtsZ, the bacterial tubulin homologue. This protein is generally admitted to be the structural scaffold required by the divisome (a complex including all the division proteins) to assemble both in rods (Egan & Vollmer, 2013) and cocci (Zapun*, et al.*, 2008). As in most bacteria, FtsZ first forms a ring structure at the septum of *S. pneumoniae* that undergoes constriction until closure of the septum in a diaphragm-like manner. FtsZ relocates to the equators in late cell cycle stages, determining the new site of peptidoglycan insertion, as observed by immunofluorescence microscopy (Morlot*, et al.*, 2003),(Morlot*, et al.*, 2004). Recent 3D structured

illumination microscopy (SIM) experiments on fixed pneumococci labeled with anti-FtsZ antibodies confirmed that FtsZ relocalizes to the equators before the PBPs, the peptidoglycan synthesis enzymes (Land*, et al.*, 2013). An interesting observation of this study was that the FtsZ-ring is not homogeneous but has a pearl-necklace structure. This was also observed in our laboratory by Maxime Jacq and Cécile Morlot, who used photo-activated localization microscopy (PALM) to determine the localization of FtsZ at high resolution in fixed pneumococci with an endogenous FtsZ:GFP fusion (personal communication). In *S. pneumoniae*, FtsZ is abundant with an estimated 3000 molecules per cell (Lara*, et al.*, 2005). This protein is highly conserved in bacteria, with more than 50% of identity between *S. pneumoniae* FtsZ amino acids sequence and those of *E. coli*, *B. subtilis*, *S. aureus*, *E. faecalis* and *E. hirae* (Massidda*, et al.*, 1998). FtsZ polymerization has been studied *in vitro*, revealing diverse structures, such as linear filaments, helixes or large sheets of protofilaments, depending on the conditions (examples in (Bramhill & Thompson, 1994),(Popp*, et al.*, 2009),(Erickson*, et al.*, 1996)). To date, *in vitro* polymerization of pneumococcus FtsZ has never been reported in the literature. However, it was successfully accomplished in our laboratory (Maxime Jacq and Cécile Morlot).

FtsA from *Thermotoga maritima* is an actin homologue harboring an extra domain that enables binding to FtsZ (van den Ent & Lowe, 2000). Consistent with this in the pneumococcus, the protein was shown to localize at the equator and septa, as does FtsZ, with an FtsA/FtsZ ratio of 1:1.5 (2200 and 3000 molecules per cell, respectively) (Lara*, et al.*, 2005). Also, in presence of ATP, *S. pneumoniae* FtsA was shown to polymerize *in vitro* with the formation of "corkscrew-like helixes" (Lara*, et al.*, 2005). In *E. coli*, FtsA tethers the FtsZ ring to the membrane.

Inactivation of the *ylmf* gene, coding for the SepF protein, resulted in some elongated pneumococcus cells with multiple aborted septa (Fadda*, et al.*, 2003). In *B. subtilis*, three properties of this protein are shared with FtsA: binding to FtsZ, binding to the membrane and polymerization (Duman*, et al.*, 2013). Indeed, purified SepF formed tubes or rings *in vitro* (depending on the pH) and it co-migrated with FtsZ and liposomes in a sucrose gradient. Given the diameter of the rings of SepF observed *in vitro* (40nm)

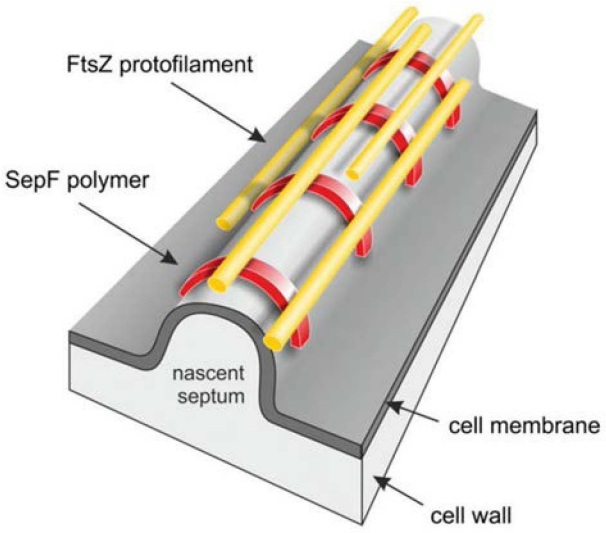


**Figure 22: Model of SepF stabilization of the membrane curvature and its interaction with FtsZ polymers (Duman*, et al.*, 2013).**

and the fact that these rings bound liposomes only to their convex side, a model has been proposed concerning the organization of SepF in division (Figure 22). Indeed, the curvature diameter of the membrane of a forming septum of *B. subtilis* is 40 nm. Thus, SepF would form half rings stabilizing the membrane curvature at the septum, while tethering FtsZ filaments to the membrane to help the division process (Figure 22). A similar role in the pneumococcus would be coherent with the observations made on mutants devoid of SepF.

ZapA and ZapB have been implicated in the stabilization of the FtsZ-ring in *E. coli* (Galli & Gerdes, 2012). In this paper, the authors showed that ZapA over-expression led to abnormal FtsZ helical structures at mid-cell, and the delocalization of both ZapA and ZapB. They also showed that they interact with each other *in vitro* and that this interaction reduces that of ZapA with FtsZ. A series of *in vitro* polymerization assays was performed using purified proteins. It demonstrated that ZapB can form filaments with no additional protein, and these filaments are bundled in the presence of ZapA. FtsZ also formed bundles of protofilaments in the presence of ZapA. A mixture of purified FtsZ and ZapB formed a mixture of distinct FtsZ and ZapB filaments, confirming that these proteins do not directly interact with each other. Finally, a mixture of the three purified proteins formed arrays of two to five aligned filament with a regularly striated pattern, and the characteristic ZapB filaments could not be detected in this preparation (Galli & Gerdes, 2012). The authors proposed that *in vivo*, the competition of FtsZ and ZapB for the interaction with ZapA would regulate the polymerization of FtsZ in a ring structure. ZapA and ZapB have been detected in the pneumococcus by sequence similarity (Massidda*, et al.*, 2013), but their specific role remains to be determined in this organism.

### *Peptidoglycan assembly-related proteins*

As the other division proteins, PBP2x localizes to the septum of *S. pneumoniae* before re-localization to the equators of daughter cells at a late stage of the division cycle (Morlot*, et al.*, 2003), (Land*, et al.*, 2013), (Peters*, et al.*, 2014). PBP2x is the mono-functional class B PBP involved in the synthesis of septal peptidoglycan in the pneumococcus. The first experimental evidence of the role of PBP2x in this organism was reported only recently (Berg*, et al.*, 2013). Pneumococci devoid of PBP2x activity take several shapes (Figure 23): elongated cells or “lemon-shaped” cells enlarged at their middle. The common characteristic of those cells is that they all have aborted septum formation, which indicates a role in division. These morphological defects have been observed in different conditions, including low PBP2x expression (Berg*, et al.*, 2013), inactive PBP2x mutant (Peters*, et al.*, 2014), or by specific inhibition of PBP2x with methicillin (Land*, et al.*, 2013), (Peters*, et al.*, 2014). As for PBP2b, these morphological defects are independent of the autolysin LytA (Figure

23). Note that similar to PBP2b, PBP2x is a major determinant of resistance against β-lactam antibiotics in the pneumococcus in that low-affinity variants of PBP2x are required for high β-lactam resistance (Hakenbeck, *et al.*, 2012).

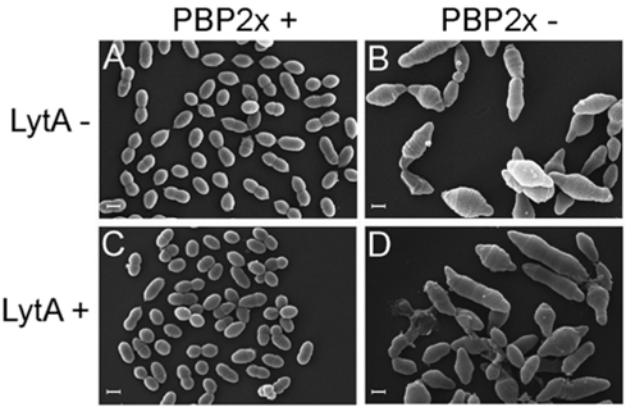


**Figure 23: Morphological defects (elongated and lemon shapes) of pneumococci devoid of PBP 2x. Scale: 1 µm. Adapted from (Berg, *et al.*, 2013).**

In addition to its role in elongation, one should not exclude the possibility that PBP1a can work in division. Also, it was suggested that its *B. subtilis* orthologue PBP1 plays a role in both mechanisms, by shuttling between the two peptidoglycan synthesis machineries (Claessen, *et al.*, 2008). By contrast with bacilli, both elongation and division machineries are overlapping in ovococci, at the resolution of regular fluorescence microscopy (Zapun, *et al.*, 2008). High-resolution 3D-SIM observations showed that PBP1a and PBP2x localize similarly at the beginning of the cell cycle (before constriction of the FtsZ ring). However, in late stages of division (septum diaphragm-like closure), PBP1a lags behind PBP2x (Land, *et al.*, 2013). Therefore, it is possible that PBP1a helps to initiate division before switching to the elongation machinery as the septum is being completed. Super-resolution localization of the other morphogenesis proteins will bring further knowledge on those mechanisms.

Depletion of PBP1a did not show division and growth rate defects (Hoskins, *et al.*, 1999), which indicates that the GT activity must be performed by either PBP1b or PBP2a in this context, and maybe also when PBP1a is present.

FtsW is an integral membrane protein with ten membrane-spanning segments (Gerard, *et al.*, 2002). This protein also localizes at mid cell in the pneumococcus before being re-localized to the equators of nascent daughter cells during division (Morlot, *et al.*, 2004). FtsW is a good candidate to be the flippase required to provide the division transpeptidase PBP2x with the di-saccharide pentapeptide precursor on the outside of the membrane (Zapun, *et al.*, 2008). Indeed, it was recently shown to belong to the divisome of *S. pneumoniae* by reconstitution of the complex *in vitro* (Noirclerc-Savoye, *et al.*, 2013). In *E. coli*, a thermo sensitive mutant of FtsW filamented under non-permissive temperatures and this protein was shown to be essential in this bacterium (Ishino, *et al.*, 1989), (Boyle, *et al.*, 1997). Although the flippase activity of *E. coli* FtsW has been characterized *in vitro* (Mohammadi, *et al.*, 2011), (Mohammadi, *et al.*, 2014), recent studies have proposed that in this organism, the flippase activity is performed by MurJ *in vivo* (Sham, *et al.*, 2014). The role of FtsW

remains unclear *in vivo* in *E. coli*. MurJ is also present in *S. pneumoniae*, and the identity of the peptidoglycan precursor flippase remains controversial.

DivIB, DivIC and FtsL are three membrane proteins required for the division of most bacteria. Their role in peptidoglycan synthesis or remodeling was suggested as they are absent from bacteria lacking a cell wall (Margolin, 2000). In *E. coli*, DivIB (FtsQ) localizes to the division site independently of the presence of DivIC (FtsB) and FtsL, but the two latter proteins require the presence of DivIB for correct localization (Buddelmeijer*, et al.*, 2002). The three proteins are then required for the recruitment of FtsW and PBP3 (FtsI), the class B division transpeptidase of *E. coli* (Buddelmeijer*, et al.*, 2002). Further, DivIC was proposed to stabilize FtsL as FtsL was not detected anymore in a strain lacking DivIC and both required the presence of each other for proper localization. DivIB, DivIC and FtsL from pneumococcus form a complex that was recovered *in vitro* with or without FtsW and PBP 2x (Noirclerc-Savoye*, et al.*, 2005), (Noirclerc-Savoye*, et al.*, 2013). These three proteins co-localized at the division site during septation, as observed by immuno-fluorescence labeling of fixed cells in exponential phase (Noirclerc-Savoye*, et al.*, 2005). However, using this technique, DivIB and FtsL were shown to have a diffuse localization at other stages of the cell cycle. It was proposed that the formation of a complex including DivIB, DivIC and FtsL was somehow regulated to transiently occur for enabling the synthesis of a peptidoglycan septum (Noirclerc-Savoye*, et al.*, 2005). Importantly, the depletion of DivIB decreased the resistance of pneumococci to β-lactam, which reinforces the hypothesis that it plays a role in the synthesis of the peptidoglycan (Le Gouellec*, et al.*, 2008). Given their membrane spanning nature, those proteins could constitute a link between the cytoplasm and the external peptidoglycan assembly. Two possible roles have been evoked for DivIB, FtsL and DivIC in ovococci, assuming that they work in septum formation (Zapun*, et al.*, 2008). First, these proteins would down-regulate the synthesis activity of the divisome as the septum disk is formed from outside to inside, and less and less material is required to complete closure of this diaphragm-like structure (Noirclerc-Savoye*, et al.*, 2005). In a second proposal, they would form a scaffold required for peptidoglycan insertion in the absence of osmotic pressure, a constraint specific to the septum.

### *Proteins involved in the separation of daughter cells*

Regarding the metabolism of the peptidoglycan, the division process comprises the synthesis of a peptidoglycan septum and the separation of the daughter cells. The latter process requires the coordinated activity of peptidoglycan hydrolases that eventually result in splitting of the septal cross wall.

LytB is a protein known to separate newly formed daughter cells at a late stage of the division (Garcia*, et al.*, 1999). Indeed, it localizes at the poles of pneumococci and LytB-depleted cells form long chains of pneumococci attached by their extremities, which can be separated by the addition of purified LytB to the culture (De Las Rivas*, et al.*, 2002). It seems that LytB is only required at a late stage of daughter cells separation, as LytB-depleted cells remain attached only by a thin segment of undigested peptidoglycan.

PcsB (for protein required for cell separation of group B streptococcus) was initially identified by analyzing the secreted proteins present in a *S. agalactiae* culture supernatant, which is consistent with its N-terminal signal peptide sequence (Reinscheid*, et al.*, 2001). The sequence of PcsB contains a cysteine- and histidine-dependent aminohydrolases/peptidases (CHAP)-domain characteristic of peptidoglycan hydrolase activity. A mutant with insertional inactivation of *pcsB* formed chains of cells that failed to separate in *S. agalactiae* (Reinscheid*, et al.*, 2001) and *S. pneumoniae* (Ng*, et al.*, 2004), (Bartual*, et al.*, 2014). Interestingly, PcsB depleted pneumococci had increased sensitivity to antibiotics, especially those directed to the cell wall (Giefing-Kroll*, et al.*, 2011). PcsB was found to localize at the septum and equators of dividing pneumococcus cells and to interact with the ABC transporter FtsE-FtsX, as shown by immunoprecipitation of PcsB after chemical cross-linking (Sham*, et al.*, 2011). The ABC transporter FtsE-FtsX is essential in a D39 pneumococcus strain devoid of its capsule (Sham*, et al.*, 2011). Low expression of FtsX or FtsE in this strain resulted in chains of pneumococci with similar phenotype than cells devoid of PcsB (Sham*, et al.*, 2011), (Sham*, et al.*, 2013). Recently, pneumococcal cells were successfully lyzed by the activity of the purified CHAP domain of PcsB *in vitro*, as evidenced by zymography analysis (Bartual*, et al.*, 2014). In this study, the structure of a pneumococcal PcsB dimer was determined by X-ray crystallography. Also, it was

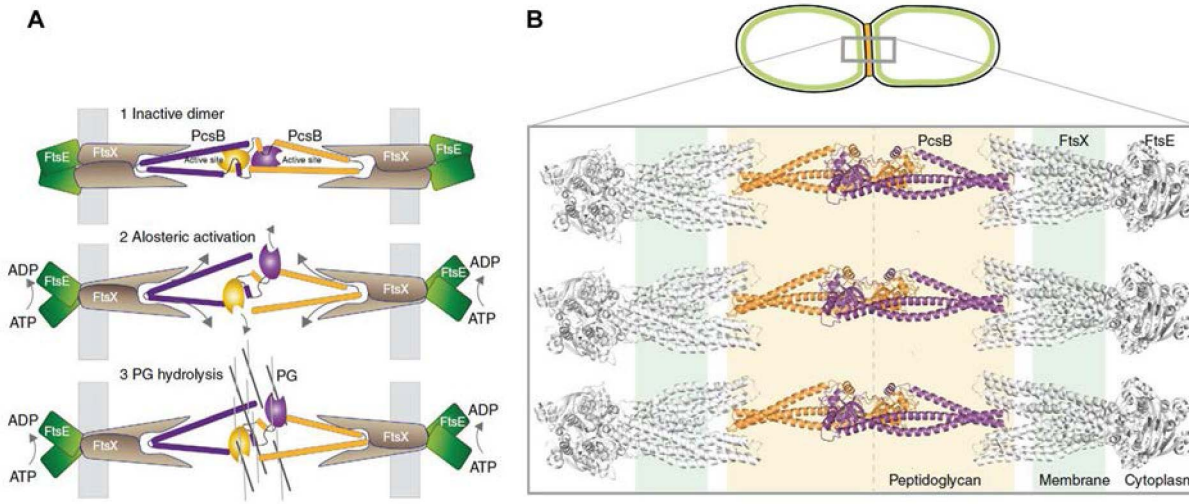


**Figure 24: Model of activation (A) and organization (B) of PcsB in *S. pneumoniae*. PG: peptidoglycan. Adapted from (Bartual*, et al.*, 2014).**

suggested that an ATP-dependent conformational change of the FtsE-FtsX ABC transporter is required to unlock the active sites of PcsB and enable peptidoglycan digestion (Figure 24A). Bartual *et al.* proposed a model in which one FtsE-FtsX ABC transporter would be attached at each extremity of the PcsB dimer, presenting the peptidoglycan hydrolase at the middle of two separating daughter cells (Figure 24B).

## Relationship between the two morphogenesis machineries

It was shown in 1990 that in ovococcal species, two independent machineries are responsible for the elongation and the division (Lleo*, et al.*, 1990). Lleo *et. al.* proposed that the function these machineries are mutually exclusive, which means that the septum is not formed before elongation is completed. However, observations indicate that it depends on the species, as *E. hirae*, *E. faecalis* and *S. pneumoniae* perform both simultaneously whereas *L. lactis* cells nearly, but not totally complete elongation before septation (Higgins & Shockman, 1970), (Wheeler*, et al.*, 2011). What is the link between the two morphogenesis machineries?

To date, the relationship between the division and the elongation machineries remains largely unclear in ovococci. The localization of the PBPs of both machineries was studied by epi-fluorescence optical microscopy in *S. pneumoniae* (Morlot*, et al.*, 2003), (Zapun*, et al.*, 2008). At the resolution of this technique (200 nm), they were shown to co-localize throughout the cell cycle. However, a pneumococcus is 1 µm long, and the area occupied by its peptidoglycan synthesis machineries is close to the resolution limit. Thus, if both the elongation and the division machineries do not physically co-localize but are both present in this zone, fine distinction of their localization is not possible by regular fluorescence microscopy. More recently, the use of three-dimensional structured illumination microscopy (3D SIM) allowed the observation of a distinct localization of PBP1a and PBP2x during the formation of the septum of *S. pneumoniae* (Land*, et al.*, 2013). Indeed, the ring of PBP2x was shown to constrict before that of PBP1a, consistent with a role of PBP1a in elongation and PBP2x in division (Figure 25). Nevertheless, as mentioned above, PBP2x and PBP1a seem to co-localize before constriction of PBP2x ring, and it is not excluded that PBP1a also plays a role in division, as proposed in *B. subtilis* (Claessen*, et al.*, 2008).

A functional interaction of PBP1a and PBP2x was also suggested based on the study of the resistance pattern of engineered penicillin-resistant strains of *S. pneumoniae*, (Zerfass*, et al.*, 2009). First, it should be mentioned that the introduction of a low-affinity mosaic PBP1a in a pneumococcus strain containing the cognate mosaic PBP2x is known to improve the resistance to β-lactams (Munoz*, et al.*, 1992). Surprisingly, when Zerfass *et al.* introduced a low-affinity mosaic PBP1a in a

pneumococcus strain having a low-affinity point mutant of PBP2x, its level of resistance decreased in the resulting strain, similarly to the disruption of PBP1a in this background (Zerfass, *et al.*, 2009). This unexpected observation is probably due to a functional relationship between PBP1a and PBP2x.

In *E. coli*, a relationship between the elongation and the division machineries was also observed. Globally, the elongasome and the divisome are physically separated in *E. coli*. This can be observed by regular fluorescence microscopy as the distance separating both machineries is large enough to avoid resolution limitations in this organism. However, in a short cell cycle phase immediately preceding the division called the "preseptal" phase, FtsZ and PBP2 (the orthologue of PBP2b) were shown to work together in the elongation of cells when MreB was inhibited by the antibiotic A22 (Varma & Young, 2009). Also, the elongation and division proteins are transiently co-localized, as shown by immunofluorescence co-localization of the elongation proteins MreB and PBP2 and the division proteins FtsZ, PBP3 and FtsN (van der Ploeg, *et al.*, 2013). Moreover in *E. coli*, a Försters Resonance Energy Transfer (FRET) was observed between of PBP2 and PBP3 fused to fluorescent proteins during the preseptal phase (van der Ploeg, *et al.*, 2013). This suggests that both proteins physically interact in this phase, as a FRET signal is possible only when the fluorophores are within 10 nm of each other. The peptidoglycan synthesis of ovoid bacteria resembles the preseptal peptidoglycan synthesis of rod-shaped bacteria in that the organization of both division and elongation also relies on FtsZ (Zapun, *et al.*, 2008), (Sham, *et al.*, 2012). An evidence for this statement in that both division and elongation proteins are found in the same pattern as FtsZ even in conditions where its localization is affected, (*eg.* upon methicillin treatment (Land, *et al.*, 2013) or in GpsB mutants (Fleurie, *et al.*, 2014)).

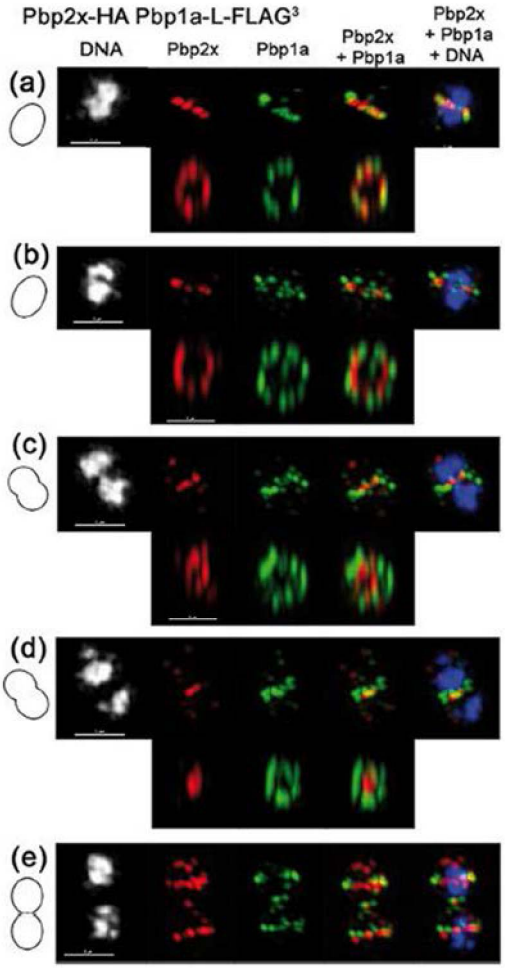


**Figure 25: 3D SIM imaging of IF localization of PBP2x, PBP1a, and DNA in *S.* pneumoniae throughout the cell cycle (Land, *et al.*, 2013).**

Several proteins have ambiguous roles in the synthesis of peptidoglycan as they seem to play a role in both the elongation and the division process of several organisms. This reinforces the hypothesis that both machineries are linked in some extent.

In *B. subtilis*, EzrA was initially shown to negatively regulate the polymerization of the FtsZ ring and to prevent it at the poles (Levin*, et al.*, 1999). Nevertheless, EzrA-depleted cells were longer than WT strains, suggesting a somewhat positive role in division (Levin*, et al.*, 1999), (Claessen*, et al.*, 2008). By contrast, EzrA mutants are thinner than the WT (Claessen*, et al.*, 2008), which suggests a role in the elongation process, as explained earlier (Young, 2010). Claessen *et al*. proposed EzrA to shuttle PBP1 (the ortholog of the pneumococcus PBP1a) from the elongation to the division machineries of *B. subtilis*, with a minor effect on the reverse shuttling (Claessen*, et al.*, 2008). EzrA has been identified in the pneumococcus by sequence similarity. Recently, EzrA was proposed to link GpsB and DivIVA to FtsZ, based on the interactions observed by surface plasmon resonance (SPR) and the similar pattern of localization of the four proteins in WT and morphologically defective mutants (Fleurie*, et al.*, 2014).

GpsB appears to have the opposite role than that of EzrA in *B. subtilis*: it allows shuttling of PBP1 from the division to the elongation peptidoglycan machinery, with a minor effect on the reverse shuttling (Claessen*, et al.*, 2008). Given this role, Land and Winkler first proposed that GpsB also promotes the elongation of the pneumococcus (Land & Winkler, 2011). However, when they depleted this protein to test this hypothesis, elongated cells were obtained, indicating that GpsB actually promotes division or impairs elongation (Land*, et al.*, 2013). In the mutant, the FtsZ ring failed to constrict, suggesting that GpsB plays a role in septal ring closure. GpsB is essential in the strain used in this study (an unencapsulated variant of the D39 strain). By contrast, it is dispensable in the D39 and TIGR4 strains (Fleurie*, et al.*, 2014). Therefore, this essentiality depends on the genetic background, and suppressive mutations may enable cells to survive depletion. In the latter study, depletion of GpsB also yielded cells with aborted division, but some were longer than those observed by

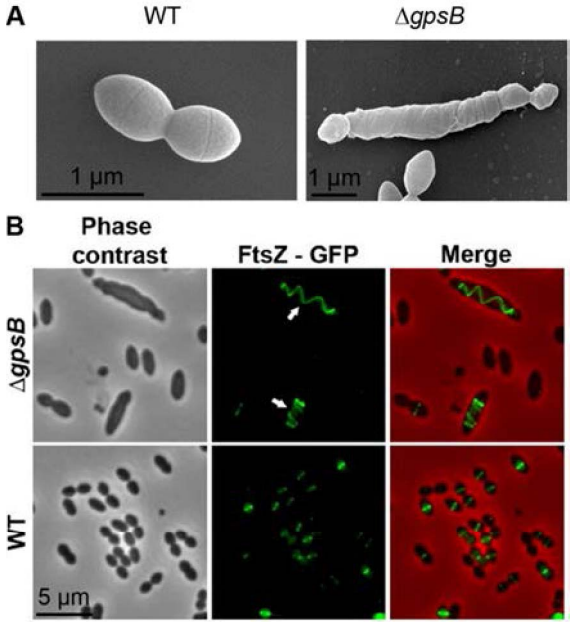


**Figure 26: Characterization of GpsB-depleted cells of pneumococcus. A: scanning electron microscopy of WT and Δ*gpsB* strains. B: helical localization of FtsZ in elongated cells devoid of GpsB. Adapted from (Fleurie*, et al.*, 2014).**

Land *et al*. Those long cells took a "twisted towel" shape and successfully inserted peptidoglycan in a helical manner, following the disposition of their morphogenesis machineries in spirals along the cell (Figure 26). In the same study, GpsB was shown to interact with StkP and to be required for its activity and localization at the division site. StkP is a serine threonine kinase known to play a role in the regulation of the morphogenesis of the pneumococcus (Fleurie*, et al.*, 2012). Taking those observations into account, it was proposed that in the pneumococcus, GpsB not only avoids excessive elongation, but it also acts upstream of StkP in the regulation of the division, by controlling its activity.

DivIVA was initially proposed to play a role in the division of the pneumococcus and in the maturation of cell poles (Fadda*, et al.*, 2007). However, lentil-shaped cells were observed upon depletion of DivIVA in the pneumococcus, similar to the phenotype observed upon depletion of PBP2b (Fadda*, et al.*, 2003), (Fleurie*, et al.*, 2014). Morever, detailed electron microscopy pictures of thin slices of the chains of DivIVA-depleted cells confirmed that those cells had successfully synthesized a septum. Also, active insertion of peptidoglycan was detected at the septum but not the periphery of DivIVA depleted pneumococci as evidenced by active insertion of fluorescent amino-acids at septa only (Fleurie*, et al.*, 2014). These observations suggest a role of DivIVA in the elongation of this ovococcus species. DivIVA localizes to the septum and poles in the pneumococcus (Fadda*, et al.*, 2007), (Fleurie*, et al.*, 2014). This localization was proposed to rely on the fact that those are the regions where the membrane has the most pronounced negative curvature, which could be recognized by this membrane-associated protein (Oliva*, et al.*, 2010).

Of note in pneumococcus, both PBP2b- and DivIVA-depleted cells formed long chains that failed to separate (Berg*, et al.*, 2013), (Fadda*, et al.*, 2003), (Fleurie*, et al.*, 2014). Both depletions suggest that the elongation process is associated with daughter cells separation in the late division phase. Indeed, both proteins seem to be essential for enabling successful peptidoglycan hydrolase activity allowing cell separation. To investigate this, Berg *et al.* added purified LytB to PBP2b-depleted pneumococci. However, this did not separate the chains, suggesting that the separation is impaired upstream to LytB action. The activity of PcsB should be investigated in this background. Indeed, a link with PcsB has been suggested by the identification of an interaction between PcsB and DivIVA by bacterial two-hybrid experiments (Fadda*, et al.*, 2007). Note that DivIVA is cytoplasmic and PcsB is secreted. Therefore, if it occurs *in vivo*, an interaction between both proteins must take place before secretion of PcsB. Also, DivIVA was proposed to recruit PcsB at the site of division (Giefing-Kroll*, et al.*, 2011).

A fundamental question has remained without clear answer for a long time in ovococcus characterization due to technical limits. Are the two peptidoglycan synthesis machineries physically separated in the cell or not? The hypothesis that both machineries form a single large molecular assembly has been evoked (Massidda*, et al.*, 2013), (Fleurie*, et al.*, 2014). However, super-resolution localization of PBP1a and PBP2x has provided a first clue that they are at least transiently separated. The adaptation of novel multicolor super-resolution microscopy techniques and *in vitro* reconstitutions will provide better insights on what really happens in the cell.

## Concluding remarks

Bacterial morphogenesis is an extremely complex mechanism that requires a wide range of proteins and enzymatic activities. Several levels of complexity should be considered including the mechanisms responsible for the localization of peptidoglycan insertion, the synthesis of peptidoglycan precursors, their assembly and the maturation of the peptidoglycan. How the pneumococcus finely coordinates these processes is just beginning to be understood. For example, the WalKR two-component system regulates the expression of peptidoglycan hydrolases including PcsB (Ng*, et al.*, 2004), (Ng*, et al.*, 2005). The serine threonine kinase StkP is involved in the regulation of the division process (Beilharz*, et al.*, 2012), (Fleurie*, et al.*, 2012). The activity of PBP3 was proposed to participate in the regulation of the rate of cross-links present in the peptidoglycan (Morlot*, et al.*, 2004).

Other surface entities should work in harmony with peptidoglycan dynamics, including the plasma membrane, the teichoic acids, the capsular polysaccharides and other surfaces molecules. This whole system should adapt to the environment, especially in the case of pathogens that interact with changing and challenging environments throughout infection. In a population of a given bacterial species, the shape remains largely homogenous, which is implies the existence of robust coordination mechanisms of the morphogenesis machineries. Also fascinating is that those mechanisms differ in distinct species, indicating that multiple complex regulation mechanisms have evolved in different backgrounds. The differing essentiality of certain morphogenesis proteins in closely related pneumococcus strains (*eg.* MreC, MreD and GpsB) attests of the complex integration of the morphogenesis with the strain-specific background.

Understanding morphogenesis is of crucial clinical importance. Indeed, several antibiotic families target the synthesis of the peptidoglycan at various levels. Many of the proteins reviewed above are exposed at the surface of the bacteria, which makes them easier to access than intracellular molecules. Also, numerous morphogenesis proteins are essential for the viability of the

bacteria. Finally, they are often conserved between serotypes, which make them good serotype-independent candidates for vaccines.

The complexity, the essentiality of many morphogenesis proteins and their hydrophobic properties make their study a hard task. However, the stress imposed by the burden caused by pathogenic bacteria in the world and the emergence of resistance against antibiotics and serotype evasion against vaccines, many researchers keep working towards the elucidation of the mechanisms of bacterial morphogenesis.

## Pneumocoque et β-lactamines

Les antibiotiques sont des molécules qui ont la propriété de tuer ou d'inhiber la croissance des bactéries. Après l'apparition de la première famille d'agents antibactériens (les sulfonamides) et des pénicillines au tout début des années quarante, de nombreuses familles d'antibiotiques ont été découvertes et adaptées pour une utilisation médicale. Cependant, depuis les années 60, la recherche sur les antibiotiques a plus apporté sur l'amélioration des antibiotiques existants que sur le développement de nouvelles familles.

Historiquement, la famille des β-lactamines a été la première à être utilisée de manière intensive, lors du traitement des troupes pendant la deuxième guerre mondiale. Les antibiotiques de cette famille ont en commun un cycle β-lactame. Celui-ci leur procure une structure similaire aux deux résidus D-Ala utilisés comme substrat par les PLPs lors de la transpeptidation, et permet la fixation de l'antibiotique dans le site actif de ces enzymes. Diverses β-lactamines existent dont les chaînes latérales et la structure globale diffèrent, ayant donc un spectre d'action, des propriétés pharmacocinétiques et une efficacité sur les pathogènes résistants différents.

Le principal mécanisme de résistance du pneumocoque est l'expression de PLPs modifiées ayant une affinité réduite pour les β-lactamines. Les variants de PBP2x, PBP2b et PBP1a sont les déterminants majeurs de la résistance.

La séquence de PLPs de souches cliniques résistantes aux β-lactamines révèle un mélange blocs de séquences retrouvés chez diverses souches. Aussi, les PLPs de faible affinité de ces souches sont qualifiées de mosaïques. Cet effet résulte de séries d'évènements de transformation-recombinations témoignant de la plasticité génétique du pneumocoque et de l'importance du transfert horizontal des gènes dans le développement de la résistance.

La modification des PLPs peut avoir des conséquences sur la croissance du pneumocoque. Aussi d'autres acteurs ayant un rôle indirect peuvent améliorer la résistance du pneumocoque. Les mieux décrits sont les gènes *murM* et *MurN*, permettant l'ajout de branchements dans les ponts peptidiques du peptidoglycane, essentiels à la résistance. D'autres protéines peuvent jouer un rôle, mais sont pour l'instant moins bien connues.

## Pneumococcus and β-lactams

Antibiotics are molecules with the property of killing or inhibiting the growth of bacteria. Most antibiotics are derived from molecules naturally produced by micro-organisms to fight other species. For example, penicillin is produced by *Penicillium* fungi and has natural antibiotic properties against many bacterial species. Semi-synthetic variants of these natural products have been generated and optimized for medical use. Some synthetic antibiotics have also been developed, with structures not found in the nature (as sulfonamides, quinolones and recently oxazolidinones). After the development of the first antibacterial agents in the late thirties (sulfonamides) (Whitby, 1938), several classes of antibiotics were added to clinical treatment during the next thirty years (Figure 27). The "golden era" of antibiotic discovery lasted until the sixties, but no more new classes of antibiotics have been discovered since then, except for oxazolidinones in 2000.

The major metabolic pathways targeted by antibiotics are the synthesis of the cell wall (by β-lactams and glycopeptides), DNA replication (by quinolones), protein synthesis (by macrolides, chloramphenicol, aminoglycosides and tetracyclines) and the metabolism of folic acid, which affects DNA synthesis (by sulfonamides and trimethoprim) (Lewis, 2013).

Most proteins involved in the synthesis of peptidoglycan have an essential activity and no homologs in mammals. Therefore, they constitute good targets for antibiotics, and all the steps of the peptidoglycan biosynthetic pathway can be inhibited by different molecules (Lovering, *et al.*, 2012). Those that have appropriate properties are used for treating bacterial infections. In this part, I will focus on the β-lactam antibiotics and the major mechanisms enabling the pneumococcus to resist them.

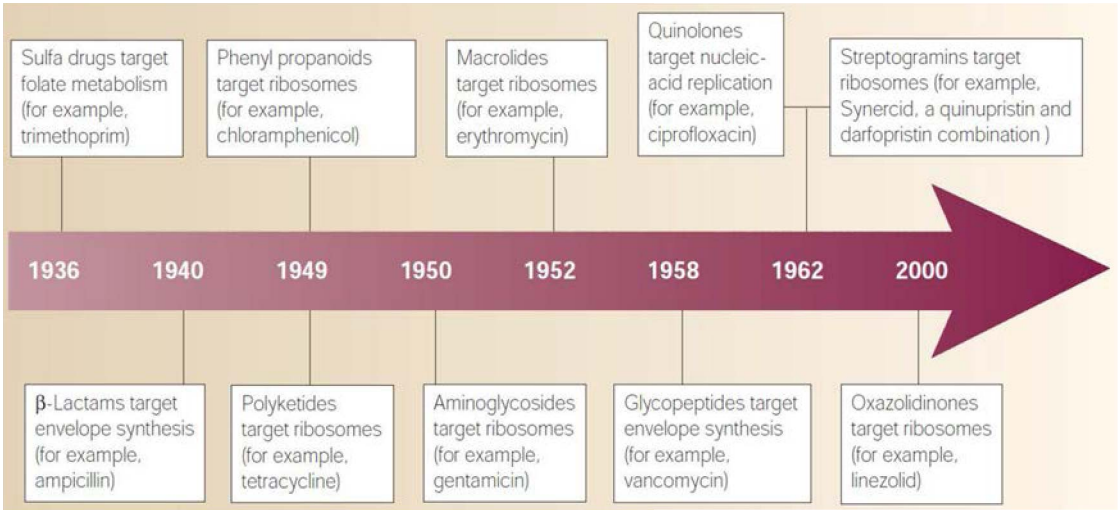


**Figure 27: Introduction of new antibiotic for clinical treatments. (Walsh, 2003)**

## β-Lactam antibiotics

β-Lactams were the first antibiotics to be used widely. The development of methods for the purification of large amounts of benzyl penicillin during World War II launched this medical revolution. The extensive use of β-lactams has led to the emergence of resistant strains and as mentioned in the first chapter of the Introduction, the pneumococcus is particularly adapted to the acquisition of resistance. Several generations of β-lactams have been developed to counteract the rapid evolution of resistance. An example of monocyclic β-lactam currently in phase I clinical trials is BAL30072 (Basilea Pharmaceutica, (Page*, et al.*, 2010)).

The common structural feature of β-lactam antibiotics is the cyclic amide, a β-lactam ring that constitutes the core of the antibiotic. With the exception of monobactams, all classes of β-lactams have a cycle harbouring a carboxyl group fused to the β-lactam ring (monobactams have a sulfonate function on the nitrogen of the β-lactam ring). β-Lactams were shown early to mimic the two D-Ala residues that are used as substrates of the TP reaction performed by the PBPs (Tipper & Strominger, 1965). Indeed, in the antibiotic structure, the distance between the carboxyl (or the sulfonate in monobactams) and the nitrogen of the β-lactam ring is identical to the distance between the carboxyl at the extremity of the D-Ala-D-Ala peptide and the nitrogen of the peptide bond between the two D-Ala residues (2.5 Å). Also, the distance between this nitrogen and that of the peptide bond between the L-Lys and the first D-Ala residue of the peptide corresponds to the distance between the nitrogen of the β-lactam ring and the first atom of the side chain present on the opposite side of the ring.

Acylation of the PBPs consists in the reaction of the carbonyl group of the β-lactam ring with the active serine of the catalytic site of the enzyme (Figure 28). The deacylation rate is negligible, which inhibits the TP activity irreversibly (Zapun*, et al.*, 2008). The acylation of the TP domain of the PBPs results in growth arrest (bacteriostatic β-lactams) or in lysis (bacteriolytic β-lactams).

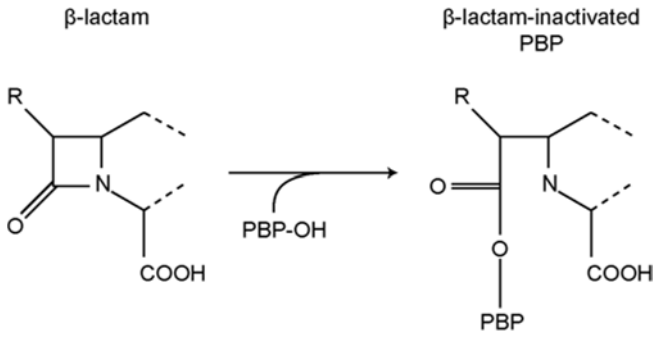


**Figure 28: Illustration of the inhibition of the TP activity of a PBP by the formation of a covalent bond between its active-site serine and a β-lactam.**

Interestingly, β-lactams that inhibit PBP2b have a lytic effect on pneumococci. It is not the case with β-lactams that do not react with PBP2b, such as cephalosporins (Hakenbeck*, et al.*, 1987). The distinct biological outcomes of different classes of β-lactam constitute another clue that the morphogenesis is a network of interconnected activities of synthesis and degradation of the peptidoglycan.

Globally, β-lactam antibiotics have a broad spectrum of bacterial targets, both Gram-negative and Gram-positive. To be effective, a relatively long time of exposition is required at concentrations above the MIC and the efficacy is not significantly improved at higher concentrations.

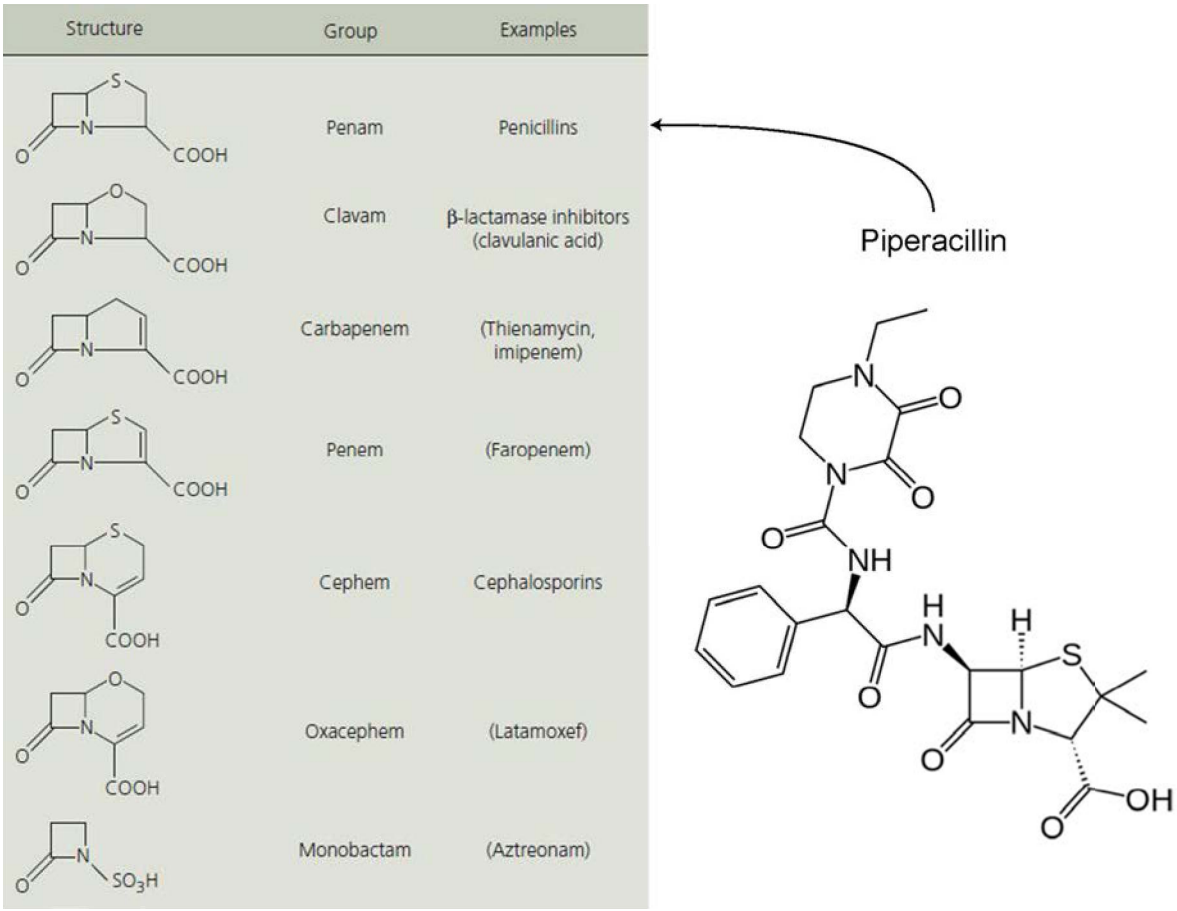


**Figure 29: Structure, name and examples of the different classes of β-lactams and detailed structure of piperacillin. Adapted from (Van Bambeke*, et al.*, 2010).**

Therefore, β-lactams are more efficient upon frequent administrations of small doses than occasional dosing of high quantities. Several classes of β-lactams have been described according to their basic structure (Figure 29). Besides their common mechanism of action, these different classes have distinct characteristics in terms of spectrum of action, pharmacokinetics and efficacy on resistant bacteria.

## Resistance of the pneumococcus against the β-lactams

Five major mechanisms of resistance have been described against β-lactams. Degradation of the antibiotic by β-lactamases, use of $_{L,D}$ transpeptidases instead of $_{D,D}$ transpeptidases, reduction of the permeability of the outer membrane (in Gram-negative organisms), export of the antibiotic from the periplasm (restricted to Gram-negative) or reduction of the affinity of the PBPs to β-lactam. The main mechanism of resistance described so far in *S. pneumoniae* is the alteration in the target enzymes, the PBPs.

Note that the term of resistance is used in clinical studies following specific rules. For example, the resistance of pneumococcus isolates is defined as follows by the European Committee on Antimicrobial Susceptibility Testing (EUCAST): susceptible strains (S) have a MIC below 0.06 mg/L and resistant strains (R), have a MIC above 2 mg/L for benzylpenicillin (http://www.eucast.org/clinical_breakpoints/). For piperacillin, the breakpoints are as follows: S < 0.5 mg/L and R > 2 mg/L. Strains with a MIC between the breakpoints are assigned to the intermediate (I) category. In the case of meningitis, a single value is provided (0.06 mg/mL benzylpenicillin) below which the organism is considered susceptible and above which it is qualified as resistant. In biochemical studies of resistance, the term is often used to designate strains with increased minimum inhibitory concentration (MIC) for a given antibiotic. This latter definition is used in the following paragraphs.

### *Alterations in the PBPs*

Single or multiple mutations can lower the affinity of the PBPs to the β-lactam associated with an increase of the MIC *in vivo* (Chesnel*, et al.*, 2003), (Pagliero*, et al.*, 2004), (Carapito*, et al.*, 2006). To decipher the structural mechanisms of this loss of affinity, the structure of PBP2b variants from the highly resistant pneumococcus clinical strain 5204 and from the susceptible laboratory strain R6 were compared (Contreras-Martel*, et al.*, 2009). Differences were found in the polar properties and charge of the TP domain, and the active site surrounding regions are more flexible in the resistant variant. These modifications decrease the affinity to β-lactam while preserving the activity on its natural substrate.

Note that the kinetic parameters of the reaction between a PBP and β-lactam depend on the identity of both the PBP and the drug. Indeed, some PBP variants have a decreased affinity to certain β-lactams but not others. The opposite is also true: a β-lactam can have a good affinity for one PBP, but not another (Hakenbeck*, et al.*, 1987).

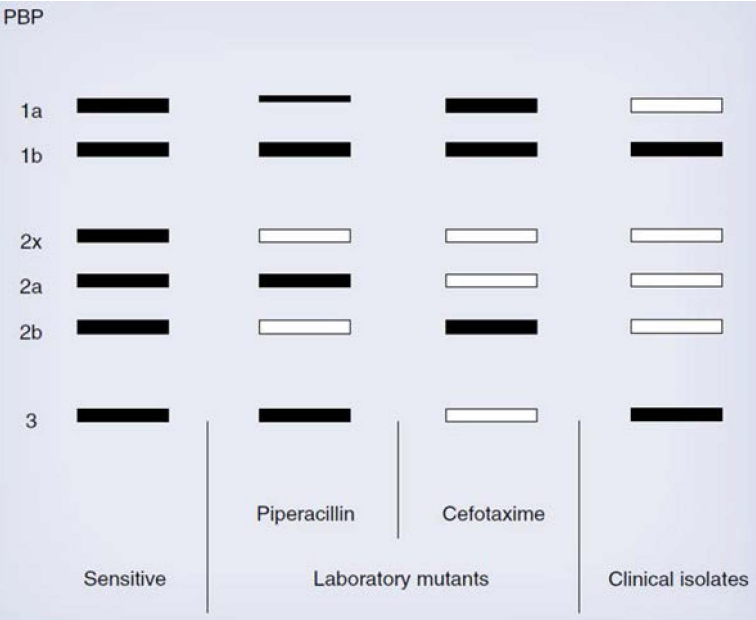


**Figure 30: Variants of PBPs shown to confer resistance against β-lactams in laboratory strains or clinical isolates of *S. pneumoniae* (white bars). Black bars are PBPs never shown to confer resistance in the different conditions. (Hakenbeck, *et al.*, 2012)**

Variants of several PBPs provide resistance to the pneumococcus (Figure 30). PBP2b and PBP2x are the primary determinants of the resistance of *S. pneumoniae* against the β-lactam antibiotics. Indeed the introduction of a variant of one of those PBP is sufficient to confer resistance to some β-lactams. For example, variants of PBP2x increase the MIC of cefotaxime (Grebe & Hakenbeck, 1996), (Chesnel, *et al.*, 2003) and variants of PBP2b confer resistance to piperacillin (Hakenbeck, *et al.*, 1994), (Grebe & Hakenbeck, 1996), (Pagliero, *et al.*, 2004). PBP1a variants confer high-level of resistance in strains with resistant PBP2b and PBP2x (Martin, *et al.*, 1992). Occasionally, PBP2a variants that confer some resistance to β-lactams have also been found in clinical isolates of *S. pneumoniae* (Smith, *et al.*, 2005), (Fani, *et al.*, 2014). No clinically relevant variants of PBP1b and PBP3 have been described in the pneumococcus so far (Hakenbeck, *et al.*, 2012), although PBP3 variants have been selected with cefotaxime in laboratory mutants (Krauss & Hakenbeck, 1997).

Despite conferring resistance, the modification of PBPs can have a fitness cost to the pneumococcus. It was shown that the introduction of variants of *pbp2b* conferring resistance resulted in longer generation time and morphological defects in the pneumococcus (Albarracin Orio, *et al.*, 2011). These defects were compensated in strains with resistant alleles of *pbp1a* and *pbp2x*. Moreover, strains with combined resistant alleles resisted to a larger β-lactam spectrum than strains with single resistant alleles (Albarracin Orio, *et al.*, 2011).

### *Mosaic genes*

Although single mutations have been shown to confer resistance in laboratory strains of *S. pneumoniae* (Hakenbeck*, et al.*, 1994), (Chesnel*, et al.*, 2003), (Carapito*, et al.*, 2006), resistant clinical isolates harbor multiple mutations in their PBPs. For example, PBP2x and PBP2b from the highly resistant clinical strain *S. pneumoniae* 5204 have 80 (Chesnel*, et al.*, 2003) and 58 amino-acid substitutions (Contreras-Martel*, et al.*, 2009), respectively, compared to the laboratory strain R6. At least half of them are in the TP domain. Sequencing of the PBP coding genes in clinical *S. pneumoniae* isolates revealed a great variability in the sequences that is not observed in susceptible clones. The sequence of the TP domain of *pbp2b* determined in fourteen penicillin-resistant strains had 14% of divergence with that of six penicillin-sensitive strains and revealed blocks of altered nucleotides (Dowson*, et al.*, 1989). This suggested transformation and recombination events with an external DNA source. Such blocks were also observed in *pbp1a* from clinical resistant isolates, with 6 to 22% of divergence in the sequence (Martin*, et al.*, 1992). Analysis of *pbp2x* genes revealed 7-18% of divergence in the nucleotides in resistant isolates, while various penicillin-susceptible isolates had only 0.4% of difference (Laible*, et al.*, 1991). Analysis in more details showed that some regions were very similar between resistant and susceptible strains (< 3%) whereas other regions presented more variations (18-23%). Based on these observations, the variants of PBPs coded by genes with such sequence blocks are referred to as mosaic PBPs. The transformation-recombination events were shown to be possible with genes from closely related species such as *Streptococcus mitis* (Dowson*, et al.*, 1993) or *Streptococcus oralis* (Sibold*, et al.*, 1994), which suggests that the commensal flora plays a role in the development of resistance. To date, no widespread mosaic structure has been described for PBP2a and PBP1b (Du Plessis*, et al.*, 2000), with a possible exception for PBP2a (Chesnel*, et al.*, 2005).

As mentioned previously, peptidoglycan with a high proportion of branched peptide bridges has been described in pneumococcus clinical isolates (Garcia-Bustos & Tomasz, 1990). Branched peptide bridges are required for resistance in that deletion of *murM*, the first gene of the operon *murMN* required for the synthesis of branched precursors, abolished resistance (Filipe & Tomasz, 2000). Also, transformation of a R6 strain with the *pbp2x*, *pbp2b* and *pbp1a* genes from a highly-resistant clinical isolate did not confer the full resistance to the R6 strain. However, when *murMN* DNA from the clinical isolate was transformed in this strain, the high level of resistance of the clinical strain was conferred to the R6 strain (Smith & Klugman, 2001). Sequencing of the *murM* gene revealed a mosaic pattern, indicating that the genetic determinants of resistance associated with

branched peptidoglycan is also horizontally transferred (Filipe, *et al.*, 2000), (Smith & Klugman, 2001), (Chesnel, *et al.*, 2005).

To explain the observations mentioned above, one could claim that mosaic PBPs require branched precursors. In this case, pneumococci devoid of branched peptides could not grow with mosaic PBPs. However, this is not the case. A strain with low-affinity mosaic PBPs and no MurM, which therefore has no branched peptides, is viable in the absence of antibiotic (Filipe & Tomasz, 2000). Despite its low-affinity PBPs, such a strain does not resist β-lactams, suggesting further complexity in the mechanisms of resistance (Filipe & Tomasz, 2000). To explain this paradox, it was proposed that branched precursors are superior competitors against β-lactams for the active site of some PBPs or that branched peptidoglycan would play some role of signalization in peptidoglycan synthesis, but no experimental evidence has been provided (Filipe & Tomasz, 2000). An alternative explanation postulates that the branched and non-branched peptidoglycan differ in their susceptibility to some hydrolases (Berg, *et al.*, 2013).

## Concluding remarks

The β-lactams used in the treatment of pneumococcus infections in France are the cefotaxime, the ceftriaxone, the amoxicillin, the cefuroxime and the cefpodoxime, as reviewed in the first chapter of the Introduction. Preventing the synthesis of the cell wall strongly incapacitates the bacteria, and the β-lactams remain widely used to fight bacterial infections. Despite the problems of resistance, the discovery of new antibiotic classes has slowed down over the last decades, and new antibacterial compounds are needed.

Major resistance determinants against β-lactams are PBP2x, PBP2b and PBP1a whereas the other PBPs play a minor role in resistance. The peptidoglycan composition has been shown to influence largely the level of resistance. In addition to those related to the peptidoglycan, additional proteins have been identified with a role in the resistance to β-lactams (Soualhine, *et al.*, 2005), (Fani, *et al.*, 2014). For example, CpoA, a putative glycosyltransferase was shown to provide pneumococci with first levels of resistance, prior to PBP2b alterations (Grebe, *et al.*, 1997). This effect was proposed to rely on modifications of the physical properties of pneumococcus membranes (Meiers, *et al.*, 2014). Similarly, variants of CiaH (part of the CiaRH two-component system related to various processes of competence, autolysis or virulence) were shown to confer resistance to cefotaxime (Guenzi, *et al.*, 1994). PstS, the phosphate-binding subunit of the phosphate ABC transporter of the pneumococcus, is expressed at a higher level in strains with low-susceptibility to penicillin (Soualhine, *et al.*, 2005). Moreover, depletion of PstS increased the susceptibility to this

antibiotic. To find genes implicated in resistance to β-lactams, Fani *et al.* transformed R6 pneumococci with the genomic DNA of penicillin-resistant clinical isolates, selected resistant clones and compared their genomes with the parental R6 strain (Fani*, et al.*, 2014). In this study, despite the confirmation of the roles of PBP2x, PBP2b, PBP1a and PBP2a in conferring β-lactam resistance, evidence was shown that other non-PBP contributors are involved. This is supported by the fact that a fitness cost is caused by antibiotics and the bacteria must compensate this stress, probably through mechanisms without direct link with the PG metabolism.

The current knowledge on the molecular mechanisms of the resistance of the pneumococcus against β-lactams is centered on low-affinity PBPs, although other mechanisms are involved. However, even the physiological effect of β-lactams and the mechanisms of PBP-mediated resistance remain unclear, and the present work brings insights on how pneumococcus deals with a piperacillin challenge.

## Objectives

The general objective of this thesis is the elucidation of the mechanisms of morphogenesis in the pneumococcus. Three aspects were especially investigated: the organization of the morphogenesis proteins, the activity of the PBPs and the specific role of the "elongation" and "division" proteins in pneumococcus morphogenesis.

The organization of the morphogenesis machineries was investigated based on the following hypothesis. The elongation of the pneumococcus is ensured by a complex of proteins called the "elongasome", while the division is performed by a "divisome". In this thesis, I used a biochemical approach (expression and co-purification of recombinant proteins) to test whether PBP2b, RodA, MreC and MreD, 4 membrane proteins involved in elongation form a complex or not.

To understand how low-affinity PBPs can avoid reacting with β-lactam antibiotics while preserving their activity on their natural substrate, an *in vitro* assay for measuring pneumococcus PBPs activities was required. In this purpose, a test of peptidoglycan synthesis *in vitro* was adapted to pneumococcus PBPs. The synthesis of lipid II (the substrate used in this test), the transglycosylase and transpeptidase activities of PBP1a, and the influence of PBP2b and PBP2x on the activities of PBP1a are reported in this manuscript.

In the third part of the Results, a manuscript just submitted for publication is provided. The aim of this part was to decipher how despite the fact that PBP2x is the main essential target of piperacillin, low-susceptibility PBP2b variants confer better resistance to this antibiotic. The specificity of piperacillin for pneumococcus PBPs and the independent effects of PBP2x and PBP2b inhibition under piperacillin treatment are described in this part.

Based on the literature and the results obtained in this thesis, a morphogenesis model is proposed, that reconciles all the observations made on the morphology of pneumococcus cells in various conditions.

# II- Material & Methods

*Louis Pasteur's microscope*

## Reconstitution of pneumococcus membrane protein complexes

### Strains, plasmids and growth conditions

**Table IV:** **Bacterial strains and plasmids utilized for the expression of recombinant proteins in *E. coli*.**

| **Bacterial strains** | **Genome / Description** | **Use** |
|---|---|---|
| *E. coli* DH5α (Invitrogen) | $F^-$ φ80*lacZ*ΔM15 Δ(*lacZYA-argF*)U169 *recA1 endA1 hsdR17*($r_K^-$, $m_K^+$) *phoA* supE44 *thi-1 gyrA*96 *relA*1 λ- | Amplification of DNA plasmids |
| *E. coli* BL21 (DE3) - RIL (Stratagene) | $F^-$ *ompT hsdS*($r_B^-$, $m_B^-$) *dcm*+ $tet^R$ *gal* λ(DE3) *endA* Hte [*argU ileY leuW* $cam^R$] | Protein over-expression |
| *S. pneumoniae* R6 | descendant of the type 2 capsule S clinical isolate (Avery, *et al.*, 1944) | Template for gene amplification |

| **Plasmids** | **Relevant content** | **Remarks** |
|---|---|---|
| pET30b (Novagen) | T7 promotor upstream of 1 MCS, $kan^R$ | Construction of protein expression vectors |
| pETduet (Novagen) | Two T7 promotors upstream of two MCS, $amp^R$ | Construction of protein expression vectors |
| pET30-2bS | *pbp2b-Strep* | Strep-tag on PBP2b C-ter |
| pET30-2xS | *pbp2x-Strep* | Strep-tag on PBP2x C-ter |
| pET30-HRA | *$His_8$-rodA* | $His_8$-tag on RodA N-ter |
| pET30-RA2b | *rodA pbp2b* | No tag |
| pET30-HRA2bS | *$His_8$-rodA pbp2b-Strep*, $kan^R$ | $His_8$-tag on RodA N-ter and Strep-tag on PBP2b C-ter |
| pETduet-MCHMD | *mreC $His_8$-mreD*, $amp^R$ | $His_8$-tag on MreD N-ter |
| pET30-MC | *mreC*, $kan^R$ | No tag |
| pETduet-SMCHMD | *Strep-mreC $His_8$-mreD*, $amp^R$ | Strep-tag on MreC N-ter and $His_8$-tag on MreD N-ter |
| pETduet-MCHMD-RA2bS | *mreC $His_8$-mreD*, *rodA pbp2b-Strep*, $amp^R$ | $His_8$-tag on MreD N-ter and Strep-tag on PBP2b C-ter, two operons (MCHMD and RA2bS) |
| pETduet-RA2bS | *rodA pbp2b-Strep*, $amp^R$ | Strep-tag on PBP2b C-ter |
| pET30-FW2xS | *ftsW pbp2x-Strep*, $kan^R$ | Strep-tag on PBP2x C-ter |
| pETduet-ICFLIB | *divIC ftsL divIB*, $amp^R$ | No tag |
| pET30-RA2bSMCHMD | *rodA pbp2b-Strep mreC $His_8$-mreD*, $kan^R$ | Strep-tag on PBP2b C-ter and $His_8$-tag on MreD N-ter |
| pETduet-RA2bSMCHMD | *rodA pbp2b-Strep mreC $His_8$-mreD*, $amp^R$ | Strep-tag on PBP2b C-ter and $His_8$-tag on MreD N-ter |

Table V: **Media used for cultivation of *E. coli* and *S. pneumoniae*.**

| Growth medium | Description / Composition (per L) | Use |
|---|---|---|
| LB (Becton Dickinson) | 1 % tryptone, 0.5 % yeast extract, 100 mM NaCl | *E. coli* liquid growth |
| LB agar (Becton Dickinson) | LB + agar 15 g/L | *E. coli* solid growth |
| SOC (prepared in the laboratory) | 2 % tryptone, 0.5 % yeast extract, 10 mM NaCl, 2.5 mM KCl, 10 mM $MgCl_2$, 10 mM $MgSO_4$, 20 mM glucose | *E. coli* transformants recovery |
| TH (Becton Dickinson) | 0.31 % beef heart infusion, 2 % peptone, 0.2 % dextrose, 40 mM NaCl, 2.5 mM $Na_3PO_4$, 25 mM $Na_2CO_3$. | *S. pneumoniae* liquid growth |
| CB agar | Columbia agar (Becton Dickinson, 1.2 % pantone, 0.6 % bitone, 0.3 % peptone, 0.1 % starch, 100 mM NaCl, 1.2 % agar), 4 % defibrinated horse blood | *S. pneumoniae* solid growth |

### *Bacterial transformation*

Two hundred nanograms of DNA were incubated with 50 µL of competent *E. coli* DH5α (for plasmid amplification) or BL21 cells (for protein expression) for 30 min on ice. A heat shock at 42°C for 45 sec followed by 2 min of incubation on ice allowed internalization of DNA. After addition of 450 µL of SOC, cells were incubated for 1 h at 37°C under shaking. Fifty (DH5α) or 500 µL of bacteria (BL21) were plated on LB agar supplemented with the appropriate antibiotic for selection (ampicillin: 100 µg/mL, kanamycin: 50 µg/mL), and placed at 37°C overnight. In the case of BL21 strains, single colonies of transformants were inoculated in 2mL LB medium containing the appropriate antibiotic and incubated at 37°C under shaking until the stationary phase. Seven hundred and fifty microliters of these cultures were added with 250 µL of 80 % sterile glycerol and stored at -80°C until use.

### *Plasmid preparation and sequencing*

Two single colonies of freshly transformed bacteria were inoculated in 5 mL of LB supplemented with the appropriate antibiotic (same concentration as above) and incubated overnight at 37°C. Plasmid isolation was performed with the Nucleospin Plasmid QuickPure kit (Macherey Nagel, or MN) following the manufacturer's recommendations except that the plasmids were eluted in distilled water to avoid any side effects of buffer components in downstream use.

The sequence of all inserts in the plasmids constructed during my PhD was verified by sequencing (Beckman Coulter).

### *Construction of pET30-RA2bSMCHMD and pETduet-RA2bSMCHMD*

To construct pET30-RA2bSMCHMD, a DNA segment containing the genes coding for Strep-MreC $His_8$-MreD was inserted in the vector pET30-RA2b downstream of the operon containing the genes *rodA* and *pbp2b*. Briefly, the plasmids pET30-RA2b and pETduet-SMCHMD were double digested with SpeI and XhoI or XbaI and XhoI, respectively (New England BioLabs, or NEB) as follows: 20 µL DNA, 3 µL buffer 4 (NEB), 3 µL distilled water, 2 µL enzyme 1 (XbaI or SpeI), 2 µL enzyme 2 (XhoI), 3 h at 37°C. After purification of the fragments of interest with a Nucleospin Gel and PCR Quick Pure kit (MN) with elution of DNA in distilled water, ligation was performed as follows: 5 µL insert (SMCHMD), 3 µL open vector (pET30-RA2b), 1 µL ligation buffer and 1 µL of T4 DNA ligase (Thermo Scientific), 1.5 h at room temperature. The ligation product was transformed in *E. coli* DH5α cells as described above, with 10 µL of ligation product and 100 µL of competent cells and selected on kanamycin. Two plasmid stocks of 40 µL were prepared and stored at -20°C for expression tests.

To construct pETduet-RA2bSMCHMD, the whole operon of pET30-RA2bSMCHMD was isolated from the vector by digestion with XbaI and SacI (NEB) following the same protocol as above. In parallel, the pETduet vector was digested with the same enzymes. After purification of both DNA fragment with the Nucleospin Gel and PCR Quick Pure kit (MN), ligation was performed with 4 µL insert (RA2bSMCHMD), 4 µL of open vector (pETduet), 1 µL ligation buffer and 1 µL of T4 DNA ligase (Thermo Scientific), 1.5 h at room temperature. *E. coli* DH5α cells were transformed as described above. Two plasmid stocks of 40 µL were prepared and stored at -20°C for expression tests.

DNA samples were analyzed at each step by electrophoresis in 1% agarose gel and run in 0.04 M Tris-acetate, 0.001 M EDTA buffer (called TAE).

### *Pneumococcus growth*

A loop of the laboratory stock of the pneumococcus R6 strain (at $OD_{600}$ = 0.3, with 20% glycerol) was inoculated on CB agar and incubated at 37°C 5% $CO_2$ for 1 or 2 days to obtain single colonies. One colony was inoculated into 100 mL TH and grown at 37°C 5% $CO_2$ until $OD_{600}$ reached 0.3. The culture was supplemented with 80 % sterile glycerol to obtain 20% glycerol final and aliquots were stored at -80°C until use.

## *Escherichia coli* expression system

### *Protein expression*

A single clone of *E. coli* BL21 was inoculated in 125 mL of LB supplemented with the appropriate antibiotic and incubated overnight at 37°C, 150 rpm. Four times 1 L of LB + antibiotic pre-warmed at 37°C were inoculated with 25 mL of pre-culture and incubated at 37°C, 150 rpm until the stationary phase ($OD_{600}$ > 2). The cultures were placed at 20°C for 20 min prior to the induction of protein expression by addition of 500 µM of isopropyl β-D-1-thiogalactopyranoside (IPTG) and overnight incubation at 20°C, 150 rpm.

### *Membranes isolation*

After overnight protein expression, bacteria were pelleted (15 min, 5000 *g*, 4°C) and resuspended in 80 mL of buffer comprised of 50 mM Tris pH 8, 200 mM NaCl, 10 mM $MgCl_2$, 10 mg/mL DNAse and RNAse and protease inhibitors: Complete EDTA-free (Roche). Cells were then mechanically lysed with a Microfluidizer (Microfluidics), in 4 passes at 10 000 psi. The lysate was centrifuged for 20 min at 40 000 *g*, 4°C to remove cellular debris, and the supernatant was ultra-centrifuged to pellet the membranes (200 000 *g*, 1 h, 4°C). Membranes were then resuspended in 6 mL of the same buffer (50 mM Tris pH 8, 200 mM NaCl, 10 mM $MgCl_2$, 10 mg/mL DNAse and RNAse and Complete EDTA-free).

The concentration of total membrane proteins was systematically measured with the BCA kit (Thermo Scientific). This allowed normalizing the amount of membranes to be solubilized for protein purification.

### *Protein purification*

#### Buffers

**Table VI: Solubilization and purification buffers**

| Name | Composition |
|---|---|
| Solubilization (S) | 50 mM Tris pH 8, 50 mM NaCl, 10 mM $MgCl_2$, 10 mM DDM |
| Wash 1 ($W_{N1}$) | 50 mM Tris pH 8, 50 mM NaCl, 10 mM $MgCl_2$, 10 mM DDM, **50 mM imidazole** |
| Wash 2 ($W_{N2}$) | 50 mM Tris pH 8, 50 mM NaCl, 10 mM $MgCl_2$, **2 mM DDM**, 50 mM imidazole |
| Wash 3 ($W_{N3}$) | 50 mM Tris pH 8, 50 mM NaCl, 10 mM $MgCl_2$, **0.3 mM DDM**, 50 mM imidazole |
| Elution ($E_N$) | 50 mM Tris pH 8, 50 mM NaCl, 10 mM $MgCl_2$, 0.3 mM DDM, **300 mM imidazole** |
| Wash 1 ($W_{S1}$) | 50 mM Tris pH 8, 50 mM NaCl, 10 mM $MgCl_2$, 10 mM DDM |
| Wash 2 ($W_{S2}$) | 50 mM Tris pH 8, 50 mM NaCl, 10 mM $MgCl_2$, **2 mM DDM** |
| Wash 3 ($W_{S3}$) | 50 mM Tris pH 8, 50 mM NaCl, 10 mM $MgCl_2$, **0.3 mM DDM** |
| Elution ($E_S$) | 50 mM Tris pH 8, 50 mM NaCl, 10 mM $MgCl_2$, 0.3 mM DDM, **2.5 mM desthiobiotin** |

#### Solubilization of the membrane samples

The appropriate amount of isolated membranes containing the proteins of interest was diluted in 20 mL final of buffer S to have 1 mg/mL of total membrane proteins. In this buffer, the detergent (DDM, for *n*-dodecyl-β-D-maltopyranoside) is in large excess to solubilize the membrane lipids. After 1 h of incubation under rotation at 4 °C, the samples were ultracentrifuged to discard aggregates (30 min, 100 000 *g*, 4°C).

#### Solubilization of mixed membrane samples

In some cases, several membrane protein samples were mixed during solubilization to test the interaction of proteins over-expressed separately. In such cases, each membrane sample was added to the concentration of 1 mg/mL of membrane proteins. Note that the total final concentration of membrane proteins became more important when several membrane samples were added to the solubilization step.

#### Ni-NTA

The solubilized membrane proteins were added to 5 mL (= 1 CV, for column volume) of Ni-NTA Superflow resin (Qiagen) previously equilibrated with buffer S and incubated overnight under rotation at 4°C. The sample was transferred to a purification gravity-flow column (BioRad), the flow-

through was collected for analysis and 3 successive washing steps were performed with 2 CV of buffer $W_{N1}$, 2 CV of buffer $W_{N2}$ and 4 CV of buffer $W_{N3}$. These washing step have two roles. First, they allow to discard the proteins that interact weakly to the chromatography resin. Second, they allow to decrease the concentration of DDM to low levels (about 2x the critical micelle concentration, or CMC) to avoid harsh conditions. Six elution steps were performed by addition of 1/2 CV of buffer $E_N$. The purified proteins were always most concentrated in the third elution fraction, which is shown in the figures.

### Strep-Tactine®

The solubilized membrane protein sample was loaded on 10 mL of Strep-Tactine® resin (IBA Lifescience) previously equilibrated with buffer S. Five washing steps were then performed with 1 CV of $W_{S1}$, 1 CV of $W_{S2}$, and 3 x 1 CV of $W_{S3}$. Six elutions of 1/2 CV were then performed using the buffer $E_S$ and as above, most purified proteins were eluted in elution 3.

### Successive purifications

To obtain better purity, two successive purification steps were sometimes performed, a Ni-NTA purification followed by a Strep-Tactin chromatography are referred to as N1S2, and the opposite order as S1N2. In both cases, the first purification step was performed as described above. The elution fractions were then analyzed by SDS-PAGE to identify which fractions contained the purified proteins of interest. The selected fractions were pooled (most of the time, elution 2 to 6) and purified in a second step. The conditions of this second purification step were the same as described above, except that all the buffers contained only 0.3 mM DDM. The second purification always resulted in protein samples too diluted for Coomassie-stained SDS-PAGE. Therefore, the elution fractions 2 to 6 were concentrated using Amicon Ultra concentration units (Merck Millipore).

## Analysis of the protein samples

### *SDS-PAGE*

For analysis, 12 µL of protein samples were supplemented with 4 µL of 4 x Laemmli blue (final concentration: 62.5 mM Tris pH 6.8, 0.4% SDS, 650 mM β-mercaptoethanol, 10% glycerol, 0.1% bromophenol blue). They were then routinely loaded on 12.5% sodium dodecyl sulfate polyacrylamide gel electrophoresis (SDS-PAGE) and ran for about 2 h at 120 V with a water-cooling

system in a vertical electrophoresis system (Hoefer). The electrophoresis buffer used was prepared in the laboratory and contained 25 mM Tris, 0.1% SDS and 200 mM glycine). The proteins were revealed by Coomassie blue staining. After the run, the gels were incubated for 30 to 60 minutes in a solution of 50% ethanol, 8% acetic acid and 0.25% Coomassie R250 and destained in a solution containing 5% ethanol and 7.5% of acetic acid for 30 to 60 minutes. Boiling the gel in either staining of de-staining solutions accelerated the process if required. If required, the density of the bands revealed by Coomassie blue staining was analyzed with the ImageJ freeware.

Of note in that the samples were not boiled before electrophoresis. With the membrane proteins I studied, this yielded better resolved band patterns.

### *Western blot*

To confirm the identity of a given protein, one way is to use antibodies that specifically bind epitopes presented by the protein. The western blot is a method that allows the identification of SDS-PAGE separated proteins based on this principle. In this work, the western blots were performed using the following protocol. After SDS-PAGE, the proteins were electro-transferred (100 V, 30 min) to a nitrocellulose membrane (BioRad) in 25 mM Tris, 200 mM glycine. The membrane was saturated for one hour in phosphate buffer saline (PBS), 0.3% Tween-20, 5% milk. Rabbit or mouse primary antibodies were added at an appropriate dilution and incubated for 1 h, prior to washing 3 times for 10 min in PBS, 0.3% Tween-20. The membrane was then incubated for 1 h with secondary anti-rabbit or anti-mouse antibodies coupled to horseradish peroxidase (HRP) diluted 10 000 times in PBS, 0.3% Tween-20, 5% milk. After 3 washin steps performed as above, the detected proteins were revealed by chemo luminescence (ECL kit, Pierce) and exposition to a photographic film (Kodak). All steps were performed at room temperature.

### *PAOL and EM sample preparation*

A sample of purified MreC/MreD complex was analyzed using the PAOL platform (Aline Leroy, Christine Ebel) and the Electron Microscopy platform (Daphna Fenel, Guy Schoehn). This sample was prepared in higher amounts than other samples with the project of obtaining large amounts of the MreC/MreD complex for crystallography assays in collaboration with Cécile Morlot. All steps of expression, membrane isolation, solubilization and protein purification were performed as described above, except for the modifications mentioned here. The proteins were expressed from the pETduet-SMCHMD vector in 4 L of culture. The membranes isolated from the 4 L were resuspended in 10 mL of buffer, which resulted in a total membrane proteins concentration of 110

mg/mL. Five milliliters of this membrane preparation was solubilized in 120 mL of solubilization buffer, and purified on 10 mL of Strep-Tactine®. The five washing steps were carried out using the buffer $W_{S3}$. An additional Strep-Tactin® chromatography was performed at this stage with the flow through fraction to recover as much material as possible. Therefore, the elution fractions 2 to 6 of both purifications were pooled and loaded onto 5 mL of Ni-NTA resin. Four times 2 CV washing steps were performed with buffer $W_{N3}$. Proteins did not require concentration to be observable on a Coomassie-stained gel under these conditions. However, they were concentrated 8x for electron microscopy analysis and 60x for PAOL analysis.

## Cell free expression system

### *Plasmids construction and preparation*

#### Plasmids

**Table VII: Plasmids used for the expression of recombinant proteins in cell free system.**

| Plasmids | Relevant content | Remarks |
|---|---|---|
| pIVEX2.4a | T7 promotor upstream to 1 MCS, *amp*$^R$ | Construction of protein expression vectors |
| pIVEX-HMC | *His$_8$-mreC*, *amp*$^R$ | Tag on MreC in N-ter |
| pIVEX-HMD | *His$_8$-mreD*, *amp*$^R$ | Tag on MreD in N-ter |
| pIVEX-SMCHMD | *Strep-mreC His$_8$-mreD*, *amp*$^R$ | Tag on MreC and MreD, both in N-ter |
| pET30-HMC | *His$_8$-mreC*, *kan*$^R$ | Tag on MreC in N-ter |
| pET30-HMD | *His$_8$-mreD*, *kan*$^R$ | Tag on MreD in N-ter |

*Note: pIVEX2.4a was provided by Lionel Imbert (IBS), pET30-HMC and pET30-HMD were made by André Zapun and Nordine Helassa (IBS). The others were constructed as described below.*

#### Construction of pIVEX-HMC, pIVEX-HMD and pIVEX-SMCHMD

The pIVEX vectors were designed by insertion of DNA inserts extracted from vectors available in the laboratory. The plasmids used were pET30-HMD, pET30-HMC, pETduet-SMCHMD and pIVEX2.4a. These vectors were transformed in *E. coli* DH5α and prepared as described in the first part of the Material and Methods. They were all digested with XbaI and XhoI (NEB) in the following conditions: 1 µg DNA, 3 µL buffer 4 (NEB), 2 µL XbaI, 2 µL XhoI and distilled water in sufficient quantity for a total volume of 30 µL, with 5 h of incubation at 37°C. The DNA fragments of interest were purified with a Nucleospin Gel and PCR Quick Pure kit (MN). Ligation was performed with 3 µL of open vector (pIVEX2.4a), 5 µL of insert (HMC, HMD or SMCHMD), 1 µL of ligation buffer and 1 µL of T4 DNA ligase (Thermo Scientific), with 1.5 h of incubation at room temperature. The ligation

product was transformed in *E. coli* DH5α cells as described above, with 10 µL of ligation product and 50 µL of competent cells and transformants were selected on ampicillin. A plasmid preparation of 40 µL was done and analyzed by restriction and verification of the size of the DNA fragments. The DNA sequence of positive samples was verified by sequencing (Beckman Coulter).

The DNA samples were analyzed between each step by electrophoresis in 1 % agarose gel and TAE buffer.

### DNA preparation for cell free expression reaction

The cell free expression reactions require high amounts of DNA. Therefore, the plasmids were purified by maxi-prep, using a NucleoBond Xtra Maxi kit (MN), which had routinely a yield of 1 µg of DNA.

### *Protein expression*

The cell free protein expression mix was prepared in the RNAse-free laboratory of the cell free platform at the IBS. Cell free reaction mixes are mixtures of crude *E. coli* cell lysate and essential components in optimized buffer and salt conditions. To enhance the expression level of the proteins, their encoding genes are under the control of a T7 promotor on the vector, and the T7 RNA polymerase is added to the reaction mix. Unless mentioned in the text, the reactions were performed in a volume of 1 mL by adding all the components listed in Table VIII.

After preparation of the mixtures, samples were incubated for 2 h at 21°C under shaking (900 rpm in a thermomixer, Eppendorf). The protein precipitates were pelleted (10 min, 20 000 *g*, 4°C) and resuspended in 1 mL of 50 mM Tris pH 8, 150 mM of NaCl and 15.6 mM of LAPAO (3-Lauramidopropyl-N,N-dimethylamine oxide) or 15 mM of FosC12 (n-Dodecylphosphocholine). These concentrations of detergent represent 10 x their CMC. Solubilization was performed for 3 h at 21°C under shaking (900 rpm). The solubilized fraction was collected after a centrifugation step (10 min, 20 000 *g*, 4°C) to remove the residual insoluble material.

**Table VIII: Example of a cell free reaction mixture for three independent reactions in 1 mL.**

| **Amino acid mix** | **Volume (µL)** |
|---|---|
| 50 mM water soluble aa each (15 mM) | 67.5 |
| 50 mM acid soluble aa each (15 mM) | 67.5 |
| 50 mM base soluble aa each (15 mM) | 67.5 |
| milliQ (sterile) | 22.5 |
| TOTAL | **225** |

| **10 x reaction mix** | **Volume (µL)** |
|---|---|
| 100 mM rGTP each (0.8 mM) | 26.40 |
| 100 mM rUTP each (0.8 mM) | 26.40 |
| 100 mM rCTP each (0.8 mM) | 26.40 |
| 2.0 M HEPES (55 mM) | 90.76 |
| 100 mM ATP (1.2 mM) | 39.60 |
| 10 mM folinic acid (68 µM) | 22.44 |
| 100 mM cyclic AMP (0.64 mM) | 21.12 |
| 500 mM DTT (3,4 mM) | 22.44 |
| 9.2 M $NH_4OAc$ (27.5 mM) | 9.87 |
| milliQ (sterile) | 44.59 |
| TOTAL | **330.03** |

| **Master mix** | **Volume (µL)** |
|---|---|
| 10 x reaction mix | 300.00 |
| 1M creatine phosphate (80 mM) | 240.00 |
| amino acid mix (1 mM)* | 200.00 |
| 4 M KGlu (208 mM) | 156.00 |
| 1.07 M $Mg(OAc)_2$ (20mM total) | 40.37 |
| 17.5 mg/ml tRNA (0.175 mg/ml) | 30.00 |
| 10 mg/ml Creatine kinase (250 µg/ml) | 75.00 |
| T7 RNA polymerase (1/100e) | 10.00 |
| TOTAL | **1051.37** |

| **Cell Free reaction mix** | **Volume (µL)** |
|---|---|
| master mix | 350.46 |
| S30 extract 09/2012 BL21 DE3 | 400.00 |
| vector (16 µg/ml) | 16.00 |
| detergent | 0.00 |
| milliQ (sterile) | 233.54 |
| TOTAL | **1000** |
| (final concentration) | |

### *Protein purification (RoBioMol platform)*

The purification of proteins was performed by the RoBioMol platform (Anne Marie Villard, IBS). Briefly, 100 µL of solubilized protein sample prepared as described above were added to 400 µL of buffer (150 mM NaCl, 50 mM Tris pH 8, 10% glycerol and 3.5 mM of LAPAO or FosC12) and 50 µL of Ni-NTA resin. After overnight incubation at 4°C, the proteins were washed twice with 1 mL of the

same buffer containing 50 mM imidazole and eluted with 100 µL of the same buffer with 300 mM imidazole.

The elution fraction was analyzed on SDS-PAGE. Twelve microliters of protein samples were added with 4 µL of 4 x Laemmli and loaded on a XT Criterion 4 – 12 % gel (BioRad). The electrophoresis was performed with MES buffer (BioRad) at 100 V with a cooling system, and revealed by Coomassie staining and analyzed by western blot as described above.

## *In vitro* reconstitution of the activities of pneumococcus PBPs

### Lipid II synthesis

#### *Preparation of* Micrococcus flavus *membranes*

*Micrococcus flavus* colonies were inoculated in 12 x 25 mL of Tryptic Soy Broth (TSB, Becton Dickinson) and incubated at 30°C, 300 rpm for 6 h. These precultures were inoculated in 12 x 1 L of TSB for overnight growth in the same conditions. At $OD_{600}$ = 4.5, cells were pelleted (30 min, 3 000 *g*, 4°C), pooled and washed by resuspension in 200 mL of 100 mM Tris-Cl pH 8 and centrifugation for 15 min at 8 000 *g*, 4°C. The pellet was resuspended in 100 mL of 100 mM Tris-Cl pH 8 supplemented with 100 µg/mL lysozyme, 20 mg of DNAse and 20 mg of RNAse. Cells were cracked by 10 passes in a cell cracker at 1 000 bar. Cell debris were pelleted by centrifugation for 1h at 8 000 *g*, 4°C and the supernatant was ultracentrifuged for 3 h at 180 000 *g*. The membranes were resuspended in 10 mL of 50 mM Tris-Cl pH 8 and stored at -20°C.

#### *Lipid II synthesis*

The reaction of lipid II synthesis was performed by adding several compounds in the order given in Table IX. Small scale synthesis tests (150 µL) first enabled to find the best synthesis conditions and a large scale reaction (150 mL) allowed to obtain large amounts of lipid II.

Small scale reactions were performed for 1 h at room temperature. Reactions products were then visualized by thin layer chromatography (TLC) as follows. Two hundred microliters of butanol – pyridine (1:1) pH 4.2 were added to the samples, vortexed and shortly centrifuged. The supernatant was washed with 100 µL of distilled $H_2O$, vortexed and quickly centrifuged. Fifteen microliters of the butanol phase (supernatant) were dried under the vacuum for 20 minutes and resuspended in 15 µL of chloroform/methanol (1:1) and vortexed. Samples were spotted on a TLC (HPTLC Silica Gel 60, Merck) and run with a chloroform/methanol/water/ammonia (440:240:50:5) mobile phase. The plate was then dried for 30 seconds at 125°C and revealed with iodine vapors.

For the large scale synthesis, the mix was stirred gently at room temperature until the reaction was complete (4.5 h). This was monitored by TLC analysis of 20 µL of sample at different time points as follows. Twenty microliters of sample were mixed with 20 µL of distilled $H_2O$ and 50 µL of butanol/pyridine (1:1) pH 4.2, vortexed and shortly centrifuged. The supernatant was washed with 50 µL of distilled $H_2O$, vortexed and quickly centrifuged. Fifteen microliters of the butanol phase (supernatant) were dried under the vacuum for 20 minutes and resuspended in 15 µL of

chloroform/methanol (1:1) and vortexed. The sample was spotted on a TLC plate and run and visualized as above. When the reaction was complete (most undecaprenol phosphate was consumed), 200 mL of butanol/pyridine (1:1) pH 4.2 were added, the solution was stirred for 20 minutes and centrifuged for 5 minutes at 2 000 *g* and stored at 4°C overnight.

**Table IX: Lipid II synthesis reaction mixture.**

| Compound | Volume (small scale) | Volume (large scale) |
|---|---|---|
| Undecaprenyl phosphate | 10 µL | 20 mL |
| 20% triton X-100 | 3.75 µL | 3.75 mL |
| Tris-Cl pH 8 | 16.25 µL (of 100 mM solution) | 7.5 mL (of 1M solution) |
| UDP-Glc*N*Ac | 10 µL (of 10 mM solution) | 123 mg |
| *S. simulans* extract (UDP-Mur*N*Ac pentapeptide) | 5 µL | 12 mL |
| milliQ $H_2O$ | *qs* 150 µL | *qs* 150 mL |
| $MgCl_2$ | 2 µL (of 500 mM solution) | 1 mL (of 1 M solution) |
| *M. flavus* membranes (MraY and MurG) | 5 or 10 or 15 µL | 5 mL |
| **TOTAL** | **150 µL** | **150 mL** |

*Note: the undecaprenyl phosphate was provided by Eefjan Breukink (Utrecht University), The S. simulans extract was made by André Zapun (IBS) and the UDPGlcNAc was purchased from Sigma®.*

### *Lipid II purification*

The butanol was evaporated using an oil pump and the synthesized lipid II was re-solubilized in 150 mL of methanol/chloroform (1:1) and loaded on a diethylaminoethyl (DEAE) cellulose anion-exchange column of 4 x 2.5 cm (height x diameter) equilibrated with 100 % methanol. After washing with chloroform/methanol/water (2:3:1), the sample was eluted with a linear gradient (1.1 L) of chloroform/methanol/water (2:3:1) to chloroform/methanol/300 mM ammonium bicarbonate (2:3:1). Elution fractions of 8 mL were collected and analyzed by TLC (20 µL samples were dried, resuspended in 15 µL chloroform/methanol (1:1) and applied to TLC). The fractions containing pure lipid II were pooled and dried with a rotary evaporator. About 50 mg of lipid II (26.7 µmol) were obtained in this experiment.

### *Dansylation of the lipid II*

Two successive reactions were performed to add a dansyl group to the lipid II (click chemistry).

First, the $NH_2$ moiety of the lysine in position 3 of the stem peptide was converted to an azide ($N_3$) moiety (the resulting molecule is referred to as LII-$N_3$). A reaction was performed with the integrality of the synthesized lipid II in 50 mL (0.5 mM), 2.7 mM imidazole-1-sulfonyl azide hydrochloride, 1 mM CuSO4, 6 mM N,N-Diisopropylethylamine (DIPEA), 0.5% Triton X-100, incubated at room temperature for 4 h. The LII-$N_3$ was purified on DEAE as follows. The sample was added with 150 mL of methanol and 100 mL of chloroform, and loaded on the DEAE column pre-equilibrated with chloroform – methanol/water (2:3:1). It was washed with 25 mL of the same solution, and 4 elution steps were done with 100; 200; 250 and 100 mL of [chloroform/methanol/100; 200; 500 and 1000 mM ammonium bicarbonate] (2:3:1), respectively. Each elution fraction was analyzed by TLC as described above. The elution fraction of 250 mL at 500 mM ammonium bicarbonate contained most of the LII-$N_3$. It was dried with a rotary evaporator and resuspended in chloroform/methanol (1:1). To estimate the concentration of the purified LII-$N_3$ obtained, it was applied on TLC in parallel with purified lipid II of known concentrations. The concentration was estimated to 2 nmol/µL.

The LII-$N_3$ was then converted to LII-DNS (lipid II with a nitrogen-carbon cycle (1,2,3-triazole) to which a dansyl moiety is attached through a $C_3$ aliphatic tail, represented in Figure 46 (Results). The carbon tail keeps the dansyl moiety distant from the nitrogen-carbon cycle to avoid impairment of the fluorescence. For this reaction, 2.6 mL of purified LII-$N_3$ were dried and added with 2 mL of 0.1 % triton X-100 in 10 mM Tris pH 8, 25 mM ascorbate, 4 mM $CuSO_4$ and 50 µL of C≡$C_3$-DNS in methanol (provided by Eefjan Breukink, Utrecht University). The reaction mix was incubated overnight at room temperature and 2 µL were analyzed by TLC as above, with both UV light and iodine vapor revelation to make sure that the observed spot was fluorescent. The reaction product was then dried using a rotary evaporator, resuspended in 10 mL chloroform/methanol/water (2:3:1) supplemented with 1 mM EDTA to eliminate the $Cu^{2+}$ ions and subsequently added with 2 mM $MgCl_2$ to titrate the EDTA and allow DEAE purification. The DEAE column was equilibrated with chloroform/methanol/water (2:3:1). The washing and the 3 elutions steps were performed with 10 mL of chloroform/methanol/0; 100; 200 and 500 mM ammonium bicarbonate (2:3:1), respectively. After TLC analysis, the 3 elution fractions were pooled and dried as they all contained fluorescent lipid II. After resuspension in 500 µL chloroform/methanol (1:1), the concentration was estimated to 3 mM compared to a lipid II solution of known concentration.

## Activity tests

### *Expression and purification of the PBPs*

PBP2x and PBP2b were purified after expression from the vectors pET30-2xS and pET30-2bS that encode for PBP2x or PBP2b with a C-terminal Strep-tag. The expression was performed as described in the first part of the Material and Methods with an *E. coli* expression system. One liter of culture was pelleted and resuspended into 35 mL of buffer containing 0.5 M NaCl, 50 mM HEPES pH7.5, 10 mM $MgCl_2$, Complete EDTA-free (Roche) and 10 µg/mL of DNAse and RNAse before sonication for 3 min 30 (2 sec ON, 8 sec OFF). The cell debris were eliminated by centrifugation (20 min, 40 000 *g*, 4 °C) and the membranes were pelleted by ultra-centrifugation of the supernatant (1 h, 200 000 *g*, 4°C). The membranes were then resuspended in 3 mL of 150 mM NaCl, 50 mM HEPES pH 7.5 and 10 mM $MgCl_2$ and stored at -20°C before use.

Membranes were solubilized in 14 mL of buffer with 150 mM NaCl, 50 mM HEPES pH 7.5, 10 mM $MgCl_2$, and 1 % triton X-100 for 1 h at 4°C. After 20 minutes of centrifugation at 40 000 *g*, 4°C, the supernatant was loaded onto a 1 mL Strep-Tactin® column equilibrated with the same buffer. The flow through was loaded a second time before the washing. The column was washed with 5 mL of loading buffer and 7 mL of buffer with only 0.02% of triton X-100. Ten fractions of 1 mL were collected after elution with 150 mM NaCl, 50 mM HEPES pH7.5, 10 mM $MgCl_2$, 0.02% triton X-100 and 2.5 mM desthiobiotin. The relevant purification fractions were analyzed by SDS-PAGE as described above confirming that the second elution fraction was the most concentrated.

The proteins were submitted to a second purification step by anion-exchange chromatography. The second elution fraction of the Strep Tactine® chromatography was diluted into 10 mL of 50 mM HEPES pH 7.5, 10 mM $MgCl_2$ to bring the NaCl concentration to 15 mM. The sample was then loaded onto a 1 mL ResourceQ column (GE Healthcare) and purified with a gradient of 15 to 1000 mM NaCl in the same buffer. Elution fractions of 500 µL were collected and analyzed by SDS-PAGE. The most concentrated fraction was stored at 4°C before use.

Purified PBP1a was provided by David Roper (Warwick University). The expression and purification protocols are described in (Zapun*, et al.*, 2013).

### *In vitro reconstitution of the activities of PBP1a*

For each reaction, a mixture of 0.25 µL of LII-DNS and 2.5 µL amidated lipid II (aLII) at 0.2 mM (provided by André Zapun, IBS) was dried under nitrogen vapors. This brought 5 µM of LII-DNS and

50 µM of aLII to the reaction mixture. The lipid II mix was resuspended in 9 µL of reaction solution comprised of 50 mM HEPES pH 7.5, 150 mM NaCl, 10 mM $MgCl_2$, 25% dimethyl sulfoxide (DMSO), 0.01% triton X-100 and 0.1 mg/mL PBP1a. This mix was subsequently added to 1 µL of distilled water (test), 5 mM moenomycin or 10 mM penicillin (negative GT and TP activity controls, respectively). The reaction was incubated overnight at 30°C.

When the cooperativity of PBP1a and a class B PBP (either PBP2x or PBP2b) was tested, the same experiment was performed in absence of DMSO and in presence of 0.1 mg/mL of both PBP1a and the tested class B PBP.

### *Analysis of the peptidoglycan synthesized in vitro*

#### SDS-PAGE,

The reaction products were analyzed on 9% polyacrylamide gels (8 x 7 cm) without stacking gel. For one gel, the following recipe was followed: 2.5 mL of [1.25 M Tris pH 8.45, 0.4% SDS], 3.3 mL of 40% acrylamide/bisacrylamide in solution (Euromedex), 15 µL of tetramethylethylene diamine (TEMED) and 30 µL of 10% ammonium persulfate (APS). The samples were added with 2 µL of loading buffer comprised of 100 mM Tris pH 8.8, 4% SDS and 40% glycerol (no bromophenol blue was added to this buffer to avoid fluorescent background). To control the electrophoresis, a sample containing loading buffer supplemented with bromophenol blue was added on the side of the gel. The cathode buffer contained 0.1 M Tris pH 8.25, 0.1 M Tricine, 0.1% SDS while the anode buffer contained 0.1 M Tris pH 8.8. The run was performed at 150 V until the bromophenol blue was at about 0.5 cm from the bottom of the gel. The gels were revealed under UV illumination using a ChemiDoc XRS+ System (BioRad).

#### Densitometry

Analysis of the density was performed using the ImageJ freeware. To discriminate between material resulting from TP activity (top band), GT activity (middle smear) or lack of activity (bottom band), the densitometry analysis was performed on adjacent successive horizontal selections covering the complete zone of migration. The density of each successive band was determined with ImageJ. The density determined in the selection corresponding to the bottom band was assigned to lipid II. The density of the top band was assigned to cross-linked material. Finally, the sum of the densities determined in the intermediary selection area was assigned to the glycan chains. The background was removed for each individual selection by subtracting the signal of an area of identical dimensions with no sample.

# III- Results

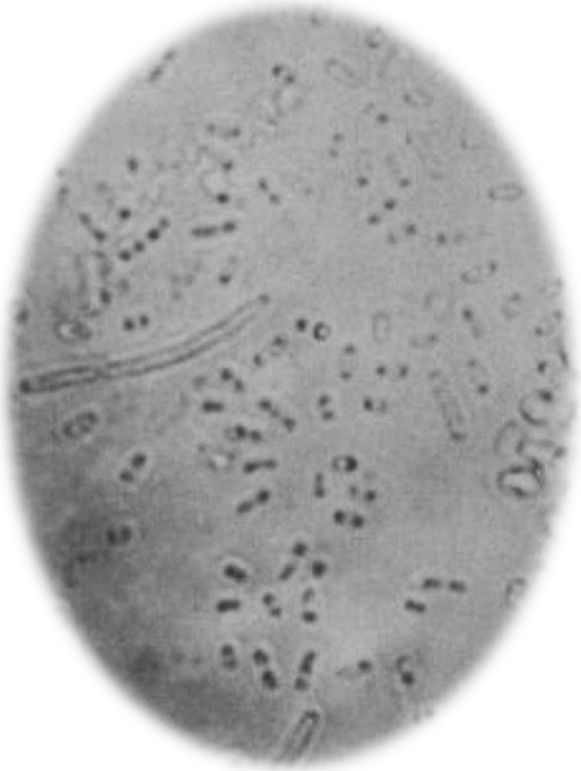

*"Bacteria from surface of bouillon" – First observation of pneumococci by George Miller Sternberg in 1881 (Sternberg, 1881).*

## Vers la reconstitution de l'élongasome du pneumocoque – résumé

L'élongasome est un complexe de protéines supposé assurer l'incorporation de peptidoglycane en périphérie du septum, entraînant une légère élongation des cellules de pneumocoque. L'existence d'un tel complexe a été proposée basée sur le rôle présumé de protéines de la morphogenèse. Pendant ma thèse, j'ai étudié cette question par une approche biochimique, consistant à reconstituer des complexes *in vitro* à l'aide de protéines recombinantes de pneumocoques.

La première stratégie employée a impliqué la co-expression des protéines membranaires MreC, MreD, RodA et PBP2b chez *E. coli*. Une fois exprimées, les bactéries ont été lysées, leurs membranes isolées puis solubilisées à l'aide de détergent. Deux étapes successives de purification ont alors suivi, permettant de séparer spécifiquement les protéines étiquetées et leurs partenaires potentiels.

Cette méthode a tout d'abord permis d'isoler un complexe comprenant MreC et MreD. Une tentative d'obtenir le complexe à forte concentration pour des essais de cristallographie a entraîné l'apparition d'agrégats ne permettant pas de poursuivre dans cette direction. L'analyse des échantillons a néanmoins permis d'envisager une stœchiométrie 1:1 pour le complexe MreC/MreD.

Un complexe comprenant MreC, MreD, RodA and PBP2b a ensuite été retrouvé dans les fractions d'élution de la deuxième purification du protocole, suggérant l'existence d'un complexe comprenant ces 4 protéines. Cependant, malgré les efforts d'optimisation et les diverses stratégies utilisées, des contaminants ont toujours été purifiés avec le complexe, remettant en question la validité de l'expérience. Pour vérifier que l'interaction observée était valide, un contrôle négatif d'interaction avec d'autres protéines membranaires était nécessaire. L'interaction a donc été testée entre MreC, MreD, PBP2x et FtsW, qui a entraîné l'élution des 4 protéines, bien qu'en présence de nombreux contaminants protéiques. Dans le même but, l'interaction entre MreC, MreD, DivIB, DivIC et FtsL a été testée. Dans ce cas, les trois dernières protéines ne semblent pas avoir été éluées, mais MreD a disparu lors de la seconde étape de purification. L'existence d'un complexe comprenant les quatre protéines MreC, MreD, RodA and PBP2b n'a donc pas pu être démontrée de façon certaine. Il n'est cependant pas exclus que l'élongasome n'existe pas *in vivo* en tant que complexe comprenant toute les protéines, mais que des interactions transitoires ou fonctionnelle permettent l'insertion appropriée de peptidoglycane dans le sacculus

Dans ce système, le taux d'expression des protéines était limitant. Ne pouvant pas augmenter ce niveau pour des raisons de toxicité pour *E. coli*, une nouvelle stratégie a été employée : le système d'expression acellulaire. Dans ce cas, les protéines ont été exprimées dans une solution contenant un extrait bactérien et un vecteur d'expression dans un tampon comprenant tous

les composés nécessaires à l'expression des protéines. Ainsi, les conditions d'expression de MreC et MreD ont été optimisées, permettant d'obtenir un niveau d'expression satisfaisant. Les outils développés permettront de poursuivre l'étude de la formation de complexes de protéines de la morphogenèse.

## Towards the reconstitution of the pneumococcus elongasome *in vitro*

To generate its ovoid shape, the pneumococcus not only inserts peptidoglycan towards the center of the bacterium to form a septum, but it also assembles some peptidoglycan at the periphery. To date, up to six proteins have been assigned to this process, as reviewed in the Introduction. It has been proposed that four of these proteins form the core of this machinery that can be called the elongasome: PBP2b, RodA, MreC and MreD (Zapun*, et al.*, 2008). A class A PBP was also included in the model, but at the time, no clues existed to designate one of the three class A PBPs of pneumococcus. A divisome was also proposed in the model, comprising PBP2x, FtsW, DivIB, DivIC, FtsL and an additional hypothetical class A PBP as core proteins of the division machinery. To test these hypotheses, we attempted to reconstitute these complexes with recombinant proteins. Marjolaine Noirclerc-Savoye in the laboratory worked on the divisome and successfully isolated a complex of recombinant proteins comprising PBP2x, FtsW, DivIB, DivIC and FtsL (Noirclerc-Savoye*, et al.*, 2013). I joined the project to work on the putative elongasome, following preliminary work by Nordine Helassa and André Zapun.

In this part, I present attempts at the *in vitro* reconstitution of complexes of membrane proteins including MreC, MreD, RodA and PBP2b. The strategy I used includes two major steps. First, the proteins were co-expressed recombinantly, two of them harboring distinct tags for affinity chromatograhy. Thereafter, two successive purification steps were performed, specific of one tag and the other, respectively. This protocol allowed the recovery of the tagged proteins that interact, together with their respective untagged partners

*E. coli* was first used to express pneumococcus membrane proteins recombinantly. As shown below, this system unfortunately introduced many contaminants which could not be discarded in the purification steps. Therefore, a cell-free expression system was used to yield promising results.

Many DNA expression vectors were designed prior to my arrival in the laboratory. Also, the choice of systematically tagging MreD for purification was made for several reasons. First, as no antibodies against MreD could be obtained in the laboratory, the histidine-tag enabled its detection with anti-His antibodies. Moreover, as expression this recombinant protein was low, it was reasoned that pulling the complex by MreD would increase the chances of recovering it in sufficient amounts for detection.

## Expression in *E. coli* membranes

### *Previously characterized complexes: PBP2b-RodA and PBP2x-FtsW*

During my Master 2, I participated in the isolation of the complex between PBP2b and RodA. The reconstitution of this complex constitutes the first step in experimentally testing the existence of an elongasome in the pneumococcus. Indeed, it includes the essential class B PBP responsible for elongation and its cognate flippase.

The complex between PBP2b and RodA was isolated as follows. The genes encoding both proteins were amplified by polymerase chain reaction (PCR) from the genome of *S. pneumoniae* R6 and inserted as an artificial operon in a pET30 vector to form the plasmid pET30-HRA2bS that encodes RodA with a N-terminal $His_8$-tag (H-RodA) and PBP2b with a C-terminal Strep-tag (PBP2b-S). This expression vector was transformed in *E. coli*, the proteins were expressed and the membranes isolated as described in Materials and Methods. After solubilization of the membranes, the complex was isolated by two successive purification steps, on Ni-NTA and Strep-Tactine®, respectively. The purified fraction was analyzed by SDS-PAGE and the proteins were stained with Coomassie blue, which showed that a pure complex of H-RodA and PBP2b-S was recovered. This experiment was published in 2014 within a review on the elongation of ovococci (Figure 31, (Philippe, *et al.*, 2014)).

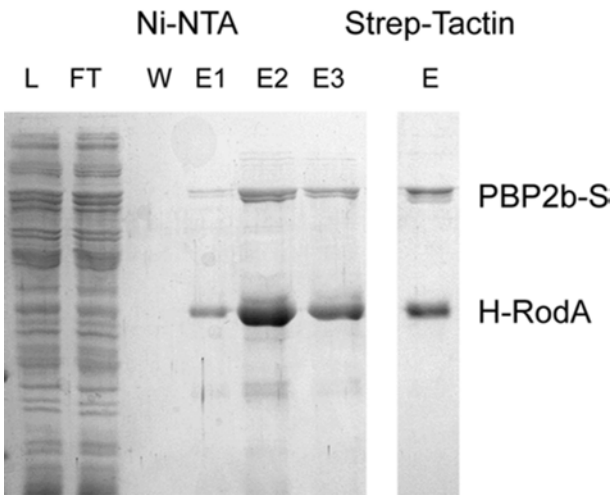


**Figure 31: Isolation of the pneumococcus RodA/PBP2b complex. Strep-tagged PBP2b and His-tagged RodA were co-expressed in *E. coli*, the membrane were isolated and solubilized before two successive purification steps, first on Ni-NTA, second on Strep-Tactin® chromatography. A picture of a Commassie-stained SDS-PAGE analysis of the complex is shown. L: load, FT: flow-through, W: wash, E: elution. (Philippe, *et al.*, 2014)**

The following experiments were performed during my PhD thesis.

### *MreC/MreD*

To verify that MreC and MreD form a complex in the pneumococcus, the plasmid pETduet-MCHMD was created in the laboratory that allows co-expression of MreC and MreD with a $His_8$-tag in N-terminus. After transformation in *E. coli*, the proteins were expressed, the membranes isolated,

solubilized and a Ni-NTA purification was performed. The fractions of interest were analyzed by SDS-PAGE and the protein identity was confirmed by western blot using an anti-MreC antibody and an anti-His antibody to detect $His_8$-MreD. Both proteins were recovered in the elution fraction, indicating their interaction in this system (Figure 32A – top panel). Note that to observe MreD by SDS-PAGE, the gel must be cooled during the run. Indeed, without this precaution, MreD precipitates and forms a smear in the gel that is not detectable with Coomassie staining (Figure 32A – bottom panel).

To rule out the possibility that the presence of MreC in the elution fraction was due to non-specific interactions with the Ni-NTA resin, a control was performed as follows. The pET30-MC vector (encoding MreC without tag) was used as above to produce recombinant MreC, which was not retained by Ni-NTA affinity chromatography, indicating that it does not interact non-specifically with the resin (Figure 32B). Some contaminants migrating between 75 and 100 kDa were observed in the MreC/MreD complex purification. Contaminants of similar size were also recovered in the negative control with MreC as the sole over-expressed protein. Therefore, they probably are *E. coli* membrane proteins that interact non-specifically with the Ni-NTA resin.

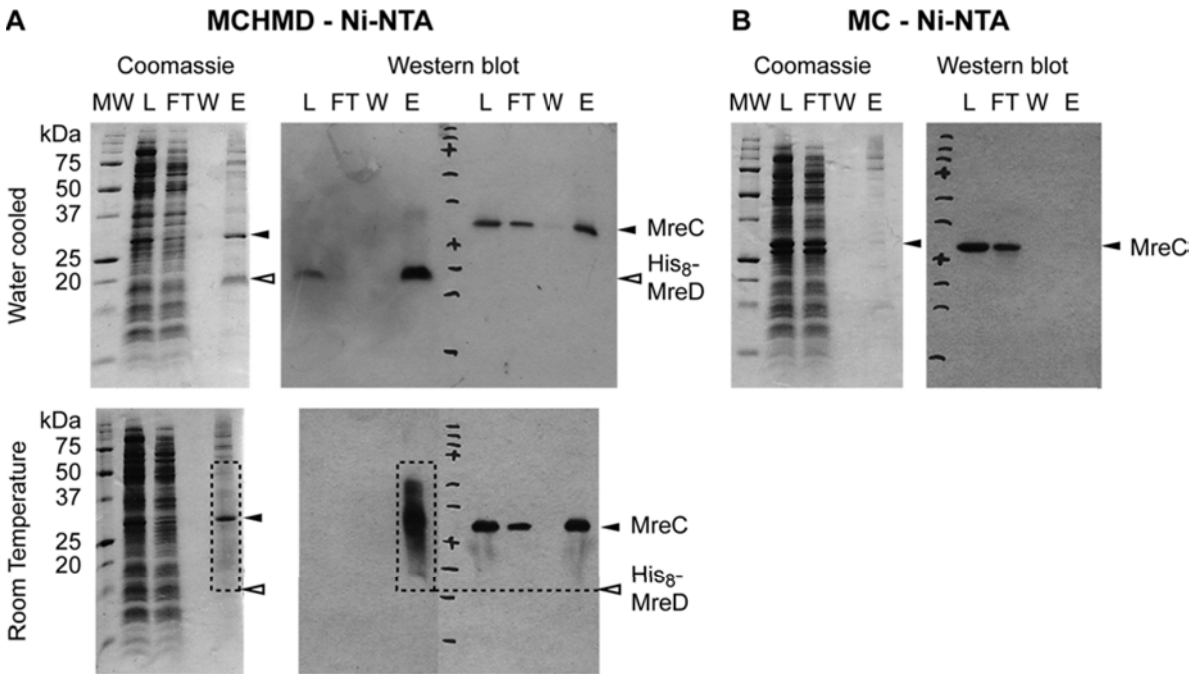


**Figure 32: Isolation of the pneumococcus MreC/MreD complex. A: MreC and His-tagged MreD were co-expressed in *E. coli*, membranes were isolated and solubilized before purification on Ni-NTA. Coomassie-stained SDS-PAGE and Western blot analysis of the purification are shown. The top and bottom panels show SDS-PAGE analysis performed with and without cooling, respectively. B: negative control lacking $His_8$-MreD. The same protocol was utilized as in A. MW: molecular weight, L: load, FT: flow-through, W: wash, E: elution.**

Following these promising results, I attempted to improve the purity of the complex for crystallization screens in collaboration with Cécile Morlot (IBS) to determine the structure of the complex by X-ray crystallography. An additional purification step that specifically targets MreC was planned to provide better purity. Therefore, another expression vector was used: pETduet-SMCHMD (encoding for MreC with a N-terminal Strep-tag and MreD with a N-terminal $His_8$-tag). The proteins were prepared in larger quantity than above (see Material and Methods) and purified by two chromatography steps: Strep-Tactine® followed by Ni-NTA, before SDS-PAGE analysis (Figure 33A). The purified fraction was analyzed by electron microscopy (EM platform, Daphna Fenel, Guy Schoehn), which revealed lots of aggregates (Figure 33B). Also, no motifs could be detected with this method, indicating that the sample was not homogenous.

To further evaluate the quality of the sample, proteins were concentrated sixty times and loaded on a size exclusion chromatography (SEC) column in line with several detectors: ultra-violet

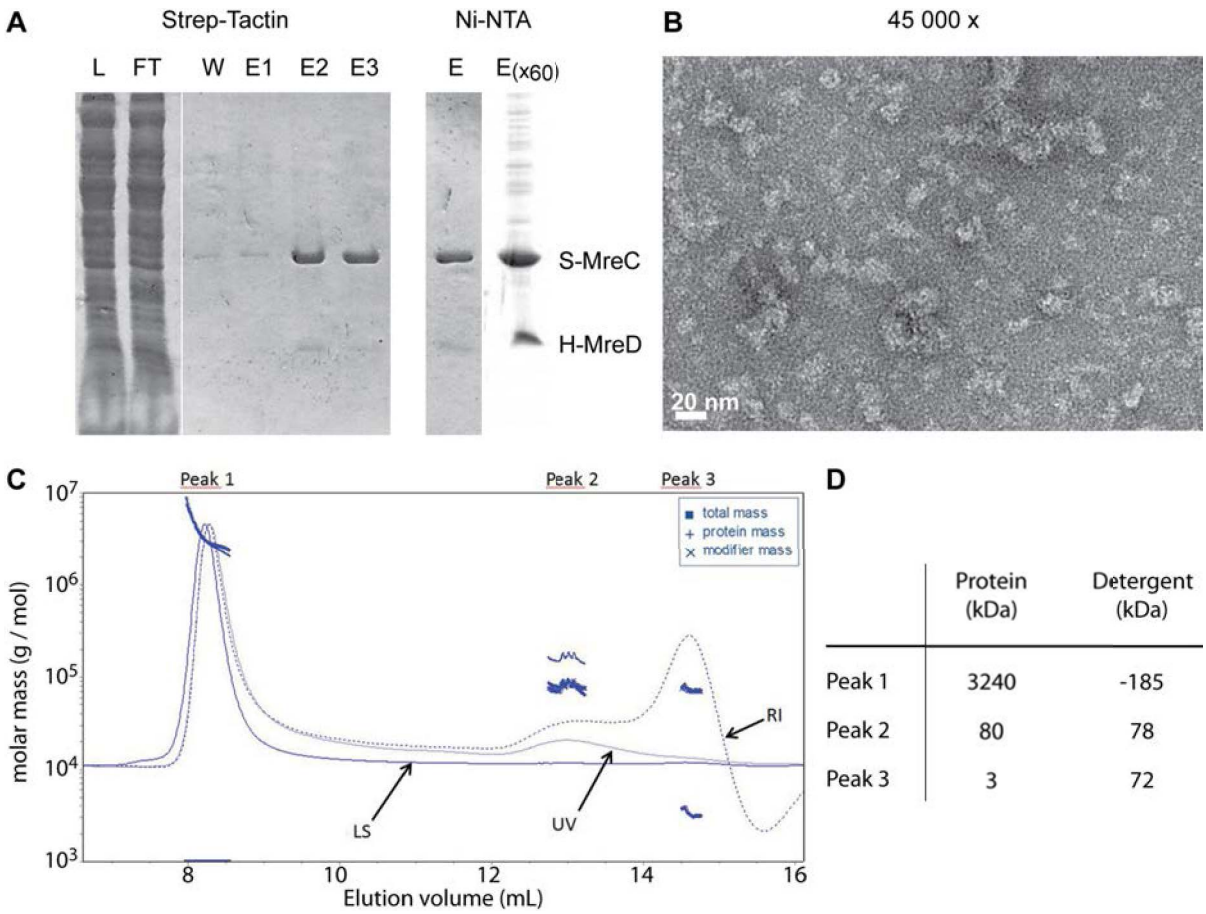


**Figure 33: Isolation of the pneumococcus MreC/MreD complex. Strep-tagged MreC and His-tagged MreD were co-expressed in *E. coli*, membrane were isolated and solubilized before two successive purification steps, first on Strep-Tactin®, then by Ni-NTA chromatography. A: Coomassie-stained SDS-PAGE analysis of the purification steps. L: load, FT: flow-through, W: wash, E: elution. B: electron microscopy picture of the Ni-NTA elution fraction after negative staining. C: SEC-MALLS profile of the Ni-NTA elution fraction concentrated 60 times. LS: light scattering, UV: ultra-violet, RI: refractive index. D: analysis of the three peaks detected in SEC-MALLS.**

(UV), multi-angle laser light scattering (MALLS), quasi-elastic light scattering (QELS) and refractive index (RI). This was carried out with the Protein Analysis On Line platform (PAOL, Aline Leroy, Christine Ebel). Three distinct fractions were separated (Figure 33C and D). The first fraction contained aggregates with a high protein molar mass (> 3000 kDa) and comparatively negligible amounts of detergent (non-relevant negative values). The second peak included particles with 80 kDa of proteins and 78 kDa of detergent. This could correspond to a protein heterotrimer comprised of two MreC molecules (2 x 30 kDa) and one MreD molecule (20 kDa) in a micelle of DDM (78 kDa). Note that the molecular weight of a micelle of DDM is estimated to be 50 kDa, but the presence of inserted proteins may increase the number of detergent molecules in the micelle, hence its weight. The last peak contained mostly detergent (72 kDa), probably comprised of detergent micelles and some protein degradation fragments (3 kDa). This analysis was performed only once and no estimation of the error was obtained.

The stoichiometry of the purified complex comprising MreC and MreD was estimated by densitometry analysis of the bands observed on SDS-PAGE (Figure 34). To discard single tagged proteins interacting with the resin, the two purification steps described above were performed as described in the Material and Methods. Also, these purification steps were performed in the two possible orders, Ni-NTA – Strep-Tactine® (N1S2), or Strep-Tactine® - Ni - NTA (S1N2) and both results were analyzed with ImageJ. The intensity of the bands corresponding to each protein was normalized according to their respective size, assumed to be proportional to their intrinsic ability to bind Coomassie blue (Figure 34, bottom table). In both cases, the ratio MreC / MreD was close to 1, differing from the SEC-MALLS analysis. Protein concentration was low and the density curves showed low signal to noise ratio.

The purification of the complex including MreC and MreD from *S. pneumoniae* has been reported in the review on the elongation of ovococci (Philippe*, et al.*, 2014).

### *MreC/MreD/PBP2b/RodA*

Two complexes comprising pneumococcus elongation proteins have been purified: MreC/MreD and RodA/PBP2b. Both include one bitopic membrane protein (PBP2b or MreC) and one integral membrane protein with multiple transmembrane segments (TM): RodA (10 TM) and MreD (5 predicted TM). The two latter are heat-sensitive, as shown by the fact that good SDS-PAGE analysis of those proteins is not possible if the samples are boiled before electrophoresis, and if the gel is not cooled during the run, in the case of MreD. Also, to avoid protein precipitation, the presence of detergent in all the proteins purification steps was required. This made analysis difficult as

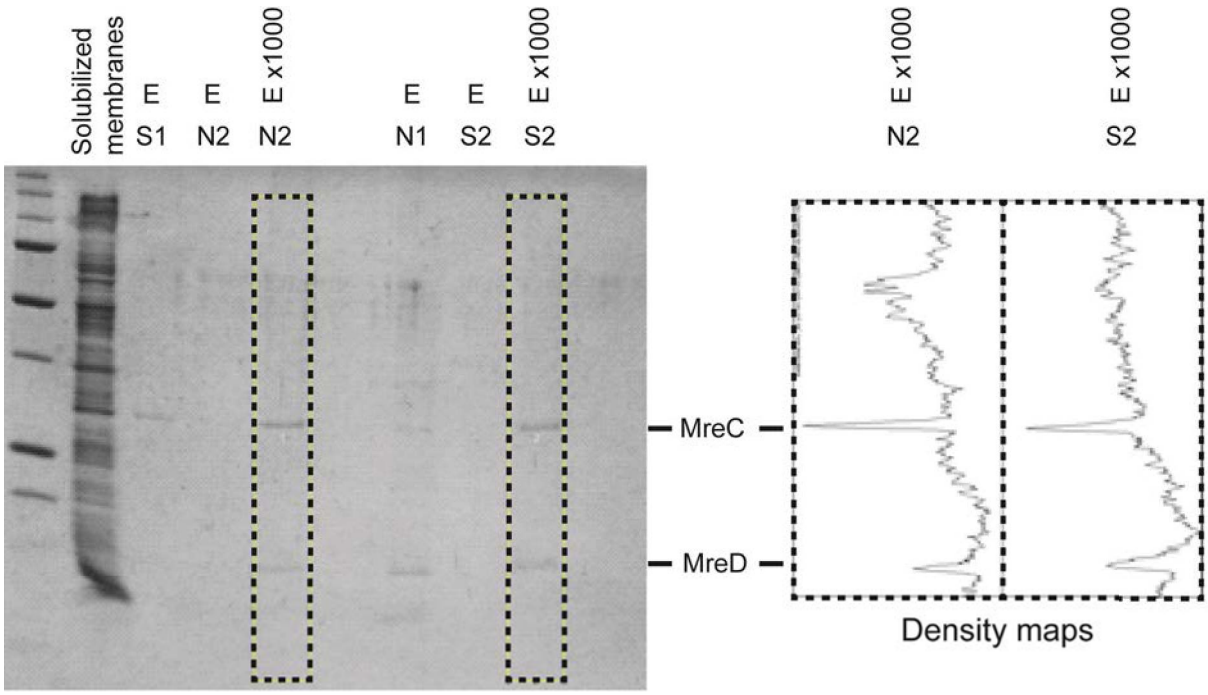


| Purification | Band | Intensity | Ratio MC/MD | Normalized* | Normalized ratio* |
|---|---|---|---|---|---|
| $S_1N_2$ | MreC | 2078 | 1.8 | 0.07 | 1.2 |
| | MreD | 1146 | | 0.06 | |
| $N_1S_2$ | MreC | 2007 | 1.2 | 0.07 | 0.8 |
| | MreD | 1629 | | 0.08 | |

*intensity / protein size (MreC = 29.738 kDa, MreD = 19.324 kDa)

**Figure 34: Densitometry analysis of purified recombinant MreC/MreD complex. Strep-tagged MreC and His-tagged MreD were co-expressed in *E. coli*, the membrane were isolated and solubilized before two successive purification steps, first on Strep-Tactin®, second on Ni-NTA chromatography (S1N2, left) or the opposite way (N1S2, right). The density curves of the elution fractions were generated with ImageJ (top-right), the area of the peaks were measured and normalized according to the theoretical size of the proteins (bottom). E: elution, S: Strep-Tactin®, N: Ni-NTA, MC: MreC, MD: MreD.**

detergents often interfere with measures routinely performed on proteins. For these reasons, handling these proteins individually is difficult, and their co-purification is even more challenging. The Conditions must be found: not too harsh to preserve the complex, but not too mild to keep the proteins soluble. Optimization of the expression and purification conditions is not always described in the following results, but was always necessary to obtain good results.

To further test the elongasome model, the next step was to investigate the possibility of a complex including MreC, MreD, RodA and PBP2b. As above, the strategy utilized was to reconstitute it *in vitro*, using recombinant *S. pneumoniae* proteins expressed in *E. coli* and purified successively in two distinct chromatography steps.

The first expression vector utilized was pETduet-MCHMD-RA2bS, which contains two operons under the control of identical IPTG-inducible T7 promotors. The first operon encodes MreC and MreD with a N-terminal $His_8$-tag. The second contains RodA and PBP2b with a C-terminal Strep tag. A single Ni-NTA purification step was first performed to avoid multiple steps and obtain sufficient amounts of proteins for Coomassie revelation. The four proteins were recovered after this purification step (Figure 35). Their identity was confirmed by western blot performed with antibodies anti-MreC, anti-His (to detect MreD), anti-RodA and anti-PBP2b (Figure 35). Note that once again, the gels were cooled to allow proper MreD migration (Figure 35, bottom panel). Several protein contaminants co-eluted with the presumed complex. Also of note is that the antibody anti-PBP2b does not seem to be highly specific of this protein as multiple bands of higher and lower molecular weight than PBP2b (74 kDa) were revealed. These bands detected in western blot could also be due to aggregation or degradation of PBP2b, however, this is unlikely as anti-Strep antibodies revealed a single band (not shown).

A control was performed to confirm that the proteins eluted were present due to specific protein interactions in a complex, rather than non-specific binding to the chromatography matrix. It was already shown that MreC does not interact with the Ni-NTA resin by itself (Figure 32B). Similarly, a plasmid with an operon encoding RodA and PBP2b with a Strep-tag in C-terminus (pETduet-RA2bS)

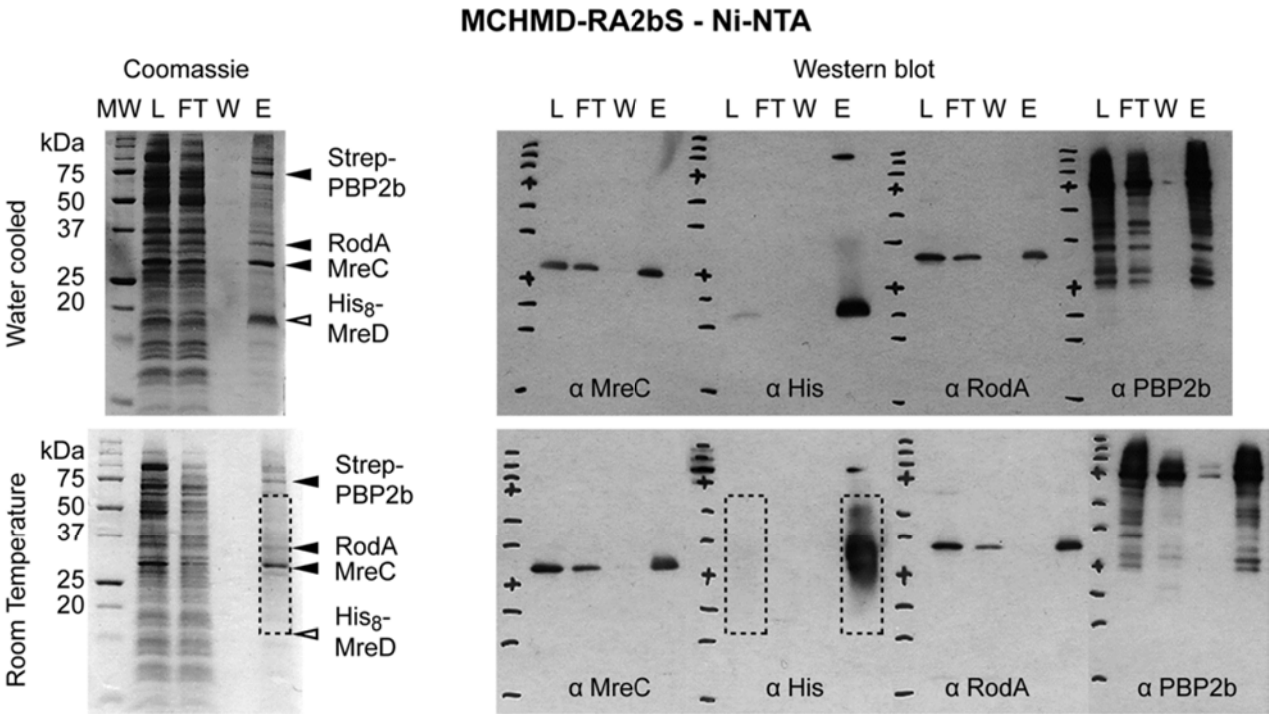


**Figure 35: Isolation of the pneumococcus complex MreC/MreD/RodA/PBP2b. MreC, His-tagged MreD, RodA and Strep-tagged PBP2b were co-expressed in *E. coli*, membranes were isolated and solubilized before purification on Ni-NTA. Coomassie-stained SDS-PAGE and Western blot analysis of the purification are shown. MW: molecular weight, L: load, FT: flow-through, W: wash, E: elution, α …: antibody + its target. The open arrows show the protein by which the complex was pulled down. The dashed area shows the smear of precipitated MreD.**

was used to verify that these proteins do not interact with the Ni-NTA resin. After transformation into *E. coli*, expression, membrane isolation and solubilization, these proteins were applied to a Ni-NTA chromatography and submitted to the same protocol as above. RodA did not interact with the resin. However, a fraction of PBP2b interacted non-specifically with the resin (Figure 36). However, the fraction of PBP2b recovered using this protocol was small compared with that recovered in presence of MreC and $His_8$-MreD (compare Figure 35 and Figure 36). Moreover, this PBP2b bound fraction did not pull down RodA in this assay.

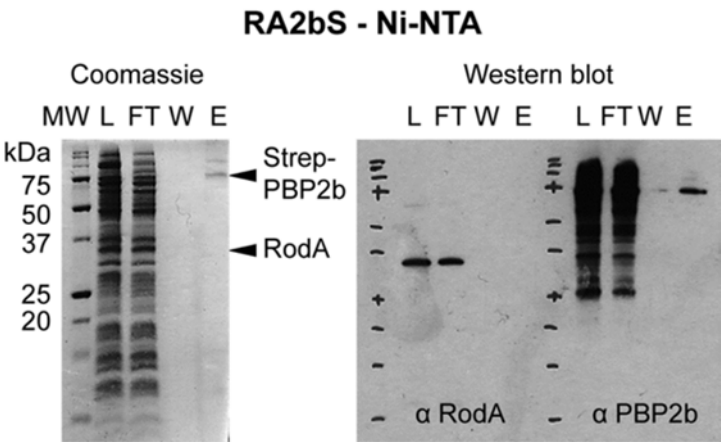


**Figure 36: Negative control of unspecific binding of RodA and PBP2b-Strep to the Ni-NTA resin. The same protocol was utilized as in Figure 35 with only RodA and PBP2b with a C-terminus Strep-tag. MW: molecular weight, L: load, FT: flow-through, W: wash, E: elution, α …: antibody + its target.**

These controls tend to confirm that the proteins observed in the elution of the purification of the complex including RodA, PBP2b, MreC and MreD are pull-down by protein interactions rather than non-specific binding of the proteins to the resin. However, the presence of protein contaminants casts doubt on the specificity of interaction between the tested proteins. In this experimental setup, the recombinant proteins are over-expressed in *E. coli*. The possibility that these proteins, which are artificially in high amounts in the membranes, would interact through their hydrophobic TM segments cannot be excluded. Therefore, better purification was pursued, and negative controls including over-expressed membrane proteins that are not expected to interact were performed. Concerning the purity, an attempt of purification on a cobalt resin was done, as it is known to provide better purity. However, the purification yield was very low and did not allow the observation of the proteins in the SDS-PAGE analysis of the elution fractions (not shown). As for the complex MreC/MreD, two successive purification steps were thus performed using the same vector (first on Ni-NTA, second on Strep-Tactine®). The results were very similar to those in Figure 35, except that the elution fraction was to be concentrated 50 x in order to visualize the proteins on the gel (not shown). The controls including other membrane proteins are shown further in this chapter.

Given the good purity of the complexes obtained using the pETduet-SMCHMD expression vector (Figure 33), a new construct was designed with a single large operon encoding RodA, PBP2b, MreC with a N-terminal Strep-tag and MreD with a N-terminal $His_8$ tag: pET30-RA2bSMCHMD. However, the expression of the four proteins was too low using this vector, which did not enable to

recover enough proteins in the elution of the purification, even after the first step of purification in both orders (not shown). Therefore, this large operon was transferred into the first multiple cloning site (MCS) of the pETduet vector, resulting in pETduet-RA2bSMCHMD.

Using this expression vector, the 4 proteins were recovered in elution in the two orders of purification: Ni-NTA followed by Strep-Tactine® (N1S2), or reversed (S1N2) (Figure 37A). The elution fraction of the second purification step had to be concentrated to become visible for SDS-PAGE analysis. Some contaminants were also recovered after this protocol, but the purity was better than that observed with pETduet-MCHMD-RA2bS. Note that a contaminant appeared around 70 kDa in the S1N2 experiment that was absent in the N1S2 experiment. The analysis of the density of the bands in either conditions suggests a protein ratio PBP2b:RodA:MreC:MreD of 1:1:4:4 (Figure 37B).

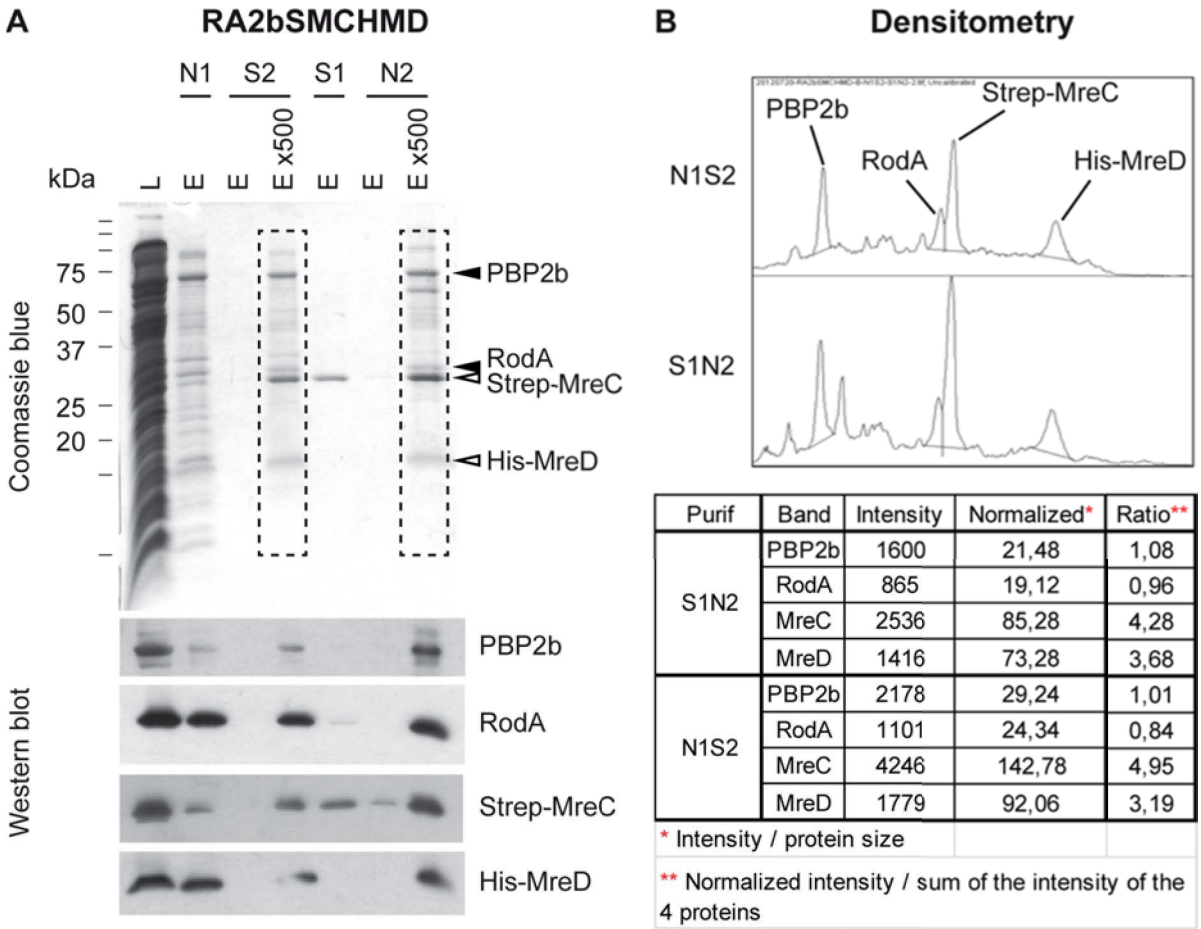


| Purif | Band | Intensity | Normalized* | Ratio** |
|---|---|---|---|---|
| S1N2 | PBP2b | 1600 | 21,48 | 1,08 |
| | RodA | 865 | 19,12 | 0,96 |
| | MreC | 2536 | 85,28 | 4,28 |
| | MreD | 1416 | 73,28 | 3,68 |
| N1S2 | PBP2b | 2178 | 29,24 | 1,01 |
| | RodA | 1101 | 24,34 | 0,84 |
| | MreC | 4246 | 142,78 | 4,95 |
| | MreD | 1779 | 92,06 | 3,19 |

* Intensity / protein size

** Normalized intensity / sum of the intensity of the 4 proteins

**Figure 37: *In vitro* reconstitution of the recombinant pneumococcus membrane protein complex MreC/MreD/RodA/PBP2b. A: Strep-tagged MreC, His-tagged MreD, RodA and PBP2b were co-expressed in *E. coli*, membranes were isolated and solubilized before two successive purification steps, first on Strep-Tactin®, second on Ni-NTA chromatography (S1N2) or the opposite way (N1S2). Coomassie-stained SDS-PAGE and western blot analysis of the purifications are shown. L: load, E: elution, S: Strep-Tactin®, N: Ni-NTA. B: Density curves of the elution fractions surrounded by in dashed rectangles in A. The area of the peaks were measured and normalized according to the theoretical size of the proteins (PBP2b: 74.5 kDa, RodA: 45.2 kDa, MreC: 29.7 kDa, MreD: 19.3 kDa).**

All together, these results support the possibility that the elongation proteins PBP2b, RodA, MreC and MreD form a complex. However, some contaminants were always recovered after co-purification of the 4 proteins, in a larger extent than those found in the samples of the complex MreC/MreD, which calls the specificity of the interaction into question. Negative controls were therefore required to validate these preliminary results.

### *MreC/MreD/PBP2x/FtsW*

In the morphogenesis model I intended to test, PBP2x and FtsW belong to a distinct protein complex than MreC and MreD (the divisome and the elongasome, respectively). A good negative interaction control would be to co-express those four proteins to check that they cannot be co-purified. To reduce the amount of expresssion vectors to build, we reasoned that we could mix *E. coli* membrane samples prepared by over-expression of either MreC/MreD or FtsW/PBP2x, and apply the co-purification protocol as previously. A positive control was first performed in which *E. coli* membranes containing the recombinant MreC/MreD complex were mixed with membranes from cells expressing RodA/PBP2b to validate the system (see Material and Methods). Membranes were isolated as usually after over-expression from pETduet-MCHMD or pETduet-RA2bS in *E. coli*. A mixture of these membranes was solubilized and the proteins were purified successively on Ni-NTA and Strep-Tactine®. The four proteins were successfully co-purified with this protocol, accompanied by protein contaminants (Figure 38A).

The same protocol was applied with pET30-FW2xS to produce membranes containing FtsW and PBP2x with a N-terminal Strep-tag instead of RodA and PBP2b-S. The purification steps were performed in both orders, (N1S2 and S1N2). Interestingly, the four proteins were co-eluted in both experiments (Figure 38B), suggesting that they do interact with each other (note that contaminants were again recovered in elution). A control was performed to verify whether or not PBP2x-Strep and FtsW interact with the Ni-NTA matrix in a non-specific manner. Similar to PBP2b-Strep, PBP2x-Strep interacted non-specifically to some extent with the resin (Figure 38C). However, more PBP2x was recovered in presence of MreC and MreD, suggesting that this non-specific binding to the resin was only responsible for the recovery of negligible amounts of the protein in the co-purification assay that includes the 4 proteins. Also, no FtsW was found in the elution fraction.

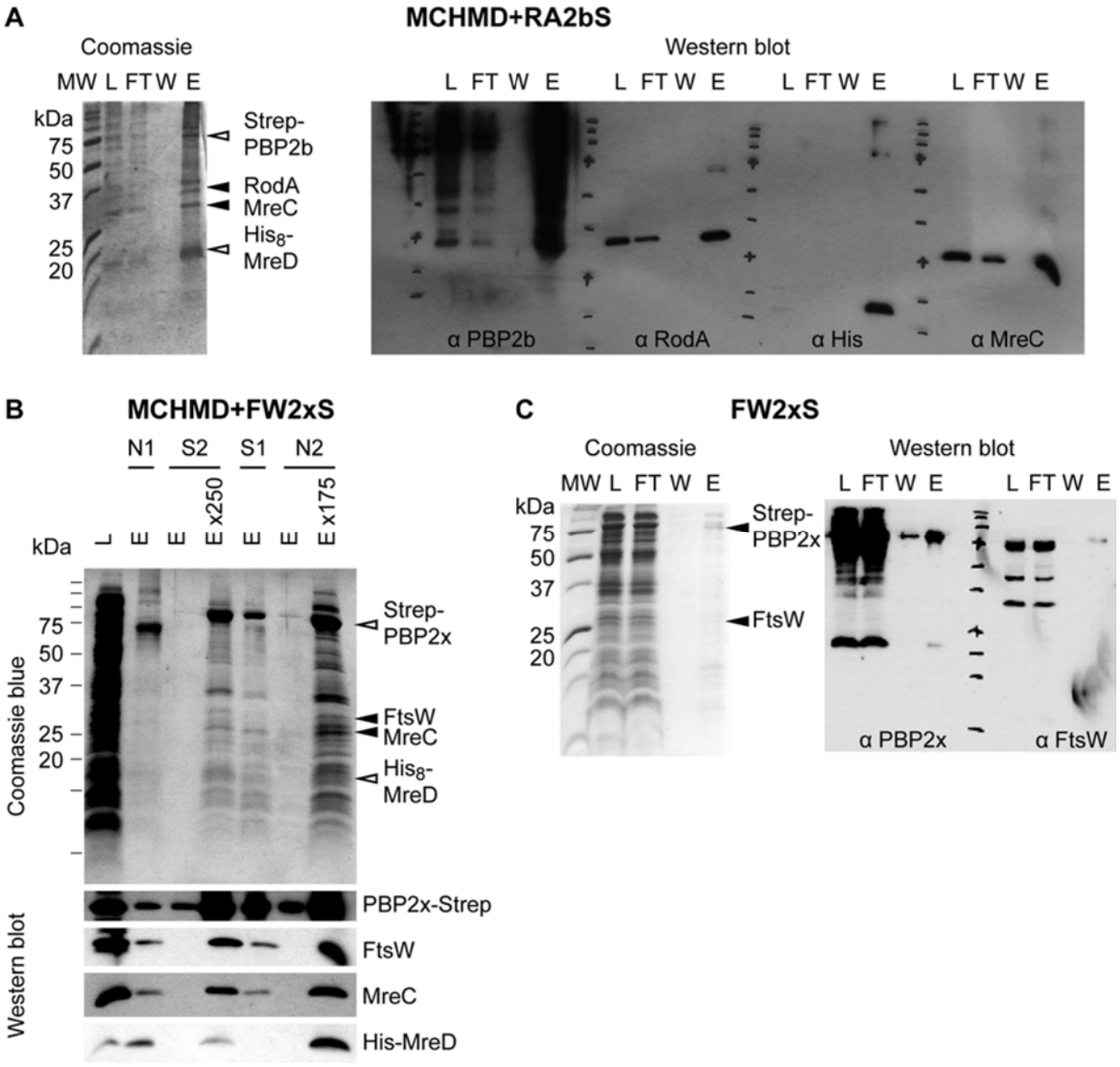


**Figure 38: FtsW and PBP2x interact with MreC and MreD. A: a mix of *E. coli* membranes containing either RodA and PBP2b with a N-terminus Strep-tag or MreC and MreD with a C-terminus $His_8$-tag were solubilized and purified successively on Ni-NTA and Strep-Tactin®. A Coomassie-stained SDS-PAGE analysis and a western blot of the Strep-Tactin® purification are shown. B: Same experiment with membranes containing FtsW and PBP2x with a N-terminus Strep-tag instead of those containing RodA and PBP2b. The two purification steps were performed in both orders. The last elution fraction was concentrated as indicated on the figure. Coomassie-stained SDS-PAGE analysis and a western blot of relevant fractions are shown. C: control of unspecific binding of FtsW and PBP2x-Strep to the Ni-NTA resin. Coomassie-stained SDS-PAGE analysis and a western blot of relevant fractions are shown. MW: molecular weight, L: load, FT: flow-through, W: wash, E: elution, α …: antibody + its target. The open arrows show the proteins by which the complex was pulled down.**

### *MreC/MreD/RodA/PBP2b/FtsW/PBP2x*

Given the unexpected co-purification of PBP2x with MreC/MreD, a competition assay was performed by mixing three distinct membrane samples. The first contained MreC and MreD with a

$His_8$-tag in N-terminus, the second contained RodA and PBP2b with a Strep-tag in C-terminus, and the third contained FtsW and PBP2x with a Strep-tag in C-terminus. After solubilization of the three membrane samples together, the proteins were purified successively on Ni-NTA and Strep-Tactine®. The low quantity of purified proteins did not allow clear observation on SDS-PAGE revealed with Coomassie blue. Nevertheless, all the proteins seemed to co-elute in both the first and second purification step, as shown by western blot (Figure 39).

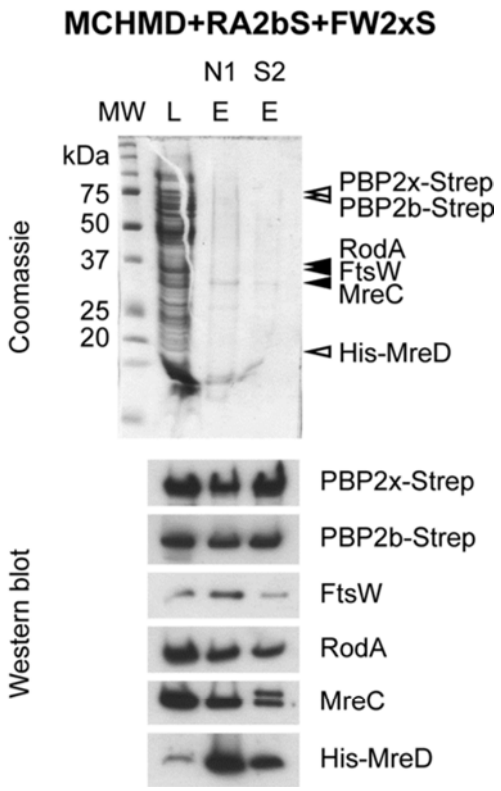


**Figure 39: Co-purification of PBP2b, PBP2x, RodA, FtsW, MreC and MreD. Three membrane samples containing MreC and H-MreD, RodA and PBP2b-S or FtsW and PBP2x-S were solubilized together before Ni-NTA and Strep-Tactine® successive purifications. SDS-PAGE and western blot analysis are shown. MW: molecular weight, L: load, E: elution. Open arrows show the proteins by which the complex was pulled down.**

Note that adding three membrane samples also bring three times more *E. coli* membrane protein contaminants. However, dividing the amount of membrane added by three would result in lower amounts of the proteins of interest. Further development of the purification conditions should be performed to obtain higher concentrations of proteins, which would allow better purity and assessment of the interactions.

### *MreC/MreD and DivIB/DivIC/FtsL*

The above experiments lacked a definitive negative control to validate the existence of the complexes. Also, available to us, the division complex DivIB/DivIC/FtsL would constitute a good control if it does not interact with the complex MreC/MreD. *E. coli* membranes with MreC/MreD were prepared by overexpression of the proteins from the vector pETduet-SMCHMD. Similarly, pETduet-ICFLIB that encodes DivIC, FtsL and DivIB without tag was used to generate membranes containing these three proteins. As above, those membrane preparations were mixed and solubilized, to be purified on Ni-NTA and Strep-Tactine® successively. The first purification step allowed the purification of a complex MreC/MreD and some residual proteins of DivIB, DivIC and FtsL (Figure 40). However, it seems that the latter three proteins were recovered to a lower extent.

Indeed, comparison between the intensity of the loaded and eluted fractions reveals that MreD is concentrated during this purification step (which is expected as it is the tagged protein) and MreC is found at the same concentration in the elution as in the load. By contrast, DivIB, DivIC and FtsL are diluted in the elution fraction compared to the load, suggesting that they might interact, but in a lower extent than MreC/MreD. The next purification step allowed MreC purification, but did not allow recovery of the four other proteins. It is surprising that MreD did not appear in the elution of the Strep-Tactin chromatography, since we know that MreC and MreD form a complex. This experiment yielded proteins not visible by Coomassie staining and at the limit of detection by western blot. The absence of interaction between the complexes MreC/MreD and DivIB/DivIC/FtsL is likely, but the conditions of purification should be improved to obtain clearer results.

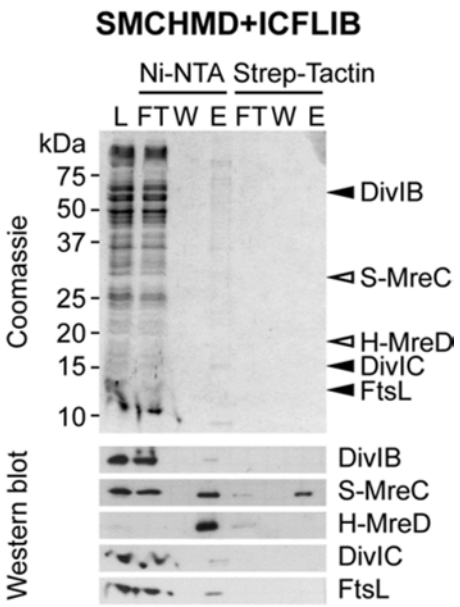


**Figure 40: MreC/MreD do not seem to interact with DivIB/DivIC/FtsL. Two membrane samples containing S-MreC and H-MreD or DivIB, DivIC and FtsL were solubilized together before Ni-NTA and Strep-Tactine® successive purifications. SDS-PAGE and western blot analysis are shown. L: load, FT: flow through, W: wash, E: elution. Open arrows show the proteins by which the complex was pulled down.**

## *Concluding remarks*

Altogether, the experiments presented above reveal that some pneumococcus morphogenesis proteins can form stable complexes that can be isolated (PBP2b/RodA, MreC/MreD).

The work with membrane proteins is a hard task for several reasons. First, the use of appropriate detergent is required to allow solubilization and retain proper folding of the proteins. Experience on membrane proteins handling tends to show that the conformation of the membrane proteins in detergent suffers from constraints imposed by the distinct properties of the detergent compared to their natural lipidic environment. Moreover, the detergent micelle can impair the proper interaction of a tagged protein with a chromatography resin or a protein partner.

To avoid this problem, I attempted to insert MreC, MreD, RodA and PBP2b into nanodiscs in collaboration with Yann Huon de Kermadec (PhD student at the IBS). However, the use of nanodiscs imposes multiple steps of purification that dilute the sample. Preliminary experiments were not promising and I did not pursue this method.

Another problem with membrane proteins is that over-expression is often toxic for the cell, which impose to lower the expression level in bacteria. In the work presented above, this problem was clearly encountered. This can be observed by the fact that the over-expressed proteins were rarely observable in the solubilized membranes analyzed on Coomassie-stained SDS-PAGE (see loaded fractions of the figures).

An emerging method allows to by-pass the problems of bacterial membrane proteins expression: the cell-free expression system. In this system, a cell extract is used to express proteins from DNA expression vectors. This aproach eliminates the problems of toxicity and the need of isolating membranes (thus, time-effective). Therefore, I tried to use this technique to determine whether a MreC/MreD/RodA/PBP2b complex could be reconstituted with proteins from *S. pneumoniae*.

## Cell-free expression

In order to determine whether the cell-free system enables the expression of MreC, MreD, RodA and PBP2b, an expression test was performed by Lionel Imbert, responsible of the cell-free platform at the IBS. The system used is based on a cell extract from *E. coli*. The expression vector used for this test was pETduet-RA2bSMCHMD, as it has the same inducible promoter (T7) than the pIVEX vectors (optimized for cell free expression). This test enabled the expression of all proteins except MreD (not shown). The lack of expression of the gene *mreD* was likely related to its last position in the operon encoded by the vector utilized. Interestingly, the expression was better in the absence of detergent, a common observation using the cell free system. Also, the cell free expression of membrane proteins without detergent results in the accumulation of a precipitate that can be subsequently solubilized by adding detergent. This method has been reported to produce good quality proteins that were active in various assays (reviewed in (Klammt*, et al.*, 2006)).

A second preliminary test was performed with the vector pETduet-MCHMD-RA2bS in which the genes are in two distinct operons under the control of a T7 promoter. This was expected to enable better expression of MreC and MreD. Once again, all proteins were expressed except MreD. We hypothesized that this was due to the fact that MreD did not support the absence of detergent. I reasoned that the use of pIVEX vectors, which are supposed to permit better protein expression in

the cell free system, would allow the presence of detergents, or would simply result in greater amounts of MreD, enabling its recovery even in absence of detergent. Also, these tests allowed to verify that the expression of MreC, RodA and PBP2b was possible even using a vector that was not optimized for cell free. Thus, I decided to construct the vectors required for the observation of a complex comprising MreC, MreD, RodA and PBP2b.

### *pIVEX vectors*

The pIVEX vectors are optimized for the expression of recombinant proteins in cell free. Four vectors were constructed: pIVEX-MC (coding for MreC), pIVEX-HMC (MreC with a $His_8$-tag in N-terminus), pIVEX-HMD (MreD with a $His_8$-tag in N-terminus) and pIVEX-SMCHMD (containing an operon coding for MreC with a Strep-tag in N-terminus and MreD with a $His_8$-tag in N-terminus). The aim was to compare the expression of MreC and MreD when performed separately or in a single experiment, which was carried out by mixing two distinct vectors in a reaction or by using a single vector with both proteins in operon.

### *Expression test*

The expression of MreC and MreD from the designed pIVEX vectors was first tested by the cell free platform (Lionel Imbert). A preliminary test was performed in absence of detergent to monitor the expression. All vectors allowed expression of the encoded proteins (Figure 41A). Note that a smear detected by western blot with anti-His antibodies appeared at the level of MreD even when no vector encoding MreD was present. The source of this problem was not identified but further experiments showed that MreD was indeed expressed (see below). Also, MreC with a Strep-tag was not be detected in this experiment as only one anti-His antibody was used. S-MreC expression was confirmed with anti-MreC antibodies in further experiments (data not shown). The addition of several detergents was tested during expression to allow better folding of the proteins. Two detergents utilized in routine in cell-free system were applied to the test (Brij35 and Brij58) as well as DDM, which successfully solubilized MreC and MreD expressed in *E. coli*. The supernatant of the reactions was analyzed (Figure 41B). MreC was successfully solubilized by all the detergents tested. The smear present around MreD impaired the analysis of the expression of this protein. Thus, another expression test was performed only with pIVEX-HMD (Figure 41C). The gel was carefully cooled during the run to avoid precipitation of MreD. It revealed that MreD was expressed in absence of detergent, with PEG (polyethylene glycol) or with DDM, but was not successfully solubilized by DDM. The other detergents did not allow MreD expression.

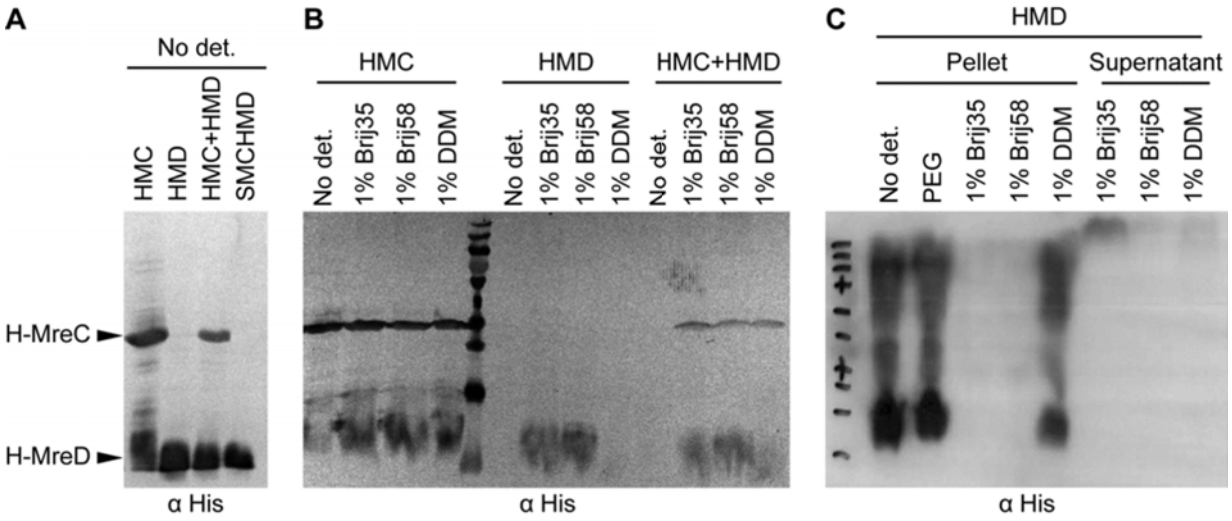


**Figure 41: Cell free expression of MreC and MreD. A: Feasibility expression test with no detergent. One microgram of pIVEX-MCH, pIVEX-MDH, 0.5 µg of each or 1 µg of pIVEX-SMCHMD were added to a 50 µL cell free reaction mix and expressed for 3 h at 37°C in absence of detergent. After centrifugation, the pellets were resuspended in Laemmli and analyzed by SDS-PAGE and western blot. B: Same as in A except that some detergents were added as indicated and the supernatants were analyzed. C: Same as B with detergents or PEG (polyethylene glycol) as indicated, and pellet and supernatant fractions are analyzed. det.: detergent.**

Given these observations, I decided to express MreC and MreD in precipitate, and solubilize them prior to purification. Two detergents were shown to successfully solubilize both proteins produced in *E. coli* in an independent detergent screen performed with the RoBioMol platform (Anne Marie Villard and Marjolaine Noirclerc-Savoye): LAPAO and FosC12, data not shown). After expression in precipitate cell-free, both proteins were successfully solubilized by both detergents (data not shown).

### *Purification of MreC and MreD after cell free expression*

After cell-free protein expression using pIVEX-HMC, pIVEX-HMD or pIVEX-SMCHMD in precipitate cell-free, the proteins were solubilized with LAPAO or FosC12 and subsequently purified on Ni-NTA (Robiomol, Anne Marie Villard, Marjolaine Noirclerc-Savoye). The proteins expressed independently were successfully purified, but not the complex (Figure 42). An interesting strategy to follow would be to solubilize MreC and MreD with LAPAO or FosC12 after precipitate cell free expression, and to exchange the detergent for a "softer" one before purification. The DDM or the MNG3 (Maltose–neopentyl glycol 3) would be good candidates as they were also shown in the detergent screen to be adapted to SMCHMD co-purification.

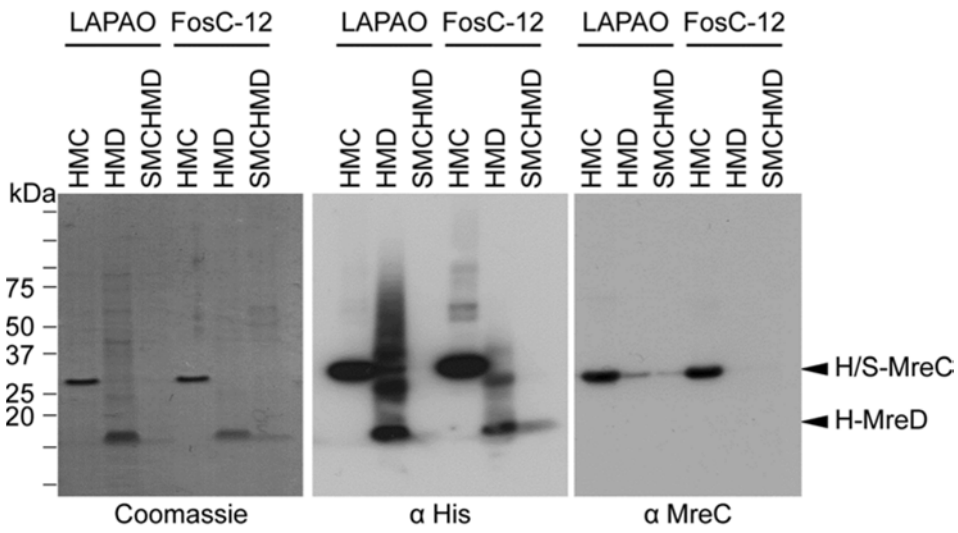


**Figure 42: Purification of MreC and MreD after cell free expression. MreC and MreD from different constructs were expressed in precipitate cell free and solubilized with LAPAO or Fos-C-12. Coomassie-stained SDS-PAGE and western blot are shown. H: histidine tag, S: strep tag.**

## Concluding remarks and perspectives

Altogether, the results presented in this part strongly support the formation of complexes including several morphogenesis proteins of the pneumococcus. The *in vitro* reconstitution of a complex comprised of pneumococcus MreC and MreD was reproducible and could be obtained in substantial concentration. Similarly, a complex of recombinant PBP2b and RodA could be isolated. However, the isolation of a stable complex MreC/MreD/RodA/PBP2b remains uncertain. Protein contaminants were always co-eluted with the complex, which casts doubts on the protein specificity of the interaction. A negative protein interaction control was obtained by showing that the MreC/MreD complex does not interact with the DivIB/DivIC/FtsL complex. The validity of this control is questionable as protein concentrations were very low.

Doubt is cast on the significance of the isolation of the complex MreC/MreD/RodA/PBP2b as two complexes containing FtsW, PBP2x along with elongation proteins were also isolated (MreC/MreD/FtsW/PBP2x and MreC/MreD/FtsW/PBP2x/RodA/PBP2b, respectively). Once again, many contaminants were presents. It is possible that since the purified tagged proteins are mostly aggregated, the co-purification of un-tagged proteins is arte-factual and biased towards recombinant overexpressed proteins. Alternatively, such recombinant complexes may have been truly isolated, but represent either true complexes that form in vivo, or artefacts of heterologous expression. The first case cannot be excluded as these proteins are mostly co-localized, even if they are ascribed to different processes. PBP2x and FtsW, may indeed interact with proteins of the elongation. In the

second case, the interaction may be real in the recombinant system, due to the fact that PBP2x and FtsW are homologues and resemble PBP2b and RodA, respectively. This interaction would not be representative of true interaction occurring in pneumococcus in the presence of all the other proteins and molecular components.

As an alternative to the recombinant strategies presented above, I attempted the co-immuno-precipitation of several members of the speculated complex from growing *S. pneumoniae* cells. The idea was to isolate pneumococcus membranes, solubilize them and immuno-precipitate proteins by the use of anti-MreC antibodies. MreC immuno-precipitation was successful, but none of PBP2b, RodA, PBP2x, FtsW, DivIB, DivIC and FtsL was co-immuno-precipitated in this assay (data not shown). The low protein concentration in the membranes (no over-expression) would have required antibodies with greater affinity.

The cell-free expression system has one drawback: it is expensive. However, it has the advantage of eliminating the problems of membrane protein over-expression toxicity and is time-effective. Also, it allows screening of many protein combinations by theoretically adding as many expression DNA vectors as desired in the expression reaction. Cell free-optimized pIVEX vectors were constructed and preliminary experiments showed promising results. The pIVEX vectors are now available at the laboratory for further investigations.

## Synthèse de peptidoglycane de pneumocoque *in vitro* – résumé

Un moyen de comprendre le fonctionnement d'un mécanisme moléculaire est de le reconstituer *in vitro*. Le développement d'un test de synthèse de peptidoglycane *in vitro* est essentiel pour étudier la morphogénèse du pneumocoque. Au début de ma thèse, ce type de test était déjà utilisé pour la synthèse de peptidoglycane par des PLPs d'*E. coli* mais n'avait jamais fonctionné avec des enzymes de bactéries à Gram positif. L'identification des enzymes responsables de l'amidation du glutamate du lipide II (ou LII) a débloqué ce champ de recherche. En effet, une des particularités du peptidoglycane des bactéries à Gram positif est qu'il présente, en deuxième position du peptide impliqué dans liaison des chaînes glycanes dans le sacculus, une glutamine (alors qu'un glutamate est retrouvé chez les Gram négatifs). L'utilisation de lipide II amidé (ou aLII) a permis la synthèse de peptidoglycane *in vitro* avec des PLPs de pneumocoque.

La réaction de synthèse utilisée est basée sur le mélange de aLII avec une PLP dans le tampon approprié. Les produits de réaction sont séparés sur gel d'acrylamide, permettant d'identifier les produits de l'activité GT et / ou TP de l'enzyme étudiée. Pour pouvoir détecter les produits de réaction, le lipide II utilisé est en fait un mélange de aLII et un variant du lipide II couplé à un fluorophore, le dansyl (ou LII-DNS). L'illumination du gel aux ultra-violets permet de détecter les bandes correspondant aux différents produits de réaction.

Le développement d'un test pour déterminer l'activité des PLPs de pneumocoques a nécessité une collaboration. Le LII a été acheté à BaCWAN (Université de Warwick) et a été amidé par André Zapun (IBS). Le LII-DNS a été synthétisé par moi-même au sein du laboratoire d'Eefjan Breukink (Université d'Utrecht). Les PLPs ont été purifiées au sein du laboratoire par André Zapun et moi-même à l'exception de PBP1a, fourni par David Roper (Université de Warwick). Enfin, le test a été mis au point et utilisé pour déterminer et caractériser l'activité de 4 PLPs (PBP1a, PBP2a, PBP2b et PBP2x) au laboratoire par André Zapun et moi-même.

Dans cette partie, je présente tout d'abord les réactions de synthèse, de purification et de dansylation du lipide II. Brièvement, la synthèse est effectuée par une réaction entre le UDP-NAG, le précurseur UDP-NAM-pentapeptide et un undécaprényl-phosphate catalysée par les enzymes MurG et MraY. Le lipide II est ensuite purifié par chromatographie échangeuse d'ions. Enfin, le fluorophore est ajoutée par chimie click.

L'activité de PBP1a a été étudiée par la suite. Le test effectué a permis de montrer que l'activité de PBP1a est meilleure sur le aLII que sur le LII dans les conditions utilisées. L'étude cinétique de la réaction a montré que les activités GT et TP de PBP1a étaient concomitantes.

La coopération entre PLPs étant été décrite avec des enzymes de *E. coli*, j'ai tenté de vérifier si elle est aussi observable sur les PLPs de pneumocoque, sans pouvoir tirer de conclusions définitives.

Globalement, les activités GT et TP de PBP1a de pneumocoque ont été confirmées *in vitro*. De plus, un test est maintenant disponible pour étudier l'impact de protéines ou de modifications dans la composition du lipide II sur l'activité des PLPs. Ceci pourra par exemple permettre de mieux comprendre le rôle des peptides branchés dans la résistance aux β-lactamines.

## Synthesis of pneumococcus peptidoglycan *in vitro*

To understand the mechanisms governing the synthesis of peptidoglycan, one strategy is to reconstitute it *in vitro*. This has been rendered possible with the development of methods to produce large quantities of lipid II (Breukink*, et al.*, 2003). The incubation of lipid II with PBPs in an appropriate buffer allows peptidoglycan chains elongation and cross-linking by the GT and TP activities, respectively. In SDS-PAGE, the glycan chains produced by the GT activity are separated according to their size. In contrast, the reticulated peptidoglycan chains cross-linked by the TP activity barely enter the gel due to their high molecular weight (Figure 43). To allow detection, a mixture of lipid II and a fluorescent variant of lipid II (with a dansyl moiety on the $Lys_3$, later called LII-DNS) is used, and the gel is revealed under UV illumination. Therefore, SDS-PAGE analysis allows discrimination between the products resulting from TP (high molecular mass material) and GT (intermediary migration) activities.

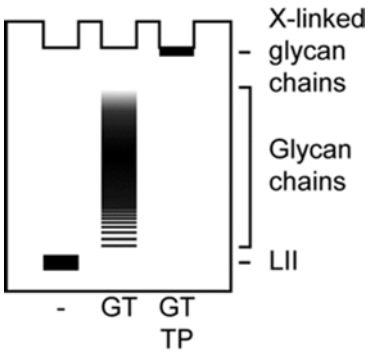


**Figure 43: Cartoon of the SDS-PAGE analysis of the reaction product of an *in vitro* peptidoglycan synthesis assay. GT: glycosyltransferase activity, TP: transpeptidase activity, X-linked: cross-linked, LII: lipid II.**

*In vitro* peptidoglycan synthesis had never been achieved with purified PBPs from Gram-positive bacteria when I began my PhD. Following the identification of the amido transferase complex MurT-GatD in *S. aureus* (Figueiredo*, et al.*, 2012), (Munch*, et al.*, 2012), André Zapun attempted PG in vitro synthesis using amidated lipid II precursor and pneumococcal PBPs. He showed that amidation of lipid II was required for the TP activity of pneumococcus PBPs, which enabled for the first time assembly of peptidoglycan with PBPs from a Gram-positive organism *in vitro*. Large amounts of lipid II were required to test the activity of pneumococcal PBPs. Unmodified Lys-containing lipid II was purchased from the BaCWAN facility (University of Warwick), which André Zapun (IBS) amidated with the assay he developed. I synthesized LII-DNS in the laboratory of Eefjan Breukink (Department of Biochemistry of membranes at the Utrecht University faculty of Chemistry). Full length PBP2x, PBP2a and PBP2b were purified by André Zapun, and David Roper (University of Warwick) provided us with purified PBP1a. As the activities of these four proteins were to be tested, the tasks were shared. I focused mainly on the activities of PBP1a and tested its co-operation with other PBPs.

In this part, several abbreviations are used when they simplify the reading. LII corresponds to unmodified Lys-containing lipid II, aLII is amidated LII (with an isoglutamine instead of a glutamate in position 2 of the stem-peptide) and LII-DNS stands for dansylated lipid II (a fluorescent variant of lipid II with a dansyl moiety attached to the 3rd residue (Lys) of the stem peptide).

I present hereafter the synthesis of LII, its dansylation and the activity tests I performed using purified recombinant pneumococcal PBPs. The LII-DNS I synthesized at Utrecht University was used in experiments of peptidoglycan synthesis with PBPs from *E. coli* and *S. pneumoniae* reported in (Banzhaf*, et al.*, 2012) and (Zapun*, et al.*, 2013), respectively. The activity test with pneumococcal PBP1a was reported in (Zapun*, et al.*, 2013).

## Lipid II synthesis

The synthesis of LII was performed based on the protocol described in (Breukink*, et al.*, 2003). In brief, it consists in mixing three precursor molecules of the lipid II: the undecaprenyl phosphate, the UDP-Mur*N*Ac-pentapeptide and the UDP-Glc*N*Ac with MurG and MraY, the enzymes required for their assembly. Eefjan Breukink (Utrecht University) provided the undecaprenyl phosphate, obtained by phosphorylation of undecaprenol purified from *Laurus nobiles* leaves as described in (Derouaux*, et al.*, 2011). The UDP-Mur*N*Ac-pentapeptide was brought in a *S. simulans* extract, which was prepared by André Zapun. The UDP-Glc*N*Ac was obtained from Sigma® and I isolated membranes of *M. flavus*, which brought the MraY and MurG activities.

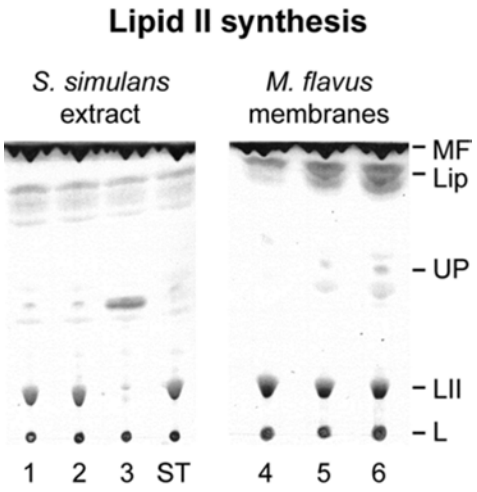


**Figure 44: Iodine-stained TLC analysis of a test of the activity of *S. simulans* extracts and *M. flavus* membranes in lipid II synthesis. Three *S. simulans* extracts (left: 1, 2, 3) and 5, 10 and 15 µL of *M. flavus* membranes were tested (right: 4, 5 and 6, respectively) as described in the Material and Methods. ST: standard with active reagents, L: load spot, LII: lipid II, UP: undecaprenyl phosphate, Lip: lipids, MF: migration front.**

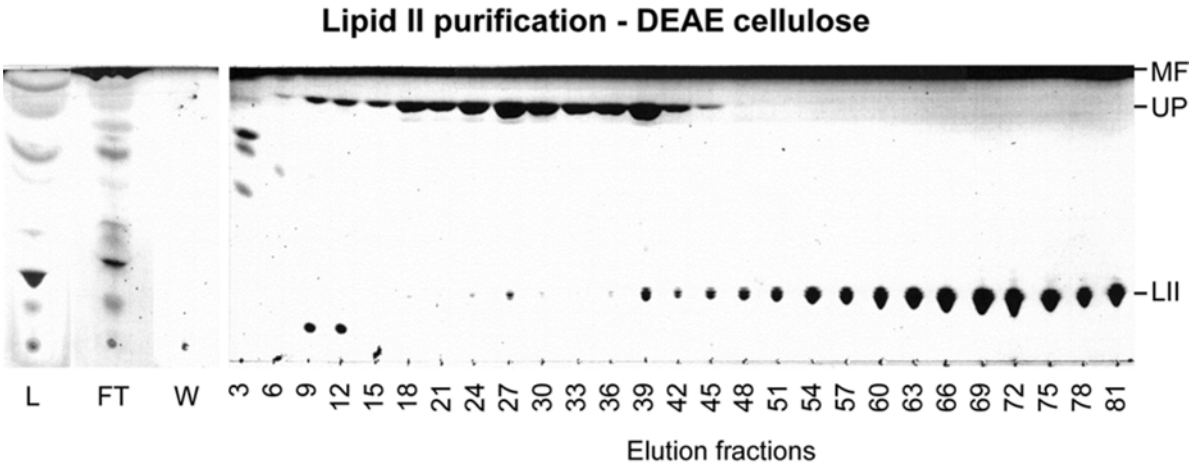


**Figure 45: Purification of lipid II. After synthesis, the lipid II was purified on DEAE-cellulose anion-exchange chromatography and several fractions were analyzed by TLC and revealed with iodine vapor. L: load, FT: flow through, W: wash, MF: migration front, UP: undecaprenyl-phosphate, LII: lipid II.**

First, small scale experiments (150 µL) were performed to verify that the *S. simulans* extract and the *M. flavus* membranes were active, as activity can vary from one preparation to another. Two of the three *S. simulans* extracts gave positive results as well as small membranes quantities (5 µL were sufficient in these conditions, Figure 44). A scale up experiment (150 mL) was then carried out using *S. simulans* extract 1 and the appropriate amount of *M. flavus* membranes. The lipid II was then purified using a DEAE cellulose anion-exchange chromatography, which enabled the separation from the residual undecaprenyl phosphate and other reaction components (Figure 45). About 50 mg of lipid II were obtained.

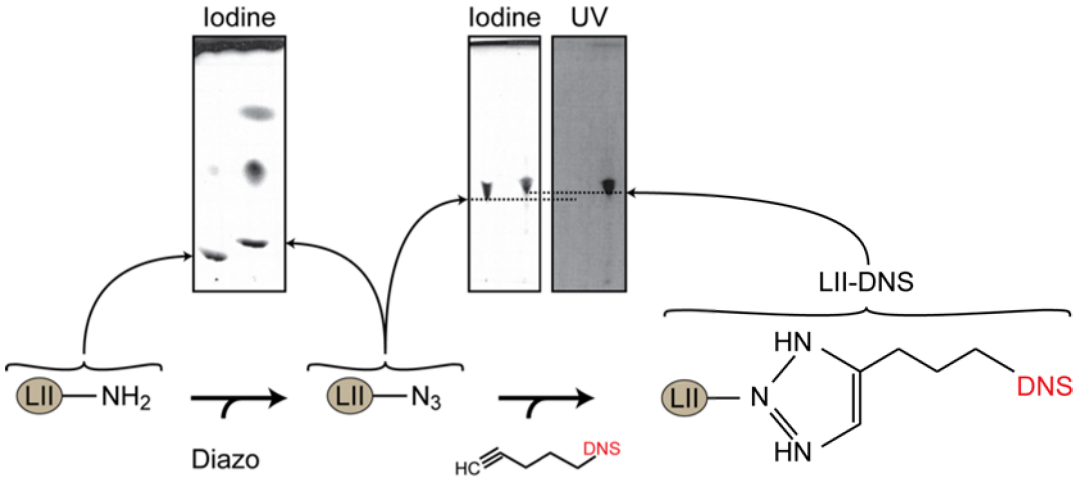


**Figure 46: Lipid II dansylation. Purified lipid II was dansylated in two steps. First, the $NH_2$ moiety at the extremity of the lysine in position 3 of the lipid II stem peptide was converted to a $N_3H_4$ moiety and the reaction product was checked by iodine-stained TLC. After purification on DEAE-cellulose anion-exchange chromatography, this intermediate was linked to a dansyl moiety through a carbon tail and purified identically. TLC analysis of the purified intermediate and final product was revealed by UV illumination and iodine-stained. LII: lipid II, DNS: dansyl.**

To attach a dansyl moiety to the lipid II, a series of reactions followed by purification steps were performed which resulted in pure dansylated lipid II (Figure 46). The modified TLC migration pattern and the spot observed under UV illumination confirmed that the reactions were complete.

## *In vitro* peptidoglycan synthesis activity of PBP1a

The synthetic activity of PBP1a was first determined using the test developed by André Zapun as described in the Material and Methods. Briefly, purified PBP1a was added to a mixture of aLII and LII-DNS in the appropriate buffer. Antibiotics were added to two samples as negative controls before incubation and SDS-PAGE analysis. PBP1a had both GT and TP activities (Figure 47). Moenomycin, an antibiotic that prevents GT activity, inhibited the elongation of glycan chains whereas the penicillin G, a β-lactam, enabled the elongation of chains, but not their cross-linking by TP activity (Figure 47). These negative controls confirmed that the band observed at the top of the gel corresponded to cross-linked glycan chains resulting from the GT and TP activities, and that the smear corresponded to the glycan chains of different length assembled by the GT activity.

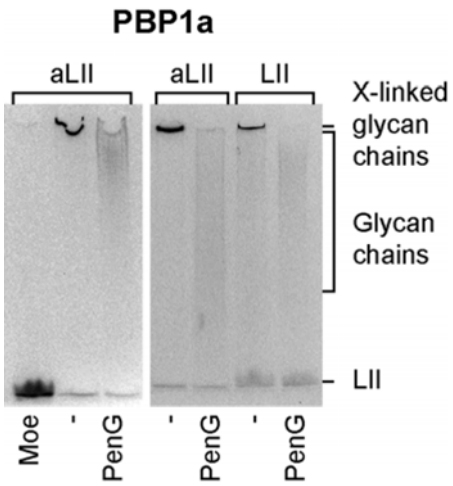


**Figure 47: The transpeptidase activity of PBP1a is better on amidated lipid II. aLII: amidated lipid II, LII: non-amidated lipid II, Moe: moenomycin, PenG: penicillin G, X-linked: cross-linked.**

To test the specificity of PBP1a for aLII, the same experiment was performed in parallel with two different lipid II mixtures: LII-DNS / LII (1 : 10) or LII-DNS / aLII (1 : 10). Although the TP activity of PBP1a was better when synthesis was performed with aLII, some activity could be detected with LII (Figure 48). This is in contrast with PBP2a, the TP activity of which is only possible with aLII (Zapun, *et al.*, 2013). This shows that in these conditions, the activity of PBP1a is facilitated by amidation of the second residue of the lipid II, but remains possible with unmodified lipid II, although with a lower efficacy.

To further investigate the reaction, a time-course analysis was performed. Samples were withdrawn at several time points after the beginning of the reaction and moenomycin and penicillin G were added to stop the reactions before SDS-PAGE analysis and UV revelation (Figure 48, right panel). To gain insights in the kinetics of the reaction, the intensity of the fluorescence signal of the top band, the smear and the lower band was determined. These signals correspond to cross-linked

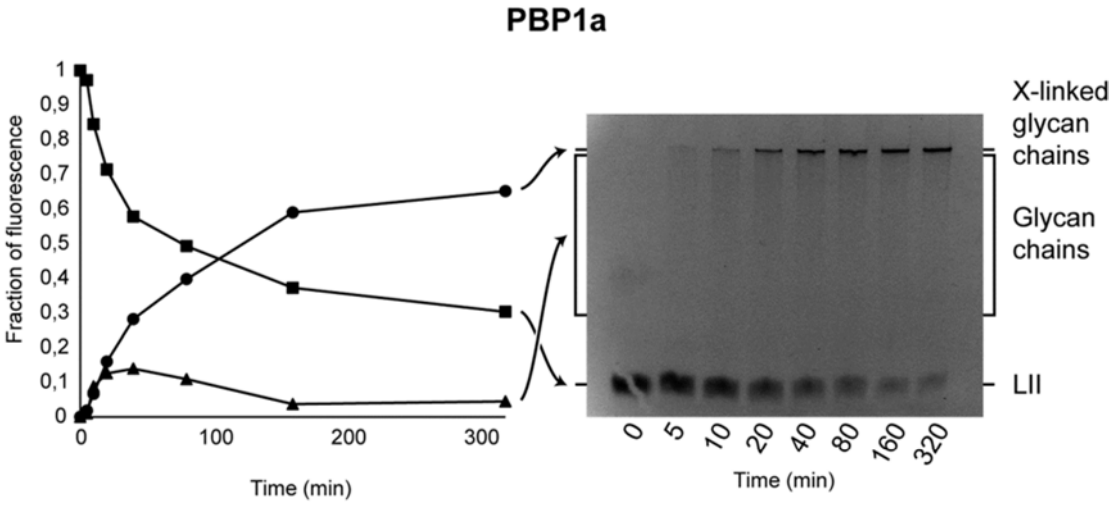


**Figure 48: Kinetics of PBP1a GT and TP activities. The peptidoglycan synthesis reaction was blocked at different times before SDS-PAGE analysis. The density of the fluorescence of the indicated gel fractions (right) was plotted for each reaction time (left). LII: lipid II, X-linked: cross-linked.**

material, elongated chains and LII. For each sample, the fraction of fluorescence was calculated as a fraction of the total fluorescence intensity of the sample and plotted over the reaction time (Figure 48, left panel). As the lipid II was consumed, the glycan chains fraction remained below 0.15 while the cross-linked glycan chains fraction increased. This suggests that the GT and TP activities of PBP1a were concomitant. The total fluorescence intensity was similar for each individual sample regardless of the advance of the reaction.

The TP activity of PBP2a was slower than that of PBP1a (data not shown). Indeed, in an experiment, a time course of PBP1a and PBP2a were performed in parallel. After 120 min, 27 and 2 % of the fluorescence was detected in the band corresponding to the cross-linked glycan chains, respectively. However at this reaction time, 63 and 65 % of the fluorescence was found in the remaining lipid II band with PBP1a and PBP2a, respectively. This suggests that in these conditions, the TP activity of PBP1a is better than that of PBP2a, but both enzymes utilize their lipid II substrate at the same rate.

Cooperation between class A and class B PBPs has been reported *in vitro* with *E. coli* proteins (Banzhaf*, et al.*, 2012). To test the cooperativity between class A and class B PBPs from *S. pneumoniae*, PBP1a was mixed with either PBP2b or PBP2x. Of note is that the DMSO contained in the buffer might disrupt potential protein interactions, possibly hiding any cooperativity effect. A preliminary test was performed where the activity of PBP1a was monitored as above, but in absence of DMSO. Although less activity was recorded for a given incubation time, GT and TP activity were possible in these conditions, and was sufficient to investigate cooperation (not shown).

An activity test was performed where both PBP1a and PBP2b or PBP2x were added to the reaction mixture, in the absence of DMSO. SDS-PAGE analysis did not reveal stimulation or inhibition of the GT or TP activities of PBP1a by either PBP2b or PBP2x (Figure 49).

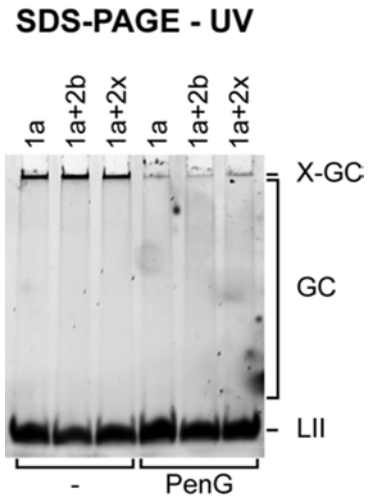


**Figure 49: Influence of class B PBPs on the activity of PBP1a. The peptidoglycan synthesis reaction was performed with PBP1a in presence or absence of PBP2b or PBP2x. X-GC: cross-linked glycan chains, GC: glycan chains, LII: residual lipid II, 1a: PBP1a, 2b: PBP2b, 2x: PBP2x, PenG: penicillin G.**

## Concluding remarks

All together, these results confirm that the pneumococcus class A PBP1a has both GT and TP activities. These activities seem to be concomitant and the TP activity is higher when amidated lipid II is used.

## Mécanismes d'action des β-lactamines sur *S. pneumoniae* : le paradoxe de la pipéracilline - Résumé

Avec l'utilisation intensive des β-lactamines dans le traitement des infections à pneumocoques, de nombreuses souches résistantes sont apparues et se sont répandues. Des solutions antibiotiques alternatives sont employées dans la lutte contre ces pathogènes, mais certains ont développé un phénotype de résistance à de multiples antibiotiques. Des souches de résistance « étendue » ont même été identifiées dans certains cas, pouvant résister à au moins un antibiotique de chaque classe, excepté la vancomycine et le linézolide. Pour perfectionner les traitements, il est maintenant nécessaire de comprendre les détails des mécanismes moléculaires permettant au pneumocoque de se développer même en présence des antibiotiques utilisés.

Les connaissances fondamentales sur la morphogenèse du pneumocoque sont de plus en plus nombreuses. Récemment, les rôles de PBP2b et PBP2x ont été déterminés de manière robuste. Ces deux protéines sont des PLPs permettant l'incorporation de nouveaux brins de peptidoglycane dans le sacculus. Alors qu'elles sont toutes deux essentielles, PBP2B est requise pour l'élongation alors que PBP2X est nécessaire pour la division du pneumocoque. Lorsqu'il exprime moins de PBP2b, le pneumocoque a un peptidoglycane plus riche en peptides branchés que quand cette protéine est normalement exprimée.

Les cibles des β-lactamines et la manière dont elles inhibent la réaction de transpeptidation sont connues. En revanche, les mécanismes entraînant l'inhibition de la croissance, voire la lyse des bactéries en présence de ces médicaments le sont peu. A partir de ce constat, nous avons étudié le paradoxe suivant. PBP2x est la cible principale de la pipéracilline, PBP2b étant touché dans une moindre mesure. Cependant, une sélection en présence de pipéracilline résulte dans un premier niveau de résistance dû à des modifications sur PBP2b, des variants de PBP2x ne pouvant être sélectionnés qu'en second lieu.

Cette partie comprend une publication scientifique qui rapporte les résultats que j'ai obtenus sur les mécanismes d'action de la pipéracilline chez le pneumocoque.

Premièrement, il est montré que la cible principale de la pipéracilline chez le pneumocoque est PBP2x *in vivo*, PBP2b et PBP3 étant affectées dans une moindre mesure. En effet, une plus grande fraction de PBP2x n'était plus réactive à la bocilline (une pénicilline fluorescente) après traitement à la pipéracilline, comparé aux autres PLPs. Les PLPs de classe A, PBP1a, PBP1b et PBP2a étaient en revanche très peu affectées par le traitement. L'observation en microscopie optique à contraste de phase a révélé que les pneumocoques avaient pris une forme de citrons ou de cellules allongées après deux heures de traitement de la culture à deux fois la concentration minimum inhibitrice (CMI) de la pipéracilline. Enfin, l'observation en microscopie électronique a montré que chez *S.*

*pneumoniae* R6, ces cellules allongées sont des cellules isolées, enflées en leur milieu. Dans un mutant qui n'exprime pas l'autolysine LytA, elles peuvent correspondent à une seule cellule enflée en son milieu, deux cellules séparées par un large septum de peptidoglycane et leur membrane plasmique, ou deux cellules séparées uniquement par leur membrane plasmique au niveau de la zone élargie.

Pour comprendre comment ce renflement apparaît, PBP2x, PBP2b et FtsZ, trois protéines essentielles de la morphogenèse, ont été marquées par fusion GFP. L'observation de ces souches en microscopie à fluorescence a révélé que la pipéracilline n'affecte pas la localisation de ces protéines, mais c'est bien l'inhibition de leur activité qui engendre les défauts observés. En effet, les protéines marquées se trouvent au milieu et aux équateurs des cellules, que ce soit en présence ou en absence d'antibiotique. L'apparition de la zone enflée a aussi été observée au cours du temps en vidéo microscopie à fluorescence, révélant que l'anneau de FtsZ suit l'élargissement du diamètre du centre de la bactérie, alors que les anneaux équatoriaux, quand ils sont présents, ne subissent pas de changement.

Dans un second temps, des souches contenant des variants résistants de PBP2b et PBP2x (appelées ici PBP2bR et PBP2xR) ont été construites. Les souches PBP2bR ont une CMI pour la pipéracilline doublée par rapport à la souche parente, alors que les souches PBP2xR ont une CMI quasiment inchangée. La corrélation des différents profils d'inhibition des PLPs dans ces souches par rapport à leur CMI a permis de déterminer la proportion minimale de PBP2b et PBP2x actives à laquelle la croissance est encore possible. Dans ce système expérimental, moins de 20% de PBP2x actifs étaient suffisants pour la croissance de pneumocoques, alors qu'au moins 50% de l'activité de PBP2b était requise. En outre, la proportion de PBP3 encore active n'affecte pas la CMI. PBP1a, PBP1b et PBP2a sont faiblement inhibées par la pipéracilline.

La cinétique d'inhibition des PLPs de pneumocoque par la pipéracilline a ensuite été comparée entre une souche PBP2xR. (dont PBP2x ne lie pas la pipéracilline à des concentrations allant jusqu'à 4 x la CMI) et sa souche parentale. Les profils d'inhibition des 6 PLPs du pneumocoque étaient similaires dans les deux souches, excepté celui de PBP2x, non inhibé dans la souche PBP2xR. Etant donné que la CMI est similaire dans ces deux souches, et que PBP2b est la seule PLP essentielle affectée, on en déduit que c'est cette dernière PLP qui est essentielle à la croissance de pneumocoques lors du traitement avec la pipéracilline.

Ce résultat est cohérent avec le fait que la pipéracilline sélectionne des mutations de PBP2b. Les changements morphologiques de la souche parentale en présence de pipéracilline (formation de « citrons ») sont quant à eux dus à l'inhibition de PBP2x dans une plus large mesure que PBP2b.

Ces résultats soulèvent une nouvelle question. Pourquoi au moins 50% de l'activité de PBP2b est requise pour la croissance du pneumocoque en présence de pipéracilline, alors que 20% de

l'activité de PBP2x suffisent ? Ceci était inattendu car une étude sur le rôle des PLPs de classe B avait montré que PBP2b est requise en moindre proportion que PBP2x en l'absence d'antibiotiques.

Une explication pourrait reposer sur le fait qu'une moindre quantité de PBP2b nécessite l'augmentation de la proportion de peptidoglycane branché dans la cellule (démontré récemment). La déplétion de PBP2b rapportée dans l'étude mentionnée plus haut s'est faite de manière progressive (sur plusieurs générations bactériennes). On peut émettre l'hypothèse que le pneumocoque dans cette situation a eu suffisamment de temps pour modifier la composition de sa paroi. En revanche, l'ajout de pipéracilline a une action très rapide. Dans ce cas, l'activité de PBP2b est inhibée avant que la quantité de liens peptidiques branchés dans le peptidoglycane ne permette la survie de la bactérie en présence d'une faible quantité de PBP2b. Cette hypothèse reste à tester.

## Mechanisms of β-lactam action in *Streptococcus pneumoniae*: the piperacillin paradox

Aiming at deciphering the role of PBP2b and PBP2x in the pneumococcus, I inhibited their activity with piperacillin. Indeed, this β-lactam does not bind the class A PBPs, while it targets PBP2b, PBP2x and PBP3. We took advantage of the fact that the only TP activities to be inhibited are those of class B PBPs, which specific role remained elusive when I initiated this project. The strategy that I followed was to treat pneumococci mutants, which PBP2b or PBP2x was substituted by a low-affinity variant. Four strains were designed, containing either PBP2b T446A, PBP2x T338A-M339F, or with the low-affinity PBP2b or PBP2x from the highly β-lactam-resistant clinical isolate 5205. As preliminary results were obtained, two studies were published by other groups reporting the role of PBP2b and PBP2x (Berg*, et al.*, 2013), (Land*, et al.*, 2013). Therefore, we decided to focus on the mechanism of β-lactam action on pneumococcal cells. The results obtained have been assembled in a document presented below and will be submitted for publication.

# Mechanism of β-Lactam Action in *Streptococcus pneumoniae*: the Piperacillin Paradox

Jules Philippe[a,b,c], Benoit Gallet[a,b,c], Cécile Morlot[a,b,c], Dalia Denapaite[d], Regine Hakenbeck[d,e], Yuxin Chen[f], Thierry Vernet[a,b,c], André Zapun[#a,b,c]

Université Grenoble Alpes, IBS, Grenoble, France[a]; CNRS, IBS, Grenoble, France[b]; CEA, IBS, Grenoble, France[c]; Department of Microbiology, University of Kaiserslautern, Kaiserslautern, Germany[d]; Alfried Krupp Wissenschaftskolleg, Greifswald, Germany[e]; University of Science and Technology of China, Hefei, China[f].

Running head: The Piperacillin Paradox

#Address correspondence to André Zapun: andre.zapun@ibs.fr

## Abstract

The human pathogen *Streptococcus pneumoniae* has been fought for decades with β-lactam antibiotics. Resistance is now widespread, mediated by the expression of mosaic variants of the target enzymes, the penicillin-binding proteins or PBPs. Understanding the mode of action of β-lactams, not only in molecular details, but also in their physiological consequences, will be crucial to improve these drugs and counter resistance. In this work, we investigate the piperacillin paradox, by which this β-lactam selects primarily variants of PBP2b, whereas its most reactive target is PBP2x. These PBPs are both essential mono-functional transpeptidases involved in peptidoglycan assembly. PBP2x participates to septal synthesis, while PBP2b functions in peripheral elongation. The formation of "lemon"-shaped cells induced by piperacillin treatment is consistent with the inhibition of PBP2x. Following the examination of treated and untreated cells by electron microscopy, localization of the PBPs by epifluorescence microscopy, and determination of the inhibition time-course of the different PBPs, we propose a model of peptidoglycan assembly that can account for the piperacillin paradox.

## INTRODUCTION

*Streptococcus pneumoniae* is a facultative bacterial pathogen that belongs to the human nasopharyngeal microbiota (1). When pneumococcus invades other areas, it can cause mild diseases such as otitis media, sinusitis and bronchitis, or life-threatening pneumonia, meningitis or septicemia. Following the introduction of β-lactams to treat bacterial infections, the first pneumococcal penicillin-resistant strain was reported in 1967 (2), and extensive multi-drug-resistant pneumococci have now emerged (3, 4). Understanding the molecular mechanisms of antibiotic resistance in pneumococcus is therefore of major importance.

β-Lactam antibiotics interfere with the assembly of peptidoglycan, the main constituent of the bacterial cell wall. The peptidoglycan is a network of glycan chains reticulated by peptide links, constituting a single macromolecule that encases the cell. This essential layer protects bacteria from the turgor pressure and provides a scaffold to anchor other surface molecules (5). Fine-tuning the dynamics of peptidoglycan assembly is essential for proper cell division and shape determination. In ovoid bacteria, synthesis of peptidoglycan is thought to involve two machineries allowing bacteria to elongate and divide, respectively (6, 7). A set of six Penicillin-Binding Proteins (PBPs) catalyzes the last step of peptidoglycan assembly in *S. pneumoniae*. The three class A PBPs (PBP1a, PBP1b and PBP2a) are bi-functional enzymes that polymerize glycan chains (glycosyltransferase activity) and cross-link them through peptide bonds (transpeptidase activity). The two class B PBPs (PBP2x and PBP2b) are mono-functional transpeptidases. PBP3 is a class C PBP with a carboxypeptidase activity, involved in the maturation of peptidoglycan (8). While the class A and C PBPs are not essential in the pneumococcus (9, 10), both class B PBPs are necessary, PBP2b being essential for elongation and PBP2x for division, respectively (11-14). In the pneumococcus, β-lactam resistant strains harbor PBP variants with reduced reactivity towards the drugs (15, 16).

An early study intended to correlate the specificity of 18 β-lactams for different PBPs and the morphological defects they caused in *S. pneumoniae* (17). A very interesting phenotype of pneumococcal cells was observed in the presence of piperacillin, an extended-spectrum β-lactam antibiotic used to cure poly-microbial infections (often in combination with tazobactam, a β-lactamase inhibitor) (18). Cells treated with half the minimal inhibitory concentration (MIC) of piperacillin for 4 h acquired a characteristic "lemon" shape, with a central bulge and pointy ends (17). In addition, it was reported that piperacillin used at the MIC inhibits about 50 % of PBP2b and PBP3 and 27% of PBP2a. However, since PBP2x was not known at that time because it co-migrated with PBP2a in the experimental setup, the reported PBP2a inhibition corresponds to that of both PBP2x and PBP2a. Accordingly PBP2x was not considered in the conclusions drawn at that time. Meanwhile it is apparent that there is a complex redundancy of the different PBPs, and the morphological, physiological and biochemical effects induced by one particular PBP remain largely open today.

Further studies investigated the resistance of pneumococcus to piperacillin in the laboratory (19-21). Pneumococci were gradually selected on increasing concentrations of piperacillin and the PBP sequences of the resulting strains were determined. Interestingly in the three selected piperacillin-resistant lineages, PBP2b variants appeared first, and PBP2x variants were found only in strains subsequently selected for higher resistance level (21). In subsequent experiments where *pbp* genes where randomly mutagenized, PBP2b variants could again be selected by piperacillin exposure (20). The T446A substitution in PBP2b, which is commonly found in resistant clinical isolates, increased the MIC for piperacillin two-fold. The same piperacillin MIC was determined for a strain having incorporated the full PBP2b sequence of a clinical isolate.

These selection studies strongly suggested that the primary essential target of piperacillin is PBP2b. However, the morphological defects induced by piperacillin challenge (*i.e.* the "lemon" shape) resemble those induced by the depletion of PBP2x (11, 13). Moreover, PBP2x was found to be the most reactive PBP with piperacillin (12, 19). In this work, we revisited the effect of piperacillin treatment on the morphology and the localization of both class B PBPs, as well as the specificity for the different PBPs. We confirm here that the primary target of piperacillin is PBP2x, causing morphological defects that are consistent with PBP2x inhibition, despite de fact that it is the lesser inhibition of PBP2b that prevents growth, a behavior that we dub the piperacillin paradox. Results are discussed in light of the recent knowledge on the respective role of PBP2x and PBP2b, and peptidoglycan composition modifications that also play a role in resistance.

## MATERIALS AND METHODS

**Bacterial strains and growth conditions.** Bacterial strains (Table 1) were grown on Columbia blood agar plates supplemented with defibrinated horse blood to 4% (herein referred to as CB agar), or in liquid C+Y medium (22), at 37°C in a 5% $CO_2$ atmosphere. A stock of each strain was prepared from exponentially growing culture ($OD_{600nm}$ between 0.2 and 0.4) and stored at -80°C in 20% glycerol.

The R6 Δ*lytA gfp-ftsZ* strain and the R6 Δ*lytA* strains with low-susceptibility PBPs (Table 1 and Fig. S1 in supplemental material) were constructed by transformation of the appropriate plasmid in R6 Δ*lytA* mother strain and homologous recombination at the *bgaA* locus. The clones of R6 Δ*lytA gfp-ftsZ* were selected on CB agar containing 2.5 µg/mL tetracycline. Clones of R6 Δ*lytA pbp2x*T338A/M339F (later called R6 Δ*lytA pbp2xR)* and R6 Δ*lytA pbp2x*5204 (later called R6 Δ*lytA pbp2x5)* were selected on CB agar containing 0.1 µg/mL cefotaxime. Clones of Δ*lytA pbp2b*T446A (later called R6 Δ*lytA pbp2bR)* and R6 Δ*lytA pbp2b*5204 (later called R6 Δ*lytA pbp2b5)* were selected on CB agar containing 0.03 µg/mL piperacillin.

The R6 Δ*lytA gfp-pbp2x* Δ*pbp2x* and R6 Δ*lytA gfp-pbp2b* Δ*pbp2b* strains were obtained by transformation of their *lytA*$^+$ parent with a PCR fragment consisting of a kanamycin resistance cassette flanked by 1000 bp-long fragments homologous to the upstream and downstream regions of the *lytA* gene, as described in (23).

Transformations of pneumococci with PCR products or plasmids were performed using the competence stimulating peptide CSP1 for convenience (24). The region surrounding the modified or introduced gene was systematically sequenced in the clones used for further experiments. In the case of R6 Δ*lytA pbp2b5*, only a partial fragment of *pbp2b5204* missing the 3' region of the gene was found to have recombined in the genome (see Results section and Fig. S1 in supplemental material). Growth curves were measured

and compared to that of the R6 Δ*lytA* strain (see protocol below). All strains grew identically (doubling time of 34 ± 2 min), except the strains grown in presence of 150 µM $ZnCl_2$, which had a longer generation time (1.3-fold).

**Growth curves.** Volumes of 2.5 mL of C+Y medium were inoculated with 250 µL of pre-culture at $OD_{600nm}$ = 0.3, in 24-well plates, sealed and grown at 37°C in a FLUOstar plate reader (BMG Labtech) equipped with a 595 nm filter. The $OD_{595nm}$ was recorded every 20 minutes after shaking. Each strain was grown in triplicates in parallel with the R6 Δ*lytA* control strain, in two independent experiments. The strains containing GFP-fusions under the control of the $P_{czcD}$ zinc-inducible promoter were grown with 150 µM $ZnCl_2$.

**Minimum inhibitory concentrations.** The minimum inhibitory concentrations (MICs) were determined in liquid cultures to determine the piperacillin concentrations to use in the various experiments. Piperacillin was from Sigma (P8396). Glycerol stocks were diluted 100-fold in 30 mL of C + Y medium. Nine hundred and fifty microliters of this dilution were added to 50 µL of a 20x piperacillin solution in 96-deep-well plates. Final piperacillin concentrations were 0, 0.02, 0.03, 0.04, 0.05, 0.06, 0.08 and 0.1 µg/mL. Cultures were incubated for 6 h at 37°C before 200 µL of culture were transferred in a 96-wells microplate to record the $OD_{595nm}$ in a FLUOstar plate reader (BMG Labtech). The lowest piperacillin concentration that did not permit growth was defined as the MIC. MIC determination was always carried out in triplicates, in two independent experiments including the R6 Δ*lytA* control strain.

**Piperacillin treatment for optical microscopy analysis.** Glycerol stocks were diluted 100-fold in 5 mL of C+Y medium and grown to $OD_{600nm}$ = 0.3. Nine hundred and fifty microliters of this culture were added to 50 µL of 20x piperacillin to obtain the desired concentrations and incubated further for 2 h. Samples were centrifuged for 3 min at 5,000 *g* and re-suspended into 50 µL of supernatant. Four microliters of concentrated bacteria were

transferred to microscope slides. Images were acquired with an Olympus BX61 microscope equipped with a UPFLN 100x O-2PH/1.3 objective, and processed using the Volocity software package (luminosity and contrast adjustment). The cells dimensions were determined using the ObjectJ plugin written by Norbert Vischer (University of Amsterdam, http://simon.bio.uva.nl/objectj/), which runs with the ImageJ software. Global representations of length and diameters were generated with ObjectJ.

**Time-lapse microscopy.** A glycerol stock of R6 Δ*lytA gfp-ftsZ* was diluted $10^7$ times in 15 mL of C+Y medium and grown overnight to $OD_{600nm}$ = 0.1. An agarose pad containing C+Y medium, 1.5 % low-melting agarose and 150 µM $ZnCl_2$ was prepared on a microscopy slide as described in (25). To avoid antibiotic degradation, the medium was incubated at 60°C until complete melting of the agarose, and piperacillin was added just prior to casting on the slide. A volume of 2.5 µL of culture was inoculated on the agarose pad. When the droplet was completely absorbed in the pad, a coverslip was mounted and samples were observed using an inverted Olympus IX81 microscope equipped with a PlanApo 60x/1.42 objective and a 37°C incubation chamber. Videos were acquired and processed using the Volocity software.

**Electron microscopy.** Glycerol stocks were diluted $10^9$ times in 50 mL of C+Y medium and incubated overnight. At $OD_{600nm}$ = 0.3, piperacillin was added to 0.06 µg/mL and incubation was pursued for 2 h. Bacteria were then centrifuged for 10 min at 3220 *g*. A pellet volume of 1.4 µL was disposed on the 200 µm side of a type A 3 mm gold platelet (Leica Microsystems), covered with the flat side of a type B 3-mm aluminium platelet (Leica Microsystems) and was vitrified by high pressure freezing using an HPM100 (Leica Microsystems). Then, the samples were freeze-substituted at -90°C for 80 h in acetone supplemented with 2% $OsO_4$ and warmed up slowly (1°C/h) to -60°C in an Automated Freeze Substitution device (AFS2, Leica Microsystems). After 8 to 12 h the temperature was raised

to -30°C (1°C/h) and the samples were kept at this temperature for another 8 to 12 h before being rinsed several times in acetone. Samples were then infiltrated with gradually increasing concentration of Epon in acetone (1:2, 1:1, 2:1 v/v and pure) for 2 to 3 h while raising the temperature. Pure Epon was added at room temperature. After polymerization at 60°C, 80 nm thin sections were obtained using an ultramicrotome UC7 (Leica Microsystems) and were collected on formvar-carbon coated 100 mesh copper grids. The thin sections were post-stained for 5 min with 5% aqueous uranyl acetate, rinsed and incubated for 2 min with lead citrate. Note that no negative staining was performed with the samples presented in Fig. S3 in the supplemental material. Samples were observed using a CM12 (Philips) or a Technai 12 (FEI) operating at 120kV with Orius CCD Camera (Gatan) at 5,000 to 45,000 x magnifications.

**Recombinant proteins purification.** Recombinant His-tagged LytA was purified from *Escherichia coli* Rosetta cells transformed with the pET28a-*his-lytA* plasmid. After induction with 500 µM of isopropyl β-D-1-thiogalactopyranoside at $OD_{600nm}$ = 0.6 and overnight expression at 25°C, the cell pellet from 2 L of culture was resuspended in 50 mL of 50 mM Tris-HCl pH 8, 500 mM NaCl, 25 mM imidazole, 10% glycerol and frozen at -80°C. Once thawed, cells were lysed using a Microfluidizer® M-110P (Microfluidics) and the lysate was centrifuged for 30 min at 40,000 *g* at 4°C. The supernatant was applied onto a 10 mL Ni-NTA column (Qiagen) in the same buffer. The protein was eluted with a 25 mM to 500 mM imidazole gradient. Pooled fractions were concentrated and further purified by size exclusion chromatography using a Superdex S200 10/300 GL column (GE Healthcare) in 25 mM Tris-HCl pH 8, 150 mM NaCl. Ten milliliters of purified $His_6$-LytA were obtained at a concentration of 500 µg/mL.

Recombinant PBP2b from R6 and from the R6 Δ*lytA pbp2b5* strain were purified as described before with a C-terminal Strep-tag (26). The *pbp2b5* gene was PCR amplified from

the genomic DNA of the R6 Δ*lytA pbp2b5* strain. PBP2b5 was expressed from a pET30-derived plasmid after cloning as described previously (26).

**PBP inhibition profiles.** PBP profiles were determined by a procedure derived from those previously reported (11, 12). Glycerol stocks were diluted 100-fold in 30 mL of C+Y medium and grown to $OD_{600}$ = 0.3. Piperacillin was added to various concentrations. Cultures were further incubated for 10 minutes at 37°C and centrifuged at room temperature for 10 min at 3220 *g*. Pellets were re-suspended in 150 µL of PBS containing 25 µg/mL of purified LytA. After complete lysis, typically obtained after 1 h at 37°C (determined visually as the samples become transparent), membrane proteomes were isolated by centrifugation at 20,000 *g* for 20 min at 4°C. Pellets were re-suspended in 150 µL of fresh PBS and stored at -20°C. The total protein concentration of each sample was estimated by the absorbance at 280 nm determined with a NanoVue$^{TM}$ Plus Spectrophotometer (GE Healthcare). Sample protein concentrations were adjusted to 1 mg/mL and 10 µL of each sample were supplemented with 0.5 µL of Bocillin™-FL (Life Technologies) at 300 µM (final concentration:15 µM) and incubated for 10 min at room temperature. After boiling for 10 min in Laemmli buffer, the proteins were separated by SDS-PAGE at 4°C using 4-12% acrylamide gradient gels (Criterion™, Biorad) with the XT MOPS running buffer (Biorad). The PBP profiles were revealed under UV illumination in a Chemidoc imager (Biorad). Densitometry of the band pattern was performed using the ImageJ freeware.

***In vitro* peptidoglycan synthesis and PBP2b inhibition.** Reactions were performed and analyzed as described previously (26). Briefly, un-labeled iso-glutamine-containing lipid II and dansylated lipid II were mixed in a 10:1 ratio and dried prior to dissolution to a final concentration of 50 and 5 µM, respectively, in the reaction mix containing 50 mM HEPES, pH 7.5, 150 mM NaCl, 10 mM $MgCl_2$ and 25% (v/v) DMSO, 0.02% (w/v) Triton X-100, 1 µM PBP2a-S410A and 0.5 µM PBP2b. Aliquots were withdrawn after various times of

incubation at 30°C and the reaction was stopped by the addition of penicillin G (1 mM) and moenomycin (0.5 mM). Samples were analyzed by SDS-PAGE and visualized with UV trans-illumination.

The reactivity of R6 PBP2b and PBP2b5 with piperacillin was evaluated by incubation of 0.5 or 0.25 μM enzyme, respectively, for 10 min at room temperature in their purification buffer with serial dilutions of the drug. Bocillin™-FL was then added to a concentration of 100 μM for a further 10 min prior to SDS-PAGE analysis and imaging under UV-trans-illumination and Coomassie-staining.

## RESULTS

**The primary target of piperacillin is PBP2x.** As piperacillin selects primarily substitutions in PBP2b of pneumococcus in the laboratory, this β-lactam is expected to inhibit specifically PBP2b. However, the most reactive PBP with piperacillin was reported to be PBP2x (12, 19). To investigate this paradoxical behavior, we set out to characterize the effect of piperacillin on pneumococcus.

The minimum inhibitory concentration (MIC) of piperacillin on the R6 strain of *S. pneumoniae* was determined (Table 2). The effect of piperacillin on the morphology of pneumococci was observed 2 h after its addition at twice the MIC (0.06 μg/mL) during exponential growth ($OD_{600mn}$ = 0.3). Cells were lemon-shaped or bulging and elongated as observed by phase contrast and differential interference contrast microscopy. However, a large proportion of cells had also lysed at this stage. To facilitate observation, we then used a R6 strain depleted of the major autolysin LytA, by substitution of the coding gene with an antibiotic resistance cassette. Autolysis was nearly inexistent in this Δ*lytA* strain and allowed the observation of morphological defects due to the toxicity of the antibiotic. The piperacillin MIC was not changed (Table 2), showing that the absence of LytA does not modify the susceptibility to piperacillin. Unless otherwise mentioned, all following experiments were performed in a Δ*lytA* background.

Piperacillin treatment of the Δ*lytA* strain also resulted in the accumulation of lemon-shaped cells with a characteristic bulge at mid-cell as observed by phase-contrast microscopy (Fig. 1A). In the absence of lysis, nearly all cells adopted abnormal shapes. Most cells were in the shape of a citrus fruit (81% of 155 analyzed misshaped cells and top two cells in Fig. 1A), that is with pointy poles bracketing a bulky mid-cell. A number of cells (19% of 155 analyzed misshaped cells and the bottom cell in Fig. 1A) were longer and tri-lobed, the middle-lobe having the wider diameter (Fig. 1A). The ratio between the cell length and the

larger diameter was greater in the presence of piperacillin (Fig. 1B). Fig. 1C represents cells sorted by length, the brightness of each vertical line is proportional to the width of a particular cell along its long axis. While sorting of control cells shows a dark zone corresponding to the constricted region at mid-cell, sorting of cells exposed to piperacillin shows a bright central region, revealing the absence of mid-cell constriction. Altogether, these data indicate that piperacillin treatment results in the enlargement of pneumococcal cells at their middle, regardless of their length. Strikingly, the morphology induced by piperacillin resembles that resulting from depletion of PBP2x ((11, 13) and Fig. 1A).

To further investigate this observation, we determined which PBPs are targeted by piperacillin. Exponentially growing cultures were incubated with different concentrations of piperacillin prior to lysis and incubation with large excess of Bocillin™-FL. Membrane proteins were finally separated by SDS-PAGE and Bocillin-labeled proteins were visualized by UV illumination. The PBP inhibition profile of the R6 strain was identical to that of its Δ*lytA* derivative, indicating that the absence of LytA did not influence the accessibility or reactivity of the PBPs to piperacillin (Fig. 4A and 4B). The band corresponding to PBP2x was the first to disappear from the fluorogram with increasing piperacillin concentration, followed by PBP3 and PBP2b (Figs. 1D and 4B). PBP2x has the strongest affinity for piperacillin, consistent with the observation that morphological defects caused by piperacillin resemble the morphological defects caused by the depletion of PBP2x (11, 13).

**Inhibition by piperacillin of PBP2b and PBP2x does not affect their localization, neither that of FtsZ.** To probe the mechanism underlying the morphological defects induced by piperacillin, we investigated whether the drug affects the localization of FtsZ and the class B PBPs. FtsZ is the tubulin-like protein that polymerizes on the cytoplasmic face of the membrane at the division site and recruits the other proteins involved in the division process (15, 27). Three different strains expressing FtsZ, PBP2x or PBP2b fused to the green

fluorescent protein (GFP) from an ectopic site under the control of a Zn-inducible promoter were created in the R6 Δ*lytA* background. In the case of GFP-PBP2x and GFP-PBP2b, the fluorescence signal observed in the initial merodiploid strains was unsatisfactory. The fluorescence signal was improved by the deletion of the endogenous copy of *pbp2x* or *pbp2b*. The GFP-PBP fusions were functional as they complemented the absence of the corresponding native proteins. The essentiality of *pbp2x* and *pbp2b* was confirmed as expression of the GFP-fused version was required and cells could not grow in the absence of zinc. GFP-PBP2x and GFP-PBP2b were localized at mid-cell and at equators as expected from previous immuno-fluorescence and GFP-fusion works (13, 14, 28, 29) (Fig. 2A, Ctl). The GFP-fusions were overexpressed compared to the native proteins (Fig. 2B). Note that an additional Bocillin-reactive species also appeared at the size of PBP2b. This product could result from the cleavage of the GFP-fusion protein, but the corresponding GFP fragment was not detected by immunoblot (Fig. S2 in supplemental material). Some synthesis of PBP2b may have been initiated from an alternative start codon. Also, a faint band is visible at the size of PBP2x in the Δ*pbp2x* strain. This protein is not a cleavage product of GFP-PBP2x, as it does not disappear in the absence of zinc, and is not detected by immunoblot with an anti-PBP2x serum (Fig. S2 in supplemental material). It may correspond to a fragment of PBP1a or PBP1b.

Also, the zinc-inducible GFP-PBPs retained their reactivity with Bocillin™-FL (Fig. 2B). The determination of the MIC of the three strains showed that induction of expression with zinc did not affect their viability or susceptibility to piperacillin (Table 2).

To localize the GFP fusions, the appropriate strains were grown with zinc to $OD_{600nm}$ = 0.3 and piperacillin was added or not to the culture at twice the MIC (0.06 µg/mL). Unexpectedly, piperacillin did not cause delocalization of the FtsZ-ring, in the sense that FtsZ was observed at mid-cell and at equators, even when the mid-cell was grossly enlarged (Fig.

2A). Similarly, the equatorial and mid-cell localization of both PBP2b and PBP2x was not affected by the action of piperacillin (Fig. 2A).

In order to get insights into the dynamics of formation of the midcell bulge, we imaged the growth of the GFP-FtsZ expressing strain using time-lapse microscopy (Fig. 2C). Pneumococci were grown to $OD_{600nm}$ = 0.3 and transferred to an agarose pad of culture medium supplemented or not with piperacillin at 0.06 µg/mL. Cells were then observed over time at 37°C. The strain expressing GFP-FtsZ in the presence of zinc is shown in Fig. 2C. In the absence of piperacillin, cells divided normally in 20 to 30 minutes. In contrast, the presence of piperacillin inhibited proper cell separation, and a mid-cell bulge appeared after 30 minutes. In some cases, cells continued to inflate until lysis after more than 1 h of piperacillin treatment. The FtsZ-ring was found to enlarge with the bulge formation at mid-cell. Remarkably, bulging occurred equally in cells that were at different stages of the cell cycle at the time of piperacillin addition. Indeed, in Fig. 2C at time t = 0', the cell on the left was at an advanced stage of the cell cycle (elongated diplococcus), whereas the cell on the right was at an early stage. In both cases, the FtsZ-ring enlarged during bulge formation.

We could not obtain good time-lapse fluorescence microscopy data with strains expressing GFP-PBPs as the illumination intensity required to obtain a good fluorescence signal caused phototoxicity.

**Morphological details of piperacillin-treated pneumococci.** To shed light on the bulge formation, piperacillin-treated cells were observed by electron microscopy. R6 Δ*lytA* cells were grown to exponential phase and treated with piperacillin as for optical microscopy. Then, cells were flash frozen under high pressure to keep cellular structures intact. Cells were then slowly brought back to room temperature while being included in Epon resin. Thin section of resin-embedded pneumococci where then negatively stained with uranyl-acetate to enhance the contrast of lipid membranes and peptide-containing peptidoglycan.

Interestingly, three distinct types of abnormal bulging cells were observed (Fig. 3). First, some bulging cells were in fact constituted of two cells adjoined by a continuous peptidoglycan septum, at least in the plane of the thin section, that apparently failed to split (Fig. 3A and B). Second, some lemons were single cells, as the membrane underlying their cell wall was clearly continuous along the bulge (Fig. 3C and D). Finally and surprisingly, some bulging shapes were formed by two distinct cells separated by their respective plasma membranes, but without a continuous peptidoglycan septum (Fig. 3C and E). To our knowledge, this is the first observation of this phenomenon in ovoid bacteria. The three types of bulging shape may result from cells that were at different stages of the cell cycle at the time of piperacillin addition, as proposed in the Discussion section.

To determine whether the absence of LytA-induced lysis plays a role in the observed morphological defects, these experiments were repeated with the R6 parental strain. In this case, cells were observed both after one and two hours of piperacilin treatment. Most cells were lysed 2 h after addition of piperacillin. However, after only 1 h, the bulging morphology was observed but none of the twenty cells observed had a septum (Fig. S3 in supplemental material). This observation suggests that upon piperacillin inhibition, LytA may be involved in the specific lysis of pneumococcal cells with a septum, through the targeted degradation of septal peptidoglycan.

**PBP2b variants confer piperacillin resistance, in contrast to PBP2x variants.** We showed that the primary target of piperacillin is PBP2x (Fig. 1D). PBP2b and PBP3 are less reactive to this β-lactam. In the late eighties, piperacillin resistant pneumococci were selected in the laboratory by successive plating on medium with increasing piperacillin concentrations (19, 20, 21). Interestingly, the first level of piperacillin resistance was conferred by low-affinity PBP2b variants. PBP2x variants did not provide pneumococci with this first level of

resistance (20). Low-affinity PBP2x variants were selected in lineages where a low-affinity PBP2b was already present, conferring a second higher level of resistance.

To further document this paradox, we constructed four strains in the R6 Δ*lytA* background. Two strains had a variant *pbp2b* allele coding either for the T446A PBP2b point-mutant (20, 30) (herein referred to as *pbp2bR*), or PBP2b from the clinical resistant strain 5204 (31, 32) (herein referred to as *pbp2b5*). Similarly, two strains had their *pbp2x* substituted with alleles coding low-affinity variants. The first allele coded for a PBP2x with the T338A/M339F mutations (herein referred to as *pbp2xR*), known to reduce its affinity to β-lactams (33). The second incorporated the *pbp2x* allele of strain 5204 (herein referred to as *pbp2x5*) (31, 33). The *pbp2b* variants were introduced by selection on piperacillin, whereas *pbp2x* variants were selected with cefotaxime.

The MIC of piperacillin was determined for the four strains (Table 2). The low-affinity PBP2b variants increased the MIC two-fold. By contrast, low-affinity PBP2x variants conferred only a modest increase of the piperacillin MIC. This modest effect on the MIC was not sufficient to select the introduction of *pbp2xR* and *pbp2x5* alleles by piperacillin, in contrast to the *pbp2bR* and *pbp2b5* alleles.

**Under piperacillin challenge, the inhibition of PBP2b prevents the growth of pneumococcus.** Given the apparent conflict between the morphological observations, which point to a predominant role of PBP2x inhibition in the action of piperacillin, and the selection experiments that indicate the importance of the inhibition of PBP2b, we determined the profile of PBP inhibition of our four resistant strains, compared to that of their parental R6 Δ*lytA* and R6 strains (Fig. 4). After 10 min of incubation with various concentrations of piperacillin below and above the MIC, the fraction of free PBP remaining reactive was determined by reaction with an excess of Bocillin™-FL and SDS-PAGE separation. All the strains were challenged in three independent experiments. For each PBP, data were

normalized against the intensity of the Bocillin™-FL labeling without piperacillin treatment. For each strain, a representative fluorogram is provided and the mean and standard deviation of the Bocillin™-FL-reactive fraction is plotted against piperacillin concentration (Fig. 4).

The PBP inhibition profiles by piperacillin were similar for the R6 strain and its Δ*lytA* derivative (Fig. 4A and 4B). At the piperacillin MIC (0.03 µg/mL), less than 20 % of PBP2x remained reactive, whereas about 50% of PBP2b and PBP3 were so. The class A PBPs were nearly not impaired (> 80% still reactive). The two strains with low affinity PBP2b variants had similar profiles, regardless of their *pbp2b* allele (Fig. 4C and 4D). Both retained more than 75% of their PBP2b with a free active site after incubation with 0.12 µg/mL of piperacillin, and PBP2b was nearly not affected at 0.03 and 0.06 µg/mL of piperacillin, which are the MIC of the parental and transformed strains, respectively. In those strains, PBP2x showed the same inhibition profile as the parental strains. At 0.03 µg/mL of piperacillin, below the MIC, most of PBP2x (>80%) was inhibited. Thus, less than 20% of the PBP2x present in the cell is sufficient to sustain growth and cell division. In these strains, the class A and C PBP inhibition profile showed no variation compared to that of the parental strains.

Both strains with variants PBP2x showed a lower affinity of PBP2x for piperacillin compared to those containing R6 *pbp2x* allele (Fig. 4E and 4F). However, whereas PBP2x5 was nearly not inhibited even at the highest piperacillin concentration, the double mutation in PBP2xR caused only a modest decrease of the reactivity for piperacillin. In this latter case, the inhibition profiles of PBP2xR is very similar to that of PBP2b. Note that despite their differing inhibition profiles, the *pbp2xR* and *pbp2x5* strains have the same MIC of piperacillin (Table 2).

In the case of the *pbp2b5* strain, the low affinity of PBP2b5 impaired Bocillin™-FL. Thus, we had to increase the concentration of Bocillin™-FL to allow reaction with PBP2b5 during the preparation of the membrane samples. With this higher concentration of Bocillin,

the SDS-PAGE profile gave a saturated fluorescent smear that was not interpretable. To avoid this, Bocillin™-FL -treated membranes of this strain were pelleted again and re-suspended in fresh PBS, removing the free Bocillin™-FL responsible for the smear. However, some material has probably been lost during this additional step, explaining why the PBP profile of this strain is less intense and the standard deviations are larger.

**Kinetics of *in vivo* inhibition of PBPs by piperacillin**. A major caveat of the experiments presented above is that they monitor different features at different time. The profiles of PBP inhibition were recorded after 10 minutes of incubation with piperacillin, whereas the morphological consequences were observed after one or two hours. MICs on the other hand were determined after inoculation in fresh medium containing the antibiotic. To verify that the observations reported above are significant, we performed time course experiments where the growth, viability, morphology and PBP inhibition profiles were determined at various time following addition of piperacillin at different concentrations. The R6 Δ*lytA* and R6 Δ*lytA pbp2x5* strains were examined and the mean of three independent experiments is shown in Fig. 5.

After 10 min at their respective piperacillin MIC, both strains continued to gain mass, as observed by the optical density of the culture (Fig. 5A and F), but they stopped multiplying (Fig. 5B and G). This result is consistent with the way the MIC was determined and its definition. At the lowest concentrations of piperacillin, PBP2x is the most inhibited PBP in the R6 Δ*lytA* strain, with PBP2b and PBP3 being impacted to a lesser extent (Fig. 5E). In the strain R6 Δ*lytA pbp2x5*, PBP2x is not affected by piperacillin, whereas PBP2b and PBP3 remain inhibited (Fig. 5J). The very limited impact of the non-inhibition of PBP2x5 on the MIC indicates that for every strain the MIC is determined by the inhibition of PBP2b, which is consistent with the selection of PBP2b variants by piperacillin.

The viability of the R6 Δ*lytA* strain decreases after 1 h of incubation with piperacillin above the MIC (Fig. 5B). This loss of viability likely correlates with the morphological aberrations ("lemon" shape) arising from the inhibition of PBP2x (Fig. 5D). Indeed, in the R6 Δ*lytA pbp2x5* strain, the viability decreases less sharply in the presence of piperacillin (Fig. 5G). Interestingly with this strain, the morphological changes observed after 1 h at the MIC of piperacillin resemble those (chained "lentils") brought by the depletion of PBP2b (Fig. 5I) (11), which is consistent with the inhibition of PBP2b and the non-inhibition of PBP2x5.

It is remarkable that the amount of Bocillin™-FL-reactive PBPs decreases with time, with the exception of PBP2x, even in the absence of piperacillin. This is particularly the case for the class A PBP1a. It is possible that the amount of PBP enzymes is down regulated upon entry in the stationary phase, when the optical density at 600 nm is approaching 1.

***In vitro* activity of PBP2b5.** To check if the activity of PBP2b in strain R6 Δ*lytA pbp2b5* was altered compared to R6 PBP2b, the *pbp2b5* gene encoding the full-length protein was cloned in a vector for expression with a C-terminal Strep-tag as described in (26). PBP2b5 differs from PBP2b from strain 5204, which served as the sequence donor for the transformation, for two reasons. Firstly, the gene fragment used lacked the sequence for the cytoplasmic and transmembrane segments. Secondly, despite the addition of a 3' extension, homologous recombination can occur within the *pbp2b* gene. Thus, PBP2b5 differs from R6 PBP2b at 29 positions, including the important T446A substitution (30). PBP2b5 also differs from 5204 PBP2b at 27 positions in the C-terminal region. The difficulty or impossibility to incorporate the 3' sequence of *pbp2b* from clinical strains in the R6 background has already been reported (30).

Recombinant PBP2b5 and R6 PBP2b were purified in parallel in the same way, as described before (26). An activity time course was performed using PBP2a-S410A to provide the glycosyltransferase activity, with a mixture of 90% amidated lipid II and 10% non-

amidated dansylated lipid II, and analyzed by SDS-PAGE. No difference of activity could be detected in this manner (Fig. 6A). Note that the polymerization of the glycan chains by PBP2a-S410A may have been limiting.

As expected from the observation *in vivo*, PBP2b5 was less reactive with piperacillin than R6 PBP2b (Fig. 6B). After 10 min of incubation at room temperature, R6 PBP2b was quantitatively titrated by piperacillin, whereas PBP2b5 was not, even with a 4-fold excess of the drug. Further doubling the concentration of piperacillin, however, resulted in complete inhibition of PBP2b5.

When *in vitro* peptidoglycan synthesis reactions were set up to test the inhibition by or resistance to piperacillin, no difference could be found between R6 PBP2b and PBP2b5, both enzymes being inhibited by piperacillin (not shown). The inhibition of the transpeptidase activity was observed even when the drug and protein concentration were the same as those used to demonstrate that PBP2b5 has a lower reactivity towards piperacillin (0.25 μM PBP2b5 and 0.5 μM piperacillin, Fig. 6B). The reason for this discrepancy is likely due to the rates of the reactions. *In vitro* assembly of the peptidoglycan is very slow and inefficient with PBP2b in the experimental conditions (requiring typically an overnight incubation). It is likely that even at very low near-stoichiometric concentration of piperacillin, PBP2b5 has time to be fully inhibited before significant transpeptidation has occurred.

## DISCUSSION

PBP2x is inhibited by piperacillin to a greater extent than PBP2b, yet this β-lactam selects low-affinity PBP2b variants. The following explanation can be proposed to solve this paradox. Even partial inhibition of PBP2b involved in the elongation signals the arrest of growth (understood as the completion of cell cycles increasing the number of cells). In the meantime, inhibition of PBP2x, which is more extensive, leads to the abortion of septation associated with the observed morphological aberrations resulting from piperacillin exposure. Note that there must be a range of low piperacillin concentrations where the partial inhibition of PBP2b stops multiplication, whereas the near complete inhibition of PBP2x is not sufficient to completely prevent cell division. In such fine-line conditions, incorporation of a "low-affinity" *pbp2b* allele is sufficient to maintain cell multiplication, which allowed us to select the strains harboring the PBP2bR or the PBP2b5 variants.

In support of this interpretation, the piperacillin MIC was nearly not affected by the presence of PBP2x variants that were not inhibited. At the MIC, this strain did not display the morphological defects associated with an inhibition of the septation, yet cells failed to multiply.

It is somewhat surprising that even a partial inhibition of PBP2b by piperacillin stops multiplication, as it was shown that depletion of PBP2b must be very extensive to achieve the same arrest ((11) and our own unpublished observation). Note that both types of experiments (β-lactam challenge and genetic depletion) were performed with R6 Δ*lytA* strains, so that cell lysis does not contribute to the different behavior. We propose here two mutually non-exclusive hypotheses to account for the large impact of the PBP2b inhibition.

At the beginning of the cell cycle, peripheral peptidoglycan is inserted, with participation of the transpeptidase activity of PBP2b. Septal synthesis is initiated using the transpeptidase activity of PBP2x. When splitting of the septal disc occurs, the peripheral

machinery, which includes PBP2b, follows the inward moving circular junction between the peripheral and the septal wall. In this configuration, PBP2b and the peripheral machinery insert material in- or onto fresh peptidoglycan assembled by the septal machinery and PBP2x. This model (Fig. 7) is consistent with the old measurements of cell wall dimension (34) and the most recent data about the localization of the synthetic machineries and their activity (12, 14, 35). Upon mild piperacillin challenge, the transpeptidase activity of PBP2x is mostly inhibited, but septal material could still be assembled by class A PBPs, although with a lower degree of cross-linking. The low PBP2x activity could be tolerated, as long as sufficient PBP2b activity in the peripheral machinery consolidates the peptidoglycan at the splitting site to produce a viable cell wall. Thus, PBP2b would be under greater selection pressure by piperacillin than PBP2x, despite being less reactive with this drug.

A second possible explanation may be related to the proportion of branched muropeptides incorporated in the peptidoglycan. In pneumococcal peptidoglycan, peptide stems can be linked either directly, with the third residue L-Lys connected to the fourth residue D-Ala of another peptide, or indirectly with an Ala-Ala or Ser-Ala intervening dipeptide. The dipeptides are added in the cytoplasm on the precursor by the MurM and MurN enzymes (36). Upon depletion of PBP2b, the fraction of cross-linked peptides containing a Ser-Ala dipeptide increases, and the deletion of *murM* increases the amount of necessary PBP2b (11). It is therefore possible that during depletion of PBP2b by dilution in medium without inducer, which requires several cell cycles, cells have time to adapt and build up a sufficient amount of branched muropeptides, whereas the effect of PBP2b inhibition by piperacillin is much more rapid and does not allow metabolic adaptation.

Some *murM* alleles are known to increase the resistance conferred by low-affinity PBPs and increase the proportion of branched muropeptides in the peptidoglycan (37). This appears to be due to the greater catalytic efficiency of the variant MurM (36). A prediction

from the above hypothesis is that a *murM* allele that increases the pool of branched precursors would decrease the susceptibility to piperacillin. We attempted to transform several of our strains with the *murM* allele from the clinical strain 5204, but failed to select transformants.

β-Lactams that inhibit PBP2b, such as piperacillin, are known to trigger lysis, whereas those that do not react with PBP2b, such as cephalosporins, are non-lytic (38). Could this observation be related to the piperacillin paradox? Now that the function of PBP2x and PBP2b in the septal and peripheral cell wall assembly, respectively, is firmly established (11, 12, 14), the different lytic responses can be rationalized. In the septal disc, new peptidoglycan can be added directly at the leading inner edge. In contrast, insertion at any other site requires cleavage of the pre-existing peptidoglycan. Without associated hydrolytic activity, the addition of new material would only result in thickening of the peptidoglycan layer. Thus, PBP2x can function without associated hydrolase, whereas PBP2b works necessarily in concert with an unidentified hydrolase. When PBP2b is inhibited, the associated hydrolytic activity would not be compensated and lysis would ensue. Note however that lysis cannot be a direct effect, since the absence of the major autolysin LytA prevents lysis when PBP2b is inhibited. Instead, the action of the PBP2b-associated hydrolytic activity may be to sensitize the cell wall to the activity of LytA. Also, piperacillin selection of low-affinity PBP2b variants in a Δ*lytA* background demonstrates that it is not the susceptibility to lysis that limits cell multiplication. Instead, a change in the peptidoglycan properties (rigidity, elasticity, shape…) brought by the imbalance between PBP2b and its cognate hydrolase may constitute the signal that stops growth.

As the morphological modifications resulting from piperacillin exposure resemble those occurring during PBP2x depletion, we conclude that the inhibition of PBP2x is driving these changes of shape. Cells adopted “lemon” or elongated bulging shapes, the latter appearing in phase contrast or differential interference microscopy as the juxtaposition of

three beads, the middle one being often larger. Electron microscopy of negatively stained cryo-thin sections showed that the elongated bulging pneumococci can have three distinct anatomies: a single elongated cell with a swollen mid-cell, two distinct cells with an abnormally extended peptidoglycan septal cross-wall, or two cells separated by their respective plasma membranes but without continuous peptidoglycan septum. We propose that these different morphologies arise from the arrest of septation by piperacillin at different stages of the cell cycle, while some peripheral cell wall building continues (Fig. 8). To explain the absence of cells with complete or partial septa in the presence of LytA, we propose that cells, which were actively inserting peptidoglycan at the septum when piperacillin was added, were lysed by the septal action of LytA. The PBPs responsible for the ongoing peripheral synthesis are unknown but could involve any of the three class A PBPs that are not affected by piperacillin and the residual activity of PBP2b, which is less affected than PBP2x.

The observation of pneumococcal cells separated by continuous membranes without cross-wall suggests that constriction of the FtsZ-ring and the membrane invagination and fission can proceed without simultaneous peptidoglycan septal growth. Note that a delay between the constriction and re-localization of FtsZ and that of PBP2x has been observed during the normal cell cycle of *S. pneumoniae* (14, 28). The piperacillin inhibition of PBP2x highlights this decoupling.

The examination of the localization of GFP-coupled FtsZ, PBP2x and PBP2b shows that the inhibition of PBPs by piperacillin does not affect the localization of the morphogenetic machineries. It is particularly notable that FtsZ remains localized at mid-cell of bulging cells. Time-lapse microscopy showed that the FtsZ-ring enlarges with the bulge. This observation supports the idea that the localization of the FtsZ-ring in ovococci occurs at the position with the largest diameter. Although no time-lapse data could be obtained with

GFP-fused PBPs, the localization of GFP-PBP2x and GFP-PBP2b indicates that the PBPs also localize at the largest cell diameter.

The observations in this report reveal the complexity of the response to β-lactam challenge. Most importantly, the most inhibited PBP by a particular β-lactam, even though the resulting morphology is consistent with the inactivation of this PBP, may not be the essential enzyme that determine the growth arrest.

## ACKNOWLEDGEMENTS

We thank E. Breukink for the generous gift of lipid II,, F. Couppey for initiating the work, and G. Cerardi for technical support in the construction of the strain sspCM99. We thank R.-L. Revel-Goyet, F. Lacroix and J.-P. Kleman (Institut de Biologie Structurale, Grenoble) for the support and access to the Microscopy Platform for time-lapse acquisitions, and G. Schoehn for the access to the Electron Microscopy Platform. J.P. was supported by a grant from la Région Rhône-Alpes. The work of R.H. and D.D. was supported by a grant from the Deutsche Forschungsgemeinschaft Ha 1011/11-1. This work was partly funded by the ‘‘coopol innovation France-Chinese’’program and by the ANR-2011-BSV5-012-01 NOBLEACH, and used platforms of the Grenoble Instruct center (ISBG: UMS3518 CNRS-CEA-UJF-EMBL) with support from FRISBI (ANR-10-INSB-05-02) and GRAL (ANR-10-LABX-49-01) within the Grenoble Partnership for Structural Biology (PSB).

## REFERENCES


1. **Bogaert D, Keijser B, Huse S, Rossen J, Veenhoven R, van Gils E, Bruin J, Montijn R, Bonten M, Sanders E.** 2011. Variability and diversity of nasopharyngeal microbiota in children: a metagenomic analysis. PLoS One **6:**e17035.
2. **Hansman DB, MM.** 1967. A resistant pneumococcus [letter]. Lancet **2:**264-265.
3. **Kang CI, Baek JY, Jeon K, Kim SH, Chung DR, Peck KR, Lee NY, Song JH.** 2012. Bacteremic pneumonia caused by extensively drug-resistant Streptococcus pneumoniae. J Clin Microbiol **50:**4175-4177.
4. **Henriques-Normak B.** 2007. Molecular epidemiology and mechanisms for antibiotic resistance in *Streptococcus pneumoniae*, p. 269-290. *In* Hakenbeck R, Chhatwal S (ed.), Molecular Biology of Streptococci. Horizon Scientific Press, Wymondham, UK.
5. **Vollmer W, Blanot D, de Pedro MA.** 2008. Peptidoglycan structure and architecture. FEMS Microbiol Rev **32:**149-167.
6. **Massidda O, Novakova L, Vollmer W.** 2013. From models to pathogens: how much have we learned about *Streptococcus pneumoniae* cell division? Environ Microbiol **15:**3133-3157.
7. **Philippe J, Vernet T, Zapun A.** 2014. The Elongation of Ovococci. Microb Drug Resist.
8. **Sauvage E, Kerff F, Terrak M, Ayala JA, Charlier P.** 2008. The penicillin-binding proteins: structure and role in peptidoglycan biosynthesis. FEMS Microbiol Rev **32:**234-258.
9. **Hoskins J, Matsushima P, Mullen DL, Tang J, Zhao G, Meier TI, Nicas TI, Jaskunas SR.** 1999. Gene disruption studies of penicillin-binding proteins 1a, 1b, and 2a in *Streptococcus pneumoniae*. J Bacteriol **181:**6552-6555.
10. **Severin A, Schuster C, Hakenbeck R, Tomasz A.** 1992. Altered murein composition in a DD-carboxypeptidase mutant of *Streptococcus pneumoniae*. J Bacteriol **174:**5152-5155.
11. **Berg KH, Stamsas GA, Straume D, Havarstein LS.** 2013. Effects of low PBP2b levels on cell morphology and peptidoglycan composition in *Streptococcus pneumoniae* R6. J Bacteriol **195:**4342-4354.
12. **Land AD, Tsui HC, Kocaoglu O, Vella SA, Shaw SL, Keen SK, Sham LT, Carlson EE, Winkler ME.** 2013. Requirement of essential Pbp2x and GpsB for septal ring closure in *Streptococcus pneumoniae* D39. Mol Microbiol **90:**939-955.
13. **Peters K, Schweizer I, Beilharz K, Stahlmann C, Veening JW, Hakenbeck R, Denapaite D.** 2014. Streptococcus pneumoniae PBP2x mid-cell localization requires the C-terminal PASTA domains and is essential for cell shape maintenance. Mol Microbiol **92:**733-755.
14. **Tsui HC, Boersma MJ, Vella SA, Kocaoglu O, Kuru E, Peceny JK, Carlson EE, VanNeuwenhze MS, Brun YV, Shaw SL, Winkler ME.** 2014. Pbp2x localizes separately from Pbp2b and other peptidoglycan synthesis proteins during later stages of cell division of *Streptococcus pneumoniae* D39. Mol Microbiol.
15. **Zapun A, Contreras-Martel C, Vernet T.** 2008. Penicillin-binding proteins and beta-lactam resistance. FEMS Microbiol Rev **32:**361-385.
16. **Hakenbeck R, Bruckner R, Denapaite D, Maurer P.** 2012. Molecular mechanisms of beta-lactam resistance in *Streptococcus pneumoniae*. Future Microbiol **7:**395-410.
17. **Williamson R, Hakenbeck R, Tomasz A.** 1980. In vivo interaction of beta-lactam antibiotics with the penicillin-binding proteins of *Streptococcus pneumoniae*. Antimicrob Agents Chemother **18:**629-637.

18. **Johnson DM, Biedenbach DJ, Jones RN.** 2002. Potency and antimicrobial spectrum update for piperacillin/tazobactam (2000): emphasis on its activity against resistant organism populations and generally untested species causing community-acquired respiratory tract infections. Diagn Microbiol Infect Dis **43:**49-60.
19. **Laible G, Hakenbeck R.** 1987. Penicillin-binding proteins in beta-lactam-resistant laboratory mutants of *Streptococcus pneumoniae*. Mol Microbiol **1:**355-363.
20. **Grebe T, Hakenbeck R.** 1996. Penicillin-binding proteins 2b and 2x of *Streptococcus pneumoniae* are primary resistance determinants for different classes of beta-lactam antibiotics. Antimicrob Agents Chemother **40:**829-834.
21. **Hakenbeck R, Martin C, Dowson C, Grebe T.** 1994. Penicillin-binding protein 2b of *Streptococcus pneumoniae* in piperacillin-resistant laboratory mutants. J Bacteriol **176:**5574-5577.
22. **Lacks S, Hotchkiss RD.** 1960. A study of the genetic material determining an enzyme in Pneumococcus. Biochim Biophys Acta **39:**508-518.
23. **Fadda D, Pischedda C, Caldara F, Whalen MB, Anderluzzi D, Domenici E, Massidda O.** 2003. Characterization of divIVA and other genes located in the chromosomal region downstream of the dcw cluster in *Streptococcus pneumoniae*. J Bacteriol **185:**6209-6214.
24. **Morrison DA.** 1997. Streptococcal competence for genetic transformation: regulation by peptide pheromones. Microb Drug Resist **3:**27-37.
25. **de Jong IG, Beilharz K, Kuipers OP, Veening JW.** 2011. Live cell imaging of *Bacillus subtilis* and *Streptococcus pneumoniae* using automated time-lapse microscopy. J Vis Exp. **53:**3145.
26. **Zapun A, Philippe J, Abrahams KA, Signor L, Roper DI, Breukink E, Vernet T.** 2013. In vitro reconstitution of peptidoglycan assembly from the Gram-positive pathogen *Streptococcus pneumoniae*. ACS Chem Biol **8:**2688-2696.
27. **Lutkenhaus J, Pichoff S, Du S.** 2012. Bacterial cytokinesis: From Z ring to divisome. Cytoskeleton (Hoboken) **69:**778-790.
28. **Morlot C, Zapun A, Dideberg O, Vernet T.** 2003. Growth and division of *Streptococcus pneumoniae*: localization of the high molecular weight penicillin-binding proteins during the cell cycle. Mol Microbiol **50:**845-855.
29. **Zapun A, Vernet T, Pinho MG.** 2008. The different shapes of cocci. FEMS Microbiol Rev **32:**345-360.
30. **Pagliero E, Chesnel L, Hopkins J, Croize J, Dideberg O, Vernet T, Di Guilmi AM.** 2004. Biochemical characterization of *Streptococcus pneumoniae* penicillin-binding protein 2b and its implication in beta-lactam resistance. Antimicrob Agents Chemother **48:**1848-1855.
31. **Chesnel L, Carapito R, Croize J, Dideberg O, Vernet T, Zapun A.** 2005. Identical penicillin-binding domains in penicillin-binding proteins of *Streptococcus pneumoniae* clinical isolates with different levels of beta-lactam resistance. Antimicrob Agents Chemother **49:**2895-2902.
32. **Contreras-Martel C, Dahout-Gonzalez C, Martins Ados S, Kotnik M, Dessen A.** 2009. PBP active site flexibility as the key mechanism for beta-lactam resistance in pneumococci. J Mol Biol **387:**899-909.
33. **Chesnel L, Pernot L, Lemaire D, Champelovier D, Croize J, Dideberg O, Vernet T, Zapun A.** 2003. The structural modifications induced by the M339F substitution in PBP2x from *Streptococcus pneumoniae* further decreases the susceptibility to beta-lactams of resistant strains. J Biol Chem **278:**44448-44456.

34. **Higgins ML, Shockman GD.** 1976. Study of cycle of cell wall assembly in *Streptococcus faecalis* by three-dimensional reconstructions of thin sections of cells. J Bacteriol **127:**1346-1358.
35. **Wheeler R, Mesnage S, Boneca IG, Hobbs JK, Foster SJ.** 2011. Super-resolution microscopy reveals cell wall dynamics and peptidoglycan architecture in ovococcal bacteria. Mol Microbiol **82:**1096-1109.
36. **Lloyd AJ, Gilbey AM, Blewett AM, De Pascale G, El Zoeiby A, Levesque RC, Catherwood AC, Tomasz A, Bugg TD, Roper DI, Dowson CG.** 2008. Characterization of tRNA-dependent peptide bond formation by MurM in the synthesis of *Streptococcus pneumoniae* peptidoglycan. J Biol Chem **283:**6402-6417.
37. **Filipe SR, Tomasz A.** 2000. Inhibition of the expression of penicillin resistance in *Streptococcus pneumoniae* by inactivation of cell wall muropeptide branching genes. Proc Natl Acad Sci U S A **97:**4891-4896.
38. **Hakenbeck R, Tornette S, Adkinson NF.** 1987. Interaction of non-lytic beta-lactams with penicillin-binding proteins in *Streptococcus pneumoniae*. J Gen Microbiol **133:**755-760.
39. **Hoskins J, Alborn WE, Jr., Arnold J, Blaszczak LC, Burgett S, DeHoff BS, Estrem ST, Fritz L, Fu DJ, Fuller W, Geringer C, Gilmour R, Glass JS, Khoja H, Kraft AR, Lagace RE, LeBlanc DJ, Lee LN, Lefkowitz EJ, Lu J, Matsushima P, McAhren SM, McHenney M, McLeaster K, Mundy CW, Nicas TI, Norris FH, O'Gara M, Peery RB, Robertson GT, Rockey P, Sun PM, Winkler ME, Yang Y, Young-Bellido M, Zhao G, Zook CA, Baltz RH, Jaskunas SR, Rosteck PR, Jr., Skatrud PL, Glass JI.** 2001. Genome of the bacterium *Streptococcus pneumoniae strain* R6. J Bacteriol **183:**5709-5717.
40. **Pagliero E, Dublet B, Frehel C, Dideberg O, Vernet T, Di Guilmi A.** 2008. The inactivation of a new peptidoglycan hydrolase Pmp23 leads to abnormal septum formation in *Streptococcus pneumoniae*. Open Microbiol J **2:**107-114.
41. **Eberhardt A, Wu LJ, Errington J, Vollmer W, Veening JW.** 2009. Cellular localization of choline-utilization proteins in *Streptococcus pneumoniae* using novel fluorescent reporter systems. Mol Microbiol **74:**395-408.

## FIGURES

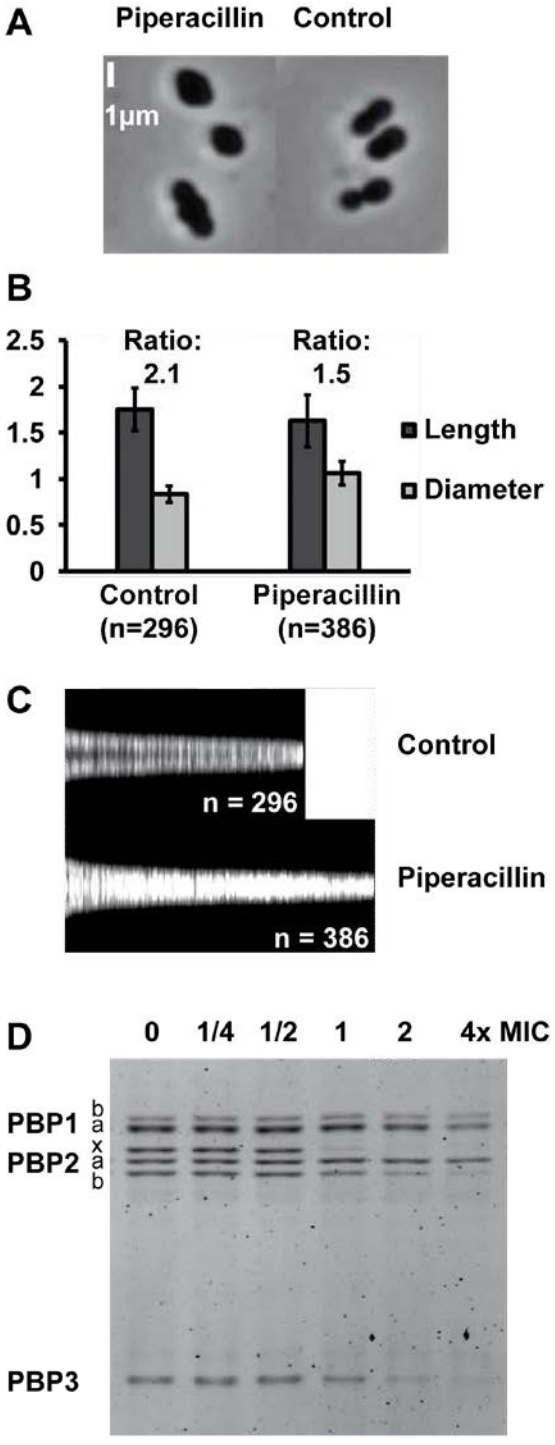


**FIG 1.** Morphological consequences of piperacillin treatment and PBP inhibition profile. (A, B and C) R6 Δ*lytA* cells were observed following 2 h of incubation at twice the piperacillin MIC (0.06 µg/mL). (A) Phase contrast microscopy. (B) Mean apparent lengths and diameters (with standard deviation). (C) Global representation of lengths and diameters. Vertical light bars represent individual cells sorted by length. The bars intensity is proportional to the cell width (perpendicular to the long axis). (D) Fluorogram showing the in vivo PBP inhibition profile by piperacillin. Cells were incubated for 10 min with the drug prior to washing, membrane isolation and PBP labeling with Bocillin™-FL.

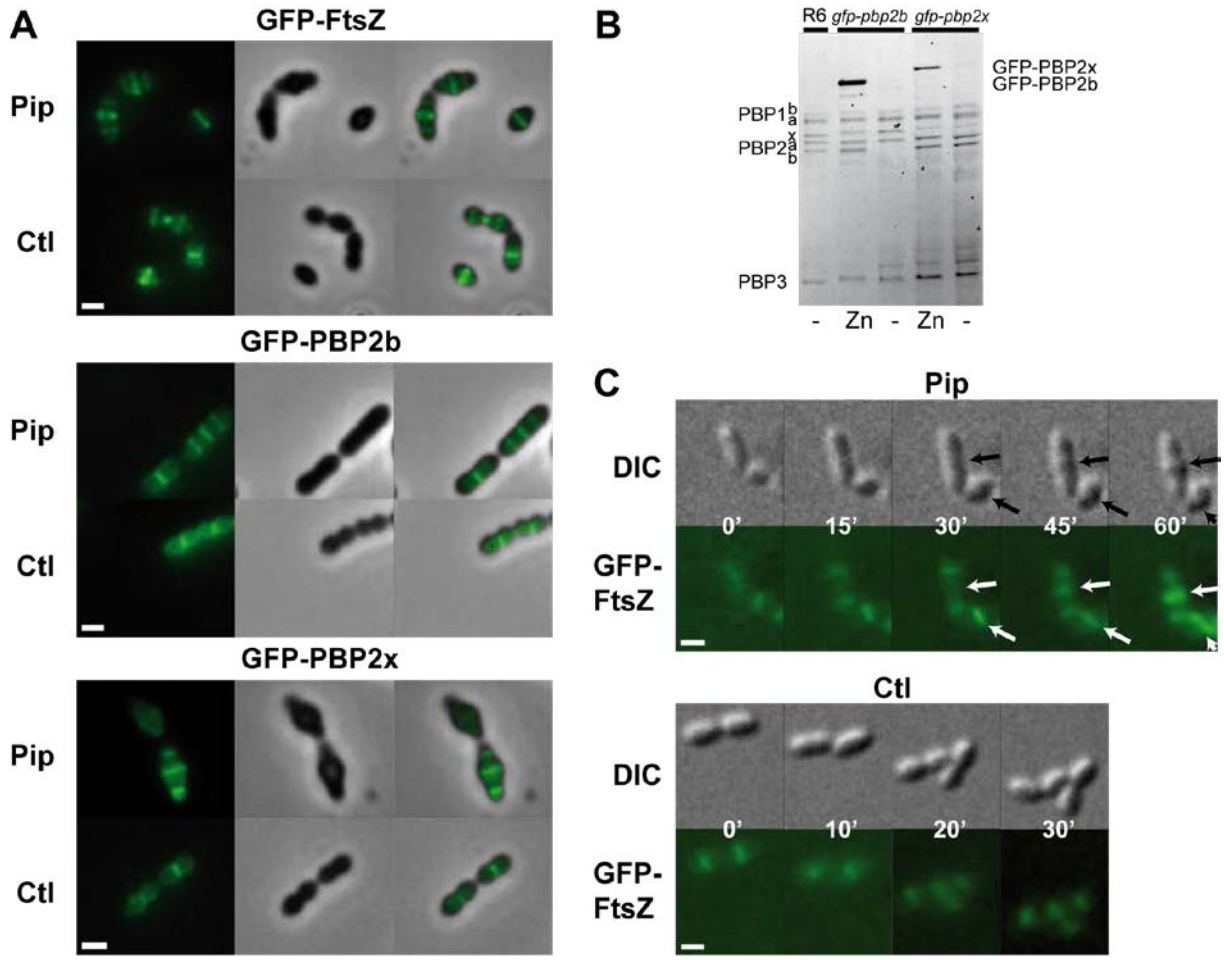


**FIG 2.** Localization of FtsZ and class B PBPs. (A) Localization of GFP-FtsZ, GFP-PBP2b and GFP-PBP2x in the presence (Pip) and absence (Ctl) of piperacillin at 2x the MIC. (B) Bocillin™-FL fluorogram of R6 Δ*lytA*, R6 Δ*lytA* Δ*pbp2x gfp-pbp2x* and R6 Δ*lytA* Δ*pbp2b gfp-pbp2b* strains in the presence or absence of inducer ($Zn^{++}$). Depletion was achieved by growing the cells to OD600nm = 0.3 with zinc, diluting the culture 16x (Δ*pbp2x*) or 256x (Δ *pbp2b*) in fresh medium without zinc and further incubation to $OD_{600nm}$ = 0.3. (C) Time-lapse localization of GFP-FtsZ in the presence (Pip) or absence (Ctl) of piperacillin at 2x the MIC. Arrows point to bulging cells. Scale bars are 1 µm.

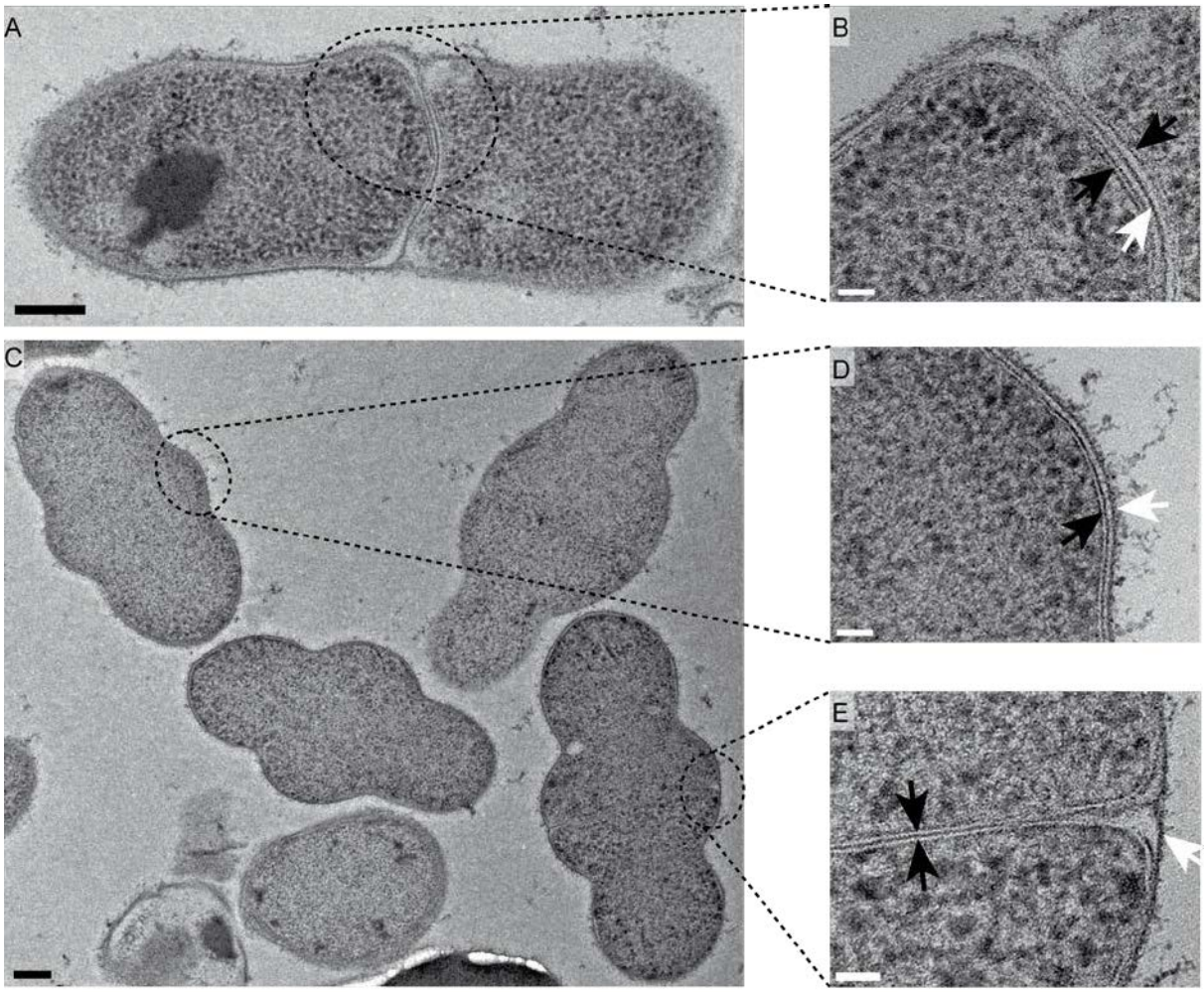


**FIG 3.** Electron micrographs of negatively stained cryo-thin sections of R6 Δ*lytA* cells treated for 2 h with 0.06 µg/mL piperacillin (2x the MIC). Bulging cells with complete (A and B), partial (C and D) or absent septum (C and E) are shown. Bars are 200 nm (A and C) and 20 nm (B, D and E). The black arrows point to the two leaflets of the plasma membrane. The white arrows point to the cell wall.

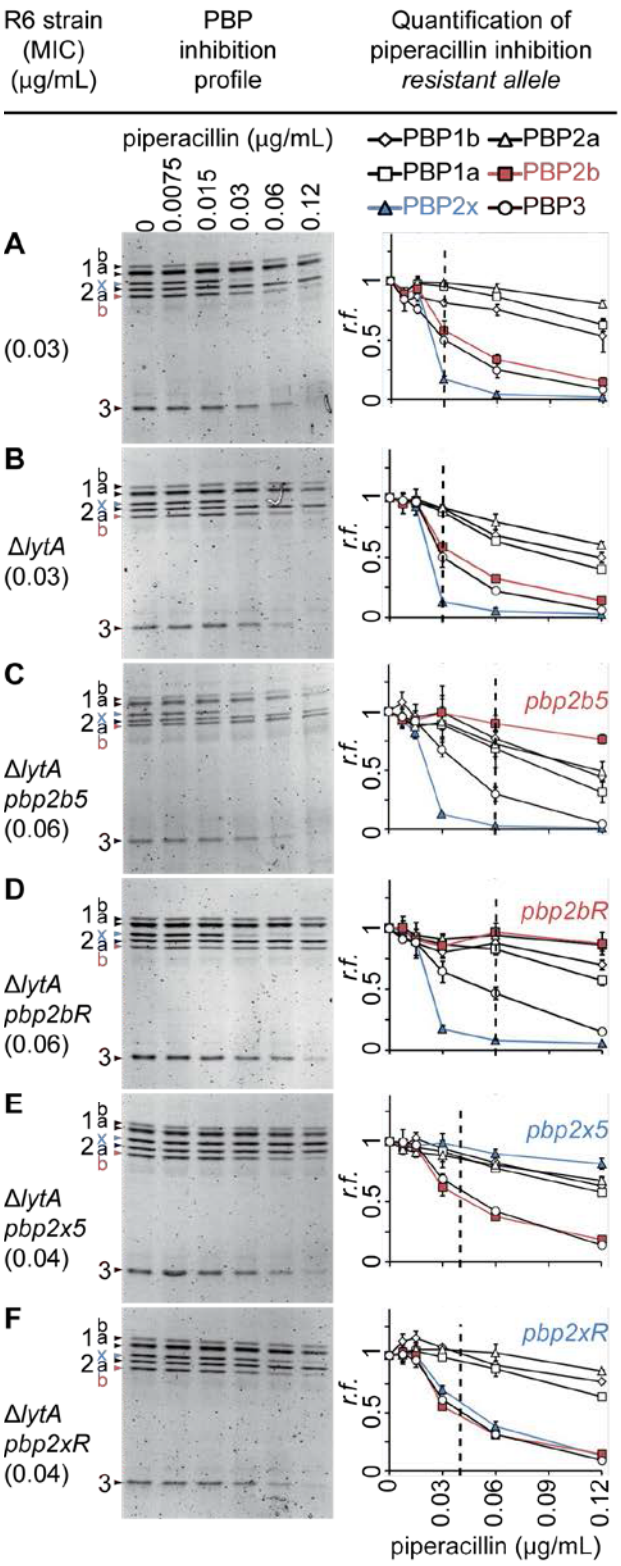


**FIG 4.** *In vivo* PBP inhibition profile by different concentrations of piperacillin. Cells were incubated for 10 min with the drug prior to washing, membrane isolation and PBP labeling with Bocillin™-FL. A representative fluorogram is shown for each strain. Bands intensity was quantified by densitometry, and results are presented for each PBP as the fraction remaining reactive (*r.f.*) with Bocillin™-FL after piperacillin treatment (means of three independent experiment, error bars are the standard deviation). The vertical dashed lines represent the MICs.

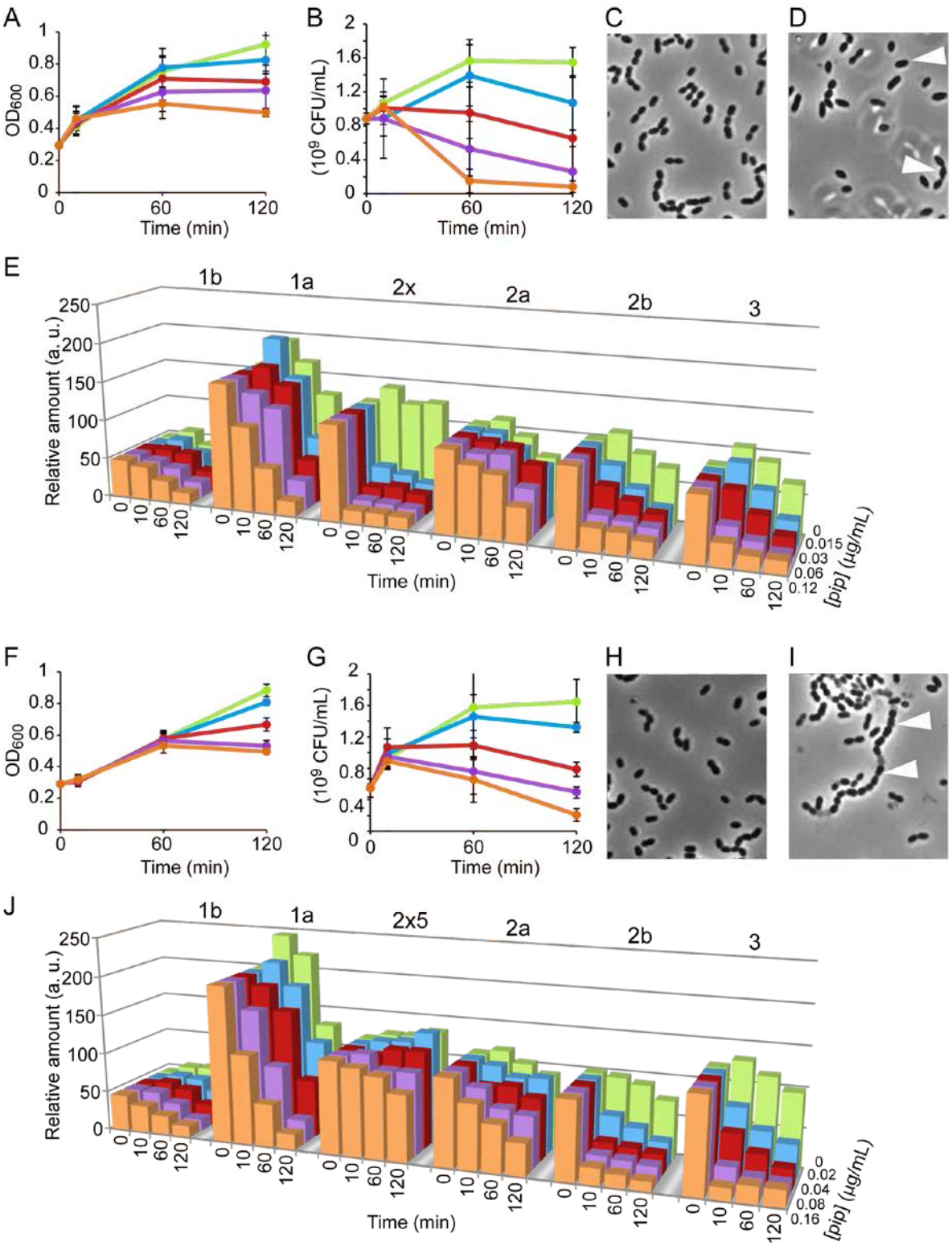


**FIG 5.** Consequences exposure of strain R6 Δ*lytA* (A to E) and R6 Δ*lytA pbp2x5* (F to J) to piperacillin at 0 (green), ½ (blue), 1 (red), 2 (purple) and 4 times (orange) the MIC. Means of three independent experiments are shown with standard deviation. (A and F) Turbidity measured after piperacillin addition. (B and G) Viability after piperacillin addition. (C and H) Morphology observed by phase contrast microscopy after one hour further incubation without piperacillin. (D and I) Morphology after one hour incubation with piperacillin at the MIC. White arrows point to lemon- (D) or lentil-shaped cells (I). (E and J) Quantification of PBP profiles. Bars represent the amount of a particular PBP that has reacted with Bocillin™-FL after incubation with piperacillin. Amounts are given relatively to that of PBP2x (or PBP2x5) at time zero (set arbitrarily to 100).

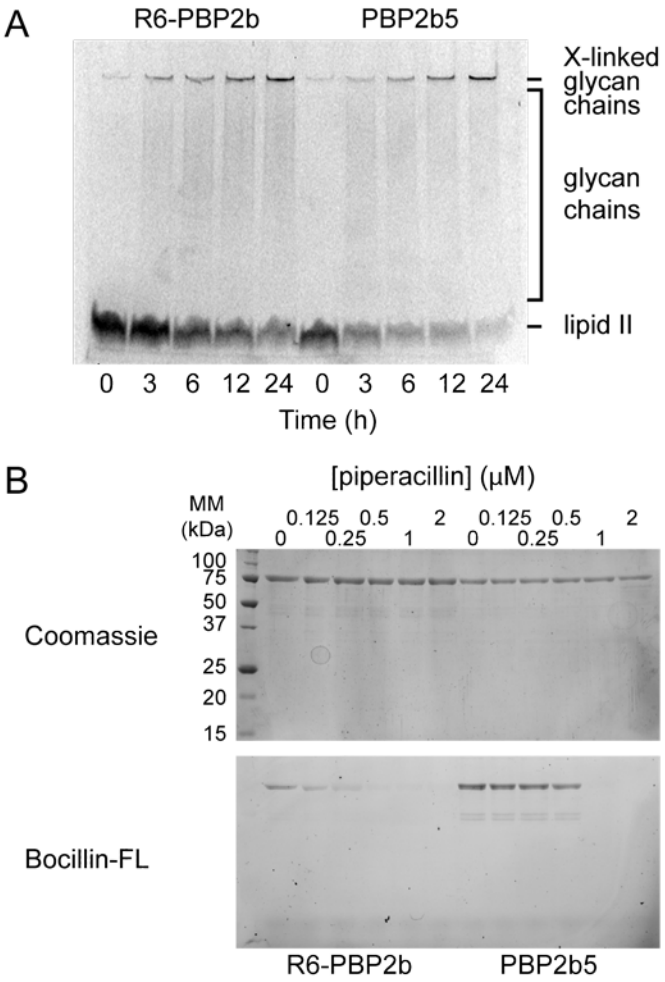


**FIG 6.** Transpeptidase activity and reactivity of PBP2b with piperacillin *in vitro*. (A) Time course of peptidoglycan synthesis by R6-PBP2b or PBP2b5 with PBP2a-S410A to provide glycosyltransferase activity. A mixture of 50 μM amidated lipid II and 5 μM non-amidated dansylated lipid II was incubated with 0.5 μM PBP2b and 1 μM PBP2a-S410A at 30°C. Aliquots were withdrawn after various time intervals and the reaction was stopped by the addition of moenomycin and penicillin G. Samples were analyzed by SDS-PAGE, and the dansyl fluorescence was imaged by UV trans-illumination. (B) 0.5 μM R6-PBP2b or 0.25 μM PBP2b5 were incubated with varying concentration of piperacillin for 10 min at room temperature prior to reaction with 100 μM Bocillin™-FL. Samples were analyzed by SDS-PAGE and fluorescence imaging and Coomassie-blue staining.

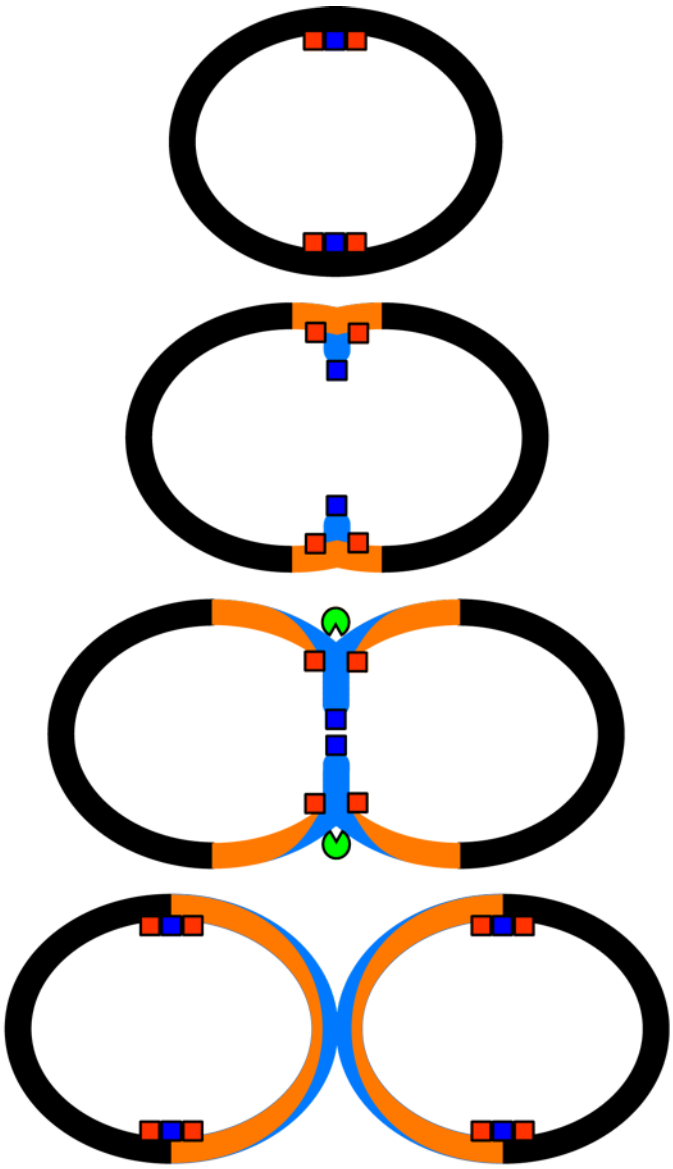

**FIG 7.** Model for the assembly of peptidoglycan in the pneumococcal cell wall. Peptidoglycan resulting from the septal machinery, which includes PBP2x (blue box), is shown in blue. Peptidoglycan resulting from the peripheral machinery including PBP2b (red box) is in orange. The septum splitting hydrolase activity is the green symbol. This model of peptidoglycan deposition can account for the greater required proportion of active PBP2b than PBP2x, since synthesis by the peripheral machinery can reinforce the material laid down by a diminished septal machinery.

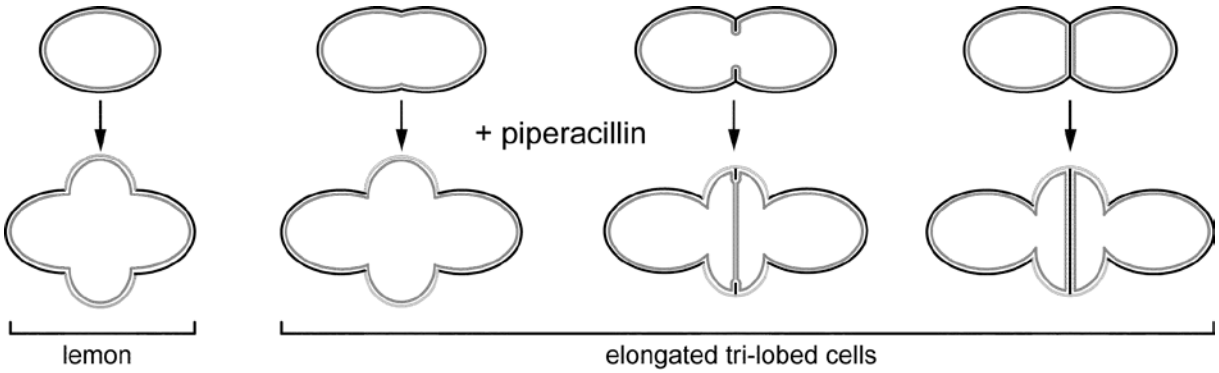


**FIG 8.** Model for the generation of abnormal morphologies following exposure to piperacillin. Depending on the stage of the cell cycle at the time of piperacillin inhibition (top row), the on-going insertion of new cell wall material (light gray) generates the abnormal bulging shapes shown on the lower row. The plasma membrane in shown in dark gray.

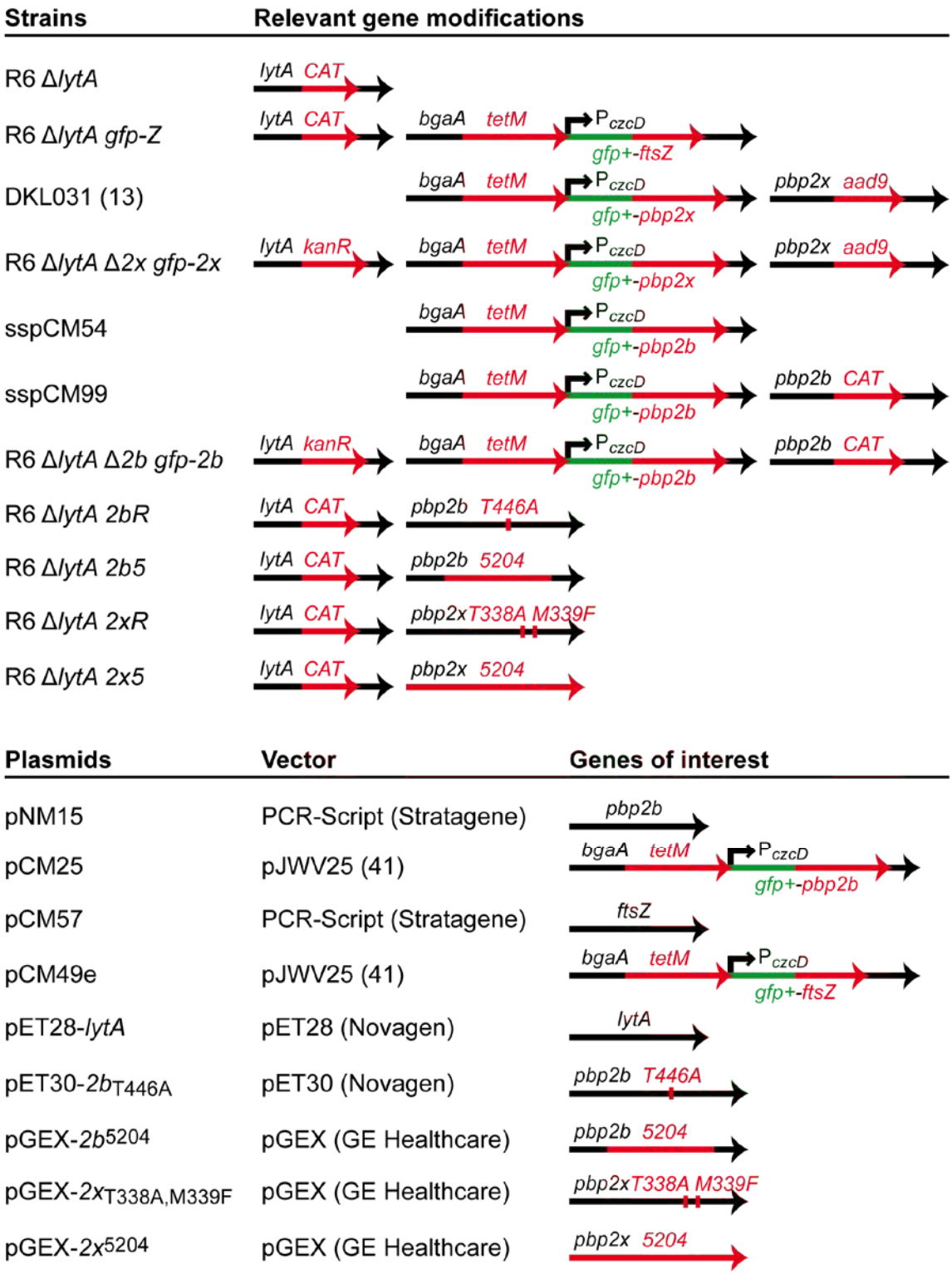


FIG S1. Schemes of the bacterial strains and DNA constructs used in this study. The insertions and genetic modifications are in red, the GFP coding sequence is in green.

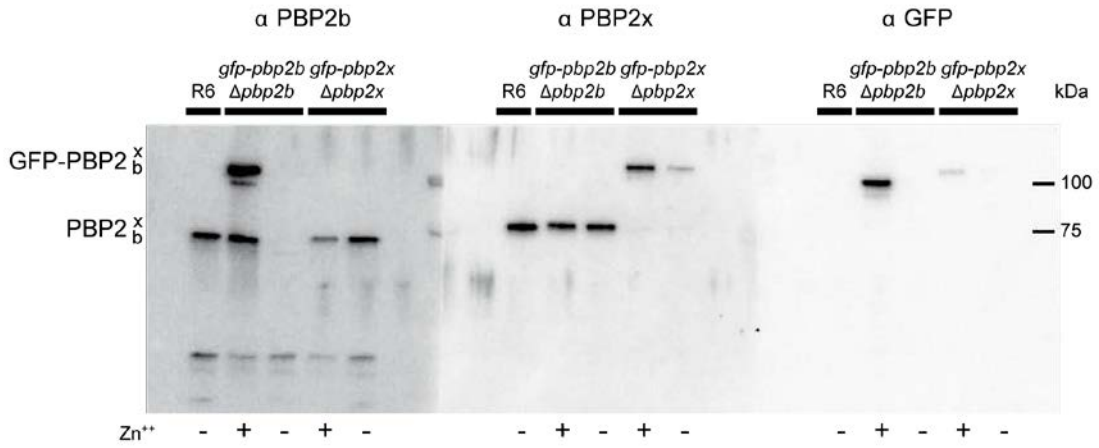


FIG S2. Western blot detection of PBP2b, PBP2x or GFP on R6 Δ*lytA*, R6 Δ*lytA gfp-pbp2x* Δ*pbp2x* and R6 Δ*lytA gfp-pbp2b* Δ*pbp2b* strains in the presence or absence of inducer (Zn++). The same samples were used as in Fig. 2B

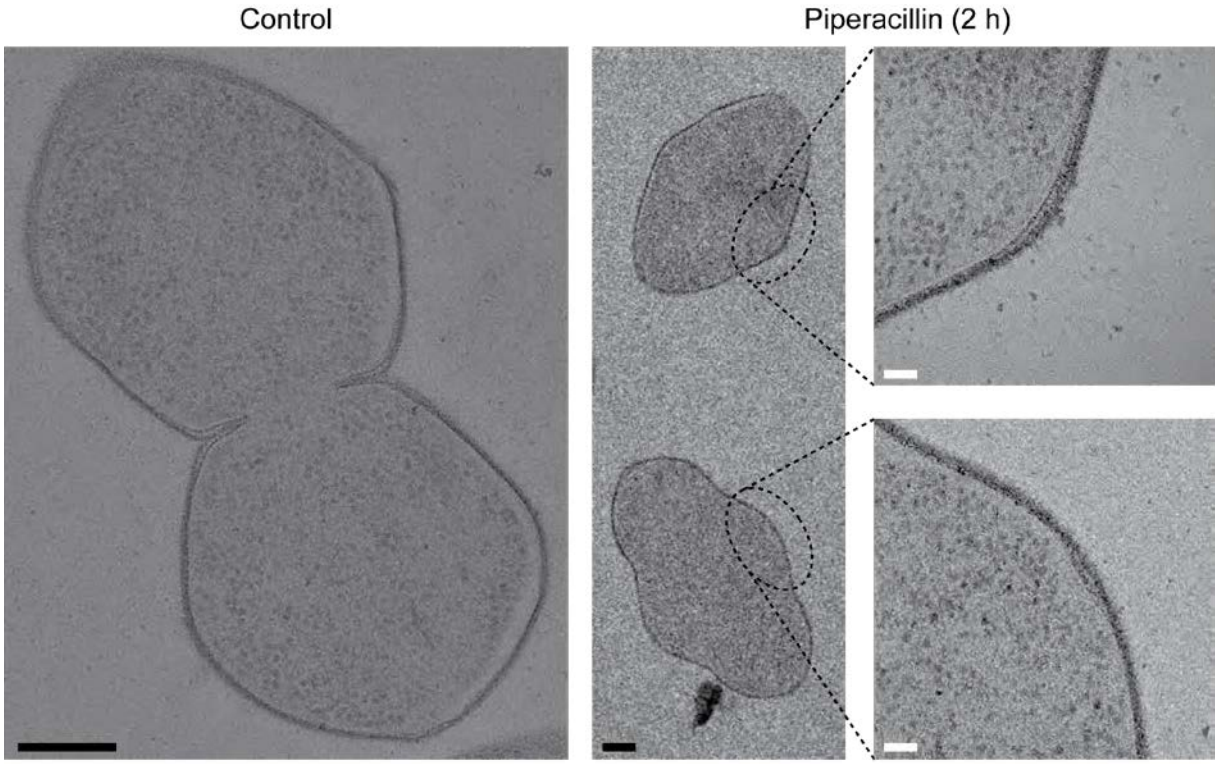


FIG S3. Electron micrographs of R6 cells treated or not (Control) for 2 h with 0.06 µg/mL piperacillin (2x the MIC). All the bulging cells observed lacked septum (middle and right panels). Black scale bars are 200 nm, white scale bars are 50 nm.

**TABLE 1** Strains and plasmids

| Strains | Relevant characteristics | Reference |
|---|---|---|
| R6 | Unencapsulated laboratory strain | (39) |
| R6 Δ*lytA* | *lytA::CAT*; $Cm^R$ | (40) |
| R6 Δ*lytA gfp-ftsZ* | *lytA::CAT bga::tetM*-$P_{czcD}$-*gfp+-ftsZ*; $Cm^R$, $Tet^R$ | This study |
| DKL031 | *bga::tetM*-$P_{czcD}$-*gfp+-pbp2x pbp2x::aad9*; $Tet^R$, $Spc^R$ | (13) |
| R6 Δ*lytA gfp-pbp2x* Δ*pbp2x* | *lytA::kanR bga::tetM*-$P_{czcD}$-*gfp+-pbp2x pbp2x::aad9*; $Kan^R$, $Tet^R$, $Spc^R$, | This study |
| sspCM54 | R6; *bga::tetM*-$P_{czcD}$-*gfp+-pbp2b*; $Tet^R$ | This study |
| sspCM99 | R6; *bga::tetM*-$P_{czcD}$-*gfp+-pbp2b pbp2b::CAT*; $Tet^R$, $Cm^R$, | This study |
| R6 Δ*lytA gfp-pbp2b* Δ*pbp2b* | *lytA::kanR bga::tetM*-$P_{czcD}$:*gfp+-pbp2b pbp2b::CAT*; $Kan^R$, $Tet^R$, $Cm^R$ | This study |
| R6 Δ*lytA pbp2bR* | Δ*lytA::CAT* $pbp2b_{T446A}$; $Cm^R$ | This study |
| R6 Δ*lytA pbp2b5* | Δ*lytA::CAT* $pbp2b^{5204}$; $Cm^R$ | This study |
| R6 Δ*lytA pbp2xR* | Δ*lytA::CAT* $pbp2x_{T338A,M339F}$; $Cm^R$ | This study |
| R6 Δ*lytA pbp2x5* | Δ*lytA::CAT* $pbp2x^{5204}$; $Cm^R$ | This study |

| Plasmids | Relevant characteristics | Reference |
|---|---|---|
| pNM15 | PCR-Script::*pbp2b*; $Cm^R$ | This study |
| pCM25 | pJWV25 (41) *bga::tetM*-$P_{czcD}$-*gfp+-pbp2b*; $Tet^R$ | This study |
| pCM57 | PCR-Script::*ftsZ*; $Cm^R$ | This study |
| pCM49e | pJWV25 (41) *bga::tetM*-$P_{czcD}$-*gfp+-ftsZ*; $Tet^R$ | This study |
| pET28-*his-lytA* | pET28a::*his-lytA* | This study |
| pET30-$2b_{T446A}$ | pET30 $pbp2b_{T446A}$; $Kan^R$ | (30) |
| pGEX-$2b^{5204}$ | pGEX $pbp2b^{5204}$; $Amp^R$ | (30) |
| pGEX-$2x_{T338A,M339F}$ | pGEX $pbp2x_{T338A,M339F}$; $Amp^R$ | (33) |
| pGEX-$2x^{5204}$ | pGEX $pbp2x^{5204}$; $Amp^R$ | (33) |

**TABLE 2** MIC of piperacillin

| Strain | MIC (μg/mL) |
|---|---|
| R6 | 0.03 |
| R6 Δ*lytA* | 0.03 |
| R6 Δ*lytA gfp-ftsZ* | 0.03 |
| R6 Δ*lytA gfp-pbp2x* Δ*pbp2x* | 0.03 |
| R6 Δ*lytA gfp-pbp2b* Δ*pbp2b* | 0.03 |
| R6 Δ*lytA pbp2b5* | 0.06 |
| R6 Δ*lytA pbp2x5* | 0.04 |
| R6 Δ*lytA pbp2bR* | 0.06 |
| R6 Δ*lytA pbp2xR* | 0.04 |

# IV- Discussion

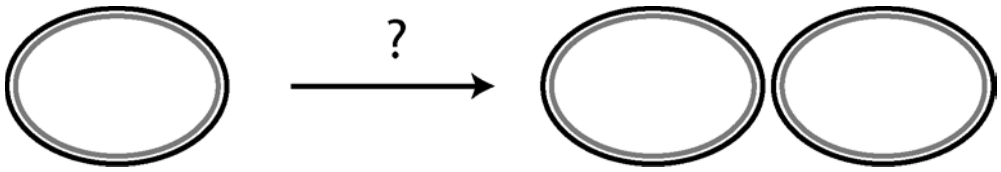

## Discussion - Résumé

Cette thèse illustre bien que les connaissances fondamentales sur un organisme pathogène sont nécessaires pour lutter contre les infections. En effet, les connaissances sur les mécanismes moléculaires de la morphogenèse du pneumocoque m'ont permis de comprendre comment la pipéracilline perturbe sa croissance. Ce type de connaissances est crucial pour améliorer les stratégies de traitement de cet organisme qui s'adapte de manière constante aux nouveaux stress infligés par les antibiotiques. Dans cette discussion, je tente de définir un modèle de morphogenèse du pneumocoque, prenant en compte mes résultats et la littérature. Ces données fondamentales suggèrent que PBP2b et les protéines associées à l'élongation sont cruciales pour le développement du pneumocoque et constituent des cibles thérapeutiques prometteuses.

La première question posée au début de ma thèse est : la morphogenèse du pneumocoque est-elle organisée par un ou deux complexes de protéines ? Probablement ni l'un, ni l'autre. En effet, plusieurs complexes ont été isolés comprenant de deux à cinq protéines de la division, de l'élongation ou un mélange des deux. La validité de certains de ces complexes reste à confirmer, mais des protéines semblent pouvoir intervenir dans les deux mécanismes. On peut alors formuler l'hypothèse suivante : des complexes fonctionnels se forment de manière transitoire au cours du cycle cellulaire. Ce système implique des mécanismes de régulation spatiale et temporelle restant peu connus à ce jour.

Un modèle de morphogenèse est proposé où l'organisation de la synthèse et de la dégradation du peptidoglycane est décrite au cours du cycle cellulaire. Au début du cycle cellulaire, un large assemblage de protéines de l'élongation (PBP2b, RodA, MreC, MreD, PBP1a) et de protéines de la division (PBP2x, FtsW, DivIB, DivIC, FtsL et une PLP de classe A) interagit avec FtsZ et les autres protéines de l'anneau de division à l'équateur de la cellule. Un signal va entraîner l'initiation de l'élongation où PBP1a va être responsable de la polymérisation des chaînes glycanes et PBP2b de leur insertion périphérique dans le sacculus « ouvert » par une activité hydrolase. La formation du septum commence ensuite par les activités de PBP1a et PBP2x (à ce moment, PBP1a est impliquée à la fois dans l'élongation et la division). Alors que le septum se referme, PcsB sépare les cellules filles en clivant le peptidoglycane septal. Celui-ci est renforcé par PBP2b qui continue aussi à intégrer les chaînes glycanes générées par PBP1a. Au niveau du septum, une autre PLP de classe A procure l'activité glycosyltransférase. Une fois les membranes refermées au centre de la cellule, l'anneau de division est relocalisé aux équateurs des cellules filles tandis que PBP2x et les autres protéines de division complètent le septum avant d'être relocalisées à leur tour aux équateurs. Alors que les protéines de l'élongation finissent leur tâche, l'activité de LytB va permettre de finaliser la séparation

de cellules filles. Enfin, les protéines de l'élongation rejoignent les protéines de la division aux équateurs.

Le pneumocoque compte six PLPs. PBP1a, PBP1b et PBP2a sont des PLPs de class A sont bi-fonctionnelles (activité glycosyltransférase et transpeptidase), les PLPs de classe B (PBP2b et PBP2x) sont mono-fonctionnelles (activité transpeptidase) et la PLP de classe C, PBP3 a une activité DD-carboxypeptidase. PBP2b et PBP2x sont impliquées dans l'élongation et la division, respectivement. En revanche, le rôle spécifique des trois PLPs de classe A n'est pas connu et la redondance de leurs activité n'est pas encore comprise, bien que PBP1a semble impliquée dans l'élongation, mais aussi dans l'initiation de la division. Le fait que la présence d'une seule PLP de classe A (PBP1a ou PBP2a) suffit pour assurer le développement du pneumocoque avec un taux de croissance inchangé suggère que ces protéines peuvent être impliquées dans l'élongation et la division.

Concernant les PLPs de classe B, mes résultats indiquent que PBP2b a un rôle prépondérant dans la morphogenèse. En effet, c'est l'inhibition de cette protéine qui impacte la croissance des pneumocoques traités à la pipéracilline. L'inhibition de PBP2x, quant à elle, est responsable des défauts morphologiques observés dans ces conditions. Ceci est en accord avec le fait que seules les β-lactamines inhibant l'activité de PBP2b sont bactériolytiques, les autres étant bactériostatiques. Deux explications sont suggérées. Premièrement, l'insertion de peptidoglycane dans le sacculus au niveau de la périphérie n'est possible que si celui-ci est « ouvert » par l'action d'hydrolases. Lorsque PBP2b est inhibé, cette activité pourrait continuer, entraînant la lyse. En revanche, l'insertion de peptidoglycane au niveau du septum peut se faire sans hydrolase, comme il est inséré sur le bord interne de la paroi septale. Son inhibition, bien qu'empêchant la multiplication du pneumocoque n'entraîne pas la lysis. La deuxième explication est basée sur le fait que le peptidoglycane septal est peut-être consolidé par l'activité de PBP2b dans le modèle proposé. Si des chaînes glycanes sont insérées au centre de la cellule mais que PBP2x est inhibée, PBP2b pourrait assumer leur réticulation. Ce modèle rend compte du fait qu'une quantité moindre de PBP2x que de PBP2b est nécessaire au pneumocoque.

Un autre mécanisme permet au pneumocoque de compenser une baisse de l'activité de PBP2b. En effet, chez *S. pneumoniae*, en présence de peptidoglycane de structure branchée, une plus faible activité de PBP2b est suffisante pour assurer la multiplication. La raison exacte n'est pas connue, on peut imaginer que cette structure affecte l'attachement ou l'activité des hydrolases sur le peptidoglycane. Une autre hypothèse est que que les propriétés de la paroi sont changées pour devenir plus élastique, permettant une meilleure résistance à la pression osmotique donnant donc la possibilité au pneumocoque de se développer alors que l'activité de PBP2b est amoindrie.

# Discussion

This thesis demonstrates that basic knowledge is necessary to fight diseases. More specifically, understanding the molecular mechanisms of the morphogenesis of *S. pneumoniae* brings insights on how β-lactams interferes with the growth of this pathogen. This knowledge is of critical importance for improving the strategies employed to combat the pneumococcus that constantly evolves in parallel with the development of new treatments. The identification of the most essential mechanisms or those that have the most multifaceted impact on peptidoglycan synthesis will provide promising targets. In this part, I discuss the results obtained during my thesis, and what they imply on the molecular mechanisms of the morphogenesis of *S. pneumoniae*. These fundamental results suggest that PBP2b and the other associated elongation proteins are promising targets to avoid the development of pneumococcal infections.

## Organization of the morphogenesis machineries in the pneumococcus

The first question I asked in this thesis is whether the morphogenesis of *S. pneumoniae* involves one or two machineries. In the light of my results and the literature, the short answer answer could be: neither. Indeed, although neither hypothesis can be ruled out, no robust observations could clearly demonstrate the existence of separated elongasome and divisome to date. But what can mine and others' observations indicate concerning the organization of the morphogenesis machineries in the pneumococcus?

A complex comprised of five division proteins, PBP2x/FtsW/DivIB/DivIC/FtsL, has been isolated *in vitro* (Noirclerc-Savoye*, et al.*, 2013). I reported the isolation of two complexes including elongation proteins: PBP2b/RodA and MreC/MreD (Philippe*, et al.*, 2014). These results indicate that some morphogenesis proteins interact in bacterial membranes. Further, I presented a result suggesting that the elongation proteins MreC, MreD can interact with the division proteins FtsW and PBP2x, as well as with the elongation proteins RodA and PBP2b. However, this surprising result was obtained in a context where recombinant pneumococcal proteins were overexpressed in *E. coli*. Three explanations can be proposed with diminishing significance. First, the interactions may be genuine and MreC and MreD may participate to both the elongasome and the divisome. Several bridges have already been reported between both putative machineries. For example, EzrA was proposed to link GpsB and DivIVA to FtsZ, based on the interactions observed by surface plasmon resonance (SPR) and the similar pattern of localization of the four proteins in WT and morphologically defective mutants (Fleurie*, et al.*, 2014). Secondly, MreC/MreD may truly interact with RodA and PBP2b, but may be "tricked" to interact with the homologues FtsW and PBP2x in the

recombinant system where the four proteins are overexpressed, because of the sequence and structural similarity and the absence of regulation and natural context. Thirdly, as many protein contaminants were recovered with the putative complexes, it is possible that overexpressed recombinant membrane proteins have a tendency to aggregate together, allowing an apparent co-purification. Further work is required to clarify the issue, ideally with alternative methods.

In *S. pneumoniae*, additional morphogenesis proteins may stabilize or impair the formation of these complexes. Therefore, to verify the physiological relevance of these complexes, they must be isolated from pneumococcus cells. For example, if one protein was immuno-precipitated with additional proteins, this would evidence the occurrence of a complex *in vivo*.

In the pneumococcus, all the proteins mentioned above were shown to localize at the septum and equators of the cell by fluorescence microscopy (Morlot*, et al.*, 2003), (Morlot*, et al.*, 2004), (Noirclerc-Savoye*, et al.*, 2005), (Zapun*, et al.*, 2008), (Land & Winkler, 2011). However, this technique has a limit of resolution of 200 nm, which would not discriminate fine localization differences if the morphogenesis proteins have a distinct localization within the zone of peptidoglycan insertion. This is supported by recent super-resolution microscopy results indicating that PBP1a can co-localize with or be separated from PBP2x depending on the stage of division (Land*, et al.*, 2013).

The hypothesis of a single large morphogenesis machinery has been proposed in the pneumococcus (Massidda*, et al.*, 2013), (Fleurie*, et al.*, 2014). Two separate morphogenesis machineries have also been suggested (Zapun*, et al.*, 2008). Whether these machineries involve physical protein interactions remains unclear. Some complexes exist and are robust, which involve a limited number of proteins: DivIB/DivIC/FtsL (Noirclerc-Savoye*, et al.*, 2005), (Noirclerc-Savoye*, et al.*, 2013), FtsW/PBP2x (Zapun*, et al.*, 2012), MreC/MreD and PBP2b/RodA (Philippe*, et al.*, 2014). A recombinant complex comprised of five division proteins (DivIB/DivIC/FtsL/FtsW/PBP2x) has been isolated but in low quantities (Noirclerc-Savoye*, et al.*, 2013). A cognate complex may exist with the elongation proteins PBP2b, RodA, MreC, MreD and/or others. A trivial explanation for the difficulty to isolate these complexes is that the detergent destabilizes the interactions, or that over-expression of the proteins is insufficient because of their toxicity when they are in too large amounts in the membranes. However, it is also possible that such complexes are intrinsically unstable and occur only transiently *in vivo*, at specific stages of the cell cycle and division process, controlled by other events. Regulatory events could be interaction with other proteins, modification such as phosphorylation or degradation, membrane composition and/or curvature modification, or substrate availability. It is likely that these large molecular complexes, if they exist *in vivo*, are transient.

The formation of protein complexes can be of functional relevance *in vivo*. A role in peptidoglycan synthesis can be envisaged, on the TP or GT activity of the PBPs or on the flippase activity, for example. An example exists in *E. coli*, where the GT activity of PBP1a (orthologue of its homonym in the pneumococcus) was shown to be enhanced in presence of PBP2 (orthologue of PBP2b) and that both proteins cooperated to attach neo-synthesized peptidoglycan to sacculi (Banzhaf*, et al.*, 2012). Now that biochemical assays are available to monitor both processes *in vitro* (Mohammadi*, et al.*, 2011), (Zapun*, et al.*, 2013), the activity of complexes of pneumococcus proteins can be compared to that of individual enzymes. However, the specific detergent conditions required for these tests may affect the interaction of the proteins and further improvements are necessary.

A simple role of the protein/protein interactions in the localization is also possible. Note that even if this cannot be ruled out, specific localization does not necessarily rely on the formation of complexes. Membrane lipid organization or local modifications in the structure of the peptidoglycan could affect localization, and may even be sufficient for proper localization. It was shown in *E. coli* in "preseptal" phase that MreC, MreD, RodA and the cytoskeletal protein MreB (absent in the pneumococcus) could localize in a ring pattern independently of each other, while PBP2 (orthologue of PBP2b) requires the presence of MreC for such localization (Vats*, et al.*, 2009). Only the FtsZ-ring was required for the localization of all these proteins in the ring pattern. It is unlikely that this dependence on the FtsZ-ring is due to direct interaction with FtsZ that would require transient binding to a large number of distinct proteins.

Although the formation of complexes between morphogenesis proteins has been demonstrated, their physiological relevance remains poorly documented. As discussed above, functional complexes may occur transiently along the cell cycle, regulated in terms of timing and spatial localization. A plausible morphogenesis model can be built in agreement with distinct transient interactions between morphogenesis along the cell cycle (Figure 56). In this model, a large complex initiates septation, where the division proteins (PBP2x, FtsW, DivIB, DivIC, FtsL and at least one class A PBP) interact with the division ring (polymers of FtsZ, SepF and FtsA) and the elongation proteins (PBP2b, RodA, MreC, MreD and a class A PBP). Thereafter, the division proteins follow the division ring during membrane constriction to form the septum. The interaction between the division proteins and the division ring is disrupted to allow the membrane fission. The division proteins complete the peptidoglycan septum while the division ring is re-localized to the equators of the daughter cells. Eventually, the division proteins re-localize to the equators of the daughter cells. Meanwhile, the elongation proteins incorporate peptidoglycan at the periphery, as the sacculus is "opened" by hydrolases. At a defined time, the separation proteins (PcsB and others) are activated and cleave the septum in its middle. From this moment, the elongation proteins incorporate peptidoglycan in the

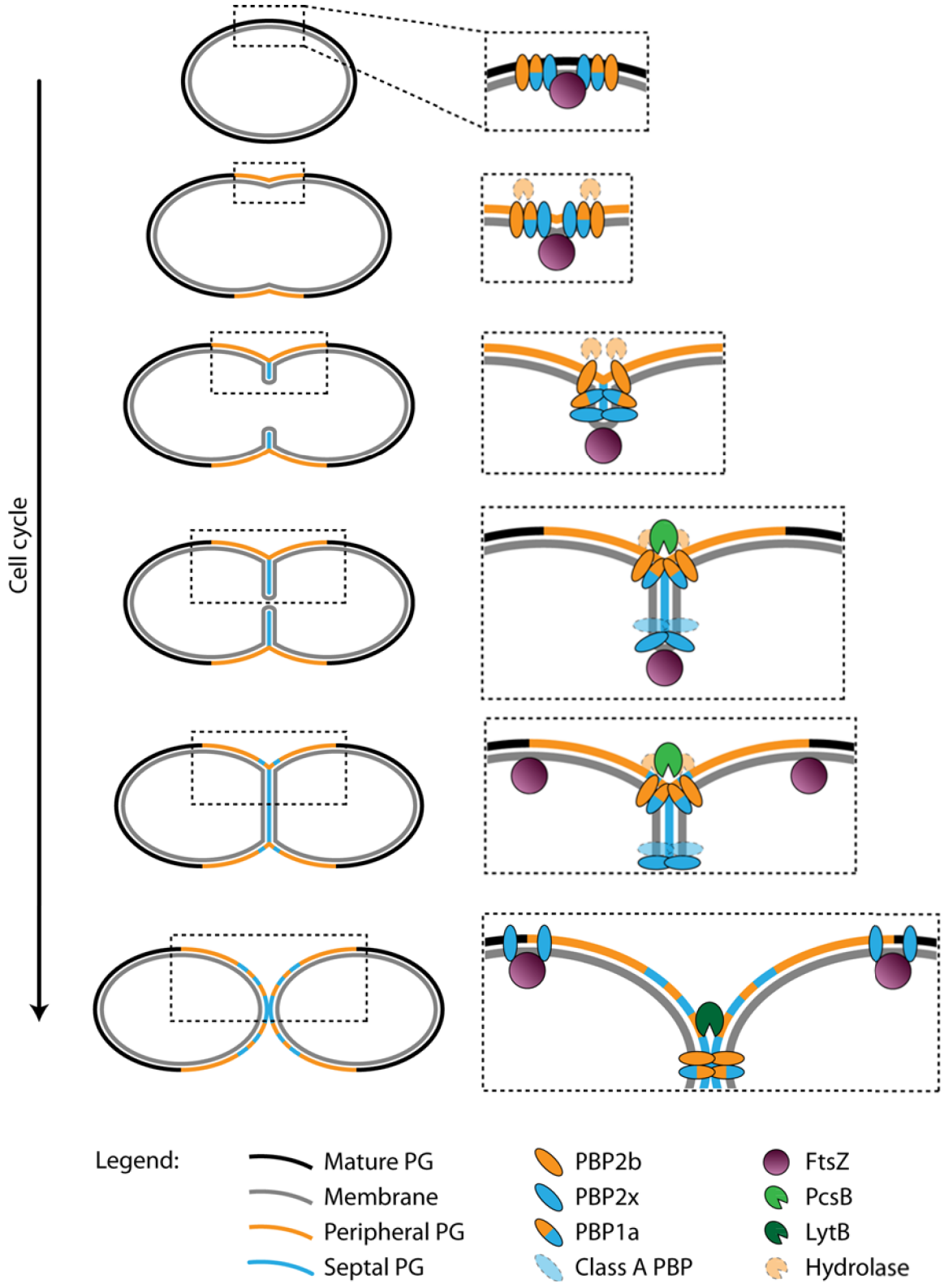


Figure 50: **Model for the morphogenesis of *S. pneumonia*. PG: peptidoglycan.**

split septum until the daughter cells are completely separated (by LytB and other hydrolytic activities).

This model implies some mechanisms of regulation to provide the signals necessary to orchestrate the changes in protein interactions, and the localization of the machineries.

## What can we learn from the activity of the PBPs?

### Redundancy of the class A PBPs

The pneumococcus genome codes for six PBPs. The class A PBPs, PBP1a, PBP1b and PBP2a are bi-functional in that they perform both GT and TP activities while the class B PBPs, PBP2b and PBP2x, are mono-functional transpeptidases. The class C PBP, PBP3, is a DD-carboxypeptidase involved in the maturation of the peptidoglycan in the sacculus. The two class B PBPs have been assigned to distinct processes, which explain the need for two class B PBPs in *S. pneumoniae*. PBP2b is required for the elongation of pneumococcal cells (Berg*, et al.*, 2013) while PBP2x allows division (Berg*, et al.*, 2013), (Land*, et al.*, 2013), (Peters*, et al.*, 2014). The specific role of the class A PBPs is much less known and only indirect observations assign PBP1a to elongation or septation, as discussed in the Introduction. To date, the reason why three enzymes with redundant activities are conserved in the pneumococcus is unclear. The three proteins are individually dispensable for growth, but at least PBP1a or PBP2a are required in the absence of PBP1b (Paik*, et al.*, 1999). Thus, the activity of PBP1b does not seem to play a major role, and that of both PBP1a and PBP2a must be able to provide glycan chains both at the septum and at the periphery. Note that Land *et al.* reported that the depletion of PBP1a yielded pneumococcus cells of slightly reduced size (Land & Winkler, 2011).

The trivial assignment of PBP1a to the elongation and PBP2a to the division is unlikely. Indeed, PBP1a may play a role in both division and elongation. More precisely, its co-localization with elongation proteins in late division steps implies that it can play a role in elongation. On the other hand, its co-localization with PBP2x at early stages of division may reflect an activity in the elongation of glycan strands used in the synthesis of a septum by PBP2x. A link between PBP1a and PBP2x was also suggested in the analysis of the level of resistance of pneumococcal strains with different combinations of low-susceptibility PBP2x and PBP1a variants (Zerfass*, et al.*, 2009). When a mosaic version of PBP2x was introduced in a R6 strain containing the cognate mosaic PBP1a, high levels of resistance to cefotaxime were obtained. By contrast, if the low-affinity PBP2x T338G mutant was used instead of the mosaic version, the resulting strain had a slightly lower resistance compared to its parent. The authors proposed that mosaic PBP1a and PBP2x evolved in parallel and

that multiple modifications increased their resistance while preserving their interaction. However, the mosaic PBPs would have lost their ability to bind WT PBP, or point mutants of the PBP. A dual role in division and elongation has also been proposed for *B. subtilis* PBP1 (orthologue of PBP1a) based on localization studies (Claessen*, et al.*, 2008). We can imagine that PBP1a is required to initiate division, providing PBP2x with glycan chains, this activity being pursued by another class A PBP.

### A preponderant role for PBP2b compared to PBP2x

Given my results and the literature, although they are both essential in the pneumococcus, the activity of PBP2b seems to be more critical than that of PBP2x. My results show that under piperacillin challenge, it is the inhibition of PBP2b that is most detrimental to the cells despite the fact that PBP2x is the preferred target and the morphological defects are due to the inhibition of PBP2x. Interestingly, Hakenbeck *et al.* showed that β-lactams that inhibit PBP2b are bacteriolytic while those that do not affect its activity are bacteriostatic (Hakenbeck*, et al.*, 1987). In this part, I propose two plausible explanations according to the current knowledge on the morphogenesis of the pneumococcus.

Insertion of new peptidoglycan strands does not have the same constraints at the septum and at the periphery. At the periphery, the sacculus must be "opened" to allow the insertion of neo-synthesized glycan chains. By contrast, to form the septum, peptidoglycan strands can be attached on the inner "edge". Therefore, it is necessary that the activity of peptidoglycan hydrolases is coupled with the GT and TP activities to in insert new peptidoglycan during elongation. Assuming this, the inhibition of PBP2b by β-lactam would prevent the cross-linking of neo-synthesized glycan chains in the peripheral sacculus. However, the hydrolases that make space for new peptidoglycan may continue to digest the cell wall, which is not reinforced by insertion of new material. This imbalance would lead to lysis of the bacterium, hence the bacteriolytic property of β-lactam that inhibit PBP2b. By contrast, the inhibition of PBP2x by β-lactam that do not target PBP2b (such as the cephalosporins) prohibit septum formation, which is not associated to a hydrolytic activity. Thus, bacterial multiplication is blocked, but no lysis ensues. The β-lactam that target PBP2x are bacteriostatic.

The second explanation relies on assumptions made from protein localization throughout the cell cycle by traditional and high-resolution fluorescence microscopy (Morlot*, et al.*, 2003), (Morlot*, et al.*, 2004), (Noirclerc-Savoye*, et al.*, 2005), (Zapun*, et al.*, 2008), (Land & Winkler, 2011), (Land*, et al.*, 2013). In the model presented above (Figure 56), splitting the septum begins after the initiation

of its synthesis by the division proteins. Splitting of the septum is concomitant with insertion of new peptidoglycan at the periphery by the elongation proteins and the elongation proteins reach the center of the septum after the division proteins. The elongation proteins may also reinforce the septal peptidoglycan that undergoes splitting. Upon challenge with a β-lactam that does not bind PBP2b, some glycan chains continue to be produced at mid-cell but cannot be "weaved" or cross-linked into the septum because of impaired TP activity. However, although the septum is not formed, PBP2b and the other elongation proteins are in the close vicinity of this septal material and can provide some compensatory TP activity. By contrast, when PBP2b is inhibited in addition to PBP2x, not only the synthesis of peripheral peptidoglycan is hampered and becomes exposed to turgor pressure without strengthening by PBP2b TP activity, but the septum that keeps being split becomes exposed to the environment without compensatory consolidation by PBP2b. A possible hydrolase activity associated with peripheral cell wall synthesis machineries fits in this model.

In conditions that are above the MIC of piperacillin in a WT strain but below that of the strains possessing the PBP2bR or PBP2b5 variants (between 0.03 and 0.06 µg/mL of piperacillin), PBP2x was nearly completely inhibited. However, the strains with PBP2bR and PBP2b5 could grow. How can the pneumococcus grow with virtually no PBP2x TP activity? Reasons could be that residual PBP2x activity may be sufficient to enable growth, or the simple interaction of the inactivated protein would give a signal to the division ring and the division proteins to initiate division, the lack of TP activity being compensated by other PBP(s), PBP2b and/or possibly class A PBPs.

In the explanations proposed above, one observation was omitted. Not only the presence, but also the activity of PBP2x is essential for pneumococcus growth. Indeed, PBP2x with a mutation in the catalytic site was still localizing at the septum, but the resulting pneumococcus could not grow (Peters*, et al.*, 2014). How of the low-affinity-PBP2b variant strains of pneumococcus could grow with less than 20% of PBP2x activity remains unclear.

### Compensation of impaired class B PBP activity

Both class B PBPs, PBP2x and PBP2b are essential in the pneumococcus. In order to protect the pneumococcus from this surface-exposed Achilles' heel, some mechanisms must have evolved to compensate the inhibition of either enzyme. A well-known mechanism is the reduction of the affinity for β-lactams. As discussed above, the inhibition of PBP2x activity might be less deleterious to the cell in that it prevents division, but likely does not induce lysis. A mechanism to compensate PBP2b lack of activity must be of higher priority as its inhibition results in lysis according to the observation and hypotheses mentioned above.

After progressive depletion of PBP2b in pneumococcus cells, it was shown that they remained viable, albeit with multiple morphological defects (Berg*, et al.*, 2013). The analysis of the composition of the peptidoglycan of PBP2b-depleted cells revealed that it had an increased proportion of branched cross-links. According to the model presented above, when PBP2b is inhibited, the peripheral peptidoglycan is digested by elongations hydrolases. The structure of the peptide bonds of the branched peptidoglycan contains an additional two amino-acids compared to linear links, which may impair the binding or activity of peptidoglycan hydrolases. The accumulation of branched cross-links may require some time, explaining why depletion of PBP2b by removal of the inducer of an ectopic copy of the gene can be well tolerated, whereas rapid inhibition by piperacillin is not.

Progressive depletion of PBP2x in pneumococcus cells did not result in major changes in the composition of the peptidoglycan. To date, no mechanisms were shown to compensate a lack in PBP2x activity, except lower affinity to β-lactam antibiotics in mosaic PBP2x.

Branched peptidoglycan has been shown to be required for the high level of resistance of the strain Pen6 against penicillin. Indeed the depletion of MurM and MurN (that add the L-Ser-L-Ala or L-Ala-L-Ala branch to the lipid II) in the Pen6 strain resulted in a peptidoglycan lacking branched links accompanied by a total loss of resistance to penicillin (Filipe & Tomasz, 2000). Why pneumococci with highly branched peptidoglycan are more resistant is not known, but it could be related to resistance to lysis following partial inhibition of PBP2b.

An observation remains unclear concerning the branched peptidoglycan and mosaic PBPs. Indeed, the Pen6 strain lost its resistance upon depletion of MurM and MurN, but could grow normally in the absence of β-lactam. Strikingly, the mutated Pen6 strain retained its low-affinity PBPs. Thus, mosaic PBPs do not require branched precursor in the absence of β-lactam challenge, and can process linear peptide at a rate that allows normal growth rate. To explain this puzzling observation, it has been proposed that branched precursors were better competitor for β-lactams than linear peptides. We propose here an alternative explanation. Low-affinity PBPs have a reduced affinity to β-lactams, but they are inhibited in some extent, albeit less than WT PBPs. We can imagine that upon penicillin challenge, the mosaic PBP2b of the Pen6 strain is inhibited in some extent, which can be compensated by the better resistance to lysis of branched peptidoglycan. In the Pen6 mutant with no branched peptides, the compensation is not possible. This is supported by the observation of Berg *et al.* that less PBP2b is required at higher branched peptides (Berg*, et al.*, 2013).

## Conclusion générale - Résumé

Les β-lactamines font partie des antibiotiques les plus efficaces et les plus utilisés au monde. Leur mécanisme d'action est étudié depuis de nombreuses années et est bien connu d'un point de vue biochimique. Ce qui est moins connu est la nature de la cascade d'évènements physiologiques provoquée par l'action des β-lactamines qui empêche le développement des bactéries traitées. Dans cette thèse, j'ai montré que l'effet le plus délétère est l'inhibition de l'activité transpeptidase de PBP2b. Le modèle de morphogenèse proposé permet d'émettre des hypothèses expliquant l'impact de la pipéracilline sur le pneumocoque.

## General conclusion

β-Lactams are some of the most efficient and of the most widely used antibiotics in the world. Also, the mode of action of β-lactams has been investigated for decades and is well understood in a biochemical point of view. To date, what is less known it the cascade of events that lead to growth arrest or death of β-lactam-treated bacteria. In this thesis, we have shown that the most deleterious effect of piperacillin on *S. pneumoniae* cells is the inhibition of the TP activity of PBP2b. The morphogenesis model that I proposed (Figure 56) based on the literature and that fits my observations allows questioning of the nature of the physiological response of the pneumococcus to β-lactams with different specificities.

# References


Albarracin Orio AG, Pinas GE, Cortes PR, Cian MB & Echenique J (2011) Compensatory evolution of pbp mutations restores the fitness cost imposed by beta-lactam resistance in Streptococcus pneumoniae. *PLoS Pathog* **7**: e1002000.

Alyahya SA, Alexander R, Costa T, Henriques AO, Emonet T & Jacobs-Wagner C (2009) RodZ, a component of the bacterial core morphogenic apparatus. *Proc Natl Acad Sci U S A* **106**: 1239-1244.

Andre G, Kulakauskas S, Chapot-Chartier MP*, et al.* (2010) Imaging the nanoscale organization of peptidoglycan in living Lactococcus lactis cells. *Nat Commun* **1**: 27.

Appelbaum PC, Bhamjee A, Scragg JN, Hallett AF, Bowen AJ & Cooper RC (1977) Streptococcus pneumoniae resistant to penicillin and chloramphenicol. *Lancet* **2**: 995-997.

Avery OT & Dubos R (1931) The Protective Action of a Specific Enzyme against Type Iii Pneumococcus Infection in Mice. *J Exp Med* **54**: 73-89.

Avery OT, Macleod CM & McCarty M (1944) Studies on the Chemical Nature of the Substance Inducing Transformation of Pneumococcal Types : Induction of Transformation by a Desoxyribonucleic Acid Fraction Isolated from Pneumococcus Type Iii. *J Exp Med* **79**: 137-158.

Banzhaf M, van den Berg van Saparoea B, Terrak M*, et al.* (2012) Cooperativity of peptidoglycan synthases active in bacterial cell elongation. *Mol Microbiol* **85**: 179-194.

Barendt SM, Sham LT & Winkler ME (2011) Characterization of mutants deficient in the L,D-carboxypeptidase (DacB) and WalRK (VicRK) regulon, involved in peptidoglycan maturation of Streptococcus pneumoniae serotype 2 strain D39. *J Bacteriol* **193**: 2290-2300.

Bartual SG, Straume D, Stamsas GA*, et al.* (2014) Structural basis of PcsB-mediated cell separation in Streptococcus pneumoniae. *Nat Commun* **5**: 3842.

Beilharz K, Novakova L, Fadda D, Branny P, Massidda O & Veening JW (2012) Control of cell division in Streptococcus pneumoniae by the conserved Ser/Thr protein kinase StkP. *Proc Natl Acad Sci U S A* **109**: E905-913.

Bendezu FO, Hale CA, Bernhardt TG & de Boer PA (2009) RodZ (YfgA) is required for proper assembly of the MreB actin cytoskeleton and cell shape in E. coli. *EMBO J* **28**: 193-204.

Benson TE, Marquardt JL, Marquardt AC, Etzkorn FA & Walsh CT (1993) Overexpression, purification, and mechanistic study of UDP-N-acetylenolpyruvylglucosamine reductase. *Biochemistry* **32**: 2024-2030.

Bera A, Herbert S, Jakob A, Vollmer W & Gotz F (2005) Why are pathogenic staphylococci so lysozyme resistant? The peptidoglycan O-acetyltransferase OatA is the major determinant for lysozyme resistance of Staphylococcus aureus. *Mol Microbiol* **55**: 778-787.

Bercovici B, Michel J, Miller J & Sacks TG (1975) Antimicrobial activity of human peritoneal fluid. *Surg Gynecol Obstet* **141**: 885-887.

Berg KH, Biornstad TJ, Johnsborg O & Havarstein LS (2012) Properties and biological role of streptococcal fratricins. *Appl Environ Microbiol* **78**: 3515-3522.

Berg KH, Stamsas GA, Straume D & Havarstein LS (2013) Effects of low PBP2b levels on cell morphology and peptidoglycan composition in Streptococcus pneumoniae R6. *J Bacteriol* **195**: 4342-4354.

Bertrand JA, Auger G, Fanchon E, Martin L, Blanot D, van Heijenoort J & Dideberg O (1997) Crystal structure of UDP-N-acetylmuramoyl-L-alanine:D-glutamate ligase from Escherichia coli. *EMBO J* **16**: 3416-3425.

Bertsche U, Breukink E, Kast T & Vollmer W (2005) In vitro murein peptidoglycan synthesis by dimers of the bifunctional transglycosylase-transpeptidase PBP1B from Escherichia coli. *J Biol Chem* **280**: 38096-38101.

Blake CC, Koenig DF, Mair GA, North AC, Phillips DC & Sarma VR (1965) Structure of hen egg-white lysozyme. A three-dimensional Fourier synthesis at 2 Angstrom resolution. *Nature* **206**: 757-761.

Bogaert D, Keijser B, Huse S*, et al.* (2011) Variability and diversity of nasopharyngeal microbiota in children: a metagenomic analysis. *PLoS One* **6**: e17035.

Boneca IG (2005) The role of peptidoglycan in pathogenesis. *Curr Opin Microbiol* **8**: 46-53.

Born P, Breukink E & Vollmer W (2006) In vitro synthesis of cross-linked murein and its attachment to sacculi by PBP1A from Escherichia coli. *J Biol Chem* **281**: 26985-26993.

Boyle DS, Khattar MM, Addinall SG, Lutkenhaus J & Donachie WD (1997) ftsW is an essential cell-division gene in Escherichia coli. *Mol Microbiol* **24**: 1263-1273.

Bramhill D & Thompson CM (1994) GTP-dependent polymerization of Escherichia coli FtsZ protein to form tubules. *Proc Natl Acad Sci U S A* **91**: 5813-5817.

Breukink E, van Heusden HE, Vollmerhaus PJ*, et al.* (2003) Lipid II is an intrinsic component of the pore induced by nisin in bacterial membranes. *J Biol Chem* **278**: 19898-19903.

Briese T & Hakenbeck R (1985) Interaction of the pneumococcal amidase with lipoteichoic acid and choline. *Eur J Biochem* **146**: 417-427.

Brisou P, Chamouilli JM, Gaillard T & Muzellec Y (2004) Infections à pneumocoque. *Encyclopédie Médico-Chirurgicale* **4-260-B-10**.

Buddelmeijer N, Judson N, Boyd D, Mekalanos JJ & Beckwith J (2002) YgbQ, a cell division protein in Escherichia coli and Vibrio cholerae, localizes in codependent fashion with FtsL to the division site. *Proc Natl Acad Sci U S A* **99**: 6316-6321.

Bui NK, Eberhardt A, Vollmer D*, et al.* (2012) Isolation and analysis of cell wall components from Streptococcus pneumoniae. *Anal Biochem* **421**: 657-666.

Carapito R, Chesnel L, Vernet T & Zapun A (2006) Pneumococcal beta-lactam resistance due to a conformational change in penicillin-binding protein 2x. *J Biol Chem* **281**: 1771-1777.

CDC (2013) Progress in Introduction of Pneumococcal Conjugate Vaccine - Worldwide, 2000–2012. *Morbidity and Mortality Weekly Report* **62**: 308-311.

Chesnel L, Carapito R, Croize J, Dideberg O, Vernet T & Zapun A (2005) Identical penicillin-binding domains in penicillin-binding proteins of Streptococcus pneumoniae clinical isolates with different levels of beta-lactam resistance. *Antimicrob Agents Chemother* **49**: 2895-2902.

Chesnel L, Pernot L, Lemaire D*, et al.* (2003) The structural modifications induced by the M339F substitution in PBP2x from Streptococcus pneumoniae further decreases the susceptibility to beta-lactams of resistant strains. *J Biol Chem* **278**: 44448-44456.

Chung BC, Zhao J, Gillespie RA*, et al.* (2013) Crystal structure of MraY, an essential membrane enzyme for bacterial cell wall synthesis. *Science* **341**: 1012-1016.

Claessen D, Emmins R, Hamoen LW, Daniel RA, Errington J & Edwards DH (2008) Control of the cell elongation-division cycle by shuttling of PBP1 protein in Bacillus subtilis. *Mol Microbiol* **68**: 1029-1046.

Contreras-Martel C, Dahout-Gonzalez C, Martins Ados S, Kotnik M & Dessen A (2009) PBP active site flexibility as the key mechanism for beta-lactam resistance in pneumococci. *J Mol Biol* **387**: 899-909.

Crisostomo MI, Vollmer W, Kharat AS, Inhulsen S, Gehre F, Buckenmaier S & Tomasz A (2006) Attenuation of penicillin resistance in a peptidoglycan O-acetyl transferase mutant of Streptococcus pneumoniae. *Mol Microbiol* **61**: 1497-1509.

Croucher NJ, Harris SR, Fraser C*, et al.* (2011) Rapid pneumococcal evolution in response to clinical interventions. *Science* **331**: 430-434.

Crum NF, Barrozo CP, Chapman FA, Ryan MA & Russell KL (2004) An outbreak of conjunctivitis due to a novel unencapsulated Streptococcus pneumoniae among military trainees. *Clin Infect Dis* **39**: 1148-1154.

Dawson MH & Sia RH (1931) In Vitro Transformation of Pneumococcal Types : I. A Technique for Inducing Transformation of Pneumococcal Types in Vitro. *J Exp Med* **54**: 681-699.

de Jong IG, Beilharz K, Kuipers OP & Veening JW (2011) Live Cell Imaging of Bacillus subtilis and Streptococcus pneumoniae using Automated Time-lapse Microscopy. *J Vis Exp* **53**: 3145.

De Las Rivas B, Garcia J, Lopez R & Garcia P (2002) Purification and polar localization of pneumococcal LytB, a putative endo-beta-N-acetylglucosaminidase: the chain-dispersing murein hydrolase. *J. Bacteriol.* **184**: 4988-5000.

Derouaux A, Turk S, Olrichs NK*, et al.* (2011) Small molecule inhibitors of peptidoglycan synthesis targeting the lipid II precursor. *Biochem Pharmacol* **81**: 1098-1105.

Di Guilmi AM, Dessen A, Dideberg O & Vernet T (2003) Functional characterization of penicillin-binding protein 1b from Streptococcus pneumoniae. *J Bacteriol* **185**: 1650-1658.

Di Guilmi AM, Dessen A, Dideberg O & Vernet T (2003) The glycosyltransferase domain of penicillin-binding protein 2a from Streptococcus pneumoniae catalyzes the polymerization of murein glycan chains. *J Bacteriol* **185**: 4418-4423.

di Guilmi AM, Mouz N, Martin L, Hoskins J, Jaskunas SR, Dideberg O & Vernet T (1999) Glycosyltransferase domain of penicillin-binding protein 2a from Streptococcus pneumoniae is membrane associated. *J Bacteriol* **181**: 2773-2781.

Dmitriev BA, Toukach FV, Schaper KJ, Holst O, Rietschel ET & Ehlers S (2003) Tertiary structure of bacterial murein: the scaffold model. *J Bacteriol* **185**: 3458-3468.

Dowson CG, Coffey TJ, Kell C & Whiley RA (1993) Evolution of penicillin resistance in Streptococcus pneumoniae; the role of Streptococcus mitis in the formation of a low affinity PBP2B in S. pneumoniae. *Mol Microbiol* **9**: 635-643.

Dowson CG, Hutchison A, Brannigan JA*, et al.* (1989) Horizontal transfer of penicillin-binding protein genes in penicillin-resistant clinical isolates of Streptococcus pneumoniae. *Proc Natl Acad Sci U S A* **86**: 8842-8846.

Du Plessis M, Smith AM & Klugman KP (2000) Analysis of penicillin-binding protein lb and 2a genes from Streptococcus pneumoniae. *Microb Drug Resist* **6**: 127-131.

Duman R, Ishikawa S, Celik I*, et al.* (2013) Structural and genetic analyses reveal the protein SepF as a new membrane anchor for the Z ring. *Proc Natl Acad Sci U S A* **110**: E4601-4610.

Eberhardt A, Wu LJ, Errington J, Vollmer W & Veening JW (2009) Cellular localization of choline-utilization proteins in Streptococcus pneumoniae using novel fluorescent reporter systems. *Mol Microbiol* **74**: 395-408.

Egan AJ & Vollmer W (2013) The physiology of bacterial cell division. *Ann N Y Acad Sci* **1277**: 8-28.

Erickson HP, Taylor DW, Taylor KA & Bramhill D (1996) Bacterial cell division protein FtsZ assembles into protofilament sheets and minirings, structural homologs of tubulin polymers. *Proc Natl Acad Sci U S A* **93**: 519-523.

Fadda D, Pischedda C, Caldara F, Whalen MB, Anderluzzi D, Domenici E & Massidda O (2003) Characterization of divIVA and other genes located in the chromosomal region downstream of the dcw cluster in Streptococcus pneumoniae. *J Bacteriol* **185**: 6209-6214.

Fadda D, Santona A, D'Ulisse V, Ghelardini P, Ennas MG, Whalen MB & Massidda O (2007) Streptococcus pneumoniae DivIVA: localization and interactions in a MinCD-free context. *J Bacteriol* **189**: 1288-1298.

Fani F, Leprohon P, Zhanel GG, Bergeron MG & Ouellette M (2014) Genomic analyses of DNA transformation and penicillin resistance in Streptococcus pneumoniae clinical isolates. *Antimicrob Agents Chemother* **58**: 1397-1403.

Figueiredo TA, Ludovice AM & Sobral RG (2014) Contribution of Peptidoglycan Amidation to Beta-Lactam and Lysozyme Resistance in Different Genetic Lineages of Staphylococcus aureus. *Microb Drug Resist* **20**: 238-249.

Figueiredo TA, Sobral RG, Ludovice AM, *et al.* (2012) Identification of genetic determinants and enzymes involved with the amidation of glutamic acid residues in the peptidoglycan of Staphylococcus aureus. *PLoS Pathog* **8**: e1002508.

Filipe SR & Tomasz A (2000) Inhibition of the expression of penicillin resistance in Streptococcus pneumoniae by inactivation of cell wall muropeptide branching genes. *Proc Natl Acad Sci U S A* **97**: 4891-4896.

Filipe SR, Pinho MG & Tomasz A (2000) Characterization of the murMN operon involved in the synthesis of branched peptidoglycan peptides in Streptococcus pneumoniae. *J Biol Chem* **275**: 27768-27774.

Filipe SR, Severina E & Tomasz A (2000) Distribution of the mosaic structured murM genes among natural populations of Streptococcus pneumoniae. *J Bacteriol* **182**: 6798-6805.

Filipe SR, Severina E & Tomasz A (2002) The murMN operon: a functional link between antibiotic resistance and antibiotic tolerance in Streptococcuspneumoniae. *Proc Natl Acad Sci U S A* **99**: 1550-1555.

Fischer W (1997) Pneumococcal lipoteichoic and teichoic acid. *Microb Drug Resist* **3**: 309-325.

Fleming A (1922) On a Remarkable Bacteriolytic Element Found in Tissues and Secretions. *Proceedings of the Royal Society B* **93**: 306-317.

Fleming A (1929) On the antibacterial action of cultures of a penicillium, with special reference to their use in the isolation of B. influenzae. *British Journal of Experimental Pathology* **10**: 226-236.

Fleurie A, Cluzel C, Guiral S, *et al.* (2012) Mutational dissection of the S/T-kinase StkP reveals crucial roles in cell division of Streptococcus pneumoniae. *Mol Microbiol* **83**: 746-758.

Fleurie A, Manuse S, Zhao C, *et al.* (2014) Interplay of the Serine/Threonine-Kinase StkP and the Paralogs DivIVA and GpsB in Pneumococcal Cell Elongation and Division. *PLoS Genet* **10**: e1004275.

Fraipont C, Sapunaric F, Zervosen A, *et al.* (2006) Glycosyl transferase activity of the Escherichia coli penicillin-binding protein 1b: specificity profile for the substrate. *Biochemistry* **45**: 4007-4013.

Galli E & Gerdes K (2012) FtsZ-ZapA-ZapB interactome of Escherichia coli. *J Bacteriol* **194**: 292-302.

Garcia-Bustos J & Tomasz A (1990) A biological price of antibiotic resistance: major changes in the peptidoglycan structure of penicillin-resistant pneumococci. *Proc Natl Acad Sci U S A* **87**: 5415-5419.

Garcia P, Gonzalez MP, Garcia E, Lopez R & Garcia JL (1999) LytB, a novel pneumococcal murein hydrolase essential for cell separation. *Mol Microbiol* **31**: 1275-1281.

Gerard P, Vernet T & Zapun A (2002) Membrane topology of the Streptococcus pneumoniae FtsW division protein. *J Bacteriol* **184**: 1925-1931.

Giefing-Kroll C, Jelencsics KE, Reipert S & Nagy E (2011) Absence of pneumococcal PcsB is associated with overexpression of LysM domain-containing proteins. *Microbiology* **157**: 1897-1909.

Goffin C & Ghuysen JM (1998) Multimodular penicillin-binding proteins: an enigmatic family of orthologs and paralogs. *Microbiol Mol Biol Rev* **62**: 1079-1093.

Grau I, Ardanuy C, Calatayud L, Schulze MH, Linares J & Pallares R (2014) Smoking and alcohol abuse are the most preventable risk factors for invasive pneumonia and other pneumococcal infections. *Int J Infect Dis* **25**: 59-64.

Grebe T & Hakenbeck R (1996) Penicillin-binding proteins 2b and 2x of Streptococcus pneumoniae are primary resistance determinants for different classes of beta-lactam antibiotics. *Antimicrob Agents Chemother* **40**: 829-834.

Grebe T, Paik J & Hakenbeck R (1997) A novel resistance mechanism against beta-lactams in Streptococcus pneumoniae involves CpoA, a putative glycosyltransferase. *J Bacteriol* **179**: 3342-3349.

Griffith F (1928) The Significance of Pneumococcal Types. *J Hyg (Lond)* **27**: 113-159.

Guenzi E, Gasc AM, Sicard MA & Hakenbeck R (1994) A two-component signal-transducing system is involved in competence and penicillin susceptibility in laboratory mutants of Streptococcus pneumoniae. *Mol Microbiol* **12**: 505-515.

Hakenbeck R, Tarpay M & Tomasz A (1980) Multiple changes of penicillin-binding proteins in penicillin-resistant clinical isolates of Streptococcus pneumoniae. *Antimicrob Agents Chemother* **17**: 364-371.

Hakenbeck R, Tornette S & Adkinson NF (1987) Interaction of non-lytic beta-lactams with penicillin-binding proteins in Streptococcus pneumoniae. *J Gen Microbiol* **133**: 755-760.

Hakenbeck R, Martin C, Dowson C & Grebe T (1994) Penicillin-binding protein 2b of Streptococcus pneumoniae in piperacillin-resistant laboratory mutants. *J Bacteriol* **176**: 5574-5577.

Hakenbeck R, Bruckner R, Denapaite D & Maurer P (2012) Molecular mechanisms of beta-lactam resistance in Streptococcus pneumoniae. *Future Microbiol* **7**: 395-410.

Hammerschmidt S, Wolff S, Hocke A, Rosseau S, Muller E & Rohde M (2005) Illustration of pneumococcal polysaccharide capsule during adherence and invasion of epithelial cells. *Infect Immun* **73**: 4653-4667.

Hansman DB, MM. (1967) A resistant pneumococcus [letter]. *Lancet* **2**: 264-265.

Hausdorff WP, Bryant J, Paradiso PR & Siber GR (2000) Which pneumococcal serogroups cause the most invasive disease: implications for conjugate vaccine formulation and use, part I. *Clin Infect Dis* **30**: 100-121.

Havarstein LS, Diep DB & Nes IF (1995) A family of bacteriocin ABC transporters carry out proteolytic processing of their substrates concomitant with export. *Mol Microbiol* **16**: 229-240.

Havarstein LS, Coomaraswamy G & Morrison DA (1995) An unmodified heptadecapeptide pheromone induces competence for genetic transformation in Streptococcus pneumoniae. *Proc Natl Acad Sci U S A* **92**: 11140-11144.

Helassa N, Vollmer W, Breukink E, Vernet T & Zapun A (2012) The membrane anchor of penicillin-binding protein PBP2a from Streptococcus pneumoniae influences peptidoglycan chain length. *FEBS J* **279**: 2071-2081.

Henriques-Normark B & Tuomanen EI (2013) The pneumococcus: epidemiology, microbiology, and pathogenesis. *Cold Spring Harb Perspect Med* **3**: a010215

Henriques AO, Glaser P, Piggot PJ & Moran CP, Jr. (1998) Control of cell shape and elongation by the rodA gene in Bacillus subtilis. *Mol Microbiol* **28**: 235-247.

Higgins ML & Shockman GD (1970) Model for cell wall growth of Streptococcus faecalis. *J Bacteriol* **101**: 643-648.

Higgins ML & Shockman GD (1976) Study of cycle of cell wall assembly in Streptococcus faecalis by three-dimensional reconstructions of thin sections of cells. *J Bacteriol* **127**: 1346-1358.

Hirst RA, Gosai B, Rutman A, Guerin CJ, Nicotera P, Andrew PW & O'Callaghan C (2008) Streptococcus pneumoniae deficient in pneumolysin or autolysin has reduced virulence in meningitis. *J Infect Dis* **197**: 744-751.

Holtje JV (1998) Growth of the stress-bearing and shape-maintaining murein sacculus of Escherichia coli. *Microbiol Mol Biol Rev* **62**: 181-203.

Hoskins J, Matsushima P, Mullen DL*, et al.* (1999) Gene disruption studies of penicillin-binding proteins 1a, 1b, and 2a in Streptococcus pneumoniae. *J Bacteriol* **181**: 6552-6555.

Hoskins J, Alborn WE, Jr., Arnold J*, et al.* (2001) Genome of the bacterium Streptococcus pneumoniae strain R6. *J Bacteriol* **183**: 5709-5717.

Howard LV & Gooder H (1974) Specificity of the autolysin of Streptococcus (Diplococcus) pneumoniae. *J Bacteriol* **117**: 796-804.

Hoyland CN, Aldridge C, Cleverley RM*, et al.* (2014) Structure of the LdcB LD-Carboxypeptidase Reveals the Molecular Basis of Peptidoglycan Recognition. *Structure* **22**(7): 949-960.

Hu Y, Chen L, Ha S*, et al.* (2003) Crystal structure of the MurG:UDP-GlcNAc complex reveals common structural principles of a superfamily of glycosyltransferases. *Proc Natl Acad Sci U S A* **100**: 845-849.

Ikeda M, Sato T, Wachi M, Jung HK, Ishino F, Kobayashi Y & Matsuhashi M (1989) Structural similarity among Escherichia coli FtsW and RodA proteins and Bacillus subtilis SpoVE protein, which function in cell division, cell elongation, and spore formation, respectively. *J Bacteriol* **171**: 6375-6378.

Ishino F, Jung HK, Ikeda M, Doi M, Wachi M & Matsuhashi M (1989) New mutations fts-36, lts-33, and ftsW clustered in the mra region of the Escherichia coli chromosome induce thermosensitive cell growth and division. *J Bacteriol* **171**: 5523-5530.

Johnsborg O & Havarstein LS (2009) Regulation of natural genetic transformation and acquisition of transforming DNA in Streptococcus pneumoniae. *FEMS Microbiol Rev* **33**: 627-642.

Johnson DM, Biedenbach DJ & Jones RN (2002) Potency and antimicrobial spectrum update for piperacillin/tazobactam (2000): emphasis on its activity against resistant organism populations and generally untested species causing community-acquired respiratory tract infections. *Diagn Microbiol Infect Dis* **43**: 49-60.

Kadioglu A, Weiser JN, Paton JC & Andrew PW (2008) The role of Streptococcus pneumoniae virulence factors in host respiratory colonization and disease. *Nat Rev Microbiol* **6**: 288-301.

Kang CI, Baek JY, Jeon K, *et al.* (2012) Bacteremic pneumonia caused by extensively drug-resistant Streptococcus pneumoniae. *J Clin Microbiol* **50**: 4175-4177.

Kawamura Y, Hou XG, Sultana F, Miura H & Ezaki T (1995) Determination of 16S rRNA sequences of Streptococcus mitis and Streptococcus gordonii and phylogenetic relationships among members of the genus Streptococcus. *Int J Syst Bacteriol* **45**: 406-408.

Keefer CB, FG. Marshall, EKJr. Lockwood, JS. Wood, WBJr. (1943) Penicillin in the treatment of infections: a report of 500 cases. *JAMA* **122**: 1217-1224.

Kelly T, Dillard JP & Yother J (1994) Effect of genetic switching of capsular type on virulence of Streptococcus pneumoniae. *Infect Immun* **62**: 1813-1819.

Klammt C, Schwarz D, Lohr F, Schneider B, Dotsch V & Bernhard F (2006) Cell-free expression as an emerging technique for the large scale production of integral membrane protein. *FEBS J* **273**: 4141-4153.

Krauss J & Hakenbeck R (1997) A mutation in the D,D-carboxypeptidase penicillin-binding protein 3 of Streptococcus pneumoniae contributes to cefotaxime resistance of the laboratory mutant C604. *Antimicrob Agents Chemother* **41**: 936-942.

Laible G, Spratt BG & Hakenbeck R (1991) Interspecies recombinational events during the evolution of altered PBP 2x genes in penicillin-resistant clinical isolates of Streptococcus pneumoniae. *Mol Microbiol* **5**: 1993-2002.

Laitinen H & Tomasz A (1990) Changes in composition of peptidoglycan during maturation of the cell wall in pneumococci. *J Bacteriol* **172**: 5961-5967.

Land AD & Winkler ME (2011) The requirement for pneumococcal MreC and MreD is relieved by inactivation of the gene encoding PBP1a. *J Bacteriol* **193**: 4166-4179.

Land AD, Tsui HC, Kocaoglu O, *et al.* (2013) Requirement of essential Pbp2x and GpsB for septal ring closure in Streptococcus pneumoniae D39. *Mol Microbiol* **90**: 939-955.

Lara B, Rico AI, Petruzzelli S, *et al.* (2005) Cell division in cocci: localization and properties of the Streptococcus pneumoniae FtsA protein. *Mol Microbiol* **55**: 699-711.

Le Gouellec A, Roux L, Fadda D, Massidda O, Vernet T & Zapun A (2008) Roles of pneumococcal DivIB in cell division. *J Bacteriol* **190**: 4501-4511.

Levin PA, Kurtser IG & Grossman AD (1999) Identification and characterization of a negative regulator of FtsZ ring formation in Bacillus subtilis. *Proc Natl Acad Sci U S A* **96**: 9642-9647.

Lewis K (2013) Platforms for antibiotic discovery. *Nat Rev Drug Discov* **12**: 371-387.

Liechti GW, Kuru E, Hall E, Kalinda A, Brun YV, VanNieuwenhze M & Maurelli AT (2014) A new metabolic cell-wall labelling method reveals peptidoglycan in Chlamydia trachomatis. *Nature* **506**: 507-510.

Lleo MM, Canepari P & Satta G (1990) Bacterial cell shape regulation: testing of additional predictions unique to the two-competing-sites model for peptidoglycan assembly and isolation of conditional rod-shaped mutants from some wild-type cocci. *J Bacteriol* **172**: 3758-3771.

Lloyd AJ, Gilbey AM, Blewett AM, *et al.* (2008) Characterization of tRNA-dependent peptide bond formation by MurM in the synthesis of Streptococcus pneumoniae peptidoglycan. *J Biol Chem* **283**: 6402-6417.

Lorian V & Atkinson B (1976) Effects of subinhibitory concentrations of antibiotics on cross walls of cocci. *Antimicrob Agents Chemother* **9**: 1043-1055.

Lovering AL, Safadi SS & Strynadka NC (2012) Structural perspective of peptidoglycan biosynthesis and assembly. *Annu Rev Biochem* **81**: 451-478.

Lutkenhaus J, Pichoff S & Du S (2012) Bacterial cytokinesis: From Z ring to divisome. *Cytoskeleton (Hoboken)* **69**: 778-790.

Margolin W (2000) Themes and variations in prokaryotic cell division. *FEMS Microbiol Rev* **24**: 531-548.

Martin C, Sibold C & Hakenbeck R (1992) Relatedness of penicillin-binding protein 1a genes from different clones of penicillin-resistant Streptococcus pneumoniae isolated in South Africa and Spain. *EMBO J* **11**: 3831-3836.

Martin M, Turco JH, Zegans ME, *et al.* (2003) An outbreak of conjunctivitis due to atypical Streptococcus pneumoniae. *N Engl J Med* **348**: 1112-1121.

Martner A, Skovbjerg S, Paton JC & Wold AE (2009) Streptococcus pneumoniae autolysis prevents phagocytosis and production of phagocyte-activating cytokines. *Infect Immun* **77**: 3826-3837.

Massidda O, Novakova L & Vollmer W (2013) From models to pathogens: how much have we learned about Streptococcus pneumoniae cell division? *Environ Microbiol* **15**: 3133-3157.

Massidda O, Anderluzzi D, Friedli L & Feger G (1998) Unconventional organization of the division and cell wall gene cluster of Streptococcus pneumoniae. *Microbiology* **144 ( Pt 11)**: 3069-3078.

Matsuzawa H, Hayakawa K, Sato T & Imahori K (1973) Characterization and genetic analysis of a mutant of Escherichia coli K-12 with rounded morphology. *J Bacteriol* **115**: 436-442.

McGee L (2007) The coming of age of niche vaccines? Effect of vaccines on resistance profiles in Streptococcus pneumoniae. *Curr Opin Microbiol* **10**: 473-478.

Meiers M, Volz C, Eisel J, Maurer P, Henrich B & Hakenbeck R (2014) Altered lipid composition in Streptococcus pneumoniae cpoA mutants. *BMC Microbiol* **14**: 12.

Mellroth P, Daniels R, Eberhardt A*, et al.* (2012) LytA, major autolysin of Streptococcus pneumoniae, requires access to nascent peptidoglycan. *J Biol Chem* **287**: 11018-11029.

Moffitt KL & Malley R (2011) Next generation pneumococcal vaccines. *Curr Opin Immunol* **23**: 407-413.

Mohammadi T, Sijbrandi R, Lutters M*, et al.* (2014) Specificity of the transport of Lipid II by FtsW in Escherichia coli. *J Biol Chem* **289**(21): 414707-18.

Mohammadi T, van Dam V, Sijbrandi R*, et al.* (2011) Identification of FtsW as a transporter of lipid-linked cell wall precursors across the membrane. *EMBO J* **30**: 1425-1432.

Morlot C, Zapun A, Dideberg O & Vernet T (2003) Growth and division of Streptococcus pneumoniae: localization of the high molecular weight penicillin-binding proteins during the cell cycle. *Mol Microbiol* **50**: 845-855.

Morlot C, Noirclerc-Savoye M, Zapun A, Dideberg O & Vernet T (2004) The D,D-carboxypeptidase PBP3 organizes the division process of Streptococcus pneumoniae. *Mol Microbiol* **51**: 1641-1648.

Morrison DA (1997) Streptococcal competence for genetic transformation: regulation by peptide pheromones. *Microb Drug Resist* **3**: 27-37.

Moscoso M & Claverys JP (2004) Release of DNA into the medium by competent Streptococcus pneumoniae: kinetics, mechanism and stability of the liberated DNA. *Mol Microbiol* **54**: 783-794.

Mosser JL & Tomasz A (1970) Choline-containing teichoic acid as a structural component of pneumococcal cell wall and its role in sensitivity to lysis by an autolytic enzyme. *J Biol Chem* **245**: 287-298.

Moynihan PJ, Sychantha D & Clarke AJ (2014) Chemical biology of peptidoglycan acetylation and deacetylation. *Bioorg Chem* **54C**: 44-50.

Munch D, Roemer T, Lee SH, Engeser M, Sahl HG & Schneider T (2012) Identification and in vitro analysis of the GatD/MurT enzyme-complex catalyzing lipid II amidation in Staphylococcus aureus. *PLoS Pathog* **8**: e1002509.

Munoz R, Dowson CG, Daniels M, Coffey TJ, Martin C, Hakenbeck R & Spratt BG (1992) Genetics of resistance to third-generation cephalosporins in clinical isolates of Streptococcus pneumoniae. *Mol Microbiol* **6**: 2461-2465.

Netter A (1887) De la meningite due au pneumocoque (avec ou sans pneumonie). *Archives Générales de Médecine* **séries 7**: 434-455.

Neufeld F & Haendel L (1910) Weitere Untersuchungen uber Pneumokokken-Heilsera. III. Mitteilung. *Arbeiten aus dem Kaiserlichen Gesundheitsamte* 293-304.

Ng WL, Kazmierczak KM & Winkler ME (2004) Defective cell wall synthesis in Streptococcus pneumoniae R6 depleted for the essential PcsB putative murein hydrolase or the VicR (YycF) response regulator. *Mol Microbiol* **53**: 1161-1175.

Ng WL, Tsui HC & Winkler ME (2005) Regulation of the pspA virulence factor and essential pcsB murein biosynthetic genes by the phosphorylated VicR (YycF) response regulator in Streptococcus pneumoniae. *J Bacteriol* **187**: 7444-7459.

Noirclerc-Savoye M, Le Gouellec A, Morlot C, Dideberg O, Vernet T & Zapun A (2005) In vitro reconstitution of a trimeric complex of DivIB, DivIC and FtsL, and their transient co-localization at the division site in Streptococcus pneumoniae. *Mol Microbiol* **55**: 413-424.

Noirclerc-Savoye M, Lantez V, Signor L, Philippe J, Vernet T & Zapun A (2013) Reconstitution of membrane protein complexes involved in pneumococcal septal cell wall assembly. *PLoS One* **8**: e75522.

Nonomura N, Giebink GS, Juhn SK, Harada T & Aeppli D (1991) Pathophysiology of Streptococcus pneumoniae otitis media: kinetics of the middle ear biochemical and cytologic host responses. *Ann Otol Rhinol Laryngol* **100**: 236-243.

Oliva MA, Halbedel S, Freund SM*, et al.* (2010) Features critical for membrane binding revealed by DivIVA crystal structure. *EMBO J* **29**: 1988-2001.

Ostash B & Walker S (2005) Bacterial transglycosylase inhibitors. *Curr Opin Chem Biol* **9**: 459-466.

Page MG, Dantier C & Desarbre E (2010) In vitro properties of BAL30072, a novel siderophore sulfactam with activity against multiresistant gram-negative bacilli. *Antimicrob Agents Chemother* **54**: 2291-2302.

Pagliero E, B D, C F, O D, T V & Di Guilmi A (2008) The Inactivation of a New Peptidoglycan Hydrolase Pmp23 Leads to Abnormal Septum Formation in Streptococcus pneumoniae. *Open Microbiol J* **2**: 107-114.

Pagliero E, Chesnel L, Hopkins J, Croize J, Dideberg O, Vernet T & Di Guilmi AM (2004) Biochemical characterization of Streptococcus pneumoniae penicillin-binding protein 2b and its implication in beta-lactam resistance. *Antimicrob Agents Chemother* **48**: 1848-1855.

Paik J, Kern I, Lurz R & Hakenbeck R (1999) Mutational analysis of the Streptococcus pneumoniae bimodular class A penicillin-binding proteins. *J Bacteriol* **181**: 3852-3856.

Pasteur L (1881) Note sur la maladie nouvelle provoquée par la salive d 'un enfant mort de la rage. *Bulletin de I'Académie de Médicine* **séries 2**: 94-103.

Patin D, Boniface A, Kovac A*, et al.* (2010) Purification and biochemical characterization of Mur ligases from Staphylococcus aureus. *Biochimie* **92**: 1793-1800.

Perez-Nunez D, Briandet R, David B*, et al.* (2011) A new morphogenesis pathway in bacteria: unbalanced activity of cell wall synthesis machineries leads to coccus-to-rod transition and filamentation in ovococci. *Mol Microbiol* **79**: 759-771.

Perlstein DL, Zhang Y, Wang TS, Kahne DE & Walker S (2007) The direction of glycan chain elongation by peptidoglycan glycosyltransferases. *J Am Chem Soc* **129**: 12674-12675.

Pestova EV, Havarstein LS & Morrison DA (1996) Regulation of competence for genetic transformation in Streptococcus pneumoniae by an auto-induced peptide pheromone and a two-component regulatory system. *Mol Microbiol* **21**: 853-862.

Peters K, Schweizer I, Beilharz K, Stahlmann C, Veening JW, Hakenbeck R & Denapaite D (2014) Streptococcus pneumoniae PBP2x mid-cell localization requires the C-terminal PASTA domains and is essential for cell shape maintenance. *Mol Microbiol* **92**: 733-755.

Philippe J, Vernet T & Zapun A (2014) The Elongation of Ovococci. *Microb Drug Resist* **20**: 215-221.

Pilishvili T, Lexau C, Farley MM*, et al.* (2010) Sustained reductions in invasive pneumococcal disease in the era of conjugate vaccine. *J Infect Dis* **201**: 32-41.

Popp D, Iwasa M, Narita A, Erickson HP & Maeda Y (2009) FtsZ condensates: an in vitro electron microscopy study. *Biopolymers* **91**: 340-350.

Raz A, Talay SR & Fischetti VA (2012) Cellular aspects of the distinct M protein and SfbI anchoring pathways in Streptococcus pyogenes. *Mol Microbiol* **84**: 631-647.

Reinscheid DJ, Gottschalk B, Schubert A, Eikmanns BJ & Chhatwal GS (2001) Identification and molecular analysis of PcsB, a protein required for cell wall separation of group B streptococcus. *J Bacteriol* **183**: 1175-1183.

Sakwinska O, Bastic Schmid V, Berger B*, et al.* (2014) Nasopharyngeal microbiota in healthy children and pneumonia patients. *J Clin Microbiol* **52**: 1590-1594.

Sauvage E, Kerff F, Terrak M, Ayala JA & Charlier P (2008) The penicillin-binding proteins: structure and role in peptidoglycan biosynthesis. *FEMS Microbiol Rev* **32**: 234-258.

Schuster C, Dobrinski B & Hakenbeck R (1990) Unusual septum formation in Streptococcus pneumoniae mutants with an alteration in the D,D-carboxypeptidase penicillin-binding protein 3. *J Bacteriol* **172**: 6499-6505.

Schwartz B, Markwalder JA & Wang Y (2001) Lipid II: total synthesis of the bacterial cell wall precursor and utilization as a substrate for glycosyltransfer and transpeptidation by penicillin binding protein (PBP) 1b of Escherichia coli. *J Am Chem Soc* **123**: 11638-11643.

Seto H & Tomasz A (1975) Protoplast formation and leakage of intramembrane cell components: induction by the competence activator substance of pneumococci. *J Bacteriol* **121**: 344-353.

Severin A, Schuster C, Hakenbeck R & Tomasz A (1992) Altered murein composition in a DD-carboxypeptidase mutant of Streptococcus pneumoniae. *J Bacteriol* **174**: 5152-5155.

Sham LT, Barendt SM, Kopecky KE & Winkler ME (2011) Essential PcsB putative peptidoglycan hydrolase interacts with the essential FtsXSpn cell division protein in Streptococcus pneumoniae D39. *Proc Natl Acad Sci U S A* **108**: E1061-1069.

Sham LT, Jensen KR, Bruce KE & Winkler ME (2013) Involvement of FtsE ATPase and FtsX extracellular loops 1 and 2 in FtsEX-PcsB complex function in cell division of Streptococcus pneumoniae D39. *MBio* **4**.

Sham LT, Tsui HC, Land AD, Barendt SM & Winkler ME (2012) Recent advances in pneumococcal peptidoglycan biosynthesis suggest new vaccine and antimicrobial targets. *Curr Opin Microbiol* **15**: 194-203.

Sham LT, Butler EK, Lebar MD, Kahne D, Bernhardt TG & Ruiz N (2014) Bacterial cell wall. MurJ is the flippase of lipid-linked precursors for peptidoglycan biogenesis. *Science* **345**: 220-222.

Shiomi D, Sakai M & Niki H (2008) Determination of bacterial rod shape by a novel cytoskeletal membrane protein. *EMBO J* **27**: 3081-3091.

Sibold C, Henrichsen J, Konig A, Martin C, Chalkley L & Hakenbeck R (1994) Mosaic pbpX genes of major clones of penicillin-resistant Streptococcus pneumoniae have evolved from pbpX genes of a penicillin-sensitive Streptococcus oralis. *Mol Microbiol* **12**: 1013-1023.

Sieger B, Schubert K, Donovan C & Bramkamp M (2013) The lipid II flippase RodA determines morphology and growth in Corynebacterium glutamicum. *Mol Microbiol* **90**: 966-982.

Skarzynski T, Mistry A, Wonacott A, Hutchinson SE, Kelly VA & Duncan K (1996) Structure of UDP-N-acetylglucosamine enolpyruvyl transferase, an enzyme essential for the synthesis of bacterial peptidoglycan, complexed with substrate UDP-N-acetylglucosamine and the drug fosfomycin. *Structure* **4**: 1465-1474.

Smith AM & Klugman KP (2001) Alterations in MurM, a cell wall muropeptide branching enzyme, increase high-level penicillin and cephalosporin resistance in Streptococcus pneumoniae. *Antimicrob Agents Chemother* **45**: 2393-2396.

Smith AM, Feldman C, Massidda O, McCarthy K, Ndiweni D & Klugman KP (2005) Altered PBP 2A and its role in the development of penicillin, cefotaxime, and ceftriaxone resistance in a clinical isolate of Streptococcus pneumoniae. *Antimicrob Agents Chemother* **49**: 2002-2007.

Song JH, Dagan R, Klugman KP & Fritzell B (2012) The relationship between pneumococcal serotypes and antibiotic resistance. *Vaccine* **30**: 2728-2737.

Sorensen UB, Henrichsen J, Chen HC & Szu SC (1990) Covalent linkage between the capsular polysaccharide and the cell wall peptidoglycan of Streptococcus pneumoniae revealed by immunochemical methods. *Microb Pathog* **8**: 325-334.

Soualhine H, Brochu V, Menard F*, et al.* (2005) A proteomic analysis of penicillin resistance in Streptococcus pneumoniae reveals a novel role for PstS, a subunit of the phosphate ABC transporter. *Mol Microbiol* **58**: 1430-1440.

Spellerberg B, Cundell DR, Sandros J, Pearce BJ, Idanpaan-Heikkila I, Rosenow C & Masure HR (1996) Pyruvate oxidase, as a determinant of virulence in Streptococcus pneumoniae. *Mol Microbiol* **19**: 803-813.

Sternberg GM (1881) Special report to national board of health - Experimental investigations relating to the ethiology of the malarial fevers. *Annual Reports of the National Board of Health* 65-86.

Sternberg GM (1881) A fatal form of septicaemia in the rabbit, produced by the subcutaneous injection of human saliva. *Annual Reports of the National Board of Health* 87-108.

Tao L, Tanzer JM & MacAlister TJ (1987) Bicarbonate and potassium regulation of the shape of Streptococcus mutans NCTC 10449S. *J Bacteriol* **169**: 2543-2547.

Tao L, MacAlister TJ & Tanzer JM (1988) Factors influencing cell shape in the mutans group of streptococci. *J Bacteriol* **170**: 3752-3755.

Thibessard A, Fernandez A, Gintz B, Leblond-Bourget N & Decaris B (2002) Effects of rodA and pbp2b disruption on cell morphology and oxidative stress response of Streptococcus thermophilus CNRZ368. *J Bacteriol* **184**: 2821-2826.

Tillett WS, Cambier MJ & Harris WH (1943) Sulfonamide-Fast Pneumococci. A Clinical Report of Two Cases of Pneumonia Together with Experimental Studies on the Effectiveness of Penicillin and Tyrothricin against Sulfonamide-Resistant Strains. *J Clin Invest* **22**: 249-255.

Tillett WS, Cambier MJ & McCormack JE (1944) The Treatment of Lobar Pneumonia and Pneumococcal Empyema with Penicillin. *Bull N Y Acad Med* **20**: 142-178.

Tipper DJ & Strominger JL (1965) Mechanism of action of penicillins: a proposal based on their structural similarity to acyl-D-alanyl-D-alanine. *Proc Natl Acad Sci U S A* **54**: 1133-1141.

Tomasz A (1968) Biological consequences of the replacement of choline by ethanolamine in the cell wall of Pneumococcus: chanin formation, loss of transformability, and loss of autolysis. *Proc Natl Acad Sci U S A* **59**: 86-93.

Tomasz A & Waks S (1975) Mechanism of action of penicillin: triggering of the pneumococcal autolytic enzyme by inhibitors of cell wall synthesis. *Proc Natl Acad Sci U S A* **72**: 4162-4166.

Tomasz A, Albino A & Zanati E (1970) Multiple antibiotic resistance in a bacterium with suppressed autolytic system. *Nature* **227**: 138-140.

Tomasz A, Moreillon P & Pozzi G (1988) Insertional inactivation of the major autolysin gene of Streptococcus pneumoniae. *J Bacteriol* **170**: 5931-5934.

Typas A, Banzhaf M, Gross CA & Vollmer W (2012) From the regulation of peptidoglycan synthesis to bacterial growth and morphology. *Nat Rev Microbiol* **10**: 123-136.

Typas A, Banzhaf M, van den Berg van Saparoea B*, et al.* (2010) Regulation of peptidoglycan synthesis by outer-membrane proteins. *Cell* **143**: 1097-1109.

Van Bambeke F, Glupczynski Y, Mingeot-Leclercq M-P & Tulkens P (2010) *Mechanisms of action - Antibiotics that act on the cell wall*.

van den Ent F & Lowe J (2000) Crystal structure of the cell division protein FtsA from Thermotoga maritima. *EMBO J* **19**: 5300-5307.

van den Ent F, Johnson CM, Persons L, de Boer P & Lowe J (2010) Bacterial actin MreB assembles in complex with cell shape protein Rod*Z*. *EMBO J* **29**: 1081-1090.

van der Ploeg R, Verheul J, Vischer NO*, et al.* (2013) Colocalization and interaction between elongasome and divisome during a preparative cell division phase in Escherichia coli. *Mol Microbiol* **87**: 1074-1087.

Varma A & Young KD (2009) In Escherichia coli, MreB and FtsZ direct the synthesis of lateral cell wall via independent pathways that require PBP 2. *J Bacteriol* **191**: 3526-3533.

Varon E, Janoir C & Gutmann L (2013) Rapport d'activité du Centre National de Référence des Pneumocoques: Epidémiologie 2012. *Centre National de Référence des Pneumocoques* **Rapport d'activité 2013**.

Vats P, Shih YL & Rothfield L (2009) Assembly of the MreB-associated cytoskeletal ring of Escherichia coli. *Mol Microbiol* **72**: 170-182.

Vollmer W (2012) Bacterial growth does require peptidoglycan hydrolases. *Mol Microbiol* **86**: 1031-1035.

Vollmer W & Tomasz A (2000) The pgdA gene encodes for a peptidoglycan N-acetylglucosamine deacetylase in Streptococcus pneumoniae. *J Biol Chem* **275**: 20496-20501.

Vollmer W, Blanot D & de Pedro MA (2008) Peptidoglycan structure and architecture. *FEMS Microbiol Rev* **32**: 149-167.

Wachi M, Doi M, Tamaki S, Park W, Nakajima-Iijima S & Matsuhashi M (1987) Mutant isolation and molecular cloning of mre genes, which determine cell shape, sensitivity to mecillinam, and amount of penicillin-binding proteins in Escherichia coli. *J Bacteriol* **169**: 4935-4940.

Walsh C (2003) Where will new antibiotics come from? *Nat Rev Microbiol* **1**: 65-70.

Wang G (2014) Human antimicrobial peptides and proteins. *Pharmaceuticals (Basel)* **7**: 545-594.

Wang TS, Manning SA, Walker S & Kahne D (2008) Isolated peptidoglycan glycosyltransferases from different organisms produce different glycan chain lengths. *J Am Chem Soc* **130**: 14068-14069.

Watson DA, Musher DM, Jacobson JW & Verhoef J (1993) A brief history of the pneumococcus in biomedical research: a panoply of scientific discovery. *Clin Infect Dis* **17**: 913-924.

Wheeler R, Mesnage S, Boneca IG, Hobbs JK & Foster SJ (2011) Super-resolution microscopy reveals cell wall dynamics and peptidoglycan architecture in ovococcal bacteria. *Mol Microbiol* **82**: 1096-1109.

Whitby L (1938) Chemotherapy of pneumococcal and other infections with 2(ρ-aminobenzenesulphonamido) pyridine. *Lancet* **I**: 1210-1212.

Williamson R, Hakenbeck R & Tomasz A (1980) In vivo interaction of beta-lactam antibiotics with the penicillin-binding proteins of Streptococcus pneumoniae. *Antimicrob Agents Chemother* **18**: 629-637.

Xu X, Meng J, Wang Y*, et al.* (2014) Serotype-independent protection against pneumococcal infections elicited by intranasal immunization with ethanol-killed pneumococcal strain, SPY1. *J Microbiol* **52**: 315-323.

Yesilkaya H, Andisi VF, Andrew PW & Bijlsma JJ (2013) Streptococcus pneumoniae and reactive oxygen species: an unusual approach to living with radicals. *Trends Microbiol* **21**: 187-195.

Young KD (2006) The selective value of bacterial shape. *Microbiol Mol Biol Rev* **70**: 660-703.

Young KD (2010) Bacterial shape: two-dimensional questions and possibilities. *Annu Rev Microbiol* **64**: 223-240.

Zapun A, Vernet T & Pinho MG (2008) The different shapes of cocci. *FEMS Microbiol Rev* **32**: 345-360.

Zapun A, Contreras-Martel C & Vernet T (2008) Penicillin-binding proteins and beta-lactam resistance. *FEMS Microbiol Rev* **32**: 361-385.

Zapun A, Noirclerc-Savoye M, Helassa N & Vernet T (2012) Peptidoglycan assembly machines: the biochemical evidence. *Microb Drug Resist* **18**: 256-260.

Zapun A, Philippe J, Abrahams KA, Signor L, Roper DI, Breukink E & Vernet T (2013) In vitro reconstitution of peptidoglycan assembly from the Gram-positive pathogen Streptococcus pneumoniae. *ACS Chem Biol* **8**: 2688-2696.

Zaufal E (1887) Mikroorganismen im Secrete der Otitis media acuta. *Prager Medicinische Wochenschrift* 225-227.

Zerfass I, Hakenbeck R & Denapaite D (2009) An important site in PBP2x of penicillin-resistant clinical isolates of Streptococcus pneumoniae: mutational analysis of Thr338. *Antimicrob Agents Chemother* **53**: 1107-1115.

Zhao G, Yeh WK, Carnahan RH, *et al.* (1997) Biochemical characterization of penicillin-resistant and -sensitive penicillin-binding protein 2x transpeptidase activities of Streptococcus pneumoniae and mechanistic implications in bacterial resistance to beta-lactam antibiotics. *J Bacteriol* **179**: 4901-4908.

# Annexes

# Summary

*Streptococcus pneumoniae*, the pneumococcus, is a bacterial pathogen that causes more than 1.5 million deaths each year in the world. β-Lactams are widely used to treat patients with pneumococcal infections. These antibiotics inhibit the synthesis of the peptidoglycan, an essential mesh of aminosugar strands encasing the cell that endows bacteria with their shape. In this thesis, the morphogenesis of the pneumococcus has been investigated under three aspects. First, complexes of morphogenesis proteins have been isolated *in vitro*, involving PBP2b, RodA, MreC and MreD. In a second time, the analysis of the activity of pneumococcus Penicillin-Binding Proteins (PBPs) has been measured following the development of an assay for peptidoglycan synthesis *in vitro*. Finally, the specific role of the two essential pneumococcus PBPs (2x and 2b) in morphogenesis has been investigated by a combination of depletion and specific inhibition with piperacillin, a β-lactam antibiotic. A morphogenesis model is built based on my results and the literature, which permits to emit hypotheses concerning the response of the pneumococcus to β-lactams.

# Résumé

*Streptococcus pneumoniae*, le pneumocoque, est une bactérie pathogène qui entraîne le décès de plus d'un million et demi de personnes dans le monde chaque année. Les β-lactamines sont très utilisées pour traiter les infections à pneumocoques. Ces antibiotiques inhibent la synthèse du peptidoglycane, une molécule qui englobe la cellule et lui confère sa forme. Trois facettes de la morphogénèse du pneumocoque ont été étudiés dans cette thèse. Premièrement, des complexes de protéines de la morphogénèse ont été isolés *in vitro*, incluant PBP2b, RodA, MreC et MreD. L'activité des Protéines Liant la Pénicilline (PLPs) du pneumocoque a été mesurée grâce à la mise au point d'un test de synthèse du peptidoglycane *in vitro*. Enfin, une combinaison de déplétion et d'inhibition spécifique par traitement à la pipéracilline, une β-lactamine, a permis de mieux comprendre le rôle spécifique des 2 PLPs essentielles du pneumocoque dans la morphogénèse (PBP2x et PBP2b). Un modèle de morphogenèse est proposé intégrant mes résultats à la littérature et permettant de formuler des hypothèses sur la réponse physiologique de *S. pneumoniae* aux β-lactamines.